

The Pennsylvania State University

The Graduate School

John and Willie Leone Family Department of Energy and Mineral Engineering

DEVELOPMENT OF AN ARTIFICIAL NEURAL NETWORK  
BASED EXPERT SYSTEM TO DETERMINE THE  
LOCATION OF HORIZONTAL WELL IN A THREE-PHASE  
RESERVOIR WITH A SIMULTANEOUS GAS CAP AND  
BOTTOM WATER DRIVE

A Thesis in

Energy and Mineral Engineering

by

Mohammed AlQusom

© 2016 Mohammed AlQusom

Submitted in Partial Fulfillment  
of the Requirements  
for the Degree of

Master of Science

August 2016

The thesis of Mohammed AlQuisom was reviewed and approved\* by the following:

Turgay Ertekin

Head, John and Willie Leone Family Department of Energy and Mineral Engineering

Professor of Petroleum and Natural Gas Engineering

George E. Trimble Chair in Earth and Mineral Sciences

Thesis Advisor

Mort D. Webster

Associate Professor of Energy Engineering

Shimin Liu

Assistant Professor of Energy and Mineral Engineering

Luis F. Ayala H.

William A. Fustos Family Professor

Professor of Petroleum and Natural Gas Engineering

Associate Department Head for Graduate Education

\*Signatures are on file in the Graduate School

## ABSTRACT

---

The oil and gas industry is continuously trying to increase hydrocarbon's recovery in order to meet the high demand for energy in the world. Increasing the production rate of hydrocarbon compromises the lifespan of the reservoir. Throughout last decades, a number of processes have been developed in the oil and gas industry to increase the hydrocarbon recovery while minimizing their effect on the life of the reservoir. One of these techniques is the horizontal well drilling. This drilling method allows higher recovery of hydrocarbons by increasing the contact area between the casing and the oil zone.

However, high production rate from the horizontal well will result in phenomenon called cresting. The time at which it occurs is called breakthrough time. The goal for any production engineer is to delay breakthrough time as much as possible. The delay of this time will result in increasing the lifetime of the reservoir by maintaining the natural driving forces represented by water drive and gas cap in the reservoir.

In this study artificial neural network is utilized to construct a reliable tool to predict the production profiles namely: oil rate, gas rate, water rate, cumulative oil, cumulative gas, cumulative water, gas oil ratio, water oil ration and water cut, that lies within the reservoir and design properties for this study. A synthetic three-phase reservoir with a gas cap and bottom water drive is constructed using a commercial reservoir simulator to simulate and validate. After that, 600 different scenarios were generated using a range of reservoir properties along with different depth at which horizontal well will be placed. These different scenarios were used to train the ANN in order to make it predict the production profiles mentioned above within an error range of 5-15%. A graphical user interface (GUI) was developed to make this model user-friendly. A user will be asked to input the required

reservoir properties and the design property in the form of numbers and then the user will be able to obtain production profiles along with gas oil ratio, water oil ratio and water cut profiles.

# TABLE OF CONTENTS

---

LIST OF TABLES .....	vii
LIST OF FIGURES .....	viii
ACKNOWLEDGMENTS .....	xviii
Chapter 1: Introduction .....	1
Chapter 2: Literature Review .....	3
2.1    Artificial Neural Networks Overview. ....	3
2.1.1    Background .....	3
2.2    Artificial Neural Network Structure .....	5
2.2.1    Single Layer Feedforward Network: .....	5
2.2.2    Multilayer Feedforward Networks: .....	6
2.2.3    Recurrent Networks.....	7
2.3    Transfer Functions .....	8
2.4    Learning Methods .....	9
2.4.1    Supervised Training Method .....	9
2.4.2    Unsupervised Training Method.....	10
2.5    Applications of Artificial Neural Network in the Petroleum Engineering Field.....	11
Chapter 3: Problem Statement.....	14
Chapter 4: Reservoir Modeling .....	18
4.1    Reservoir Description .....	18

4.2	Grid Block Sensitivity Analysis .....	20
4.3	Data Generation and Compilation of Results .....	23
Chapter 5: Artificial Neural Network Development .....		24
5.1	Artificial Neural Network Structure .....	24
5.2	Artificial Neural Network Training .....	24
5.2.1	Number of Dataset.....	24
5.2.2	Training Algorithm and Transfer Function .....	28
5.2.3	ANN Structure (Layers and Neurons).....	28
5.3	Result and Error Analysis .....	31
Chapter 6: Graphical User Interface (GUI) Development .....		57
Chapter 7: Conclusion .....		59
References .....		62
Appendix (A) Test Cases results .....		66
Appendix (B) Properties Distribution .....		129
Appendix (C) ANN MATLAB Code.....		137

## LIST OF TABLES

---

TABLE 1: SUMMARY OF TRANSFER FUNCTION ( HAGAN ET AL. ,2002) .....	9
TABLE 2: RANGE OF RESERVOIR PROPERTIES USED IN THE MODEL .....	19
TABLE 3: ANN STRUCTURE WITH NUMBER OF NEURONS FOR EACH LAYER .....	29
TABLE 4: INPUT, FUNCTIONAL LINKS AND OUTPUT COMPONENTS FOR THE DEVELOPED MODEL .....	30
TABLE 5: MEAN ERROR COMPARISON FOR OIL, GAS AND WATER RATE FOR DIFFERENT ANN STRUCTURES WITH DIFFERENT NUMBER OF LAYERS AND NEURONS .....	34
TABLE 6: MEAN ERROR COMPARISON FOR CUMULATIVE OIL, GAS AND WATER FOR DIFFERENT ANN STRUCTURES WITH DIFFERENT NUMBER OF LAYERS AND NEURONS .....	34
TABLE 7: MEAN ERROR COMPARISON FOR WOR, GOR AND WATER CUT FOR DIFFERENT ANN STRUCTURES WITH DIFFERENT NUMBER OF LAYERS AND NEURONS .....	34
TABLE 8: CASE 51 RESERVOIR PROPERTIES .....	42
TABLE 9: CASE 79 RESERVOIR PROPERTIES .....	45
TABLE 10: CASE 51 RESERVOIR PROPERTIES .....	48
TABLE 11: CASE 334 RESERVOIR PROPERTIES .....	51
TABLE 12: CASE 340 RESERVOIR PROPERTIES .....	54

# LIST OF FIGURES

---

FIGURE 1: SCHEMATIC FOR BOTH BIOLOGICAL NEURON ON THE LEFT AND ARTIFICIAL NEURON ON THE RIGHT (SUZUKI, 2011).....	4
FIGURE 2: SINGLE LAYER ARCHITECTURE (HAGAN ET AL. , 2002).....	6
FIGURE 3: MULTILAYER FEEDFORWARD NETWORK ARCHITECTURE (HAGAN ET AL. , 2002).....	7
FIGURE 4: RECURRENT NETWORK STRUCTURE (HAGAN ET AL. ,2002) .....	7
FIGURE 5: LOG-SIGMOID TRANSFER FUNCTION (HAGAN ET AL., 2002).....	8
FIGURE 6: SCHEMATIC DIAGRAM THAT REPRESENTS SUPERVISED LEARNING MODEL (PRIDDY ET AL. ,2005) .....	10
FIGURE 7: SCHEMATIC DIAGRAM REPRESENTING UNSUPERVISED TRAINING (PRIDDY ET AL. ,2005)	11
FIGURE 8: SCHEMATIC DIAGRAM REPRESENTING THE WATER AND GAS CRESTING FOR A HORIZONTAL WELL.....	15
FIGURE 9: FLOW CHART SUMMARIZING RESEARCH STEPS.....	17
FIGURE 10: THREE-DIMENSIONAL CROSS-SECTIONAL AREA OF THE RESERVOIR MODEL .....	18
FIGURE 11: CUMULATIVE GAS PRODUCTION FOR ALL GRID BLOCK CASES (11X11X12 TO 33X33X12).....	21
FIGURE 12: CUMULATIVE OIL PRODUCTION FOR ALL GRID BLOCK CASES (11X11X12 TO 33X33X12) .....	21
FIGURE 13: CUMULATIVE GAS PRODUCTION FOR GRID BLOCK CASES (27X27 - 33X33) .....	22
FIGURE 14: CUMULATIVE OIL PRODUCTION FOR GRID BLOCK CASES (27X27 - 33X33) .....	22
FIGURE 15: PERFORMANCE PLOT THAT SHOWS THE PROGRESS DURING THE ANN TRAINING WITHOUT OVERTRAINING.....	26



FIGURE 16: PERFORMANCE PLOT THAT SHOWS THE PROGRESS DURING THE ANN TRAINING AT WHICH OVERTRAINING OCCURRED .....	27
FIGURE 17: COMPARISON OF DIFFERENT ANN STRUCTURES WITH DIFFERENT NUMBER OF LAYERS AND NEURONS .....	33
FIGURE 18: OBTAINED REGRESSION WITH THE TRAINED ANN WITH 7 HIDDEN LAYERS.....	35
FIGURE 19: ERROR FOR EACH TESTING CASE FOR CUMULATIVE GAS .....	36
FIGURE 20: ERROR FOR EACH TESTING CASE FOR CUMULATIVE OIL .....	36
FIGURE 21: ERROR FOR EACH TESTING CASE FOR CUMULATIVE WATER .....	37
FIGURE 22: ERROR FOR EACH TESTING CASE FOR GAS RATE .....	37
FIGURE 23: ERROR FOR EACH TESTING CASE FOR GAS OIL RATIO (GOR).....	38
FIGURE 24: ERROR FOR EACH TESTING CASE FOR OIL RATE .....	38
FIGURE 25: ERROR FOR EACH TESTING CASE FOR WATER RATE .....	39
FIGURE 26: ERROR FOR EACH TESTING CASE FOR WATER OIL RATIO (WOR).....	39
FIGURE 27: ERROR FOR EACH TESTING CASE FOR WATER CUT (WC) .....	40
FIGURE 29: COMPARISON OF PRODUCTION PROFILES GENERATED BY ANN AND NUMERICAL SIMULATOR (CASE-51) .....	42
FIGURE 30: COMPARISON OF CUMULATIVE PRODUCTION PROFILES GENERATED BY ANN AND NUMERICAL SIMULATOR (CASE-51) .....	43
FIGURE 31: COMPARISON OF GAS OIL RATION, WATER OIL RATIO AND WATER CUT PRODUCTION PROFILES GENERATED BY ANN AND NUMERICAL SIMULATOR (CASE-51).....	44
FIGURE 32: COMPARISON OF PRODUCTION PROFILES GENERATED BY ANN AND NUMERICAL SIMULATOR (CASE-79).....	45

FIGURE 33: COMPARISON OF CUMULATIVE PRODUCTION PROFILES GENERATED BY ANN AND NUMERICAL SIMULATOR (CASE-79) .....	46
FIGURE 34: COMPARISON OF GAS OIL RATION, WATER OIL RATIO AND WATER CUT PRODUCTION PROFILES GENERATED BY ANN AND NUMERICAL SIMULATOR (CASE-79).....	47
FIGURE 35: COMPARISON OF PRODUCTION PROFILES GENERATED BY ANN AND NUMERICAL SIMULATOR (CASE-214) .....	48
FIGURE 36: COMPARISON OF CUMULATIVE PRODUCTION PROFILES GENERATED BY ANN AND NUMERICAL SIMULATOR (CASE-214) .....	49
FIGURE 37: COMPARISON OF GAS OIL RATION, WATER OIL RATIO AND WATER CUT PRODUCTION PROFILES GENERATED BY ANN AND NUMERICAL SIMULATOR (CASE-214).....	50
FIGURE 38: COMPARISON OF PRODUCTION PROFILES GENERATED BY ANN AND NUMERICAL SIMULATOR (CASE-334).....	51
FIGURE 39: COMPARISON OF CUMULATIVE PRODUCTION PROFILES GENERATED BY ANN AND NUMERICAL SIMULATOR (CASE-334) .....	52
FIGURE 40: COMPARISON OF GAS OIL RATION, WATER OIL RATIO AND WATER CUT PRODUCTION PROFILES GENERATED BY ANN AND NUMERICAL SIMULATOR (CASE-334).....	53
FIGURE 41: COMPARISON OF PRODUCTION PROFILES GENERATED BY ANN AND NUMERICAL SIMULATOR (CASE-340) .....	54
FIGURE 42: COMPARISON OF CUMULATIVE PRODUCTION PROFILES GENERATED BY ANN AND NUMERICAL SIMULATOR (CASE-340) .....	55
FIGURE 43: COMPARISON OF GAS OIL RATION, WATER OIL RATIO AND WATER CUT PRODUCTION PROFILES GENERATED BY ANN AND NUMERICAL SIMULATOR (CASE-340).....	56
FIGURE 44: DEVELOPED GRAPHICAL USER INTERFACE (GUI) .....	58

FIGURE 45: COMPARISON OF PRODUCTION PROFILES GENERATED BY ANN AND NUMERICAL SIMULATOR (CASE-6) .....	66
FIGURE 46: COMPARISON OF CUMULATIVE PRODUCTION PROFILES GENERATED BY ANN AND NUMERICAL SIMULATOR (CASE-6) .....	67
FIGURE 47: COMPARISON OF GAS OIL RATION, WATER OIL RATIO AND WATER CUT PRODUCTION PROFILES GENERATED BY ANN AND NUMERICAL SIMULATOR (CASE-6).....	68
FIGURE 48: COMPARISON OF PRODUCTION PROFILES GENERATED BY ANN AND NUMERICAL SIMULATOR (CASE-9).....	69
FIGURE 49: COMPARISON OF CUMULATIVE PRODUCTION PROFILES GENERATED BY ANN AND NUMERICAL SIMULATOR (CASE-9) .....	70
FIGURE 50: COMPARISON OF GAS OIL RATION, WATER OIL RATIO AND WATER CUT PRODUCTION PROFILES GENERATED BY ANN AND NUMERICAL SIMULATOR (CASE-9).....	71
FIGURE 51: COMPARISON OF PRODUCTION PROFILES GENERATED BY ANN AND NUMERICAL SIMULATOR (CASE-11) .....	72
FIGURE 52: COMPARISON OF CUMULATIVE PRODUCTION PROFILES GENERATED BY ANN AND NUMERICAL SIMULATOR (CASE-6) .....	73
FIGURE 53: COMPARISON OF GAS OIL RATION, WATER OIL RATIO AND WATER CUT PRODUCTION PROFILES GENERATED BY ANN AND NUMERICAL SIMULATOR (CASE-11).....	74
FIGURE 54: COMPARISON OF PRODUCTION PROFILES GENERATED BY ANN AND NUMERICAL SIMULATOR (CASE-19).....	75
FIGURE 55: COMPARISON OF CUMULATIVE PRODUCTION PROFILES GENERATED BY ANN AND NUMERICAL SIMULATOR (CASE-19) .....	76

FIGURE 56: COMPARISON OF GAS OIL RATION, WATER OIL RATIO AND WATER CUT PRODUCTION PROFILES GENERATED BY ANN AND NUMERICAL SIMULATOR (CASE-19).....	77
FIGURE 57: COMPARISON OF PRODUCTION PROFILES GENERATED BY ANN AND NUMERICAL SIMULATOR (CASE-72).....	78
FIGURE 58: COMPARISON OF CUMULATIVE PRODUCTION PROFILES GENERATED BY ANN AND NUMERICAL SIMULATOR (CASE-72).....	79
FIGURE 59: COMPARISON OF GAS OIL RATION, WATER OIL RATIO AND WATER CUT PRODUCTION PROFILES GENERATED BY ANN AND NUMERICAL SIMULATOR (CASE-72).....	80
FIGURE 60: COMPARISON OF PRODUCTION PROFILES GENERATED BY ANN AND NUMERICAL SIMULATOR (CASE-89).....	81
FIGURE 61: COMPARISON OF CUMULATIVE PRODUCTION PROFILES GENERATED BY ANN AND NUMERICAL SIMULATOR (CASE-89).....	82
FIGURE 62: COMPARISON OF GAS OIL RATION, WATER OIL RATIO AND WATER CUT PRODUCTION PROFILES GENERATED BY ANN AND NUMERICAL SIMULATOR (CASE-89).....	83
FIGURE 63: COMPARISON OF PRODUCTION PROFILES GENERATED BY ANN AND NUMERICAL SIMULATOR (CASE-94).....	84
FIGURE 64: COMPARISON OF CUMULATIVE PRODUCTION PROFILES GENERATED BY ANN AND NUMERICAL SIMULATOR (CASE-94).....	85
FIGURE 65: COMPARISON OF GAS OIL RATION, WATER OIL RATIO AND WATER CUT PRODUCTION PROFILES GENERATED BY ANN AND NUMERICAL SIMULATOR (CASE-94).....	86
FIGURE 66: COMPARISON OF PRODUCTION PROFILES GENERATED BY ANN AND NUMERICAL SIMULATOR (CASE-125).....	87

FIGURE 67: COMPARISON OF CUMULATIVE PRODUCTION PROFILES GENERATED BY ANN AND NUMERICAL SIMULATOR (CASE-125) .....	88
FIGURE 68: COMPARISON OF GAS OIL RATION, WATER OIL RATIO AND WATER CUT PRODUCTION PROFILES GENERATED BY ANN AND NUMERICAL SIMULATOR (CASE-125).....	89
FIGURE 69: COMPARISON OF PRODUCTION PROFILES GENERATED BY ANN AND NUMERICAL SIMULATOR (CASE-134) .....	90
FIGURE 70: COMPARISON OF CUMULATIVE PRODUCTION PROFILES GENERATED BY ANN AND NUMERICAL SIMULATOR (CASE-134) .....	91
FIGURE 71: COMPARISON OF GAS OIL RATION, WATER OIL RATIO AND WATER CUT PRODUCTION PROFILES GENERATED BY ANN AND NUMERICAL SIMULATOR (CASE134).....	92
FIGURE 72: COMPARISON OF PRODUCTION PROFILES GENERATED BY ANN AND NUMERICAL SIMULATOR (CASE-147) .....	93
FIGURE 73: COMPARISON OF CUMULATIVE PRODUCTION PROFILES GENERATED BY ANN AND NUMERICAL SIMULATOR (CASE-147) .....	94
FIGURE 74: COMPARISON OF GAS OIL RATION, WATER OIL RATIO AND WATER CUT PRODUCTION PROFILES GENERATED BY ANN AND NUMERICAL SIMULATOR (CASE-147).....	95
FIGURE 75: COMPARISON OF PRODUCTION PROFILES GENERATED BY ANN AND NUMERICAL SIMULATOR (CASE-157).....	96
FIGURE 76: COMPARISON OF CUMULATIVE PRODUCTION PROFILES GENERATED BY ANN AND NUMERICAL SIMULATOR (CASE-157) .....	97
FIGURE 77: COMPARISON OF GAS OIL RATION, WATER OIL RATIO AND WATER CUT PRODUCTION PROFILES GENERATED BY ANN AND NUMERICAL SIMULATOR (CASE-157).....	98

FIGURE 78: COMPARISON OF PRODUCTION PROFILES GENERATED BY ANN AND NUMERICAL SIMULATOR (CASE-180) .....	99
FIGURE 79: COMPARISON OF CUMULATIVE PRODUCTION PROFILES GENERATED BY ANN AND NUMERICAL SIMULATOR (CASE-180) .....	100
FIGURE 80: COMPARISON OF GAS OIL RATION, WATER OIL RATIO AND WATER CUT PRODUCTION PROFILES GENERATED BY ANN AND NUMERICAL SIMULATOR (CASE-180).....	101
FIGURE 81: COMPARISON OF PRODUCTION PROFILES GENERATED BY ANN AND NUMERICAL SIMULATOR (CASE-195).....	102
FIGURE 82: COMPARISON OF CUMULATIVE PRODUCTION PROFILES GENERATED BY ANN AND NUMERICAL SIMULATOR (CASE-195) .....	103
FIGURE 83: COMPARISON OF GAS OIL RATION, WATER OIL RATIO AND WATER CUT PRODUCTION PROFILES GENERATED BY ANN AND NUMERICAL SIMULATOR (CASE-195).....	104
FIGURE 84: COMPARISON OF PRODUCTION PROFILES GENERATED BY ANN AND NUMERICAL SIMULATOR (CASE-203) .....	105
FIGURE 85: COMPARISON OF CUMULATIVE PRODUCTION PROFILES GENERATED BY ANN AND NUMERICAL SIMULATOR (CASE-203) .....	106
FIGURE 86: COMPARISON OF GAS OIL RATION, WATER OIL RATIO AND WATER CUT PRODUCTION PROFILES GENERATED BY ANN AND NUMERICAL SIMULATOR (CASE-203).....	107
FIGURE 87: COMPARISON OF PRODUCTION PROFILES GENERATED BY ANN AND NUMERICAL SIMULATOR (CASE-219).....	108
FIGURE 88: COMPARISON OF CUMULATIVE PRODUCTION PROFILES GENERATED BY ANN AND NUMERICAL SIMULATOR (CASE-219) .....	109

FIGURE 89: COMPARISON OF GAS OIL RATION, WATER OIL RATIO AND WATER CUT PRODUCTION PROFILES GENERATED BY ANN AND NUMERICAL SIMULATOR (CASE-219).....	110
FIGURE 90: COMPARISON OF PRODUCTION PROFILES GENERATED BY ANN AND NUMERICAL SIMULATOR (CASE-221).....	111
FIGURE 91: COMPARISON OF CUMULATIVE PRODUCTION PROFILES GENERATED BY ANN AND NUMERICAL SIMULATOR (CASE-221) .....	112
FIGURE 92: COMPARISON OF GAS OIL RATION, WATER OIL RATIO AND WATER CUT PRODUCTION PROFILES GENERATED BY ANN AND NUMERICAL SIMULATOR (CASE-221).....	113
FIGURE 93: COMPARISON OF PRODUCTION PROFILES GENERATED BY ANN AND NUMERICAL SIMULATOR (CASE-275).....	114
FIGURE 94: COMPARISON OF CUMULATIVE PRODUCTION PROFILES GENERATED BY ANN AND NUMERICAL SIMULATOR (CASE-275) .....	115
FIGURE 95: COMPARISON OF GAS OIL RATION, WATER OIL RATIO AND WATER CUT PRODUCTION PROFILES GENERATED BY ANN AND NUMERICAL SIMULATOR (CASE-275).....	116
FIGURE 96: COMPARISON OF PRODUCTION PROFILES GENERATED BY ANN AND NUMERICAL SIMULATOR (CASE-277).....	117
FIGURE 97: COMPARISON OF CUMULATIVE PRODUCTION PROFILES GENERATED BY ANN AND NUMERICAL SIMULATOR (CASE-277) .....	118
FIGURE 98: COMPARISON OF GAS OIL RATION, WATER OIL RATIO AND WATER CUT PRODUCTION PROFILES GENERATED BY ANN AND NUMERICAL SIMULATOR (CASE-277).....	119
FIGURE 99: COMPARISON OF PRODUCTION PROFILES GENERATED BY ANN AND NUMERICAL SIMULATOR (CASE-278) .....	120

FIGURE 100: COMPARISON OF CUMULATIVE PRODUCTION PROFILES GENERATED BY ANN AND NUMERICAL SIMULATOR (CASE-278) .....	121
FIGURE 101: COMPARISON OF GAS OIL RATION, WATER OIL RATIO AND WATER CUT PRODUCTION PROFILES GENERATED BY ANN AND NUMERICAL SIMULATOR (CASE-278).....	122
FIGURE 102: COMPARISON OF PRODUCTION PROFILES GENERATED BY ANN AND NUMERICAL SIMULATOR (CASE-324) .....	123
FIGURE 103: COMPARISON OF CUMULATIVE PRODUCTION PROFILES GENERATED BY ANN AND NUMERICAL SIMULATOR (CASE-324) .....	124
FIGURE 104: COMPARISON OF GAS OIL RATION, WATER OIL RATIO AND WATER CUT PRODUCTION PROFILES GENERATED BY ANN AND NUMERICAL SIMULATOR (CASE-324).....	125
FIGURE 105: COMPARISON OF PRODUCTION PROFILES GENERATED BY ANN AND NUMERICAL SIMULATOR (CASE-328) .....	126
FIGURE 106: COMPARISON OF CUMULATIVE PRODUCTION PROFILES GENERATED BY ANN AND NUMERICAL SIMULATOR (CASE-328) .....	127
FIGURE 107: COMPARISON OF GAS OIL RATION, WATER OIL RATIO AND WATER CUT PRODUCTION PROFILES GENERATED BY ANN AND NUMERICAL SIMULATOR (CASE-328).....	128
FIGURE 108: GAS DENSITY DISTRIBUTION.....	129
FIGURE 109: OIL DENSITY DISTRIBUTION.....	129
FIGURE 110: GRID BLOCK LENGTH IN THE X AND Y DIRECTIONS DISTRIBUTION.....	130
FIGURE 111: RESERVOIR TEMPERATURE DISTRIBUTION .....	130
FIGURE 112: WATER SATURATION DISTRIBUTION.....	131
FIGURE 113: OIL SATURATION DISTRIBUTION.....	131
FIGURE 114: POROSITY DISTRIBUTION .....	132



FIGURE 115: PERMEABILITY IN THE K DIRECTION DISTRIBUTION.....	132
FIGURE 116: PERMEABILITY IN THE I AND J DIRECTIONS DISTRIBUTION.....	133
FIGURE 117: ROCK COMPRESSIBILITY DISTRIBUTION.....	133
FIGURE 118: RESERVOIR THICKNESS DISTRIBUTION .....	134
FIGURE 119: LOCATION OF THE HORIZONTAL WELL IN TERM OF LAYER NUMBER DISTRIBUTION ...	134
FIGURE 120: PERMEABILITY VERSUS POROSITY DISTRIBUTION .....	135
FIGURE 121: HORIZONTAL WELL LOCATION VERSUS PERMEABILITY DISTRIBUTION .....	135
FIGURE 122: POROSITY VERSUS WELL LOCATION DISTRIBUTION.....	136
FIGURE 123: TEMPERATURE VERSUS PRESSURE DISTRIBUTION .....	136

## ACKNOWLEDGMENTS

---

I begin in the name of Allah, The Beneficent, The Merciful. First and for most, I thank God for his continuous blessings throughout my life. I find myself speechless, and nothing can express my feelings toward my parents, my father Mattoq and my mother Madenah. Without their caring, prays, and support I would not make it to this stage in my life.

I would like to express my sincere gratitude and appreciation to Dr. Turgay Ertekin, research advisor. His continuous support and guidance enabled me to successfully complete my master program. I am really honored and proud to be in Dr. Ertekin's research group and grateful to know and work with him as teacher, advisor and friend. Also, I would like to extend my appreciation to Dr. Mort Webster and Dr. Shimin Liu to be in my committee.

My sincere appreciation to my sponsor Ministry of Higher Education represented by Saudi Arabian Cultural Mission (SACM) for sponsoring my education for both Undergraduate and Graduate degrees.

Also, I would like to thank all of my friends and colleagues here at Penn State for helping me and making my six years here a great and rich experience.

Finally, I would like to thank my brother and sisters for their endless support and love.

Mohammed AlQusom  
*University Park, Pennsylvania.*  
*August, 2016*

## Chapter 1: Introduction

---

Maximizing the hydrocarbon recovery has been the main goal for the oil and gas industry in order to meet the continuously increasing world's demand for energy. The development of different drilling and production techniques has helped in making the production and drilling processes more efficient yielding a higher recovery factor of hydrocarbons.

In 1909, Hughes and Sharps patent the first roller-cone drill with two cones made of steel (*SPE, n.d., 2016*). After that, H. John Eastman introduced the controlled directional drilling in 1929, which revalorized the oil industry at that time and increased the hydrocarbon recovery to a great extent. In 1933, Hughes came up with the first tricone roller-cone drill bit. The horizontal drilling technique was first used by Alexander Grigoryan in drilling a well in Azerbaijan in 1941 (*SPE, n.d., 2016*)

Horizontal drilling technique has shown its advantage in recovering more hydrocarbons than the vertical drilling technique due to the large contact area that the horizontal well will have with the reservoir compare to that for the vertical well. Nevertheless, having a large contact area with the reservoir has its disadvantage in controlling the water and gas cresting. This phenomenon, which reduces the hydrocarbons recovery due to other fluids, gas and water, being produced with the oil simultaneously. This phenomenon happens at what is known as the breakthrough time, a time at which water and gas will reach the production casing and will be produced with the oil. However, it is not always the case that horizontal well will recover more hydrocarbons there are cases in which vertical will recover more hydrocarbons.

Despite all these technologies the most important factor in recovering more hydrocarbons is having enough data which will allow petroleum engineers and geologists to mark accurately the

sweet spots they want to target. However, these information can be difficult and expensive to obtain either from lab results/experiments or field measurements. The use of commercial reservoir simulators is crucial in the oil and gas industry and as it unveils various important reservoir behaviors that might give simulation and production engineers a good indication to use specific drilling and production techniques. Nevertheless, the use of these commercial reservoir simulators can be time-consuming especially if there is no enough data available. Artificial Neural Network (ANN) has proven itself in being able to solve complex problems in various fields, i.e. engineering, science and medical fields. The ANN can solve complex problems by using simple mathematical functions and it takes very short time to perform these computations to obtain required results which make it more attractive for the industry.

In this study, artificial neural network is developed to predict the production profiles for a horizontal well that can be placed at different depths between gas cap and bottom water drive. A commercial reservoir simulator, CMG<sup>1</sup>, was used to build a three-phase reservoir and then CMG-CMOST<sup>2</sup> was used to generate and simulate different cases and collect production profile (oil rate, gas rate, water rate, cumulative oil rate, cumulative gas rate, cumulative water rate, gas oil ratio, Water oil Ratio and water cut). After that, the predesigned ANN toolbox in MATLAB<sup>3</sup> is used to perform this study and adjust the structure of the neural network accordingly to reach an error difference between ANN and simulator results of 5-15%.

---

<sup>1</sup>CMG: Computer Modeling Group

<sup>2</sup>CMG-CMOST: Computer Modeling Group Computer Assisted History Matching, Optimization and Uncertainty Assessment Tool

<sup>3</sup>MATLAB: MATrix LABoratory

## Chapter 2: Literature Review

---

One of the first papers that discussed the phenomena of conning and the physics behind it introduced in 1935 and in that paper they have listed a number of factors that affect the water-conning namely; length of perforation interval and production rate. In another paper a study on water-conning effect in a vertical well was conducted to know what parameters affect the water-conning and also in that study a correlation was developed to predict the rate or critical rate, breakthrough time and water cut after water production (*Kui and DesBrisay, 1983*). Furthermore, numerical studies were performed on the water-conning phenomena to better understand the parameters affecting the conning processes (*Byrne and Morsse, 1973, Mungan, 1975, Blades and Stright 1975*). In 1991, after the horizontal well was widely used Yang and Wattenbarger studied the water-conning in both horizontal and vertical wells and came up with a method to calculate the breakthrough time and water cut after water production (*Yang and Wattenburg, 1991*).

### 2.1 Artificial Neural Networks Overview.

#### 2.1.1 Background

The artificial neural networks are mathematical simulators in which it will process information in the same way that a biological neural system works with respect to its complexity and functionality (*Shahab, 2000*). A simple definition of an artificial neural network is delineated input space to an output space (*Priddy et al. 2005*). This definition can be more generalized by comparing the ANN to a biological nervous system in which it will learn from previous experiences. That process will generate a new output after understanding the characteristics of the inputs (*Bailey & Thompson, 1990*). The biological neuron is the fundamental building block of the nerves system

which consists of soma, dendrites and axon. The information in the form of electrical signals are detected by the dendrites, processed by the soma and then passed over to the axon. The same thing is happening in the Artificial neuron networks; the artificial neuron is the basic building block of the artificial neuron network in which information in the form of inputs multiplied by weights along with bias entering the artificial neuron to a summing function and passed over the summation to a transfer function to an output. (Suzuki, 2011). Figure 1 shows both the biological and artificial neuron schematic diagrams.

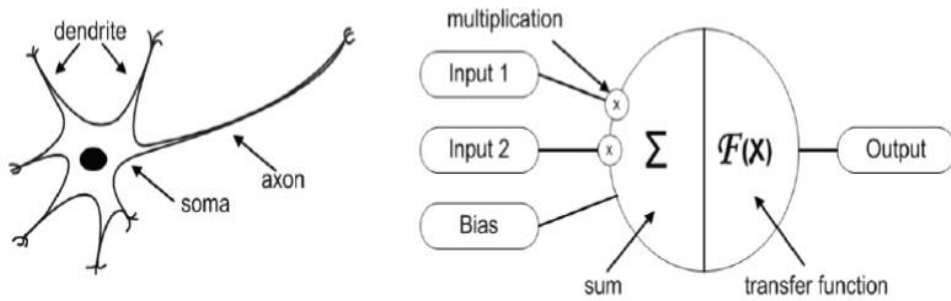


Figure 1: Schematic for both Biological neuron on the left and artificial neuron on the right (Suzuki, 2011)

In a mathematical representation, the sum of the weighted inputs and biased from the net input signal can be represented by the following equation:

$$net_k = \sum_{i=1}^n w_{ki}x_i + b_k$$

Where  $w$  is the weight,  $x$  is the input element,  $b$  is the bias term. The bias acts as a weight except it has a constant value of 1 and it is introduced to shift the activation function to the right or left.

## 2.2 Artificial Neural Network Structure

Depending on how complex the problem you are trying to solve the appropriate structure can be chosen. In general, a single neuron will not be helpful in solving many problems. Often, a number of neurons are arranged in a specific order forming what is called layers of neurons.

Networks are mainly classified into three types: single layer feedforward, multilayers feedforward networks, and recurrent networks.

### 2.2.1 Single Layer Feedforward Network:

The single layer feedforward networks include the input vector, weight matrix, bias vector, summation functions, transfer function, and the output vector. *Figure 2* shows an example of a single layer Architecture. Every single input is being connected to a weight matrix and each neuron has a bias, summation, transfer function, and output. The output vector is being formed by combining the outputs. In some texts, they refer to the processing layer as a hidden layer since it does not interact with the surrounding of the network. The way in which this structure has been developed gave the name of feedforward because each layer is being connected to the next layer respectively starting with the input and ending with outputs as shown in *Figure 2*.

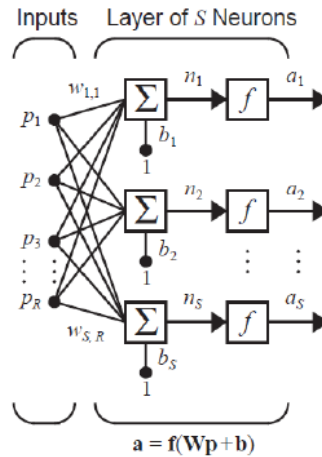


Figure 2: Single Layer Architecture (Hagan et al. , 2002)

### 2.2.2 Multilayer Feedforward Networks:

In a multilayer networks, it is basically a multiple single layer network connected to each other as shown in *Figure 3*. In this structure, each layer has its own weight matrix, bias vector, a net input vector, and an output vector (*Hagan et al. , 2002*). Such structures are used to solve complex non-linear problems that single layer networks cannot solve. In general, the required number of hidden layers and/or neurons depend on the complexity of the problem (*Beale, Hagan, & Demuth, 2014*). Trial and error are the most common technique used in order to approach the optimum number of neurons and layers for the structure (*Beale et al. , 2014; Karsoliya, 2012*). Others gave a specific instruction on how to choose the number of neurons i.e. the number of neurons in the hidden layers should not exceed twice the neurons in the input layer and has to be within 70-90% of both the input and output layers (*kaesoliya 2001*).



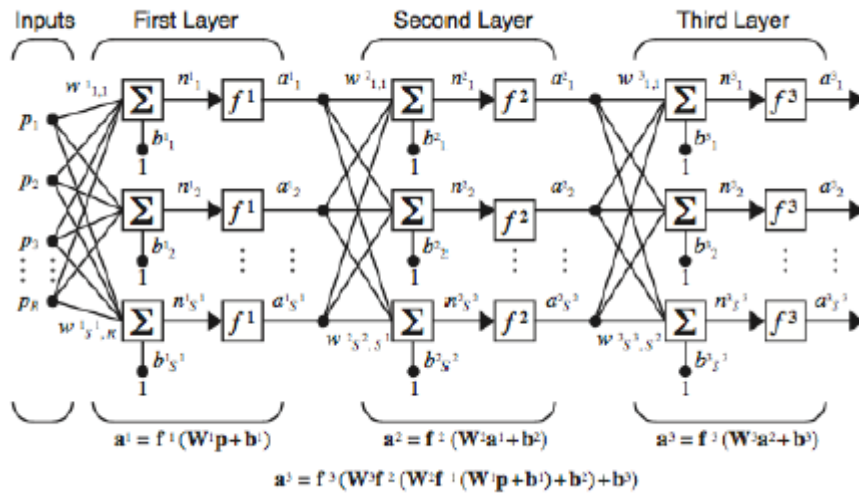


Figure 3: Multilayer Feedforward Network Architecture (*Hagan et al. , 2002*)

### 2.2.3 Recurrent Networks

The recurrent network as it can be seen from *Figure 4* are different because there is a feedback loop that connects the output to the input. The initial conditions are being supplied by the input vector. After that, the subsequent outputs are calculated from the previous outputs which mean that the output is the input but in the previous time step.

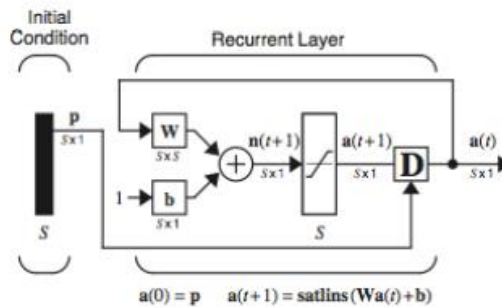


Figure 4: Recurrent Network Structure (*Hagan et al. ,2002*)

## 2.3 Transfer Functions

Transfer functions are used to activate neurons and scale its response to an external stimulus (Maren, Harston, & Pap, 1990). Transfer functions can be either linear or non-linear. The selection between transfer functions depends mainly on how complex the problem is. For example, simple problem could be solved using a single layer with a linear transfer function. On the other side, a more complex problem requires the use of multilayer network with a non-linear transfer function (Hagan et al. ,2002). The commonly used transfer functions in a multilayer network are namely; *logsig* and *purelin* transfer functions. *Logsig*, also known as log-sigmoid, transfer function is a non-linear function, which scales output values to range from 0 to 1. Whereas for the *purelin* transfer function is a linear function and it is commonly being used in the last output layer of a multilayer networks.

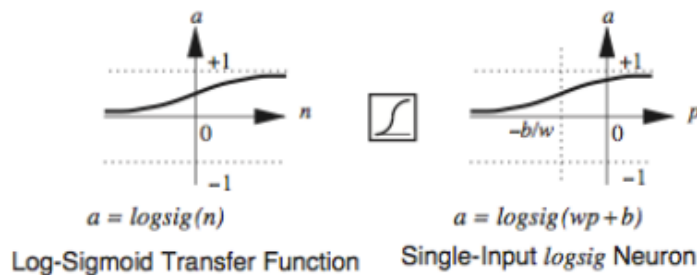


Figure 5: Log-sigmoid transfer function (Hagan et al., 2002)

Table 1: Summary of transfer function ( Hagan et al. ,2002)

Name	Input/Output Relation	Icon	MATLAB Function
Hard Limit	$a = 0 \quad n < 0$ $a = 1 \quad n \geq 0$		hardlim
Symmetrical Hard Limit	$a = -1 \quad n < 0$ $a = +1 \quad n \geq 0$		hardlims
Linear	$a = n$		purelin
Saturating Linear	$a = 0 \quad n < 0$ $a = n \quad 0 \leq n \leq 1$ $a = 1 \quad n > 1$		satlin
Symmetric Saturating Linear	$a = -1 \quad n < -1$ $a = n \quad -1 \leq n \leq 1$ $a = 1 \quad n > 1$		satlins
Log-Sigmoid	$a = \frac{1}{1 + e^{-n}}$		logsig
Hyperbolic Tangent Sigmoid	$a = \frac{e^n - e^{-n}}{e^n + e^{-n}}$		tansig
Positive Linear	$a = 0 \quad n < 0$ $a = n \quad 0 \leq n$		poslin
Competitive	$a = 1 \quad \text{neuron with max } n$ $a = 0 \quad \text{all other neurons}$		compet

## 2.4 Learning Methods

The artificial neural network could be trained using two learning methods: supervised and unsupervised training.

### 2.4.1 Supervised Training Method

Supervised training requires a guidance that tells the network what is the desired response to a given stimulus should be. A simpler example is a student having a teacher who guides the student through what is needed to be learned and how to learn it. Figure 6 shows that the learning system is being exposed to the environment represented by measurement vector which is at the

same time represents as expectancy teacher who knows what is the desired response. Based on that an error signal will be created to adapt the weights of the learning system. Meanwhile, each input feature has it corresponding output vector, which is used to train the artificial neural network (Priddy *et al.* ,2005). In general, supervised training requires both input and the associated output to train the network.

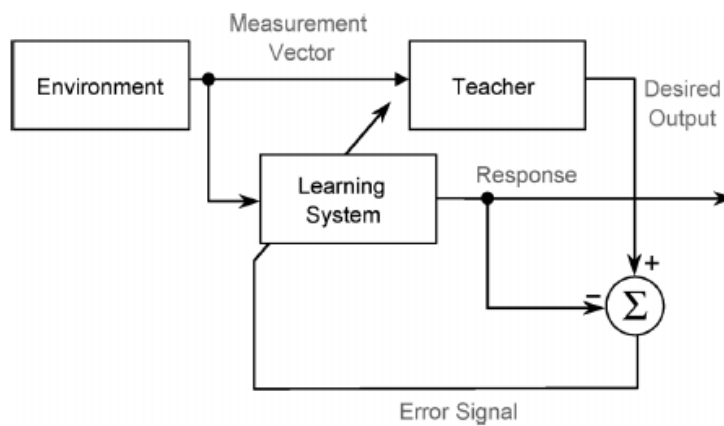


Figure 6: Schematic Diagram that represents supervised learning model (Priddy *et al.* ,2005)

### 2.4.2 Unsupervised Training Method

In the unsupervised training, the training method is the same as the supervised training except that teacher is not there. So, unsupervised training is like a self-study. The student will not have a teacher who knows what should be the response to a given stimulus. Figure 7 shows that the measurement vector is being fed to the learning system and based on the response obtained by the system an adaptation rule is utilized to generate an error signal to adjust the responses of the system to the desired performance. Two of the widely used unsupervised learning techniques are Self-Organized Map (SOM) and the Adaptive Resonance Theory (ART) network. SOM was developed

by Teuvo Kohonen and ART was developed by Stephen Grossberg and Gail Carpenter (*Priddy et al. ,2005*).

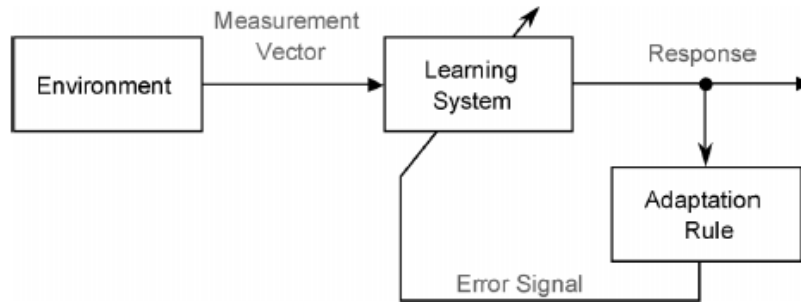


Figure 7: Schematic diagram representing unsupervised training (*Priddy et al. ,2005*)

## 2.5 Applications of Artificial Neural Network in the Petroleum Engineering Field

In the petroleum engineering field, the Artificial neural network had been introduced back in the 1980's when researchers found that it has a huge potential in solving many related problems in the industry in different petroleum engineering segments such as well testing, reservoir characterization, enhanced oil recovery, reservoir stimulation and drilling. In 1994 (*Ali, 1994*) a study was conducted that characterize the ANN applications in the oil and gas industry based on the problem type such as:

- Control Application
- Prediction and correlation
- Optimization
- Pattern or cluster analysis
- Signal or image processing

An unconventional oil reservoir located in West Texas was characterized using Artificial Neural System. The Artificial Expert System that was developed was able to produce a synthetic well log and identifying payzones. Moreover, high and low-resolution logs were predicted using both average and 3D seismic data. These logs then were used to locate and identify payzones ( *Gharehlo, 2012*).

Also, for the same field production maps were generated utilizing the artificial neural system. The main goal of this expert system was to predict the production profiles for cumulative oil and gas quarterly for a total of two years. The produced result when it was compared to the actual field data it shows a close matching between both of them. These results were used then to approximate the placement of new infill drilling with the aid of the surface maps (*Bansal, 2011*)

Another application in developing a neuro-simulation expert system based tool is to predict a wide range of reservoir properties. These properties are porosity, permeability, thickness, relative permeability values and end point saturations. A field data from Perry reservoir located in Brayton fields, west of Corpus Christi, Texas were used in this neuro-simulation tool and the obtained results compared to the production data show a good history matching ( *Childamnaram, 2009*)

A study was conducted utilizing Artificial Neural Network to predict the relative permeability for two-phase, liquid/liquid or liquid/gas. The database for this study was collected from literature to train the network. However, for the testing and validation parts, experimental data were used. A total of five ANNs were developed for the liquid/liquid relative permeability in which different combination of input properties and functional links were used. In conclusion, the most sophisticated ANN in terms of the number of layers, input parameters, and functional

links produced the best results compared to the actual experimental results. On the other hand, the ANN for the liquid/gas relative permeability was developed and its results were compared with the prediction produced from Corry's and Honarpour's correlations and they had a good matching ( *Silpangarmlers, et al., 2002*)

## Chapter 3: Problem Statement

---

With all the challenges that are going on in the oil and gas industry, optimizing the overall process which allows more hydrocarbons recovery is being the main goal. Optimizing the process not only allows companies to recover more of hydrocarbon it pushes them to be more efficient which then will be reflected on the time, money and manpower required to complete the task successfully.

Drilling a horizontal well and place it at different depth will have a different impact on the reservoir's life. On one side, it will result in producing different production profiles and on the other side, it will affect the natural driving forces that act as primary production mechanism for the well. The process of selecting the depth which will yield high oil production while maintaining the natural driving force for that reservoir represented by the gas cap and water drive is the ultimate goal for any drilling design in this case. Water and gas cresting towards a horizontal well, either simultaneous or not, will significantly affect the productivity of the well. Delaying the breakthrough time for water and gas is the main goal and this could be achieved by understanding fluids characteristics in that reservoir and how these fluids will flow in the porous media and effect each other. Figure 8 is a schematic representation of the water and gas cresting around a horizontal well.



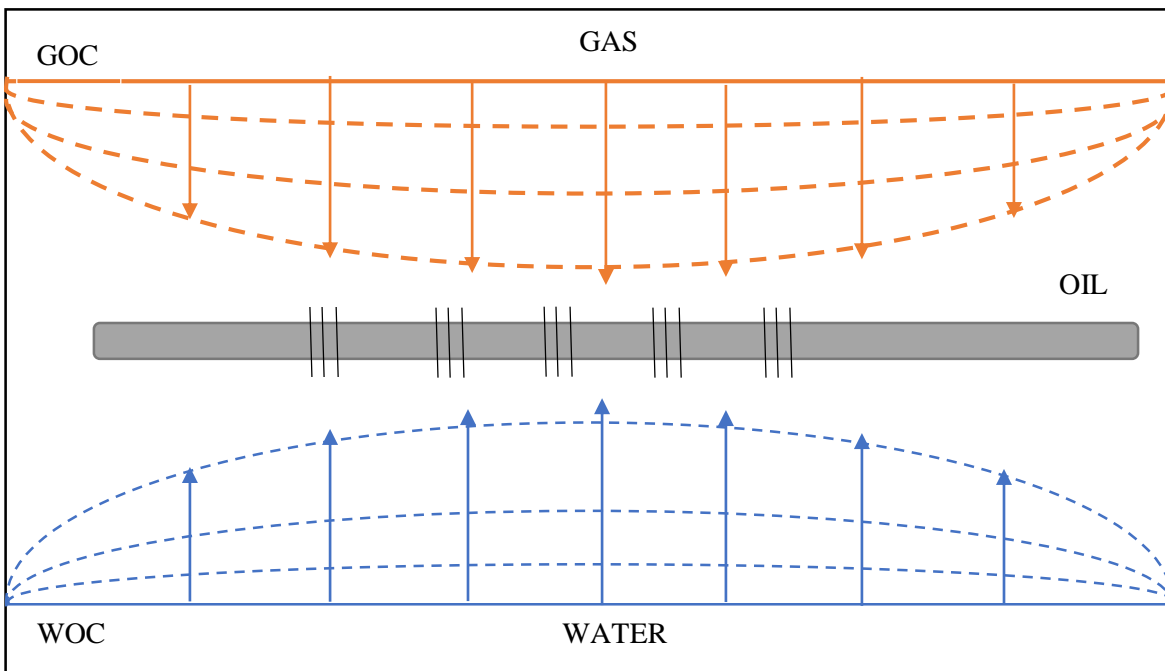


Figure 8: Schematic diagram representing the water and gas cresting for a horizontal well

The process of constructing reservoir model using a commercial simulator to simulate and study various production scenarios for the effect of gas and water cresting can be time-consuming. However, this could be overcome by utilizing the artificial neural network, which has the capability of predicting production profiles for different scenarios in seconds only. Having all the scenarios will allow the drilling engineer to select the best depth to place the horizontal well at; avoiding early breakthrough and consequently increasing the lifetime of the reservoir and the recovery factor. This process of eliminating number of scenarios will allow drilling or reservoir engineer to focus on very few cases rather than all scenarios and study them intensively.

The main objective of this study is to construct a reliable Artificial Neural Network model that predicts the production profiles: oil-rate, gas-rate, water-rate, cumulative oil, cumulative gas, cumulative water, gas oil ratio, water oil ratio and water cut within an error of 5-10% for different

synthetic scenarios between the simulator results and ANN predictions. Figure 9 shows the steps that this study will go through to achieve the goal described here.

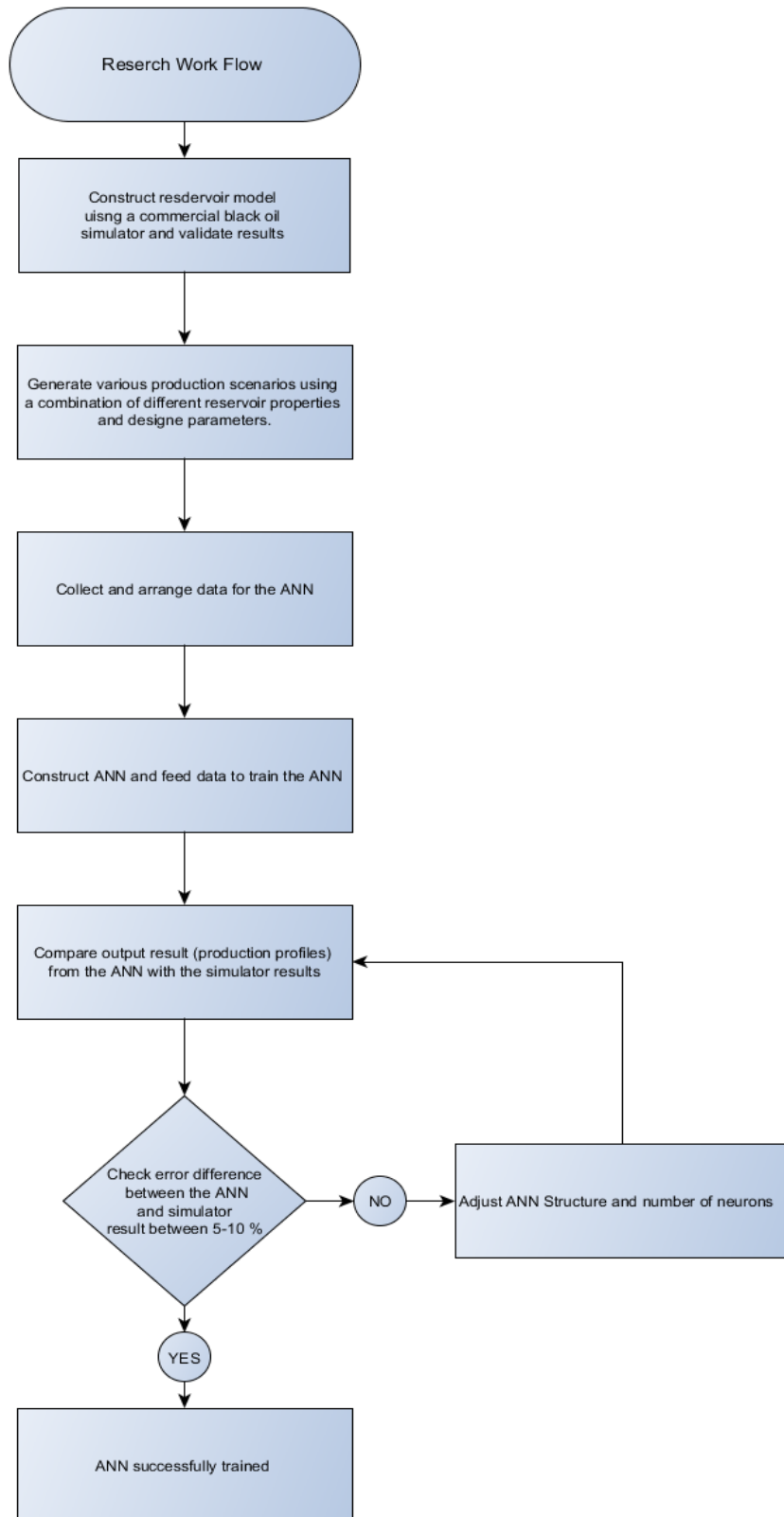


Figure 9: Flow chart summarizing research steps

## Chapter 4: Reservoir Modeling

---

CMG-IMEX Black Oil Simulator, version 2012.20, was used in this study to build the reservoir model and generate simulation results. Further details for the steps and methodology in constructing the reservoir models are discussed in the following sections.

### 4.1 Reservoir Description

This reservoir is a three-dimensional Cartesian reservoir. The reservoir is divided into three main layers; gas, oil and water aquifer. With the oil layer being divided into ten equal layers. Figure 10 shows a three-dimensional cross-sectional area of the reservoir model. The reservoir is constructed as a 29x29x12 grid-block model. The reservoir has one horizontal well placed initially at layer 7.

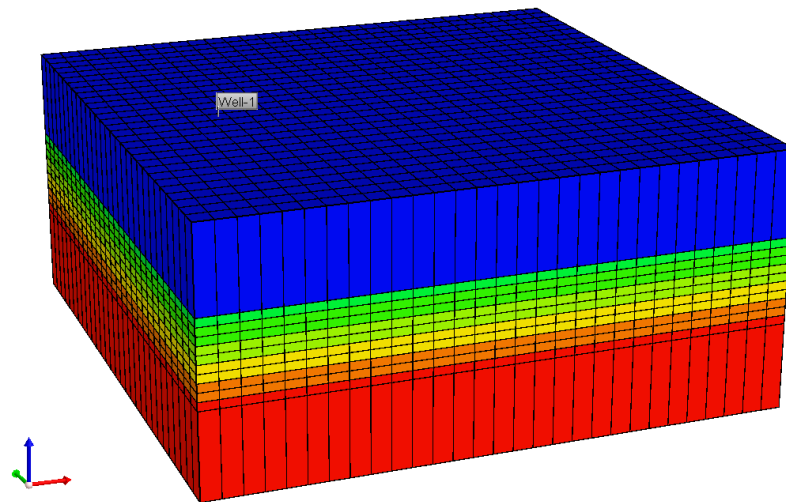


Figure 10: Three-dimensional cross-sectional area of the reservoir model

Table 2: Range of reservoir properties used in the model

<b>Reservoir Property</b>	<b>Unit</b>	<b>Min</b>	<b>Max</b>
Reservoir Thickness (h)	ft	30	150
Porosity ( $\phi$ )	Fraction	0.1	0.3
Permeability ( $k_i$ & $K_j$ )	md	5	250
Permeability ( $k_k$ )	md	10	150
Reservoir Pressure (P)	psi	3000	8000
Rock Compressibility (R_Comp)	1/psi	1.00E-07	1.00E-06
Water Saturation ( $S_w$ )	%	3	7
Oil Saturation ( $S_o$ )	%	2	5
Reservoir Temperature (T)	°F	150	250
Horizontal well Location (L)	Layer	3	10
Drainage Area (A)	Acers	494.25	950.67
Gas Density ( $\rho_g$ )	lb/ft <sup>3</sup>	0.04	0.08
	air Density=1	0.6	1.04
Oil Density	API	20	40

## 4.2 Grid Block Sensitivity Analysis

It is very important to perform grid sensitivity analysis to find the optimum number of grid blocks that should be used in constructing the reservoir model. In general, the higher the number of grid blocks the more accurate or, the higher the resolution is for the model. However, there is a point at which the accuracy or the resolution of the model will not change which then will not affect results obtained. However, it will require more time for the simulator to finish the simulation due to the high number of grid blocks and this what is needed to be avoided.

Cumulative production of gas and oil were collected for a various number of grid blocks ranging from 11x11x12 to 33x33x12. The cumulative production was found to be the same for grid block 27x27x12 to 33x33x12 and based on that grid block 29x29x12 was selected. Figure 11, and 12 show cumulative gas and oil production respectfully. Figure 13 and 14 shows cumulative oil and gas production for grid blocks 27x27x12 – 33x33x12. From these figures, especially figures 13 and 14, it is clear that both cumulative oil and cumulative gas production profiles started to be the same from grid-block size 27x27x12 and afterwards. For this reason, grid-block size 29x29x12 was selected to be the optimum grid-block size for this study.

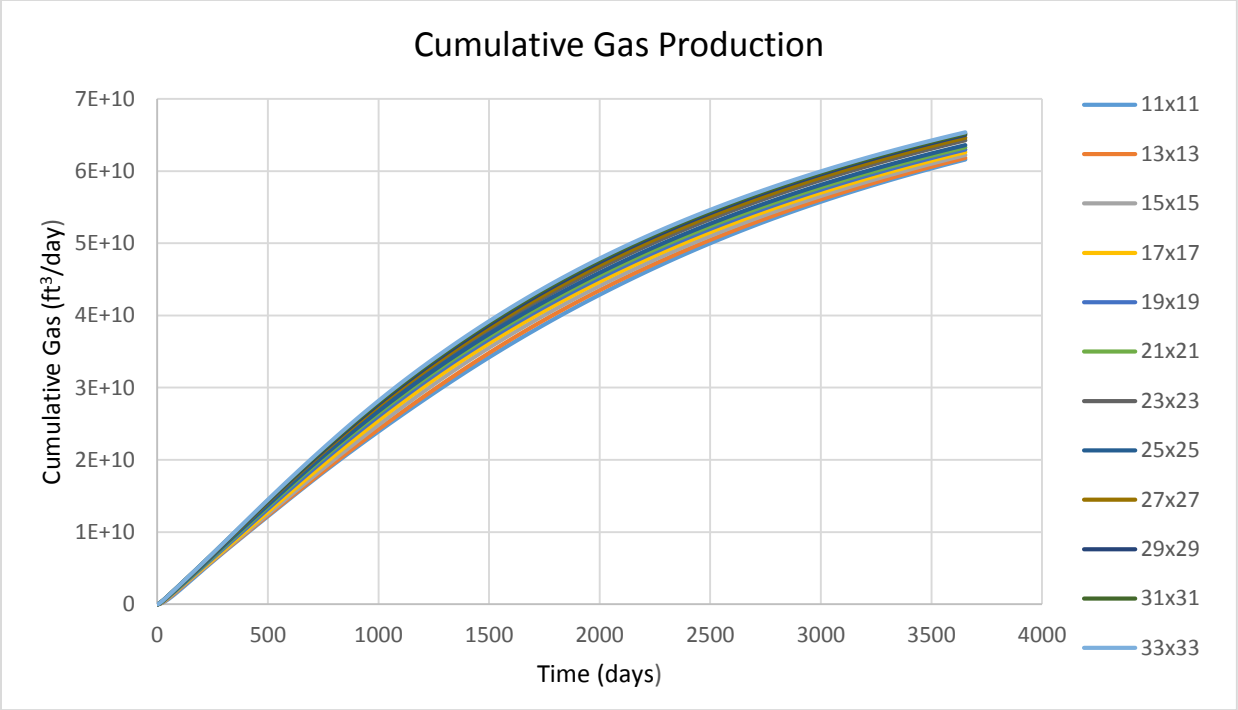


Figure 11: Cumulative Gas Production for all Grid Block cases (11x11x12 to 33x33x12)

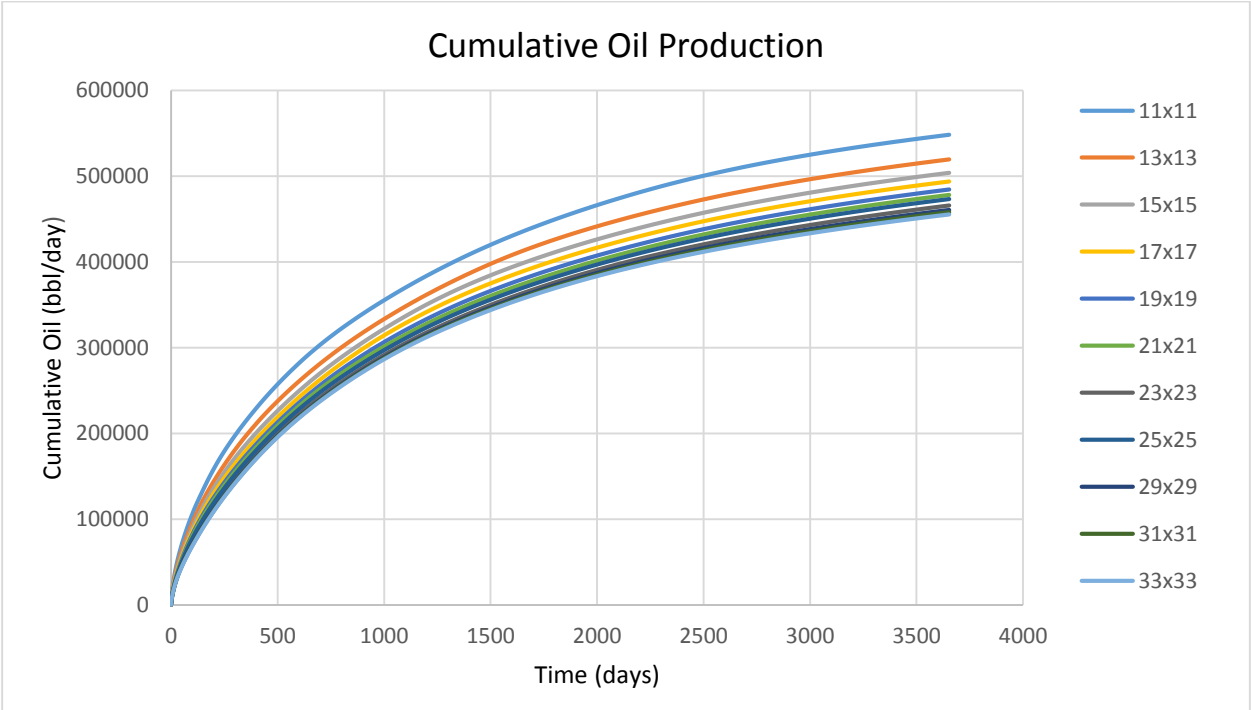


Figure 12: Cumulative Oil Production for all Grid Block cases (11x11x12 to 33x33x12)

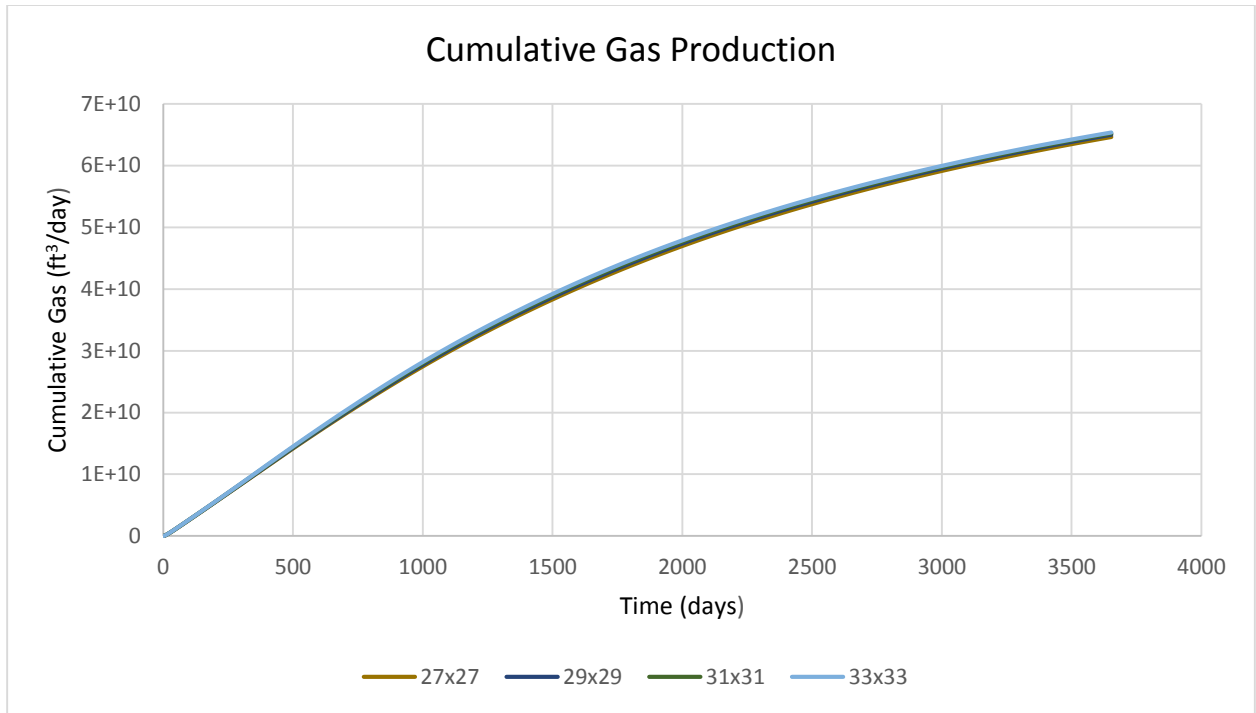


Figure 13: Cumulative Gas Production for Grid Block Cases (27x27x12 - 33x33x12)

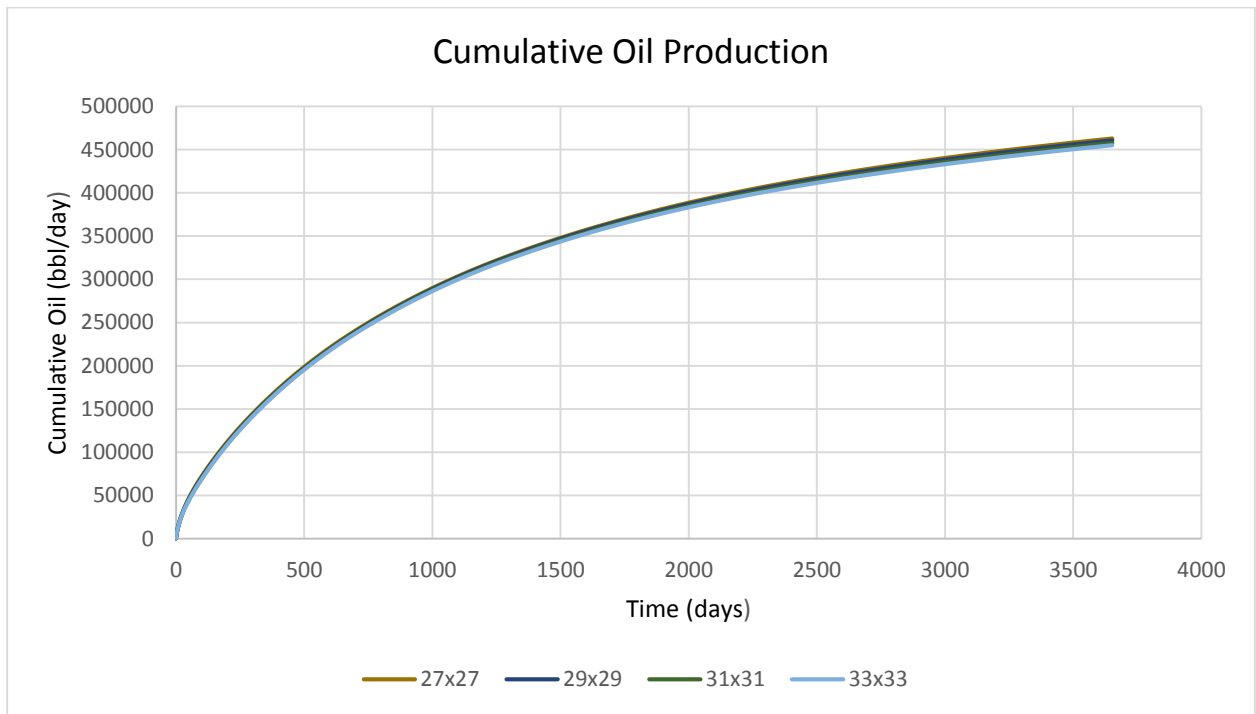


Figure 14: Cumulative Oil Production for Grid Block Cases (27x27x12 - 33x33x12)



### 4.3 Data Generation and Compilation of Results

After validating the initial model presented in the previous section. CMG-CMOST was used to generate different cases using the range of reservoir and design properties shown in table 2 section 4.1. However, supplying the ANN with the optimum number of training data is essential here since providing relatively large range of dataset could lead to what is called an ANN memorization or over-fitting problem and this is a problem that needs to be avoided in order to build a reliable ANN expert system which can predict production profiles not memorize. Initially, 1250 different seniors were generated to be used as training sets. Using these 1250 different seniors it was observed that the ANN failed to capture and predict production profiles. The intensive number of dataset fed to the ANN led to an early memorization. This was an indication to reduce the number of datasets from 1250 to a lower number. After several trials, the number of training cases were reduced to almost half of the initial number we have started with ending up with 600 cases. The generated 600 different scenarios were sent to the CMG-IMEX black oil simulator to simulate and collect production profiles for oil rate, gas rate, water rate, cumulative oil, cumulative gas, cumulative water, gas oil ratio and water oil ratio. All results were collected monthly for the first four years just to make sure that the ANN will have enough data at the beginning of each production period since the production behavior will change rapidly at early production time and then will relatively stabilize. Afterward, the production data will be collected quarterly, each three months, for the remaining of the six years.

## Chapter 5: Artificial Neural Network Development

---

This chapter will discuss the process of developing the structure of the artificial neural network used in this study to predict the production profiles along with the gas oil ratio and the water oil ratio.

### 5.1 Artificial Neural Network Structure

In the process of developing the Artificial Neural Network model, trial and error process was the main technique used to initial build and adjust the structure of the ANN along with the number of neurons. The desired or the optimum structure is being selected based on the error percentage between the ANN and the simulator results. An error margin of 10% or lower is desired in such case and based on the obtained result from both the blind test cases and the training cases the structure of the ANN was adjusted accordingly.

### 5.2 Artificial Neural Network Training

#### 5.2.1 Number of Dataset

A total number of 600 different scenarios were used with their production profiles to train the ANN. The data were randomly divided, using *dividerand* function in MATLAB, as follow: 90% for training, 5% for validation, and 5% for testing. The random division of the data has the advantage of covering a wide range of input properties without repeating. Moreover, the validation and the testing were monitored as shown in figure 15 to ensure that the ANN will not be over-trained or memorized. Overtraining occurs when the validation and/or the testing line deviate away from the training line as shown in figure 16. Besides monitoring the validation and testing

performance plot as shown in figure 15, the error difference between the ANN and simulator results were compared for both the training and testing cases to be close to the targeted error of 5-15% and the ANN structure was adjusted consequently to reduce the error to the desired target.

The error, however, was calculated by comparing the results of the simulator and those predicted by the ANN. The absolute difference was calculated using the following equation:

$$Error \% = \left| \frac{Result_{simulator} - Result_{ANN}}{Result_{simulator}} \right| \times 100$$

For the blind testing mean error average calculation, the following formula was used to calculate the average error for each case.

$$Average Error \% = \frac{\sum_{i=1}^N \left| \frac{Result_{simulator} - Result_{ANN}}{Result_{simulator}} \right| \times 100}{N}$$

Where N represents the time-frequency each test case has been collected. As mentioned in chapter 4 section 4.3 a total number of time frequency of collecting data for this study is 99.

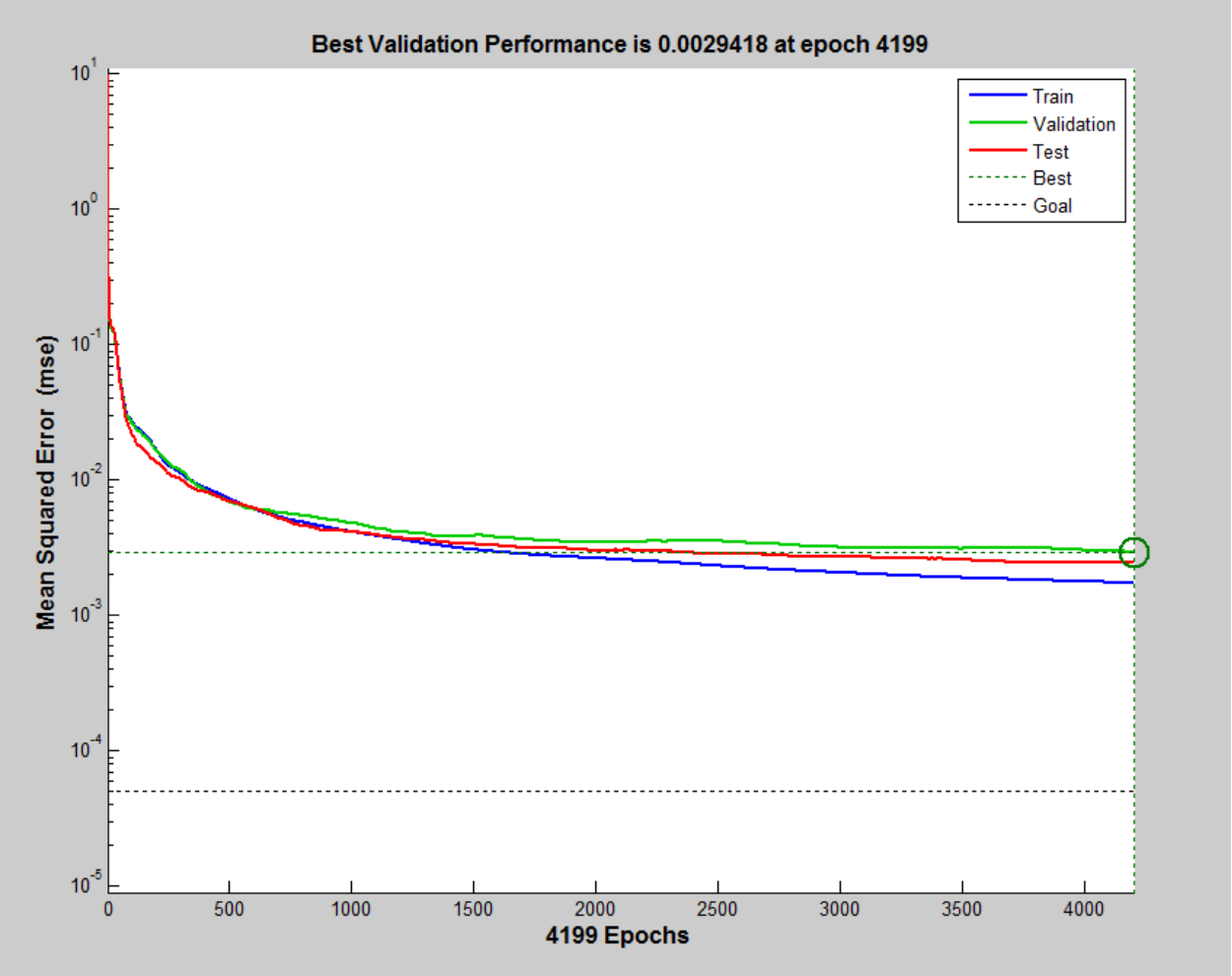


Figure 15: Performance plot that shows the progress during the ANN training without overtraining

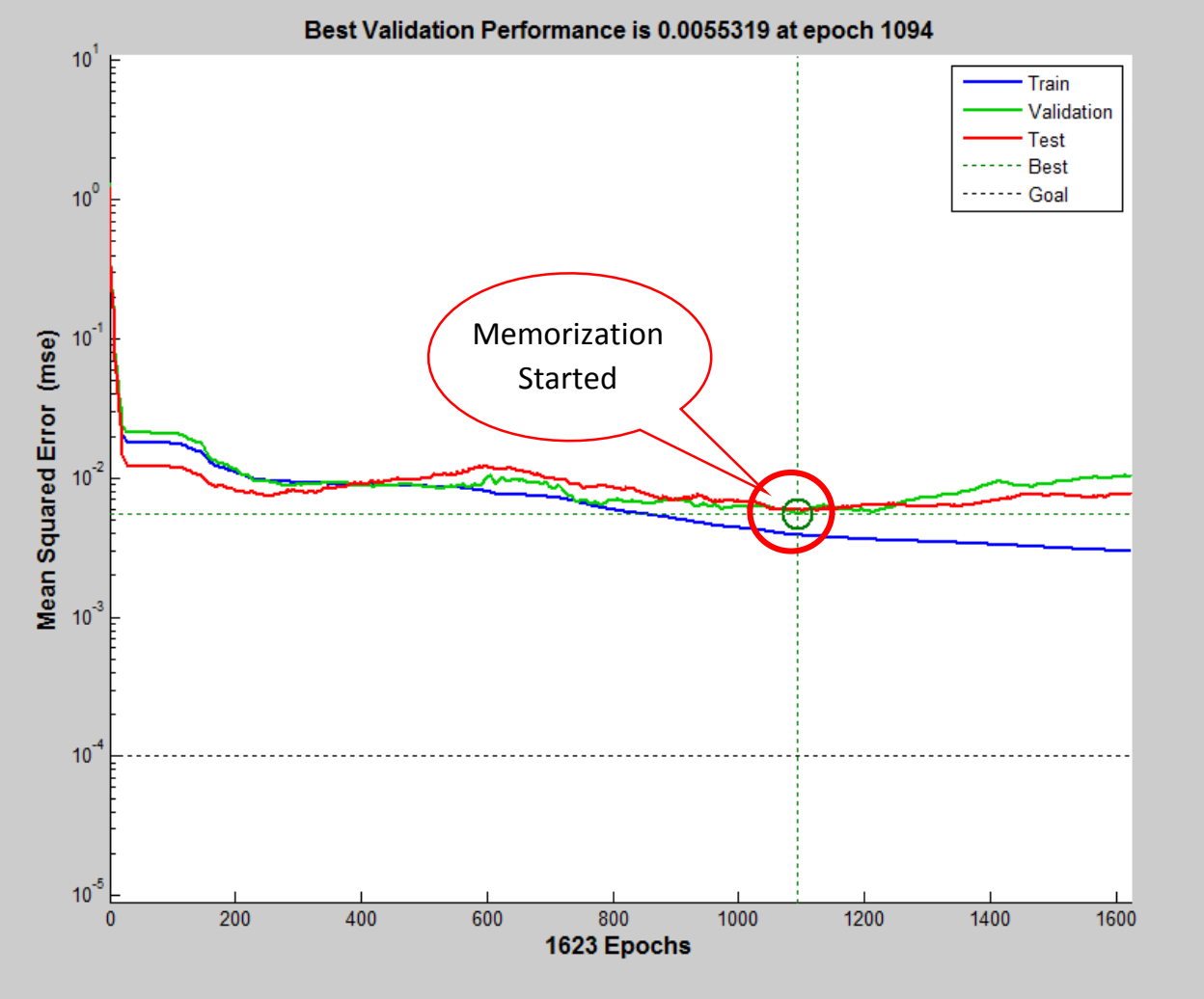


Figure 16: Performance plot that shows the progress during the ANN training at which overtraining occurred

### 5.2.2 Training Algorithm and Transfer Function

For the training algorithms, two of the commonly used training algorithms were tested, scaled conjugate gradient training algorithm (*trainscg*) and resilient backpropagation training algorithm (*trainrp*), however, *trainscg* produced the least mean error for the production profiles compared to other training algorithms available in the MATLAB's tool box. Moreover, for the transfer-function log-sigmoid (*logsig*) transfer function was used and found to perform better than other transfer links. In addition, the performance of the network was controlled using the mean sum of squares of the network error with regularization performance function (*msereg*) and gradient descent with momentum weight and bias (*learnngdm*) was used as learning algorithm.

### 5.2.3 ANN Structure (Layers and Neurons)

Initially, a network with an input layer that has 13 neurons, and output layer that has 49 neurons with a single hidden layer was setup. To determine the number of neurons along with the number of hidden layers required a loop adding 2 neurons each time until it reaches 100 neurons for the first hidden layer. For each structure, the trained and the experimental data were compared to compare the error using equations 1 and 2. If the first layer didn't produce low average error, another layer is added, and the same loop will run and compare the trained result. Going through this process the final ANN structure that produces the least mean error for all the production profiles is summarized in table 3. The data set was trained using scaled conjugate gradient training function (*trainscg*) and a transfer function (*logsig*). Other training and transfer functions were used, and the results were not comparable with the results produced by the training function (*trainscg*) and transfer link (*logsig*).

Table 3: ANN Structure with number of neurons for each layer

<b>Layer</b>	<b>Number of Neurons</b>
Input ( Reservoir + Design)	13
Input (Functional Links)	13
Hidden Layer 1	19
Hidden Layer 2	19
Hidden Layer 3	33
Hidden Layer 4	39
Hidden Layer 5	42
Hidden Layer 6	43
Hidden Layer 7	49
Output (production Profiles)	320

Table 4: Input, functional links and output components for the developed model

<b>Input</b>	Reservoir Properties	Reservoir Thickness Porosity Permeability in the $\hat{i}$ & $\hat{j}$ direction Permeability $\hat{k}$ direction Reservoir Pressure Rock Compressibility Water Saturation Oil Saturation reservoir temperature Drainage area Oil Density (API) Gas Density
	Design Parameters	Horizontal well Location
	Functional Links	Permeability $\hat{i}$ / Permeability $\hat{k}$ Permeability $\hat{j}$ / Permeability $\hat{k}$ Permeability $\hat{i}$ + Permeability $\hat{k}$ /10 Water Saturation / Oil saturation Oil Saturation + Water Saturation Rock Compressibility x Pressure x 1000 Reservoir Thickness x Drainage area (Oil Density) <sup>0.5</sup> (Water Saturation) <sup>0.75</sup> (Oil Saturation) <sup>0.75</sup> (Permeability $\hat{i}, \hat{j}$ ) <sup>0.25</sup> (Permeability $\hat{k}$ ) <sup>0.25</sup> 1/(Drainage Area x Reservoir Thickness)
<b>Output</b>	Oil Rate Gas Rate Water Rate Cumulative Oil Cumulative Gas Cumulative Water Gas Oil Ratio Water oil Ratio Water Cut	Data Collection frequency 99



### 5.3 Result and Error Analysis

Through this problem, the main target is to be able to regenerate or predict the production profiles generated originally from commercial simulator but this time using the ANN. The mean average error target is to be set around 5-10%. Throughout the obtained result: oil rate, gas rate, water rate, cumulative oil, cumulative gas, cumulative water, gas oil ratio, water oil ratio and water cut, water rate and cumulative water are the two most difficult profiles to predict accurately due to the fact that the range of data for these two profiles ranges widely, since we have an infinitely large aquifer connected to the bottom of the reservoir. This made the ANN construction somehow challenging and time-consuming. Starting with one hidden layer and 13 neurons in the input layer and 49 neurons in the output layer without the use of any functional links, the produced results were not nearly close to where they should be. A continuous adjustment of the ANN's structure in terms of the hidden layers and number of neurons for each hidden layer added the reproduced result started to be more representative. However, at the early times of production, first 2-4 years, the behavior of the production profiles were changing extensively in a way that was difficult for the ANN to capture that trend with the given data points. Increasing the frequency at which data were collected for the production profiles for the first four years to be collected monthly instead of quarterly. After the fourth year, data were collected each quarter. At this point, the produced result still did not fall within the mean error target set early. The introduction of functional links for both input and output did change the produced result significantly. As it is shown in table 4, a list of the functional links that have been used. In addition, a comparison between different ANN structures was conducted to show the improvements in each production profiles needed to be predicted. Figure 17 summarizes the findings and it is clear that the ANN with 7 hidden layers produced the most accurate with the least mean error average for the overall training and consequently for the testing cases. It is worth

mentioning that during the training and comparison between different ANN structures, fixed number of training, validating and testing data sets were used instead of making the neural network select random cases for the sake of comparison. It allows to compare each testing case against the other from different ANN structures and compare the improvement not only the mean average error because the mean average error might not be that accurate if we want to make sure that the ANN is indeed capturing the trend of the production profiles. Tables 5, 6 and 7 show a detailed comparison between different ANN structures with the corresponding error percentage for each production profile. There are some production profiles that have low mean error percentage for hidden layers 3, 4, 5 and 7 but overall ANN with 7 hidden layers produced the lowest mean error percentage for all the production profiles as it is shown in figure 17. In addition to that, figure 15 and figure 18 show the training performance for this ANN tool. Cross-checking all three figures 15, 17 and 18 give us a clear indication that the ANN has received appropriate training and has not memorized.

Comparing the testing cases for the result generated by the ANN against the results generated by the simulator for each production profiles are presented in figures 19-27. From these figures we can see the following observations:

- For the cumulative gas and gas rate profiles, 75% of the testing cases have an error of 10% or less compared to the results from the simulator.
- For the cumulative oil profiles, 70% of the testing cases have an error of 10% or less compared to the simulator's results.
- For the cumulative water profiles, 60% of the testing cases have an error of 10% or less compared to the results from the simulator.
- For the oil rate profiles, 65% of the testing cases have an error of 10% or less compared to the results from the simulator.

- For the water rate profiles, 40% of the testing cases have an error of 10% or less compared to the simulator's results.
- For the water oil ratio and gas oil ratio profiles, 80% of the testing cases have an error of 10% or less compared to the simulator's results.
- For the water cut profiles, 65% of the testing cases have an error of 10% or less compared to the simulator's results.

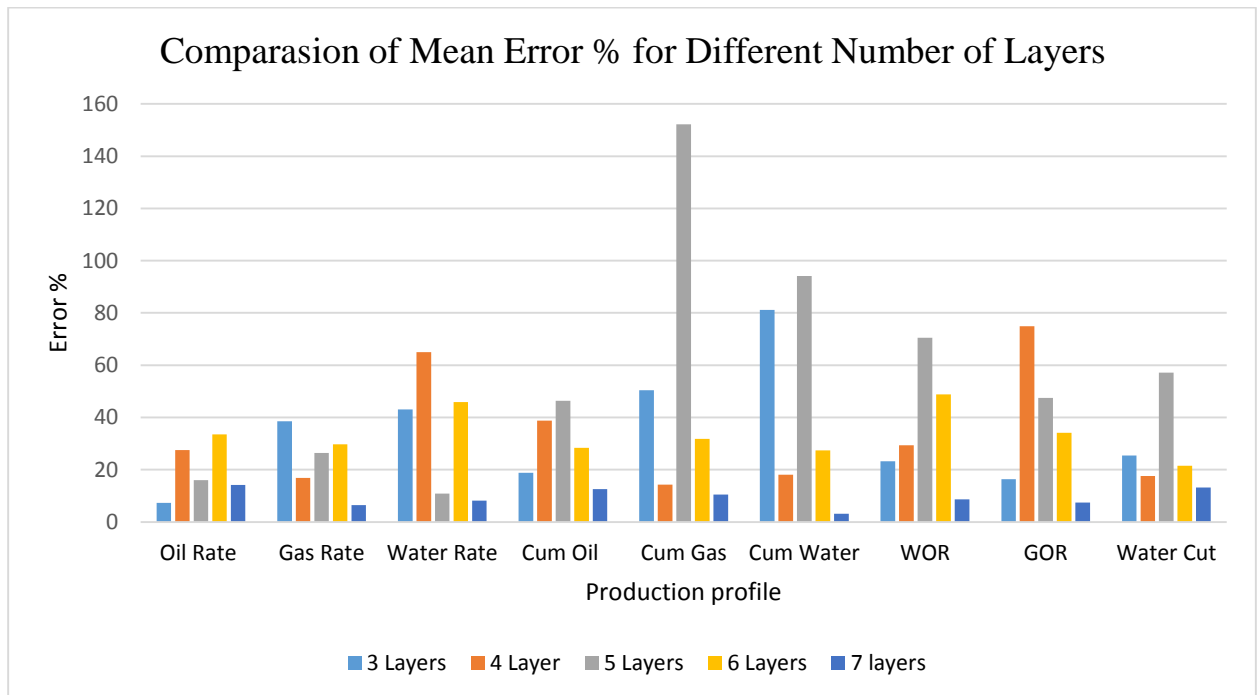


Figure 17: Comparison of Different ANN structures with different number of layers and neurons

Table 5: Mean Error Comparison for oil, gas and water rate for different ANN structures with different number of layers and neurons

Number of Hidden Layers	Number of neurons	Mean Error		
		Oil Rate	Gas Rate	Water Rate
3	13, 15,19	7.340%	38.510%	43.010%
4	13,33,35,45	27.530%	16.870%	64.950%
5	13,13,35,52,51	15.940%	26.410%	10.840%
6	13,33,33,45,52,51	33.510%	29.740%	45.840%
7	13,19,33,39,42,43,49	14.210%	6.450%	8.130%

Table 6: Mean Error Comparison for Cumulative oil, gas and water for different ANN structures with different number of layers and neurons

Number of Hidden Layers	Number of neurons	Mean Error		
		Cum Oil	Cum Gas	Cum Water
3	13, 15,19	18.840%	50.460%	81.140%
4	13,33,35,45	38.730%	14.300%	18.110%
5	13,13,35,52,51	46.340%	152.140%	94.160%
6	13,33,33,45,52,51	28.420%	31.850%	27.350%
7	13,19,33,39,42,43,49	12.570%	10.530%	3.140%

Table 7: Mean Error Comparison for WOR, GOR and water cut for different ANN structures with different number of layers and neurons

Number of Hidden Layers	Number of neurons	Mean Error		
		WOR	GOR	Water Cut
3	13, 15,19	23.240%	16.420%	25.480%
4	13,33,35,45	29.330%	74.960%	17.590%
5	13,13,35,52,51	70.460%	47.520%	57.180%
6	13,33,33,45,52,51	48.770%	34.100%	21.460%
7	13,19,33,39,42,43,49	8.640%	7.450%	13.210%

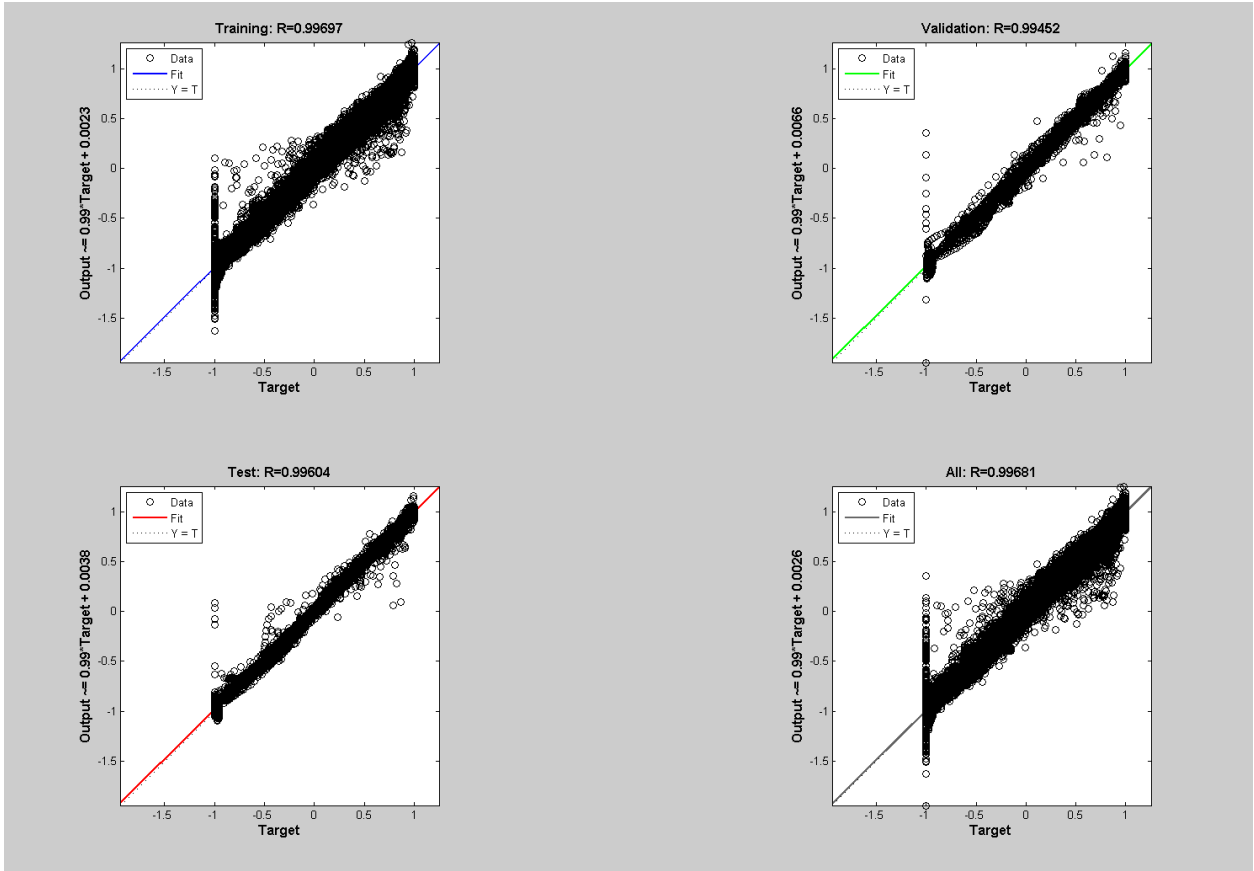


Figure 18: Obtained regression with the trained ANN with 7 hidden Layers

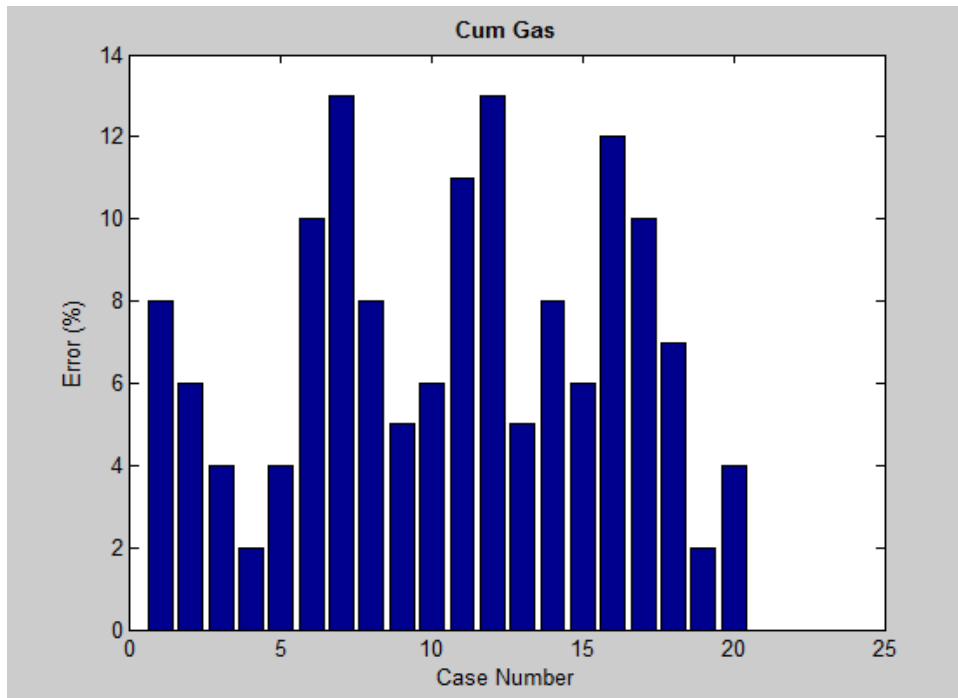


Figure 19: Error for each testing case for cumulative gas

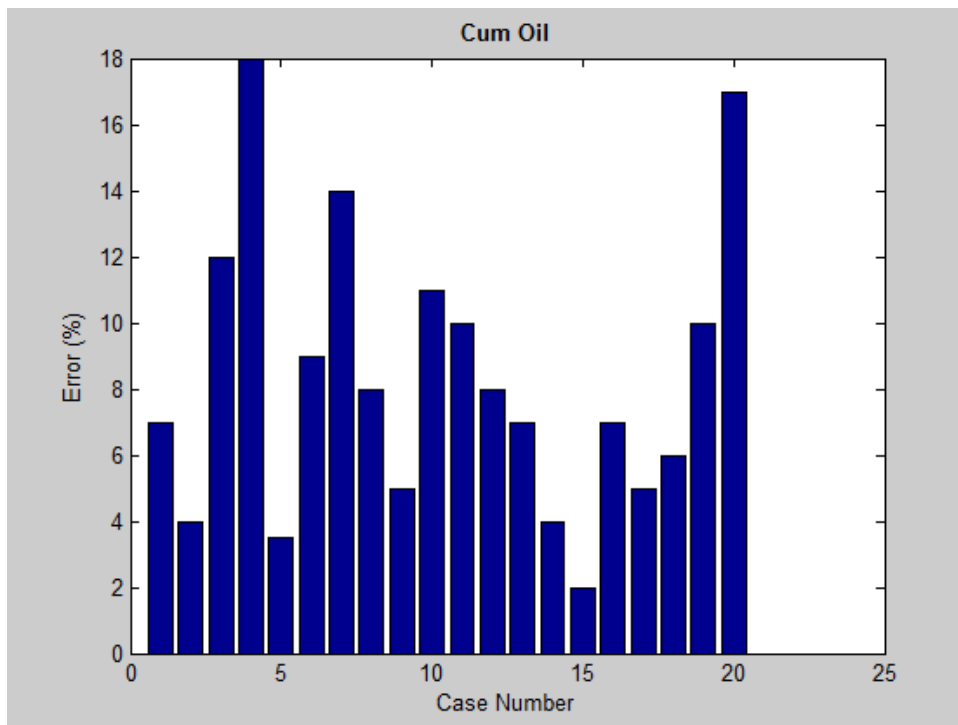


Figure 20: Error for each testing case for cumulative oil

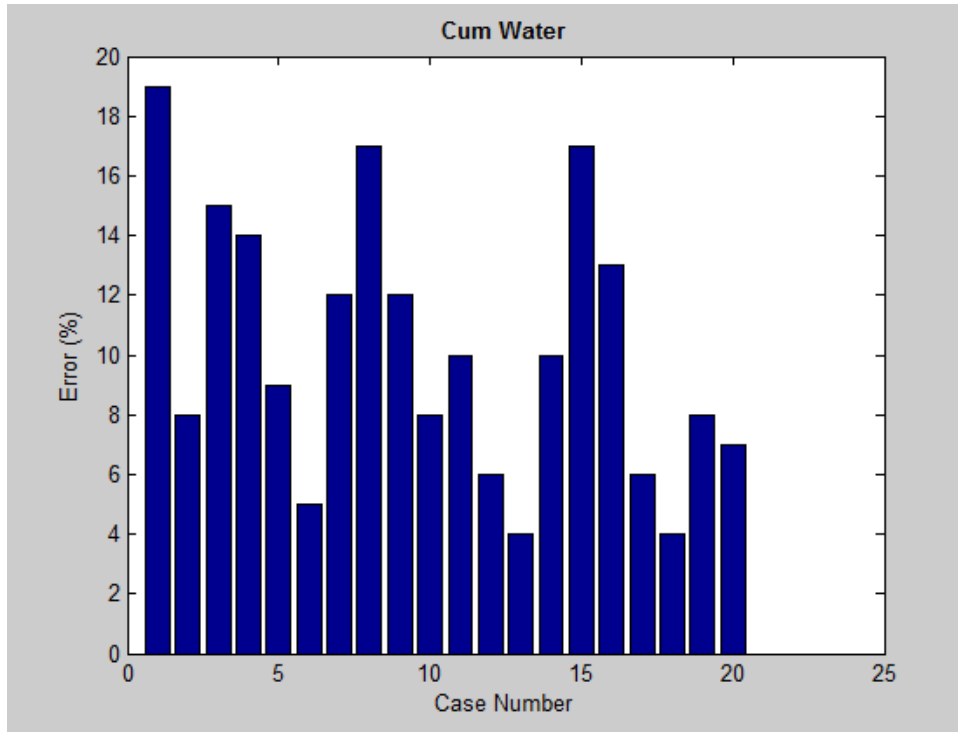


Figure 21: Error for each testing case for cumulative water

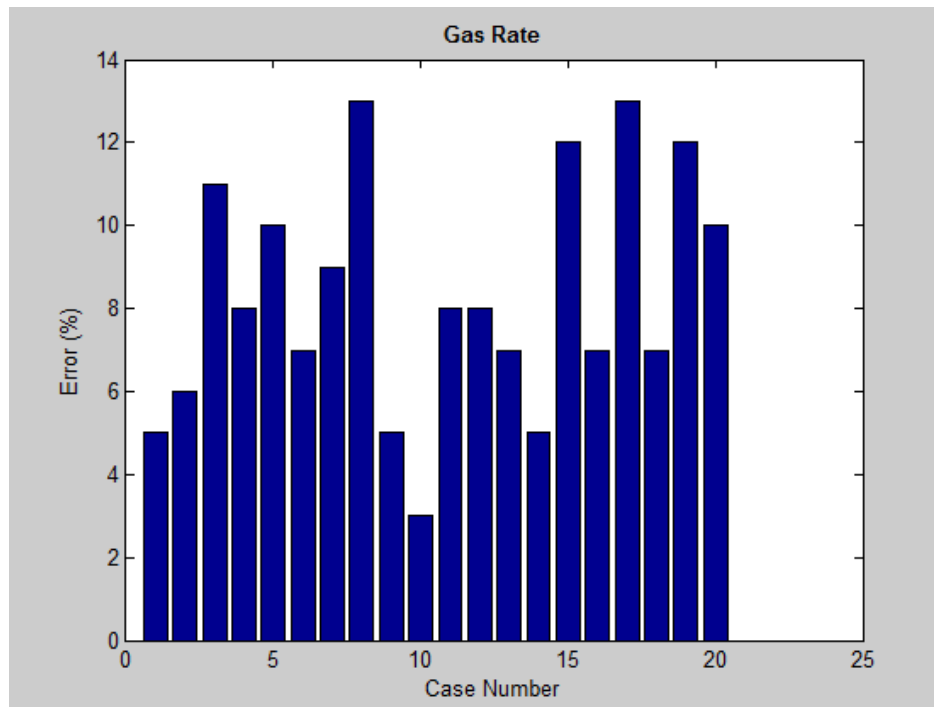


Figure 22: Error for each testing case for gas rate

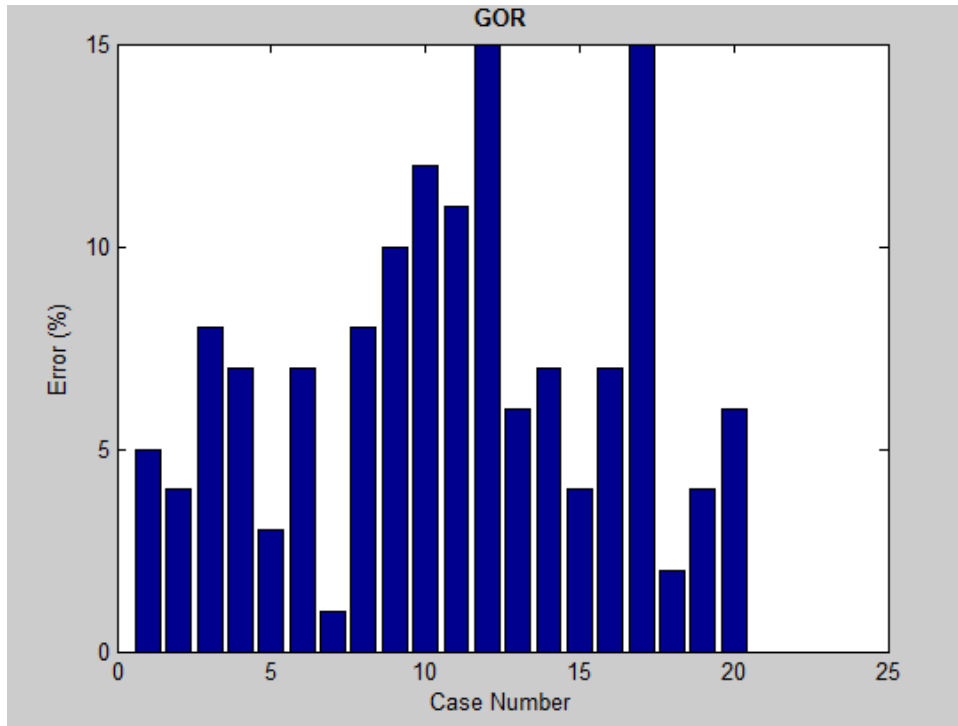


Figure 23: Error for each testing case for Gas Oil Ratio (GOR)

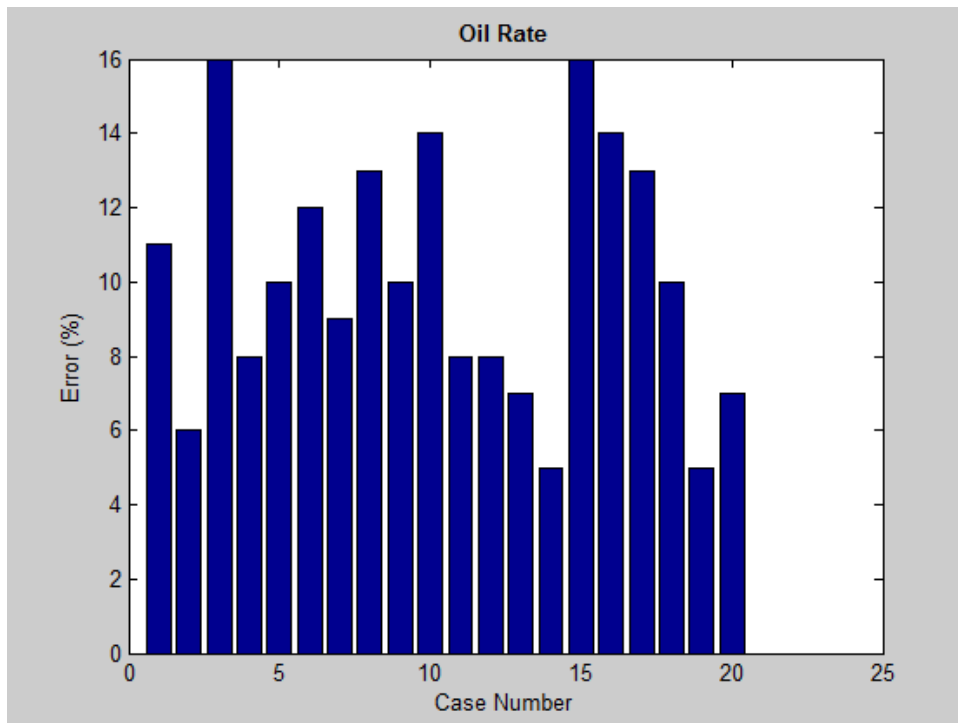


Figure 24: Error for each testing case for oil rate



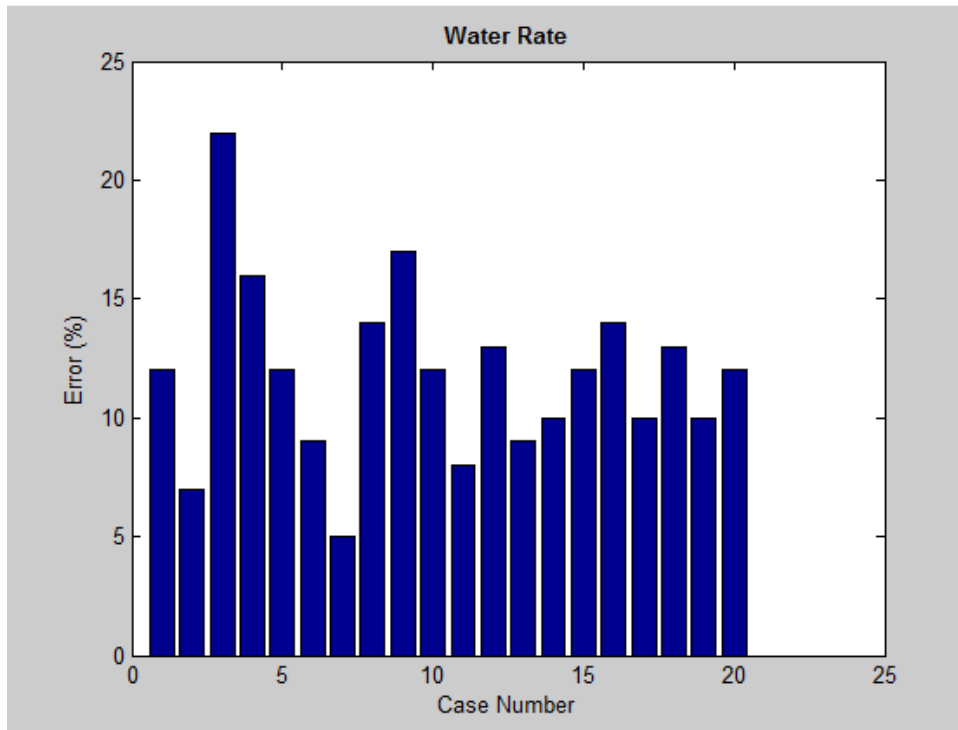


Figure 25: Error for each testing case for water rate

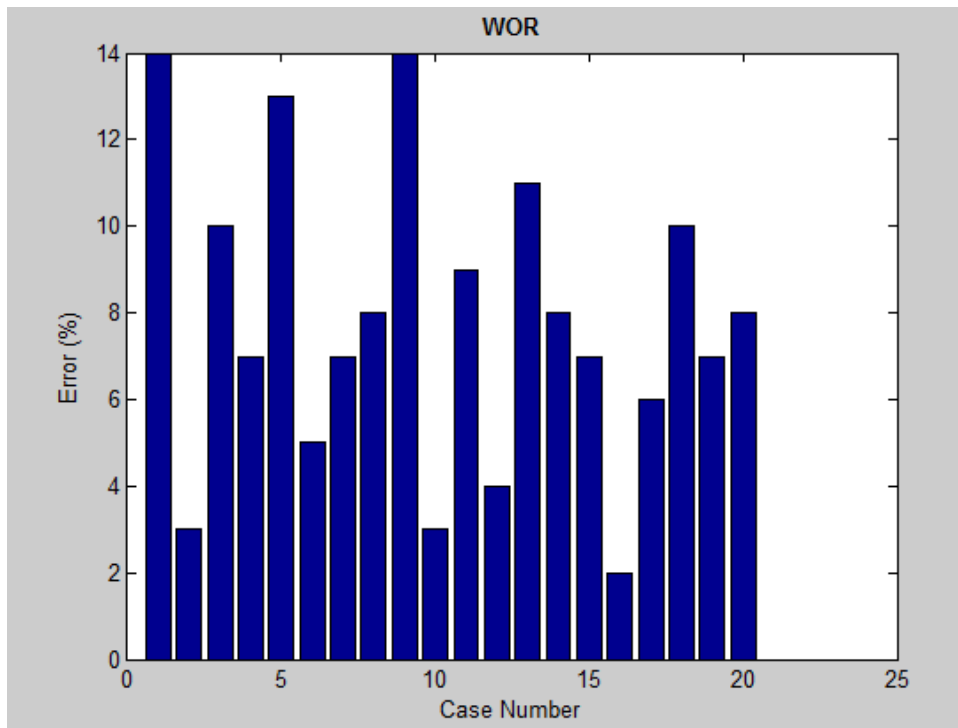


Figure 26: Error for each testing case for Water Oil Ratio (WOR)

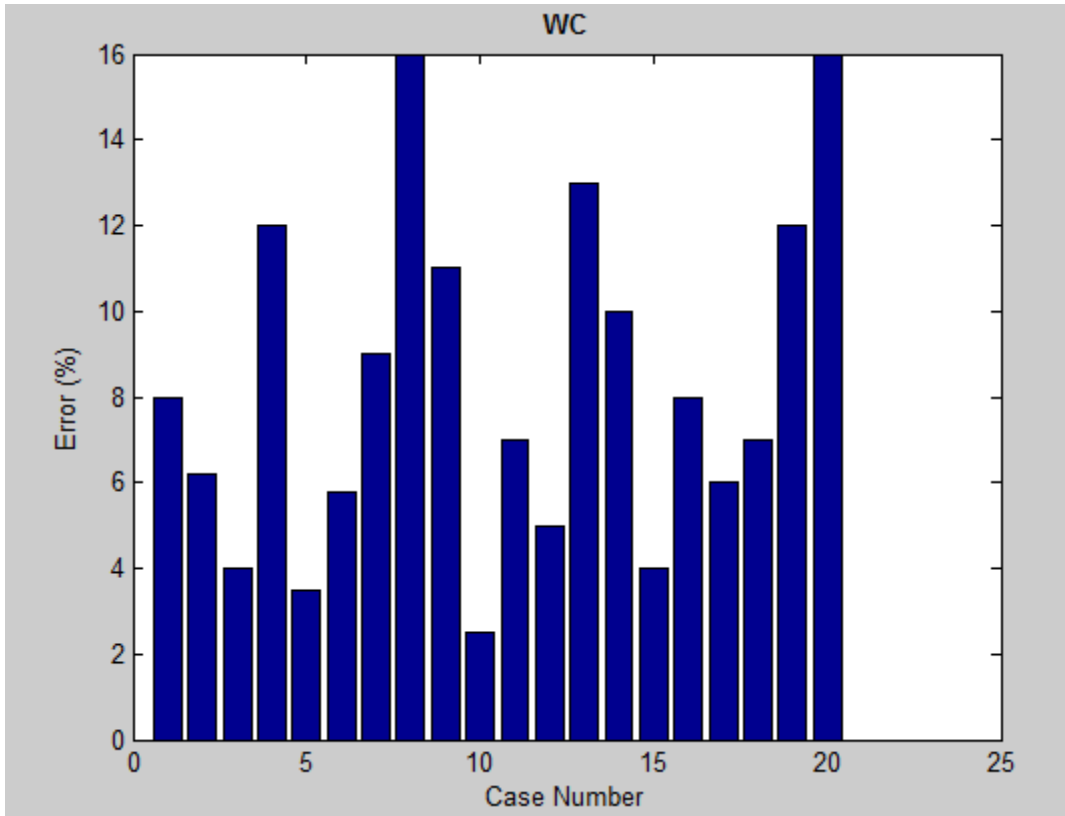


Figure 27: Error for each testing case for Water cut (WC)

Having a closer look at the blind test case results, we have chosen two of the best cases, case # 214 and case # 334 and three of the worst cases, case # 51, # 79 and # 340. Comparing all the results we can see that the ANN is predicting the production profiles and capturing their behaviors best when API values are less than 30. On the other hand, when the difference between the horizontal permeability and the vertical permeability is very large like cases 51, 79 and 340, it is clear that the ANN does not predict the production profiles behavior at high accuracy level. However, that does not mean that the ANN is not capturing the behavior for the production profiles but for some production profiles, there is an offset between the simulator result and the ANN result. For example, for case # 51 in figure 28 the oil rate production curve generated by the simulator is not being predicted by the ANN accurately especially at early production period. This could be due

to the few data points available for the ANN to be trained, as it was mentioned in the previous chapter for the first 4 years the production data were collected each month and afterward they were collected every three-month period for the rest of the 6 years. For the cases where we have an offset in some specific periods between the simulator result and ANN prediction there might be not enough data points that cover these periods and consequently the ANN predicts that maximum or minimum peak either at an early time like what is shown in figure 28 for the water rate or at later time like the water oil ratio in figure 36.

This issue of having an offset or shift between the ANN and the simulator results could be overcome if we used a fitting function instead of the discrete points. However, it might be somehow challenging to find a function that could be suitable for a production profile with a wide range of output like the water rate since it is the reservoir is connected to an infinity large source of water and depends on the location of the horizontal well the amount of water being produced will vary significantly.

Table 8: Case 51 reservoir properties

L.C	Area (Acers)	$K_{ij}$ (md)	$k_k$ (md)	$\phi$	P (psi)	R_Comp (1/psi)	$S_o$	$S_w$	T (F)	H (ft)	API	$\rho_{gas}$
9	701.45	245	50	0.163	5244.9	5.00E-07	0.34	0.20	165.79	86	33	0.978

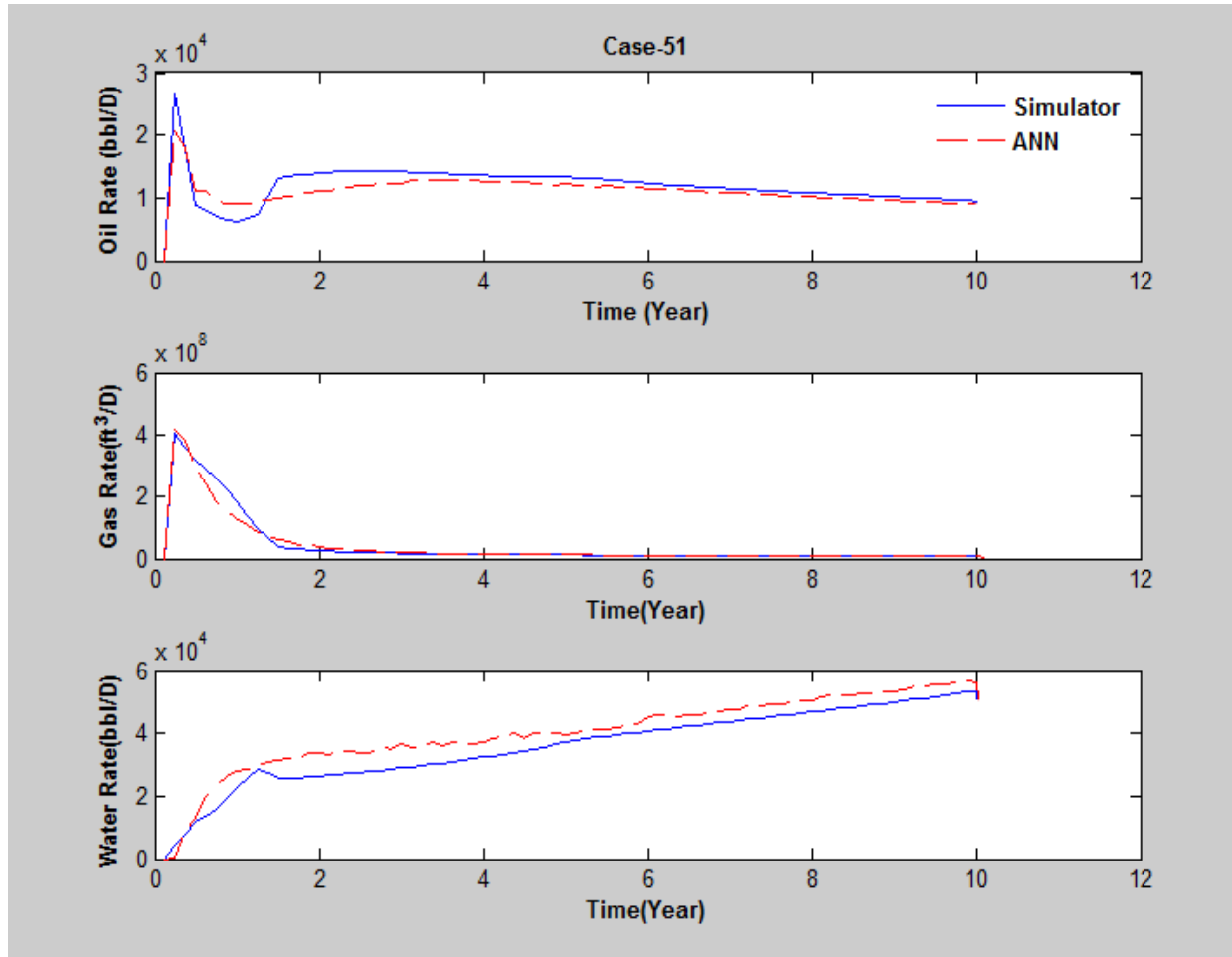


Figure 28: Comparison of production profiles generated by ANN and numerical simulator (Case-51)

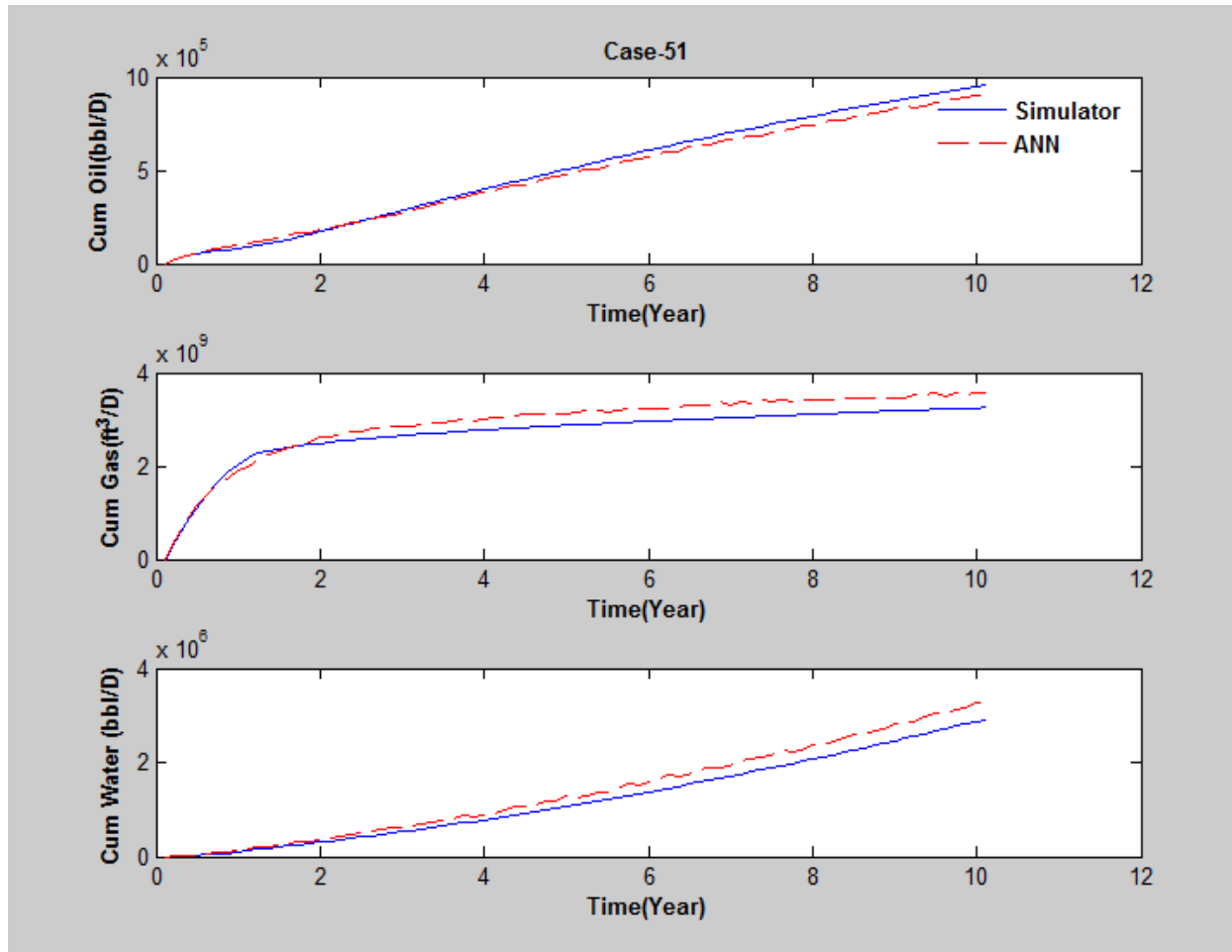


Figure 29: Comparison of cumulative production profiles generated by ANN and numerical simulator (Case-51)

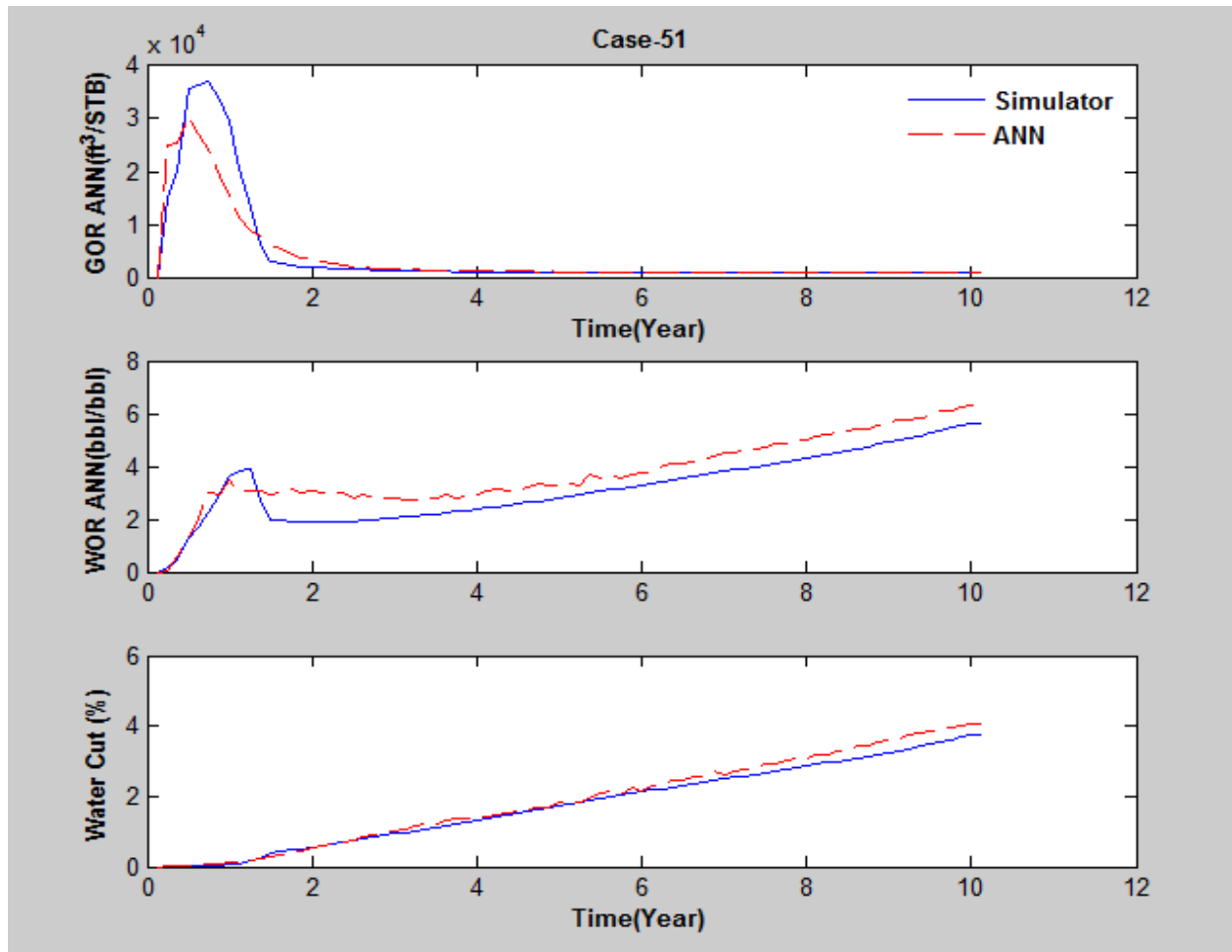


Figure 30: Comparison of Gas Oil Ratio, Water Oil Ratio and water cut production profiles generated by ANN and numerical simulator (Case-51)

Table 9: Case 79 reservoir properties

L.C	Area (Acers)	$K_{ij}$ (md)	$k_k$ (md)	$\phi$	P (psi)	R_Comp (1/psi)	$S_o$	$S_w$	T (F)	H (ft)	API	$\rho_{gas}$
8	545.95	145	81.42	0.194	5704.1	6.00E-07	0.36	0.5	250	126	36	0.823

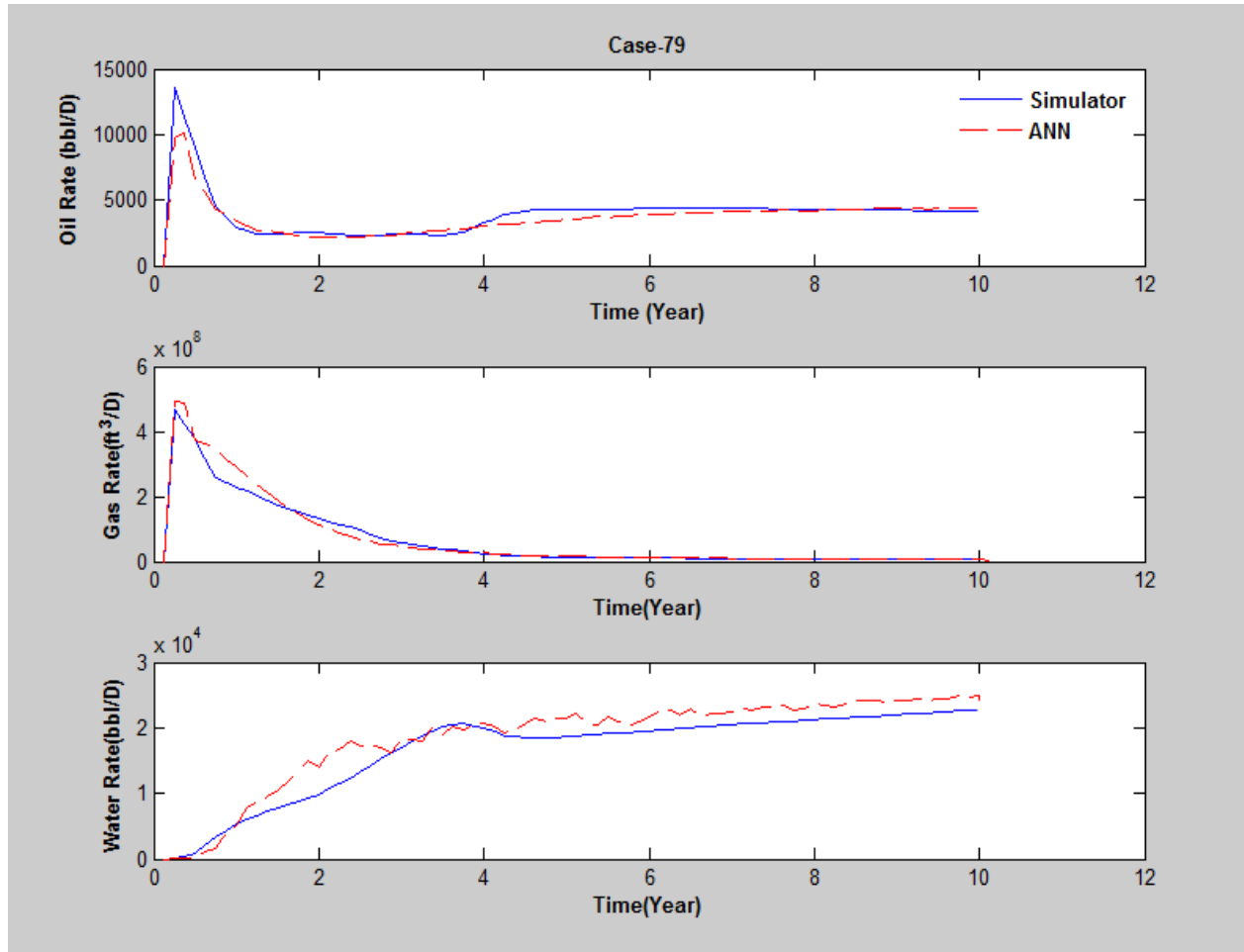


Figure 31: Comparison of production profiles generated by ANN and numerical simulator (Case-79)

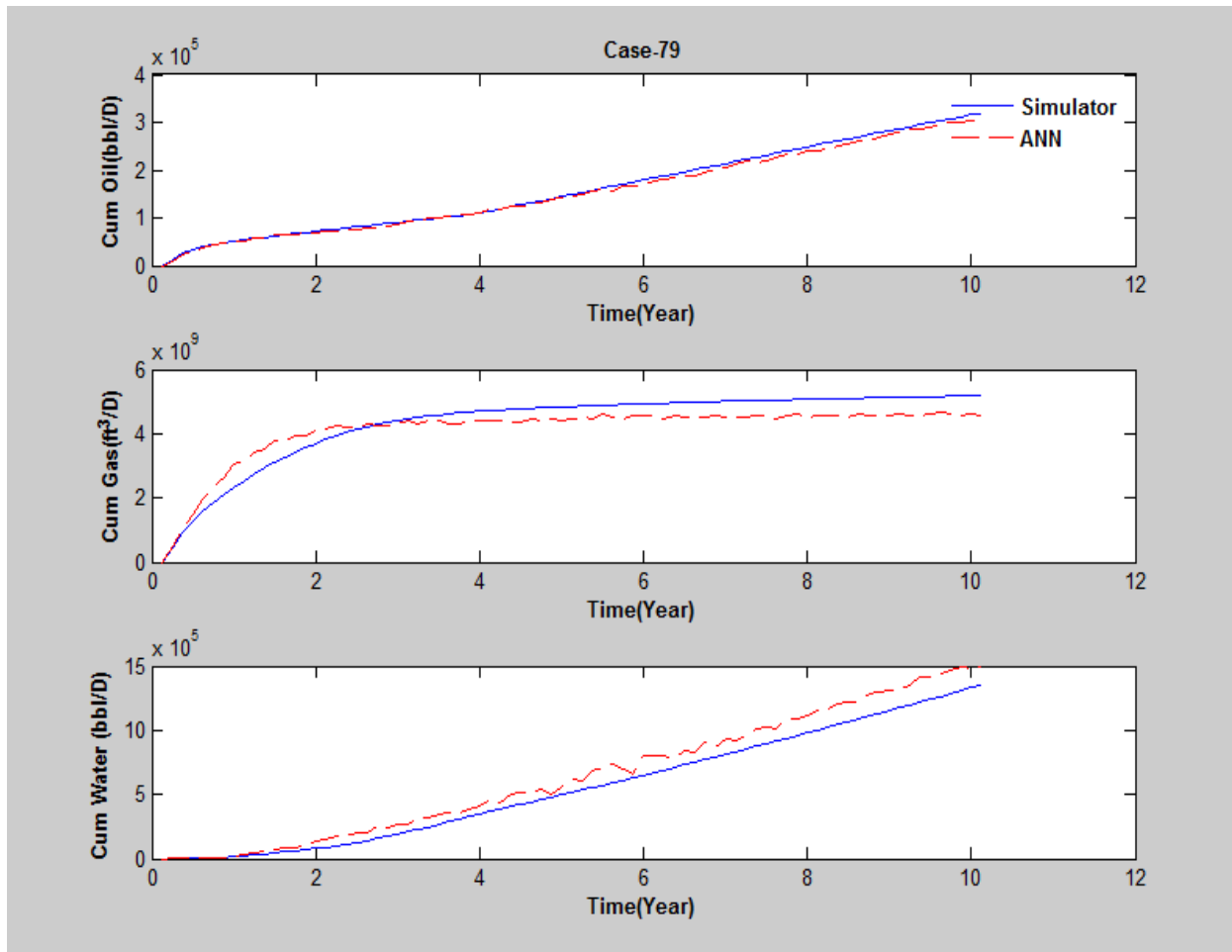


Figure 32: Comparison of cumulative production profiles generated by ANN and numerical simulator (Case-79)



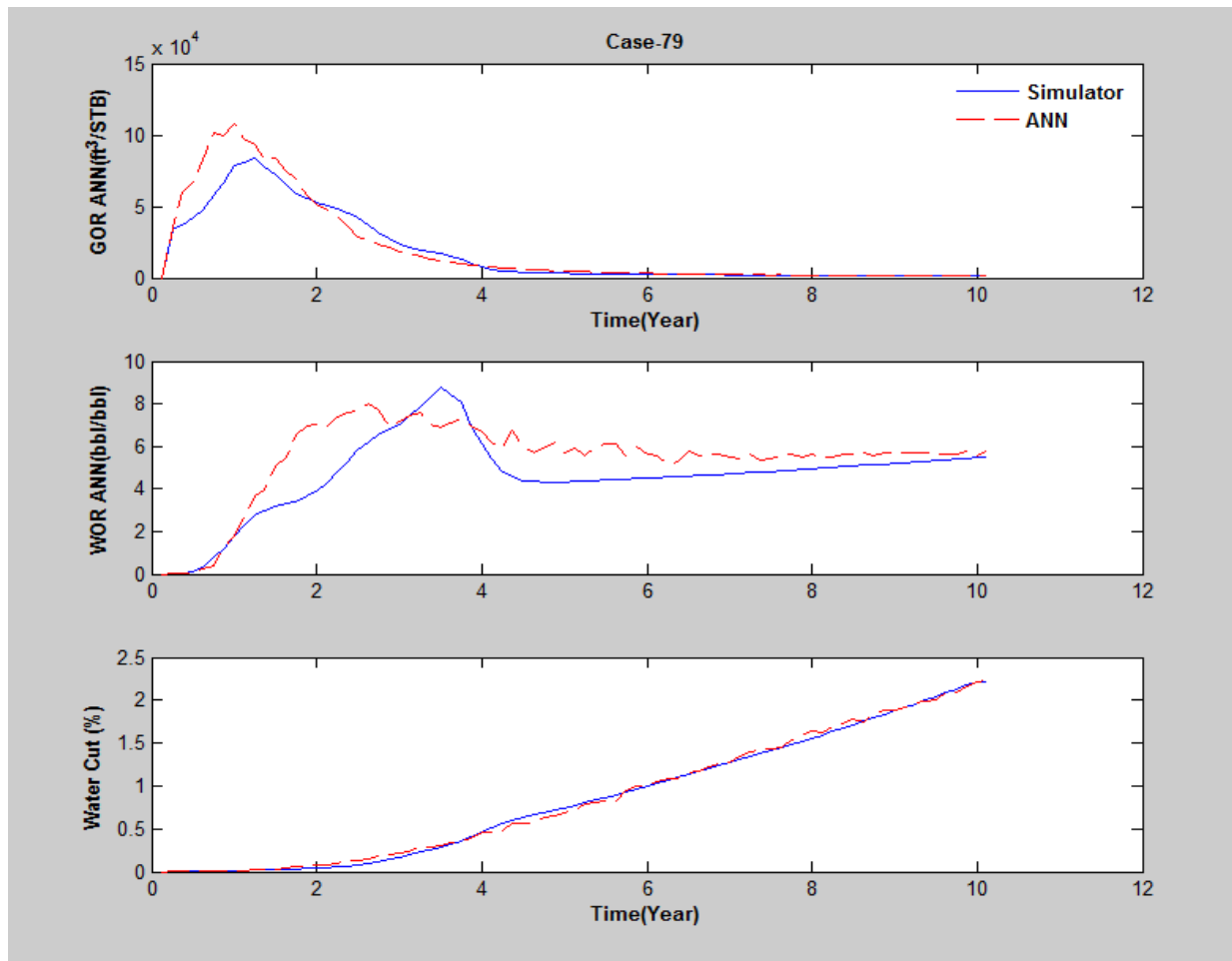


Figure 33: Comparison of Gas Oil Ratio, Water Oil Ratio and water cut production profiles generated by ANN and numerical simulator (Case-79)

Table 10: Case 51 reservoir properties

L.C	Area (Acers)	$K_{ij}$ (md)	$k_k$ (md)	$\phi$	P (psi)	R_Comp (1/psi)	$S_o$	$S_w$	T (F)	H (ft)	API	$\rho_{gas}$
7	856.739	5	15.714	0.142	4418.4	6.00E-07	0.53	0.25	186.84	99	25	0.981

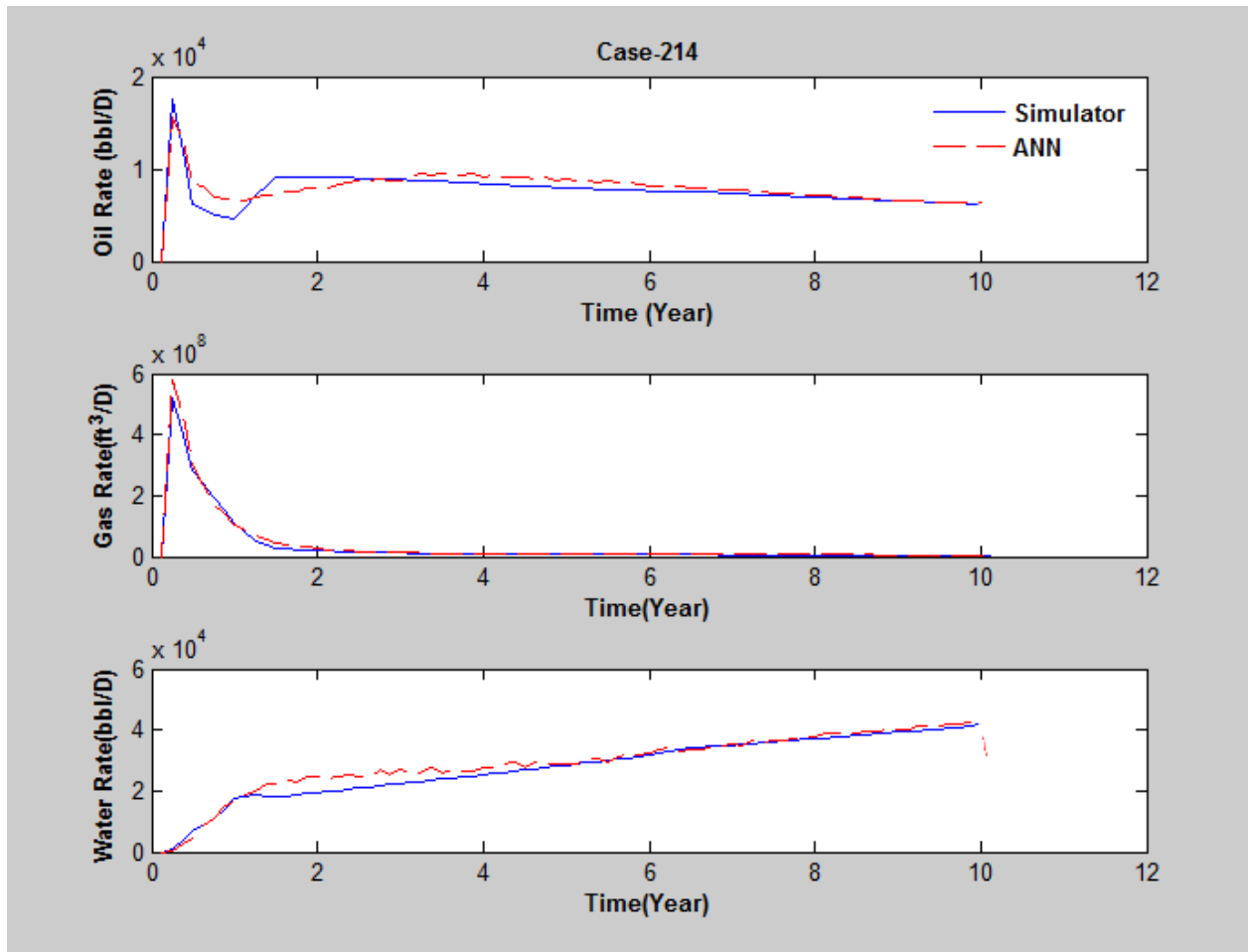


Figure 34: Comparison of production profiles generated by ANN and numerical simulator (Case-214)

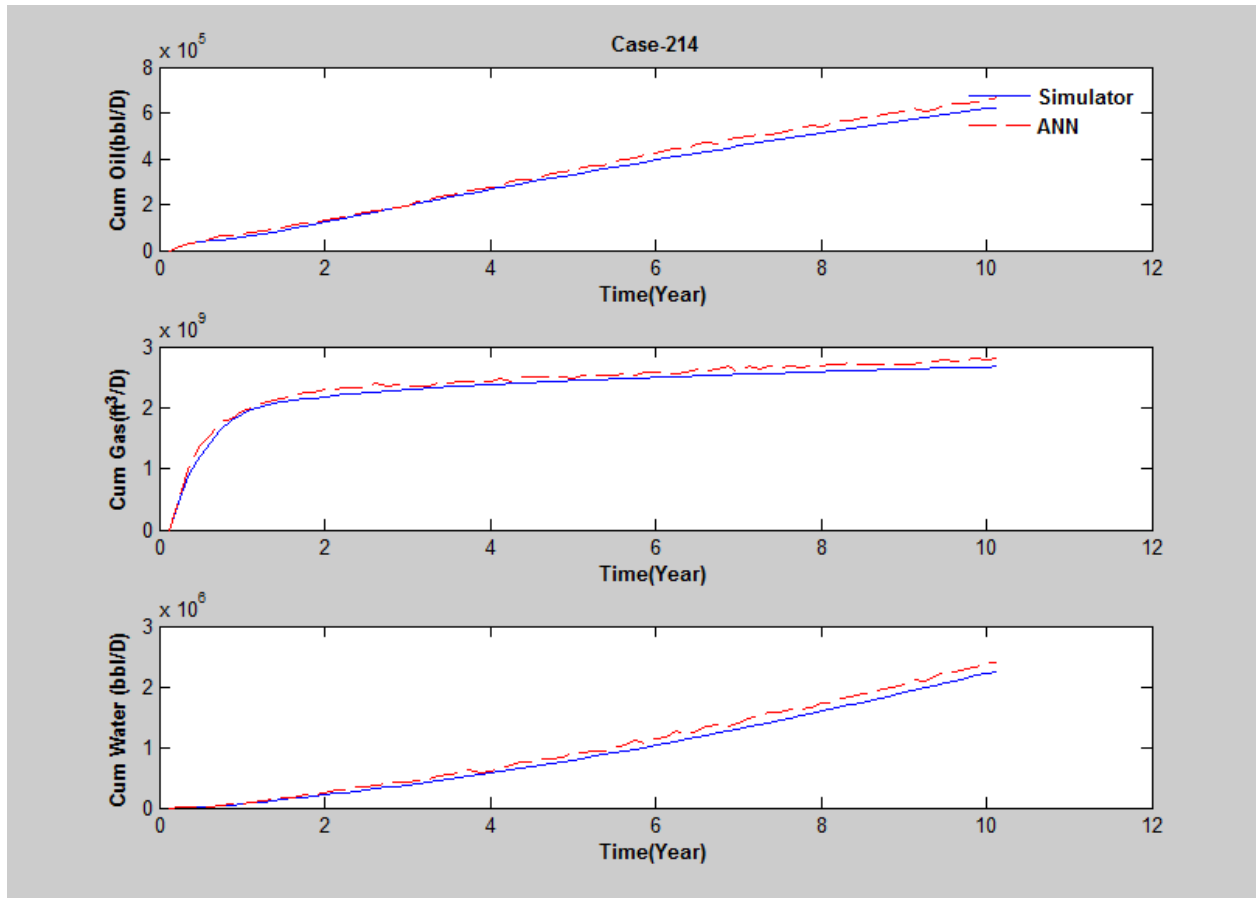


Figure 35: Comparison of cumulative production profiles generated by ANN and numerical simulator (Case-214)

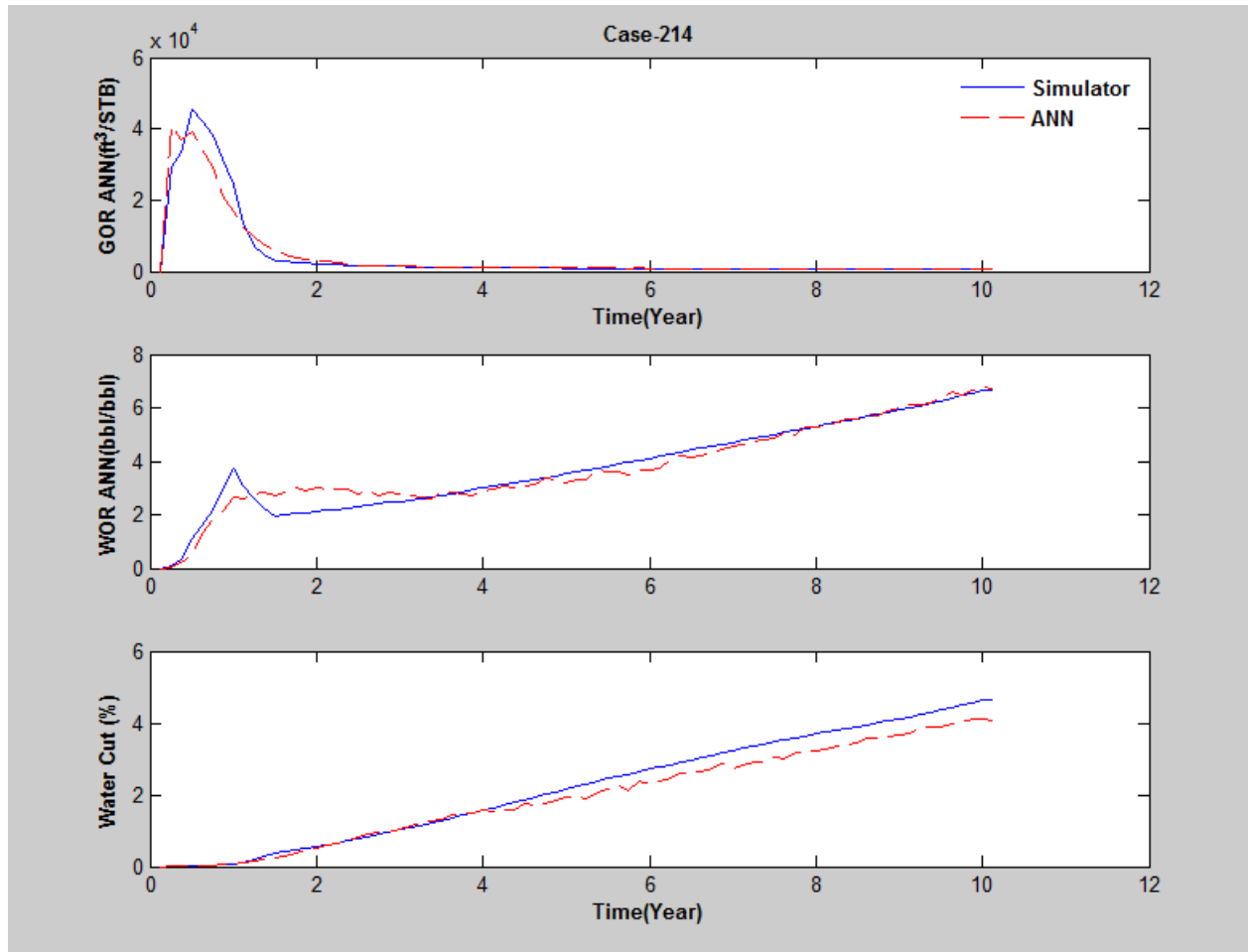


Figure 36: Comparison of Gas Oil Ratio, Water Oil Ratio and water cut production profiles generated by ANN and numerical simulator (Case-214)

Table 11: Case 334 reservoir properties

L.C	Area (Acers)	$K_{i,j}$ (md)	$k_k$ (md)	$\phi$	P (psi)	R_Comp (1/psi)	$S_o$	$S_w$	T (F)	H (ft)	API	$\rho_{gas}$
3	920.097	90	52.85	0.1	6806.1	4.00E-07	0.48	0.28	234.21	142	20	1.001

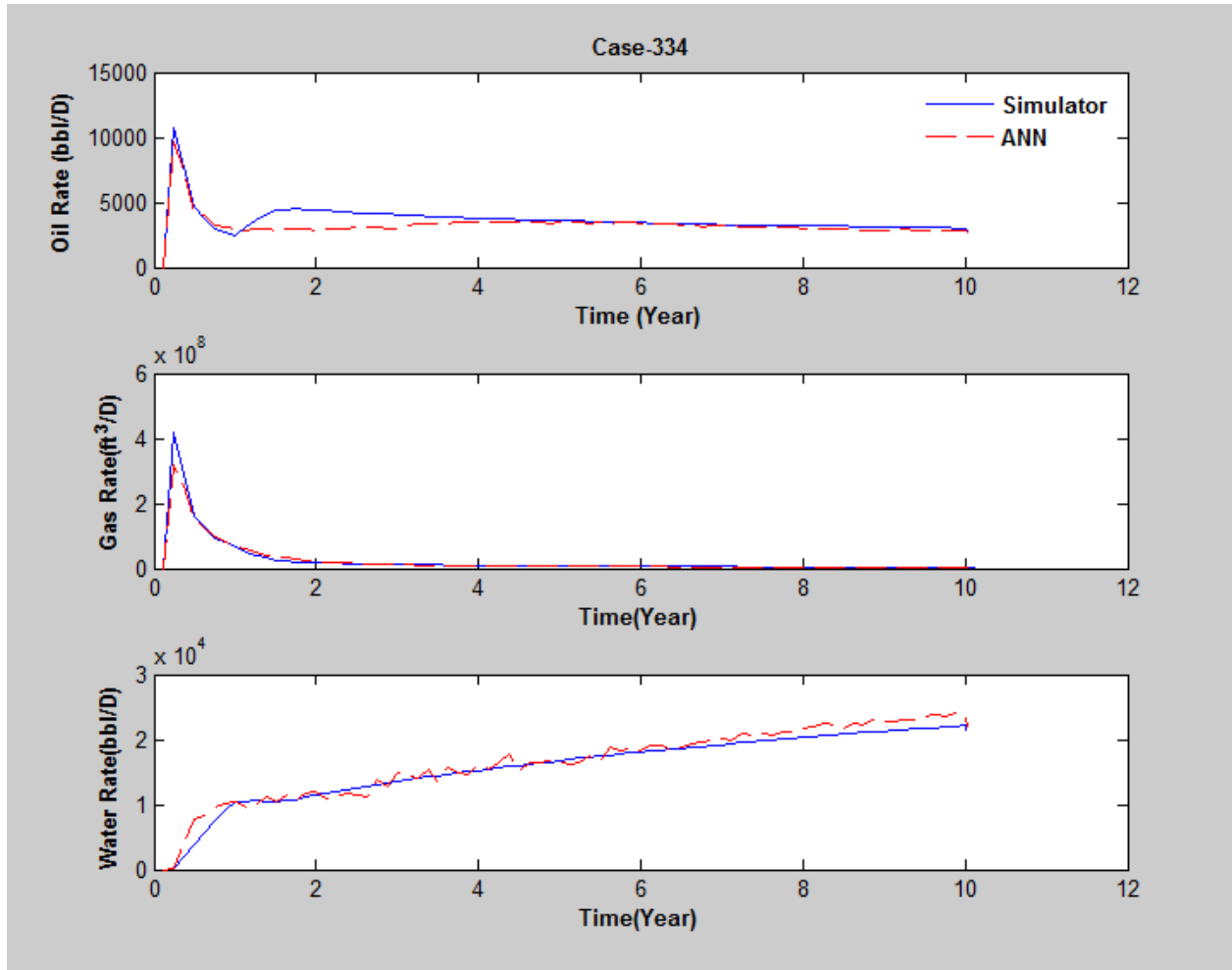


Figure 37: Comparison of production profiles generated by ANN and numerical simulator (Case-334)

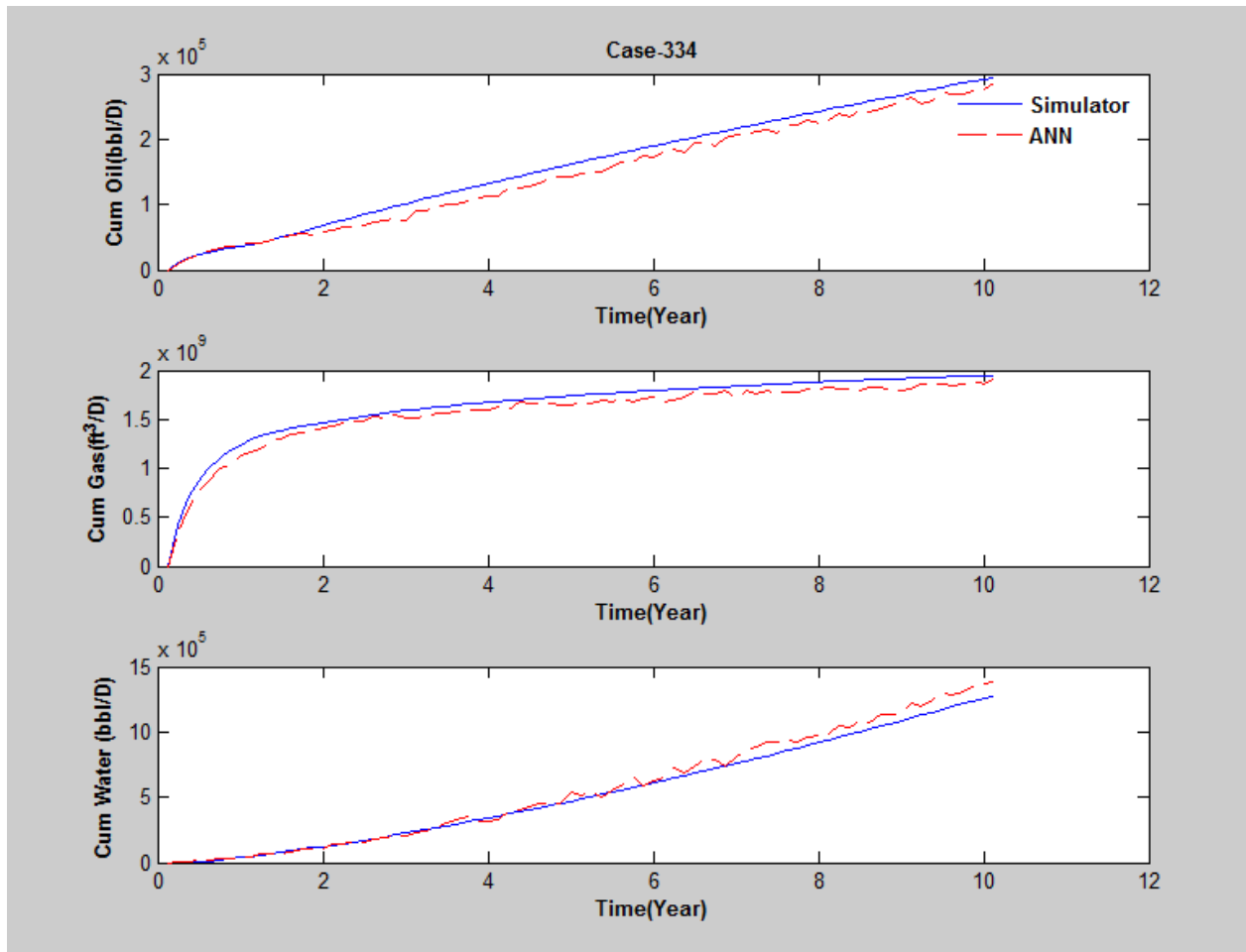


Figure 38: Comparison of cumulative production profiles generated by ANN and numerical simulator (Case-334)

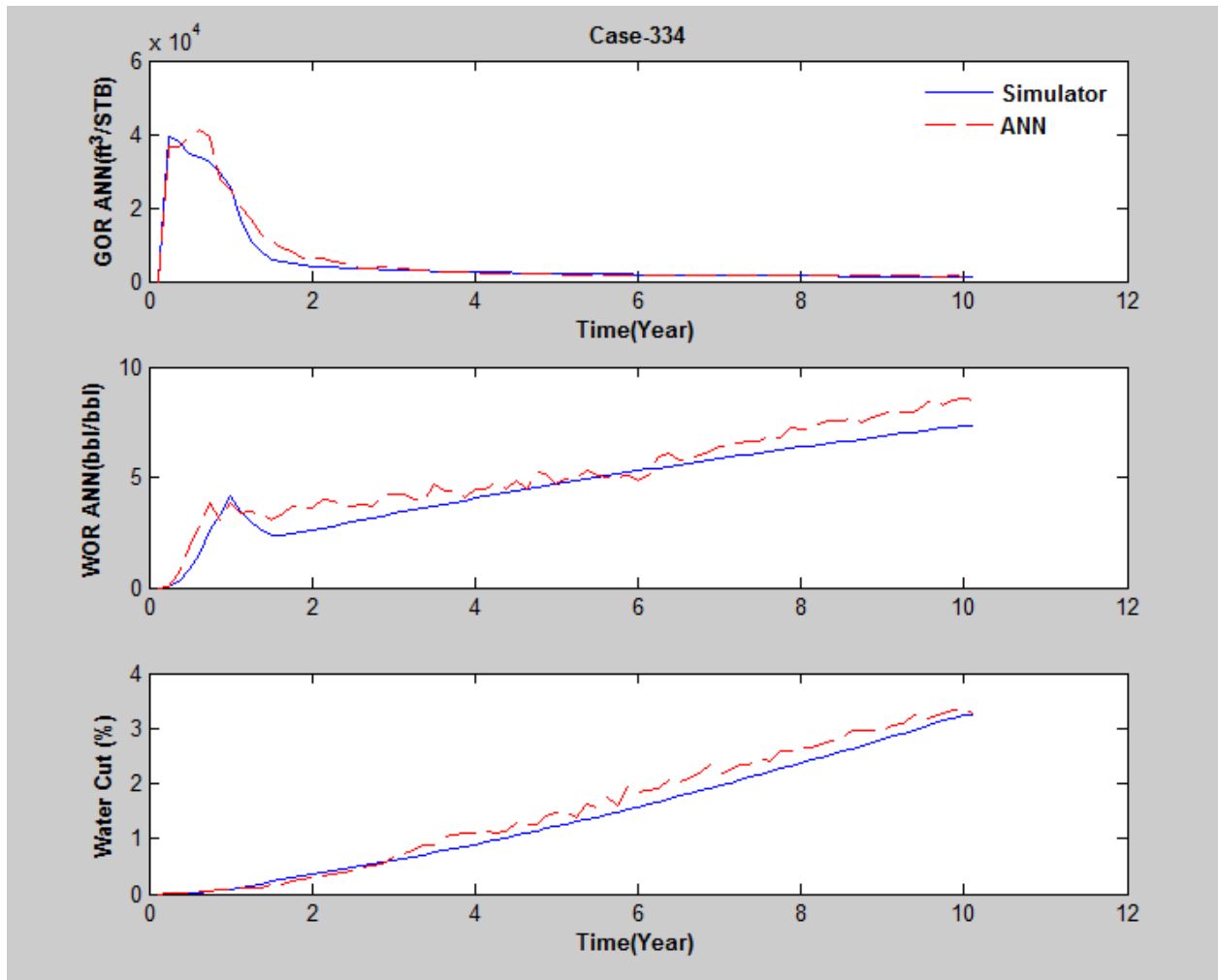


Figure 39: Comparison of Gas Oil Ratio, Water Oil Ratio and water cut production profiles generated by ANN and numerical simulator (Case-334)

Table 12: Case 340 reservoir properties

L.C	Area (Acers)	$K_{ij}$ (md)	$k_k$ (md)	$\phi$	P (psi)	R_Comp (1/psi)	$S_o$	$S_w$	T (F)	H (ft)	API	$\rho_{gas}$
5	944.837	110	12.857	0.257	5704.1	9.00E-07	0.37	0.43	234.21	139	29	1.002

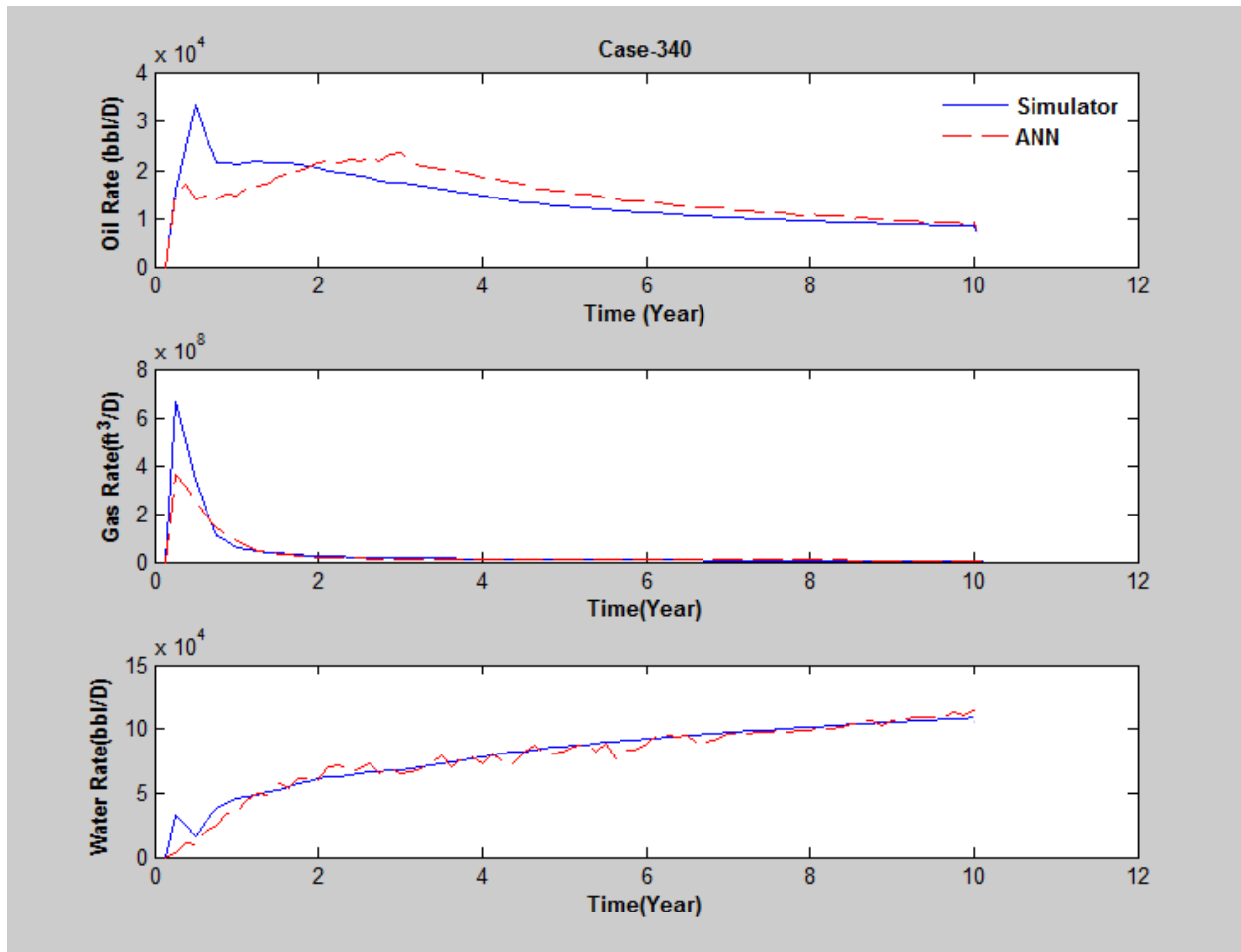


Figure 40: Comparison of production profiles generated by ANN and numerical simulator (Case-340)



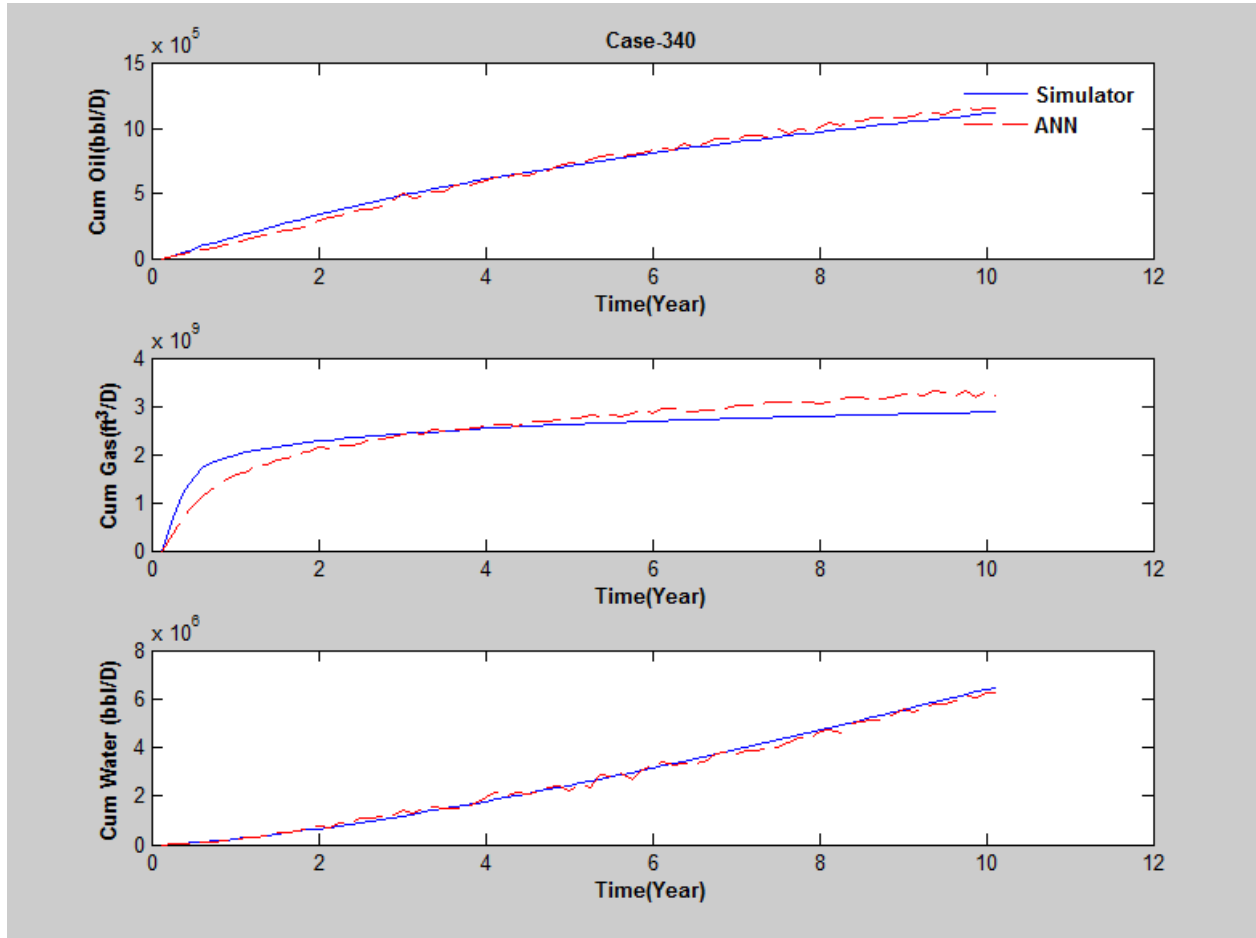


Figure 41: Comparison of cumulative production profiles generated by ANN and numerical simulator (Case-340)

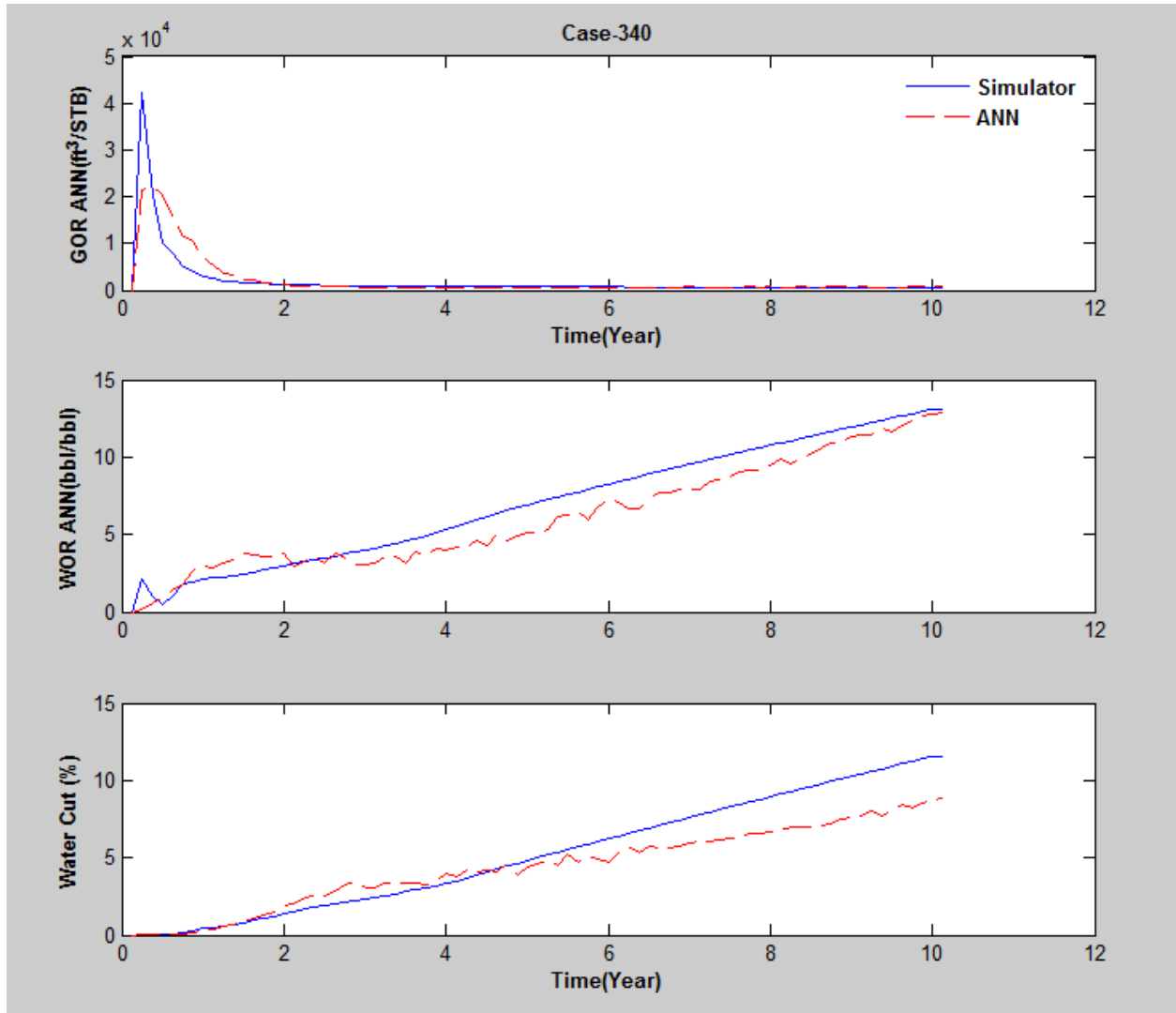


Figure 42: Comparison of Gas Oil Ratio, Water Oil Ratio and water cut production profiles generated by ANN and numerical simulator (Case-340)

## **Chapter 6: Graphical User Interface (GUI) Development**

---

Dealing with the ANN code to produce the required production profiles might not be practical especially for a user who does not have some background about it. For that reason, a graphical user interface is an essential tool since it will provide a user-friendly environment, which is an easily accessible interface that does not require the user to have a knowledge to use it. Also, it is very easy in this case for reservoir and drilling engineers to use it and take advantage of all its features and in the same time, they do not necessary need to have an extensive background to use the artificial neural network. In MATLAB the GUIDE tool provides this option to represent the ANN in an exertive and representative way to be used.

This GUI is consist of one window that has mainly two parts; the first part is for the user to input all the reservoir properties the user wants to obtain the production profiles for it. The second part is the part where all the production profiles will be presented in the form of graphs. A total of nine graphs that contains; oil rate, gas rate, water rate, cumulative oil, cumulative gas, cumulative water, gas oil ratio, water oil ratio and water cut will be generated ones the user input all the required properties in that window. Figure 44 shows the developed GUI for this research.

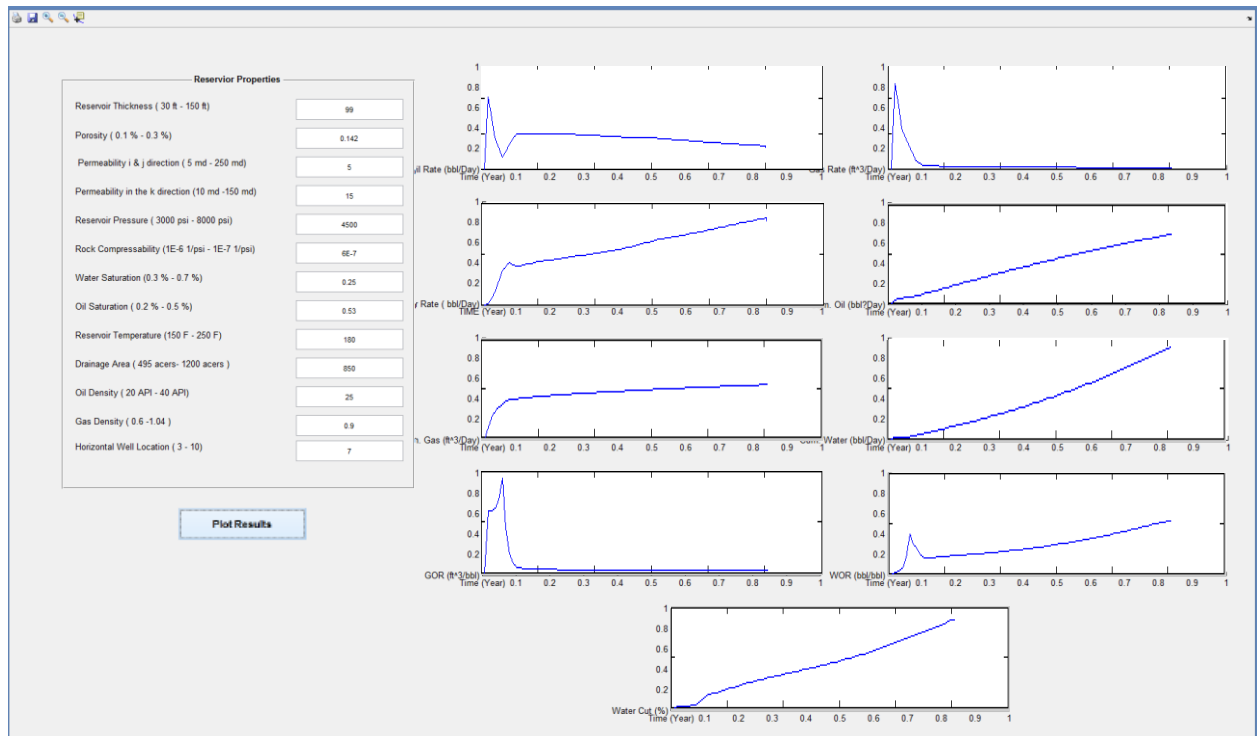


Figure 43: Developed Graphical User Interface (GUI)

## Chapter 7: Conclusion

---

Drilling is one of the most important stages in developing a new reservoir. The well location is so crucial that could affect the productivity of the well if it is done in the wrong way. The location or the depth at which horizontal well must be placed at in order to yield a high recovery factor while preserving the natural driving forces, represented by the gas cap and water drive, allowing natural production without the need to use other methods to enhance the recovery at least at early stages of the production time. In addition to that, placing horizontal well between and gas cap and an infinitely large water drive source will lead to a cresting phenomenon. However, this phenomenon cannot be avoided but instead, it could be delayed so that the most of the oil will be recovered before reaching the breakthrough time at which creasing occurs. The main objective of this study is to develop an Artificial Neural Network expert tool that will help in evaluating different production scenarios at which the horizontal could be placed at a different depth.

The model developed in the study will predict the production profiles for nine main performance indicators:

- Oil Rate
- Gas Rate
- Water Rate
- Cumulative Oil
- Cumulative Gas
- Cumulative Water
- Gas Oil Ratio
- Water Oil Ratio
- Water Cut

For this model, the optimum ANN structure was found to have 7 hidden layers that contained a total of 558 neurons. The predicted production profiles match the ones generated by the commercial simulator with an average error as follow; oil rate 14.21%, Gas rate 6.45, water rate 8.13%, cumulative oil 12.57%, cumulative gas 10.52%, cumulative water 3.140%, Gas oil Ratio 8.64%, water oil ratio 7.45% and water cut 13.21%.

The development of Graphical User Interface makes this model accessible and easy to use by drilling and/or reservoir engineers without the need for them to have a knowledge of the Artificial Neural Network code.

Through this study there are some specific conclusions that could be summarized as follow:

- Optimizing the number of data sets needed to be fed to the network so that it will cover the whole range without having a clustering in the data set overall and more specifically in any property used in the study.
- Avoid generating too many scenarios for properties with small range because it will affect the ANN training significantly since the intervals between each case and the other will be very narrow.
- In this study, although there were some cases that fewer hidden layer produces somehow reasonable results. However, the most accurate results with the lowest mean error produced by the 7 hidden layers.
- The use of functional links in the input and output layer significantly improve the results in term of capturing the profile trend and low the error difference.

- Different training and functional links algorithms were used. However, scaled conjugate gradient backpropagation training algorithm (*trainscg*) and log-sigmoid (*logsig*) functional link produced the best results for this study.
- Location of the horizontal well along with the water and oil saturation were found the most sensitive parameters that will affect the production profiles. Consequently, most of the functional links in the input and output layer these parameters were used mostly.
- Water rate and cumulative water profiles were the two most difficult profiles to predict due to the fact that it has a wide range since it is connected to an infinitely large water source.
- The use of discrete points for the production profiles generated by the simulator as a feed to the ANN did not work for all the cases in terms of allowing the ANN to capture the production profiles accurately.

## References

---

- Abu-Qudais, M. K., & Al-Nimr, M. a. (1996). a Theoretical and Experimental Study. *International Journal of Solar Energy*, 18(5), 137–146. doi:10.1080/01425919608914312
- AlGhazal, M. (2015). DEVELOPMENT AND TESTING OF ARTIFICIAL NEURAL NETWORK BASED MODELS FOR WATER FLOODING AND POLYMER GEL FLOODING IN NATURALLY FRACTURED RESERVOIRS. *The Pennsylvania State University*, (August).
- Ali, J. K. (1994). Neural Networks: A New Tool for the Petroleum Industry? *European Petroleum Computer Conference*, 217–231. doi:10.2118/27561-ms
- AlMousa, T. S., & Ertekin, T. (2013). Development and Utilization of Integrated Artificial Expert Systems for Designing Multi-Lateral Well Configurations Estimating Reservoir Properties and Forecasting Reservoir Performance. *SPE Middle East Intelligent Energy Conference and Exhibition*, (August). doi:10.2118/167462-MS
- Badde, D. S., Gupta, A., & Patki, V. K. (2009). Cascade and Feed Forward Back propagation Artificial Neural Network Models for Prediction of Compressive Strength of Ready Mix Concrete. *IOSR Journal of Mechanical and Civil Engineering (IOSR-JMCE)*, 1-6, 2278–1684.
- Bansal, Y. (2011). *Forecasting the Production Performance of Wells Located in Tight Oil Plays Using Artificial Expert Systems*. University Park: The Pennsylvania State University.
- Beale, M. H., Hagan, M. T., & Demuth, H. B. (2014). *Neural Network Toolbox: User's Guide R2014a*. Natick, MA: The MathWorks Inc.



- BuKhamseen, N. (2014). *Applications of Artificial Expert Systems in the Diagnosis and Analysis of Unexpected Spatial and Temporal Changes in Reservoir Production Behavior*. The Pennsylvania State University.
- Byrne, W. B. and Morse, R. A. (1973). The Effects of Various Reservoir and Well Parameters on Water Coning Performance. *SPE*, (4287).
- Chidambaram, P. (2009). *Development and Testing of an Artificial Neural Network Based History Matching Protocol to Characterize Reservoir Properties*. University Park: The Pennsylvania State University.
- Discussions, L. C. (2014). Learning methods, (August).
- Fausett, L. (1994). *Fundamentals of Neural Networks: Architectures, Algorithms and Applications*. Englewood Cliffs, NJ: Prentice-Hall.
- Gharehlo, A. M. (2012). *Development of Artificial Expert Reservoir Characterization Tools for Unconventional Reservoirs*. University Park: The Pennsylvania State University.
- Holand, Left A. Papatzacos, Paul. Skjaeveland, S. M. (1989). Critical Rate for Water Coning: Correlation and Analytical Solution. *SPE Journal*, (SPE 15855), 495–502.
- Khandwala, S. M., Rani, A. M. A., & Rahman, M. N. A. (1984). Field Development Planning For The Semangkok Field Offshore Pen Insular Malaysia. *Southeast Asia Show*.  
doi:10.2118/12410-MS
- Ltd., C. M. G. (2012). User's Guide CMOST: Computer Modeling Group Computer Assisted History Matching, Optimization and Uncertainty Assessment Tool.
- Lucas, S. K. (2004). Maximizing output from oil reservoirs without water breakthrough.

- Makinde, F. A. (2011). Water Coning in Horizontal Wells : Prediction of Post-Breakthrough Performance, (February).
- Mohaghegh, S. (2000). Virtual-Intelligence Applications in Petroleum Engineering: Part 3—Fuzzy Logic. *Journal of Petroleum Technology*, 52(11), 82–87. doi:10.2118/62415-JPT
- Mungan, N. (n.d.). A Theoretical and Experimental Coning Study. *SPE*, 221–236.
- Muskat, M., and Wycko, H. D. (1935). Approximate Theory of Water Coning in Oil Production. *Trans AIME*, 114(144-63).
- Robertson, S., & Morison, a. (1998). Development of an artificial neural network for automated age estimation, (98/105).
- Salavatov, T. S., & Ghareeb, A. S. (2009). PREDICTING THE BEHAVIOR OF WATER AND GAS CONING.
- Shahab, M. (2000). Virtual-Intelligence Applications in Petroleum Engineering. *Journal of Petroleum Technology*, 52(9), 64–71. Retrieved from <http://doi.org/10.2118/58046-MS>
- Silpngarmlers, N., Guler, B., Ertekin, T. & Grader, A. S. (2002). evelopment and Testing of Two-Phase Relative Permeability Predictors Using Artificial Neural Networks. *SPE Journal*, (7(3)), 299–308.
- Singhal, A. K. (n.d.). WATER AND GAS CONING CRESTING A TECHNOLOGY.
- SPE. (n.d.). Petroleum Engineering Technology Timeline. Retrieved from <http://www.spe.org/industry/history/timeline.php>
- Stright, D. N. B. D. H., Blades, D. N., & Stright, D. H. (1969). PREDICTING HIGH VOLUME LIFT PERFORMANCE IN Predicting High \ 1 olume Lift Perfonnance in Wells Coning \ -

Vater, *LI*.

Suzuki, K. (2011). *Artificial Neural Network- Methodological Advances and Biomedical Applications*. Rijeka, Croatia: InTech.

Watson, R. (2011). A STUDY ON THE ANALYSIS OF THE FORMATION OF HIGH by,  
(December).

Yang, Weiping, Wattenbarger, R. A. (1991). Water Coning Calculations for Vertical and Horizontal Wells. *SPE*, 22931.

## Appendix (A) Test Cases results

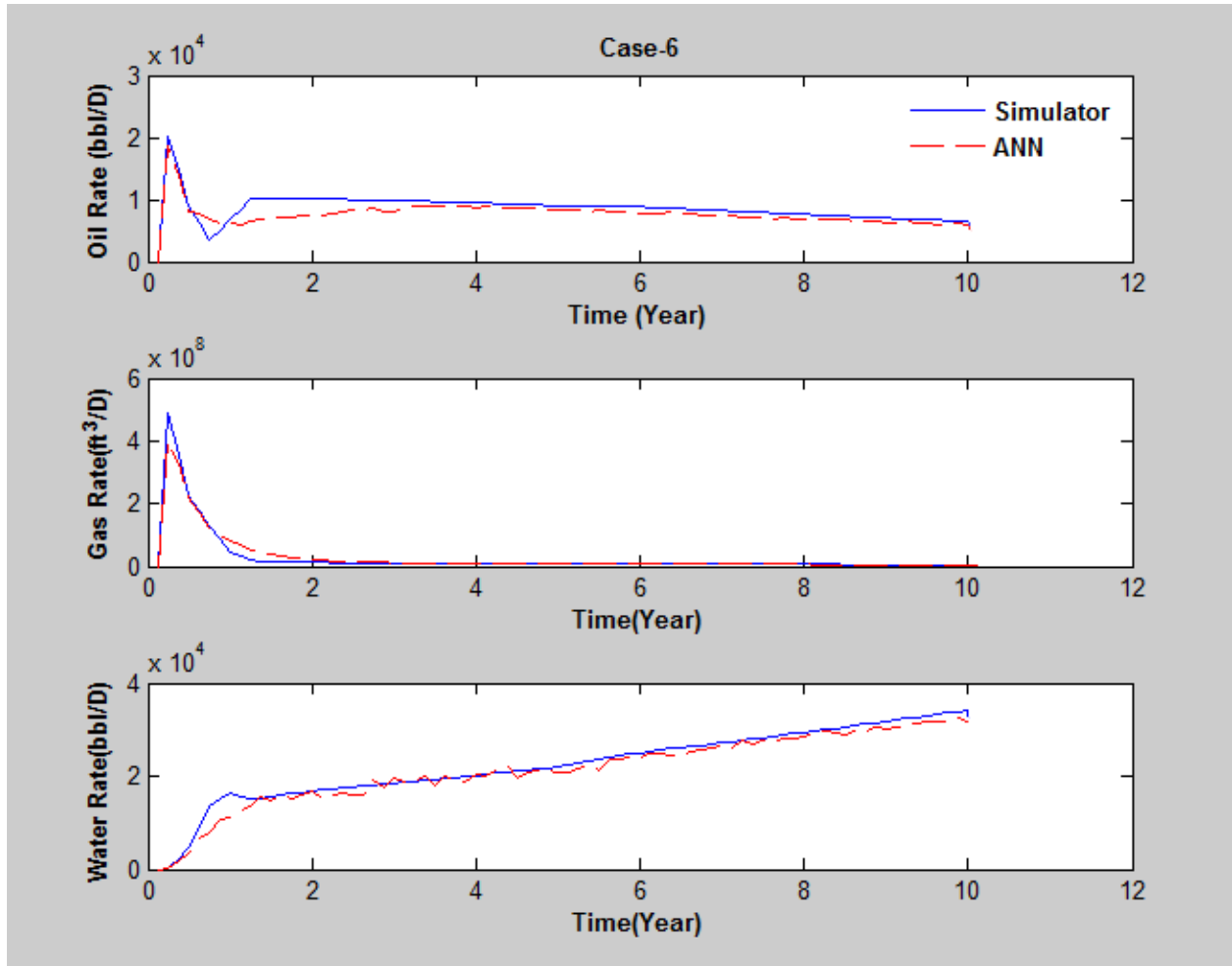


Figure 44: Comparison of production profiles generated by ANN and numerical simulator (Case-6)

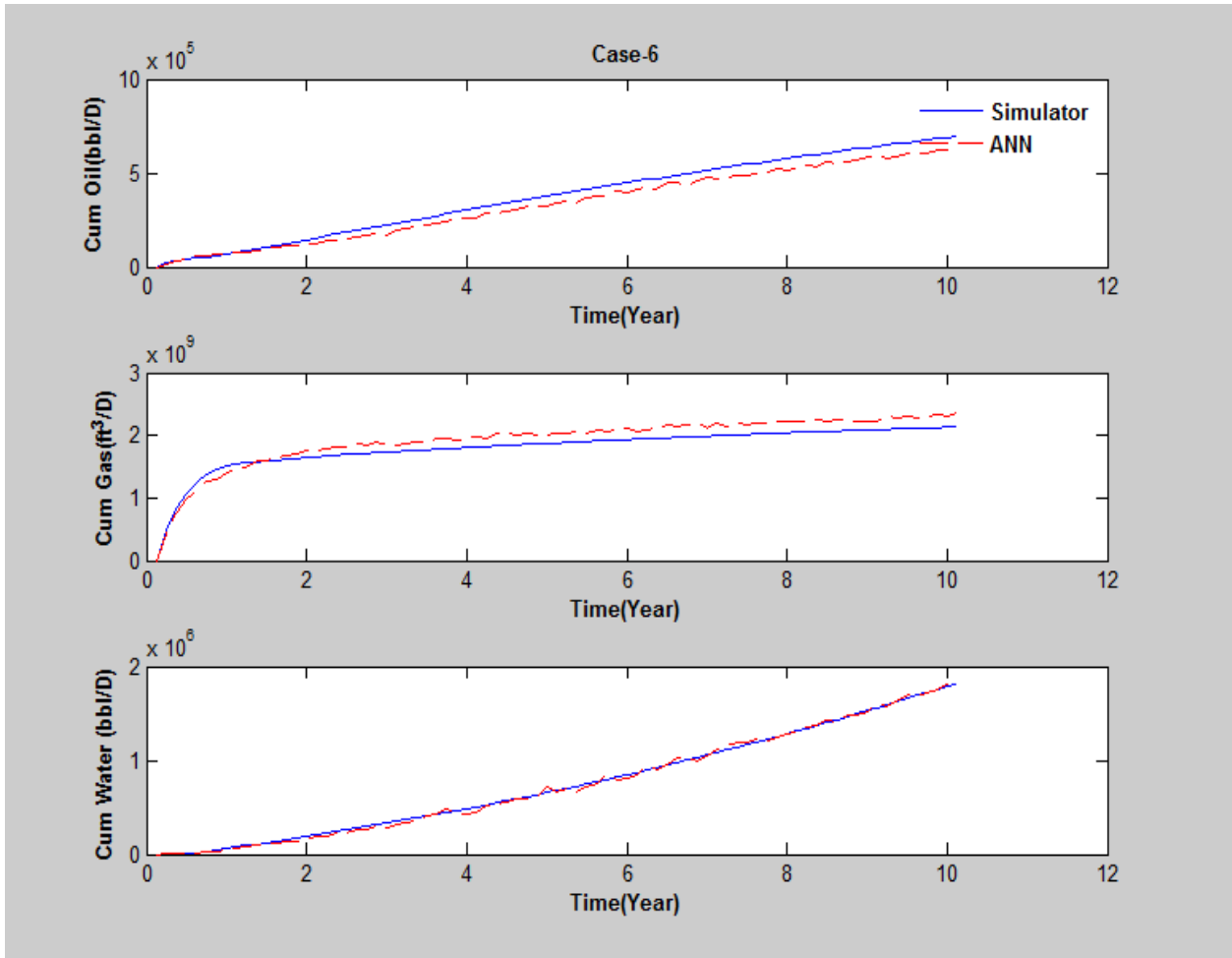


Figure 45: Comparison of cumulative production profiles generated by ANN and numerical simulator (Case-6)

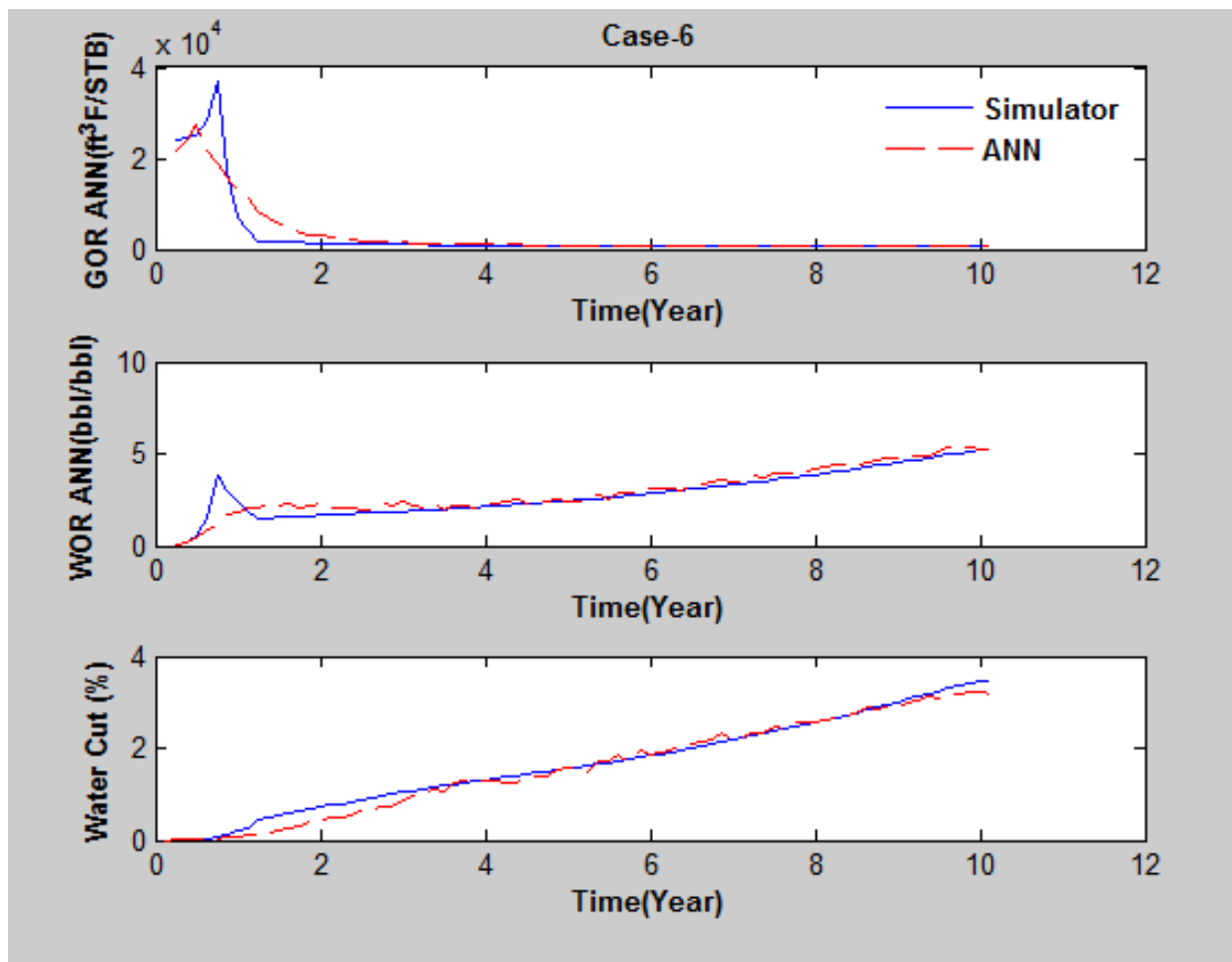


Figure 46: Comparison of Gas Oil Ratio, Water Oil Ratio and water cut production profiles generated by ANN and numerical simulator (Case-6)

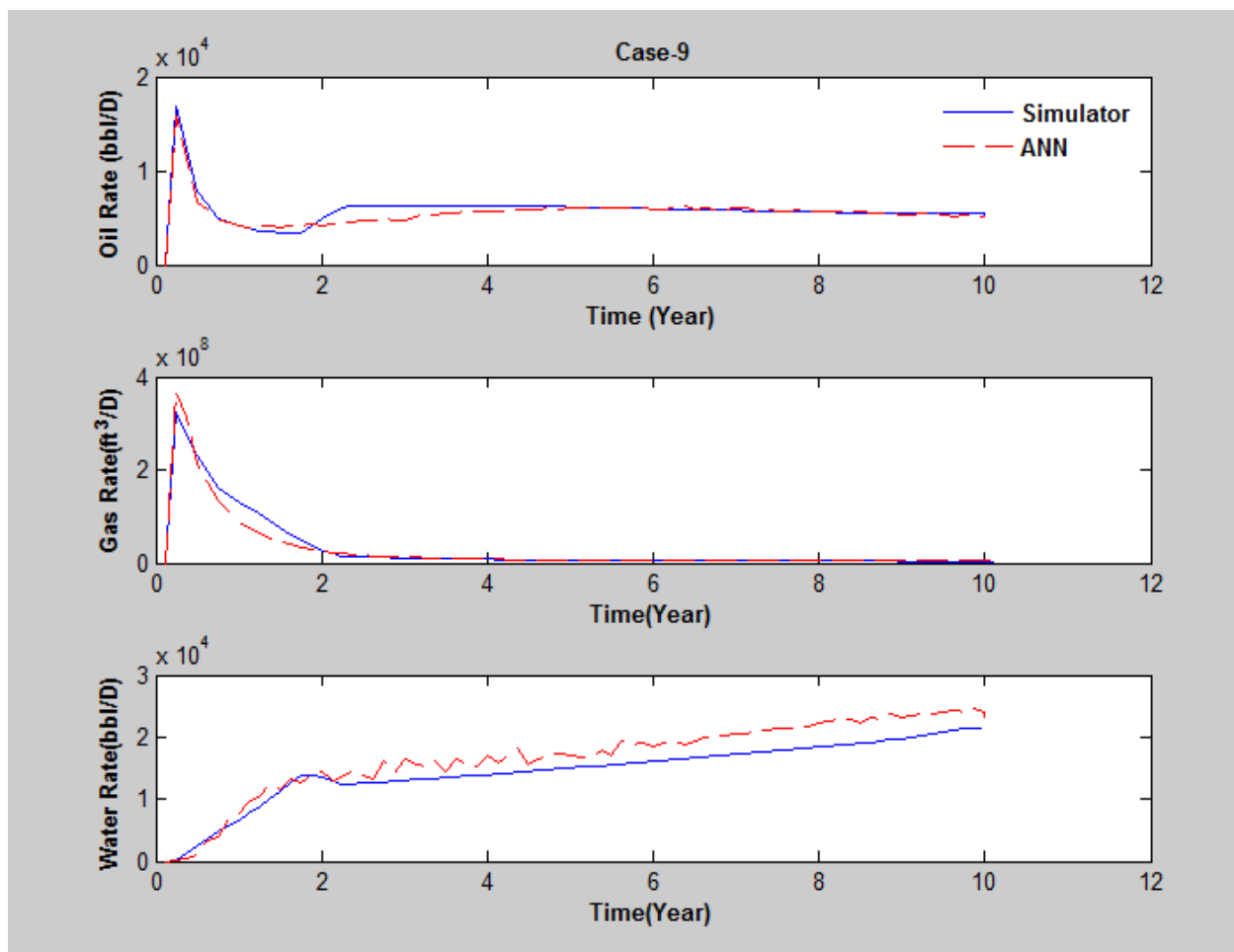


Figure 47: Comparison of production profiles generated by ANN and numerical simulator (Case-9)

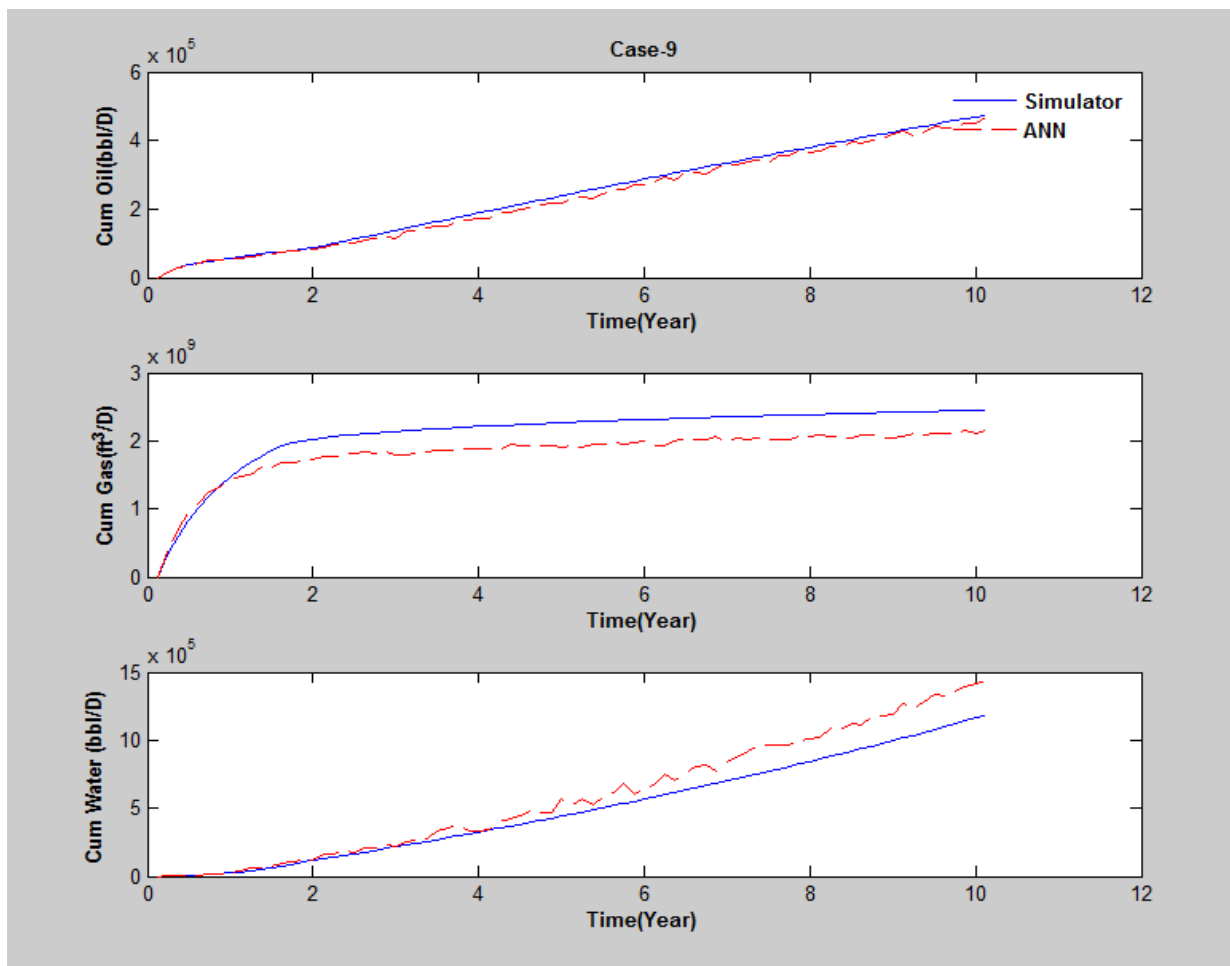


Figure 48: Comparison of cumulative production profiles generated by ANN and numerical simulator (Case-9)



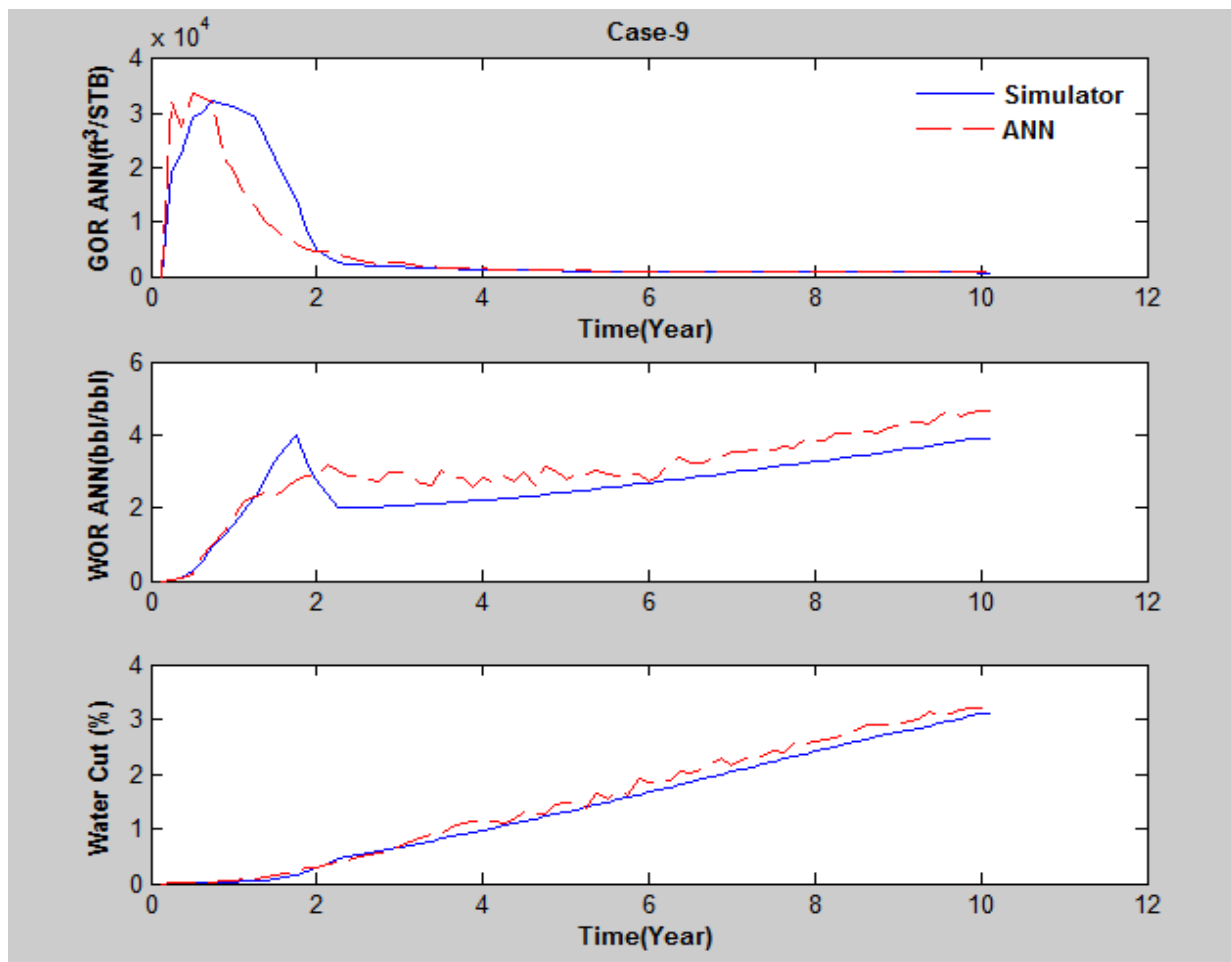


Figure 49: Comparison of Gas Oil Ratio, Water Oil Ratio and water cut production profiles generated by ANN and numerical simulator (Case-9)

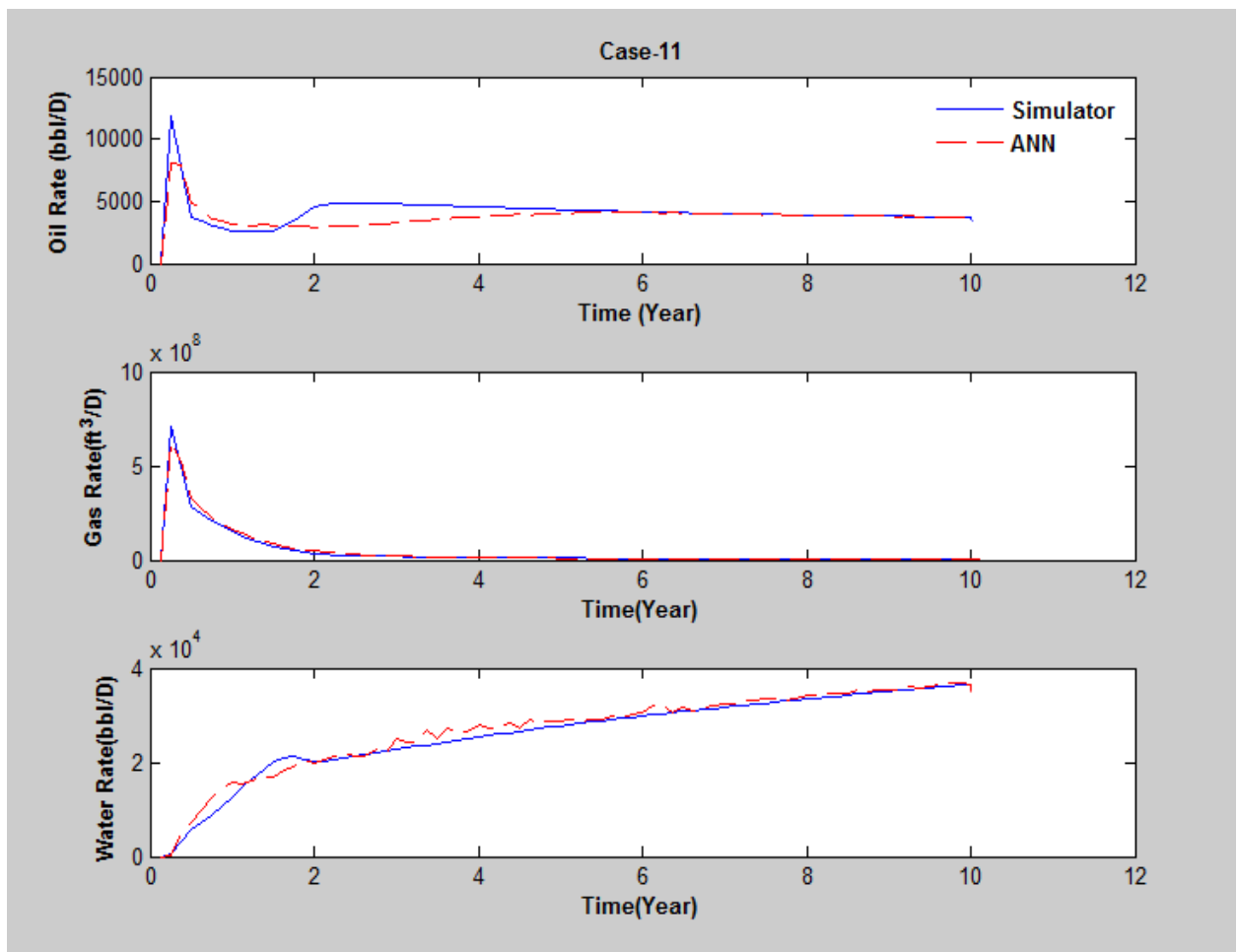


Figure 50: Comparison of production profiles generated by ANN and numerical simulator (Case-11)

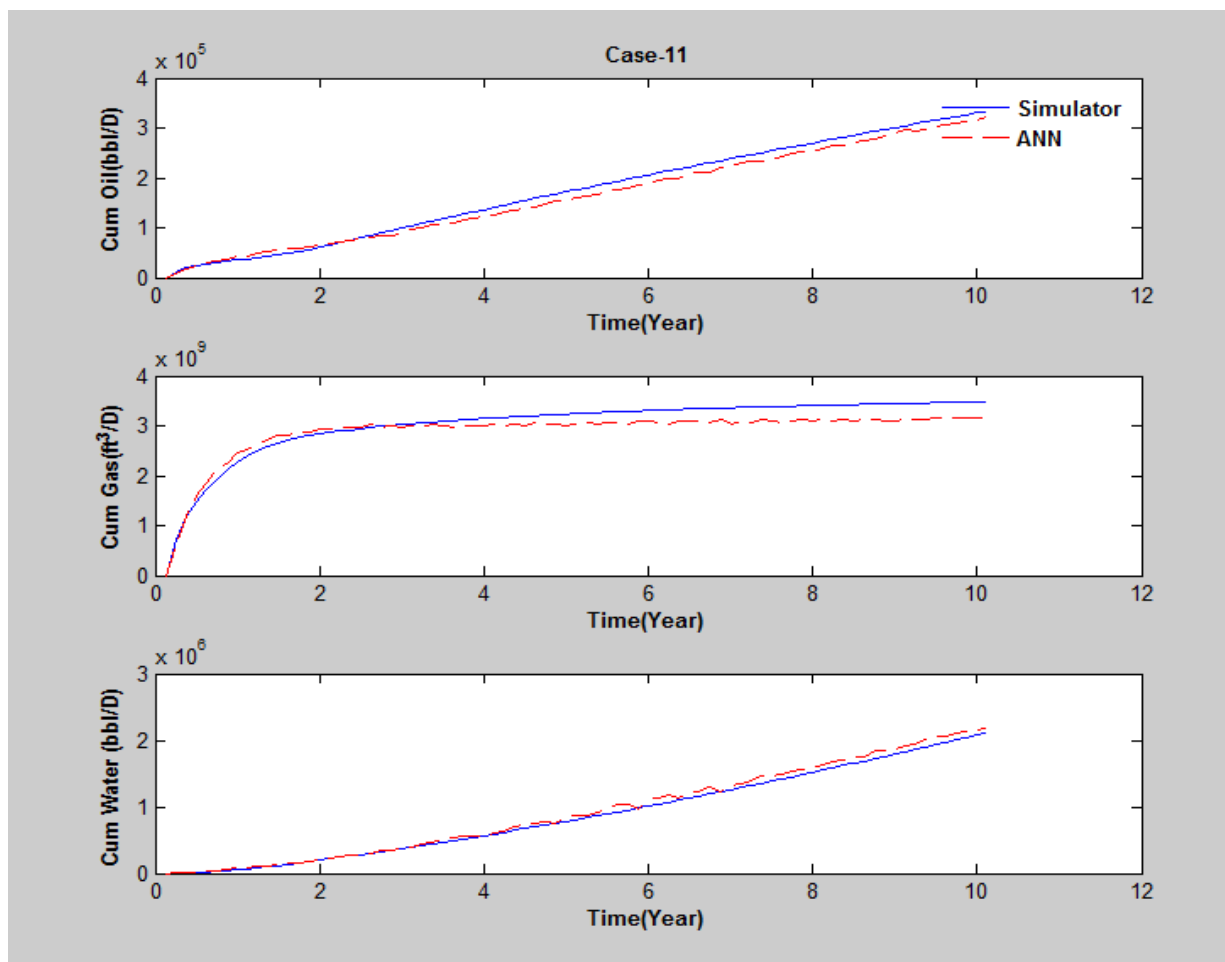


Figure 51: Comparison of cumulative production profiles generated by ANN and numerical simulator (Case-6)

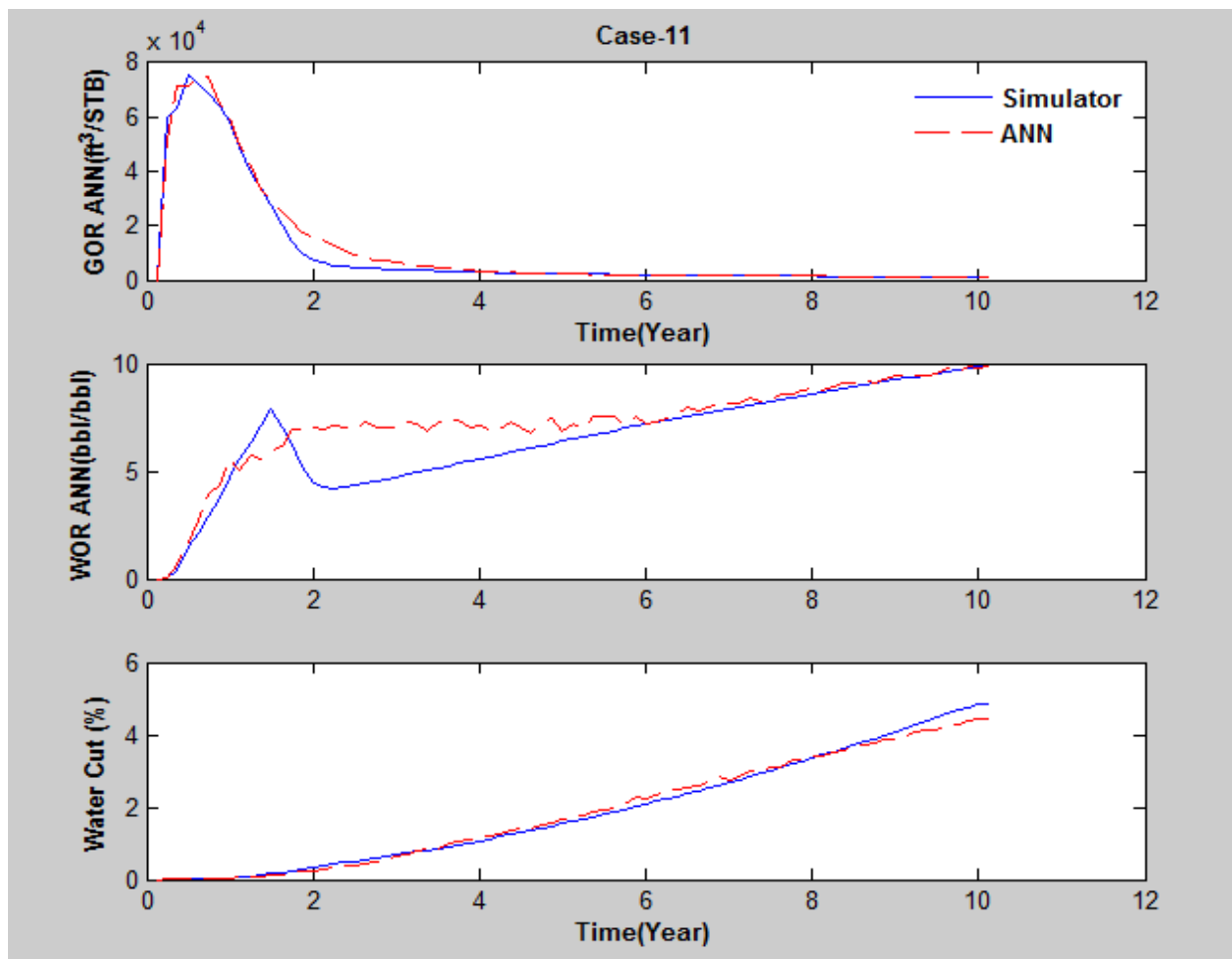


Figure 52: Comparison of Gas Oil Ratio, Water Oil Ratio and water cut production profiles generated by ANN and numerical simulator (Case-11)

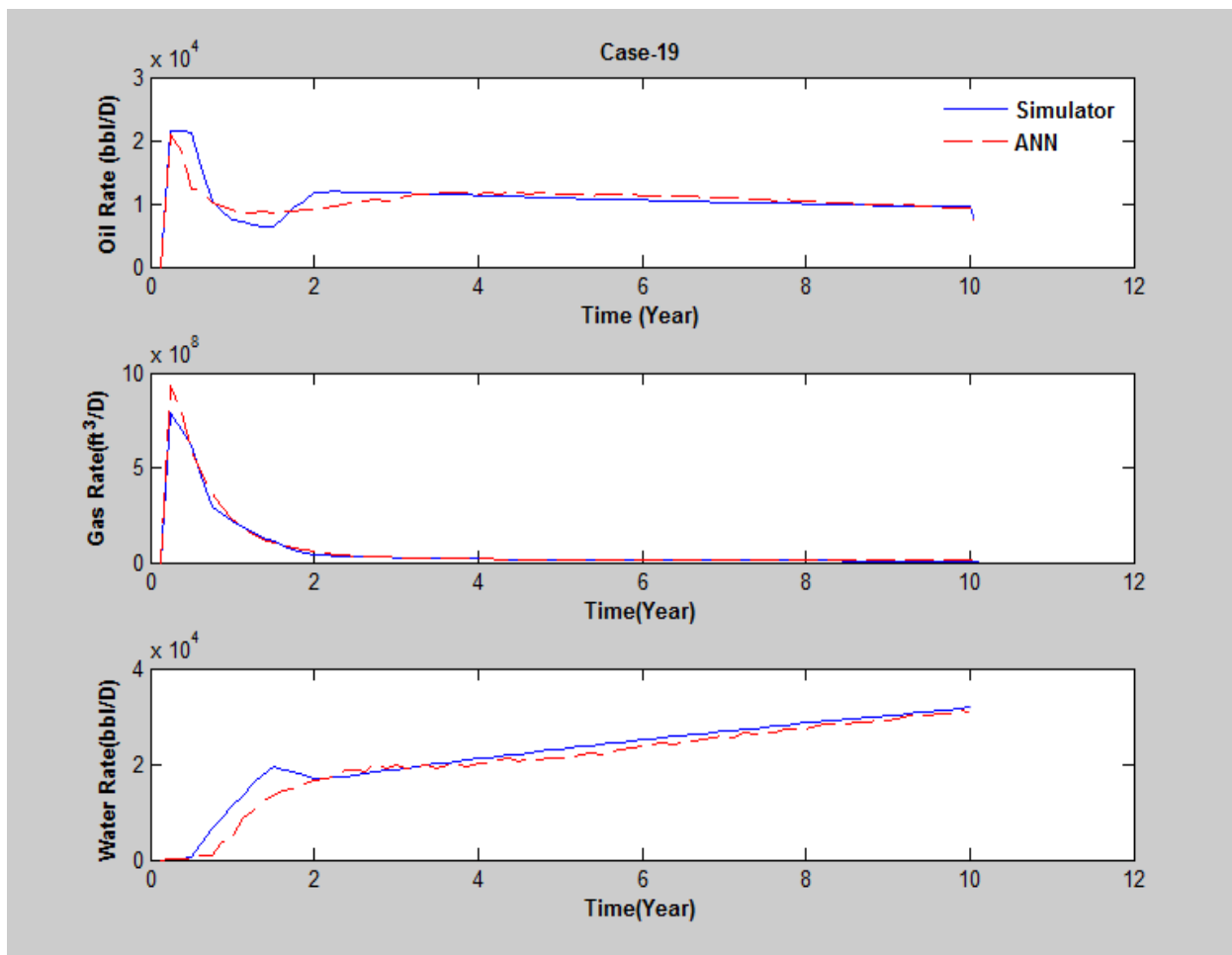


Figure 53: Comparison of production profiles generated by ANN and numerical simulator (Case-19)

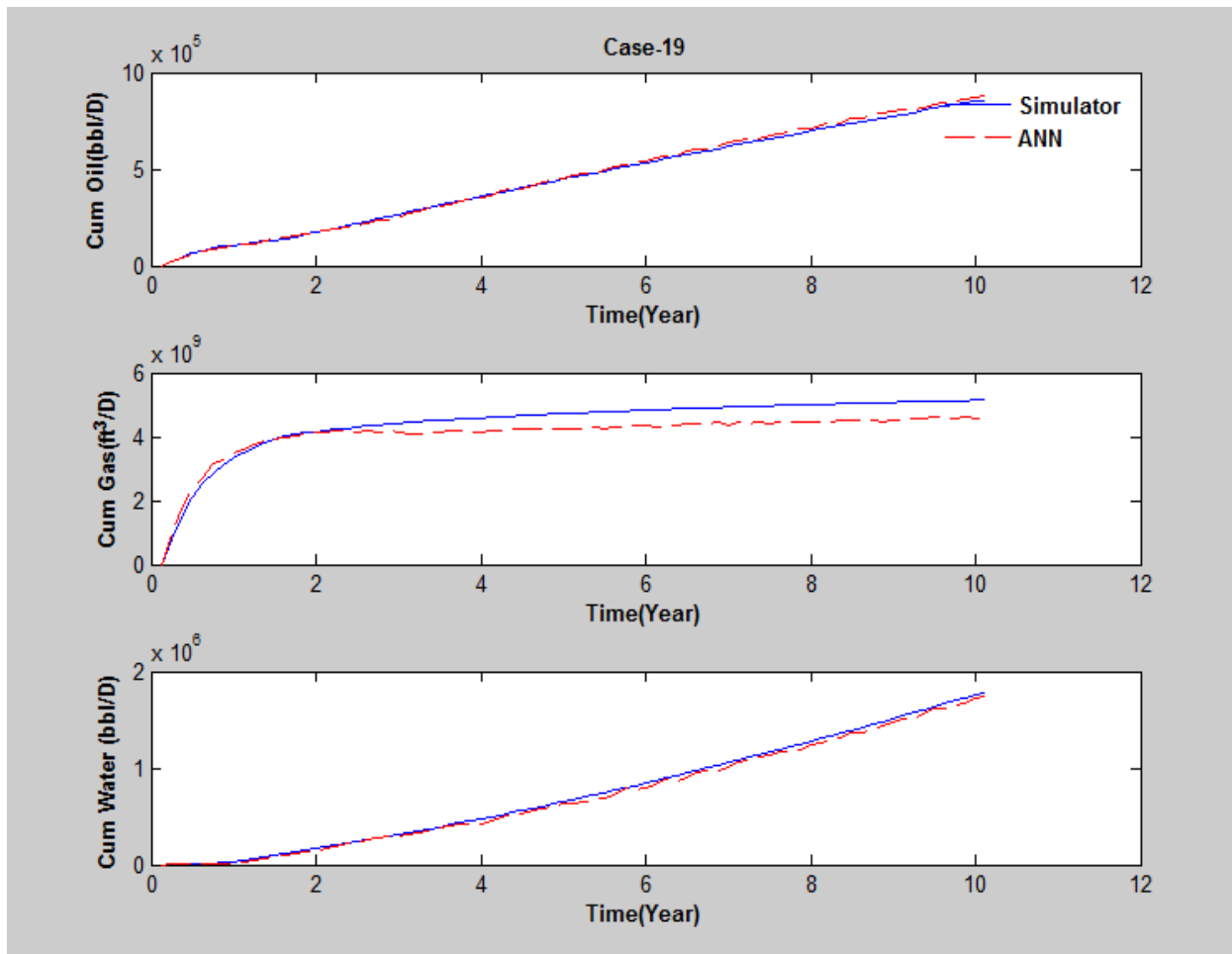


Figure 54: Comparison of cumulative production profiles generated by ANN and numerical simulator (Case-19)

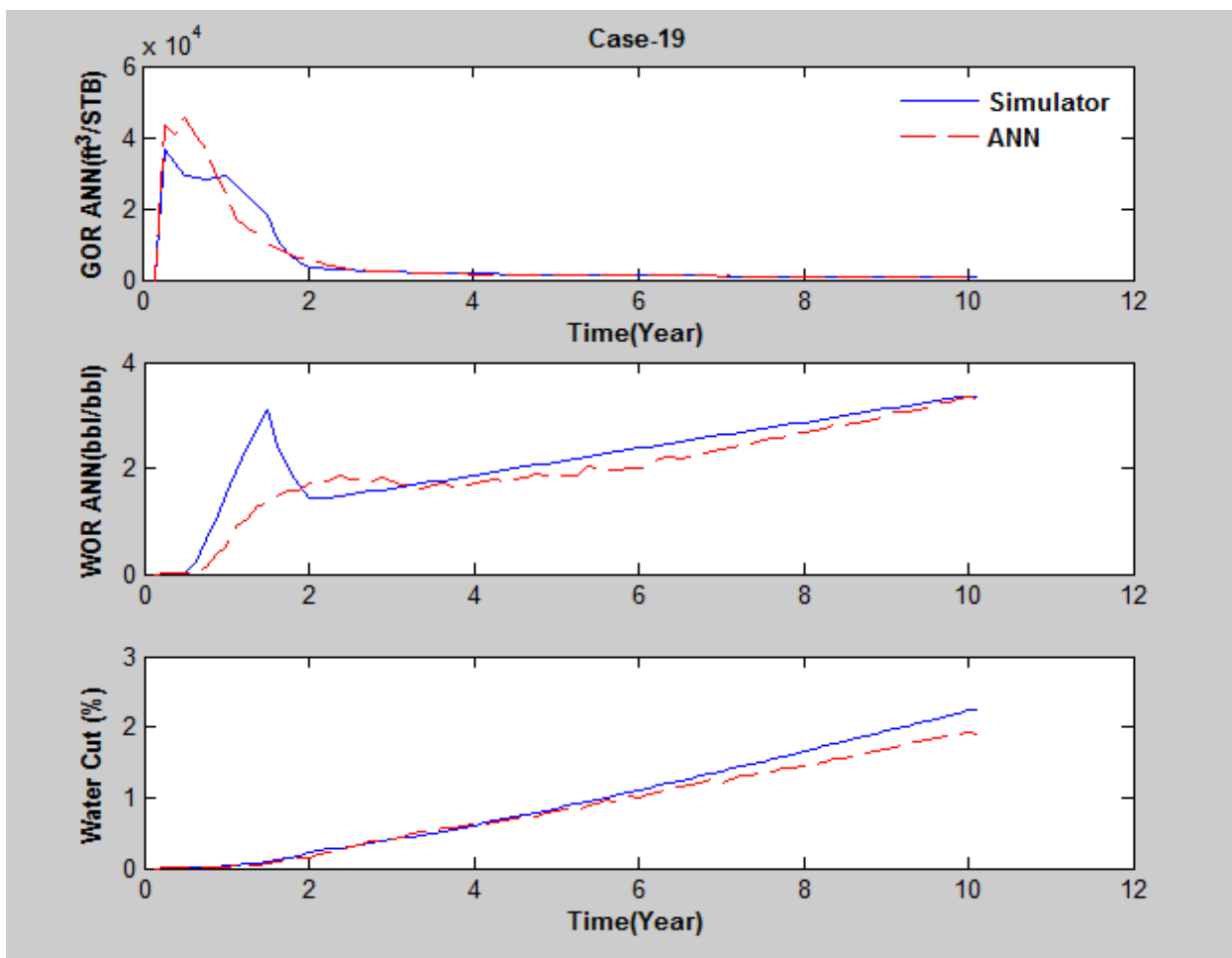


Figure 55: Comparison of Gas Oil Ratio, Water Oil Ratio and water cut production profiles generated by ANN and numerical simulator (Case-19)

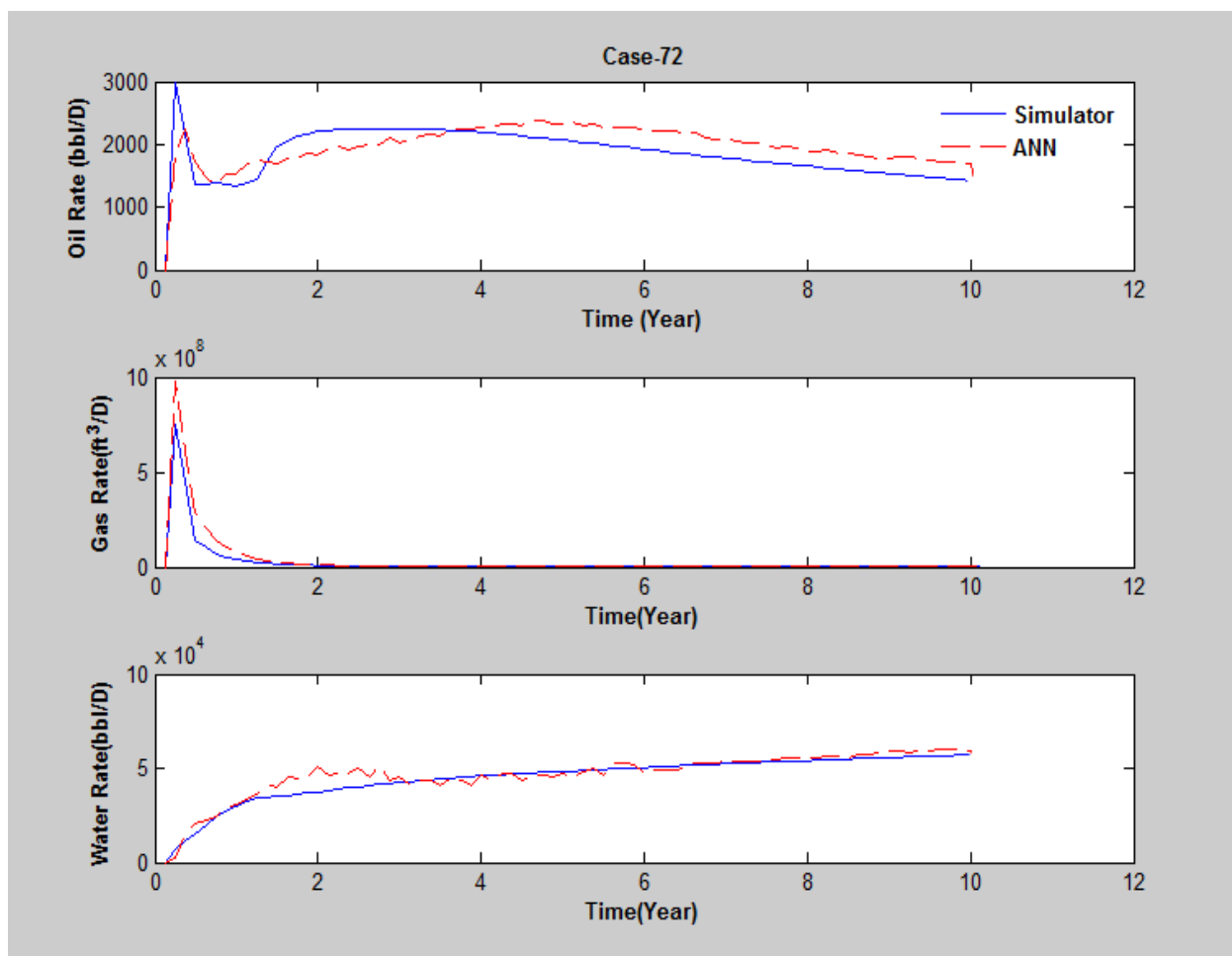


Figure 56: Comparison of production profiles generated by ANN and numerical simulator (Case-72)



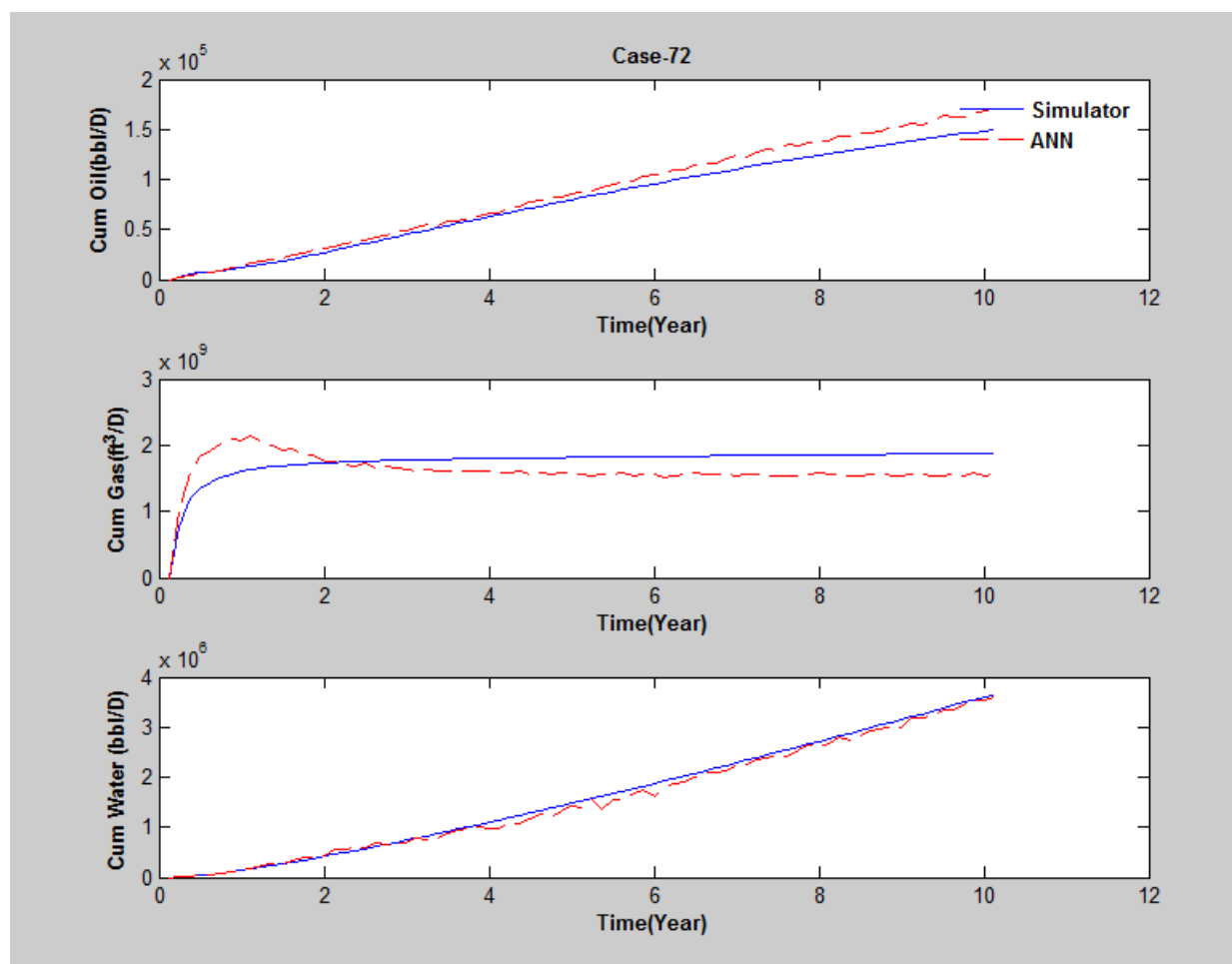


Figure 57: Comparison of cumulative production profiles generated by ANN and numerical simulator (Case-72)

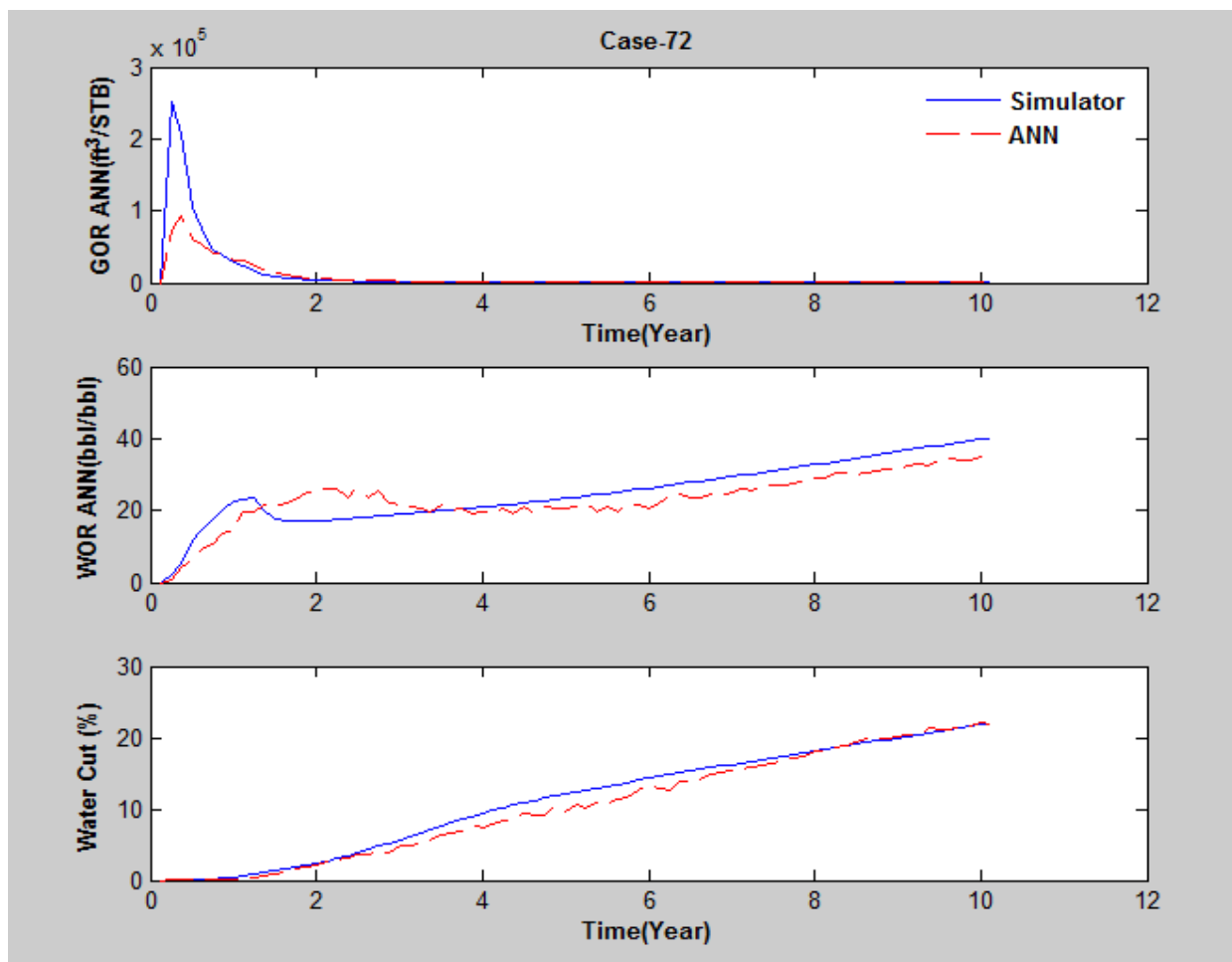


Figure 58: Comparison of Gas Oil Ratio, Water Oil Ratio and water cut production profiles generated by ANN and numerical simulator (Case-72)

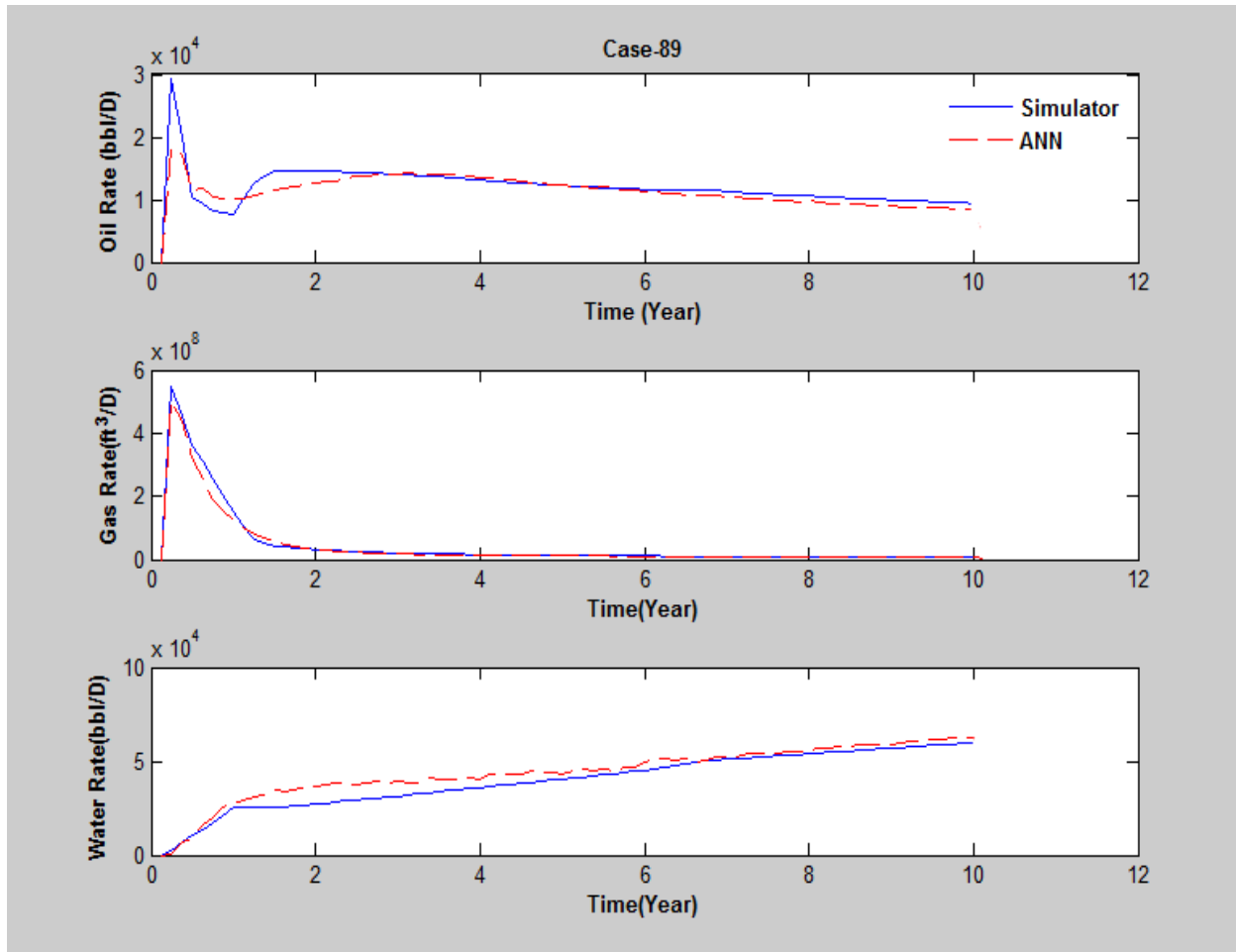


Figure 59: Comparison of production profiles generated by ANN and numerical simulator (Case-89)

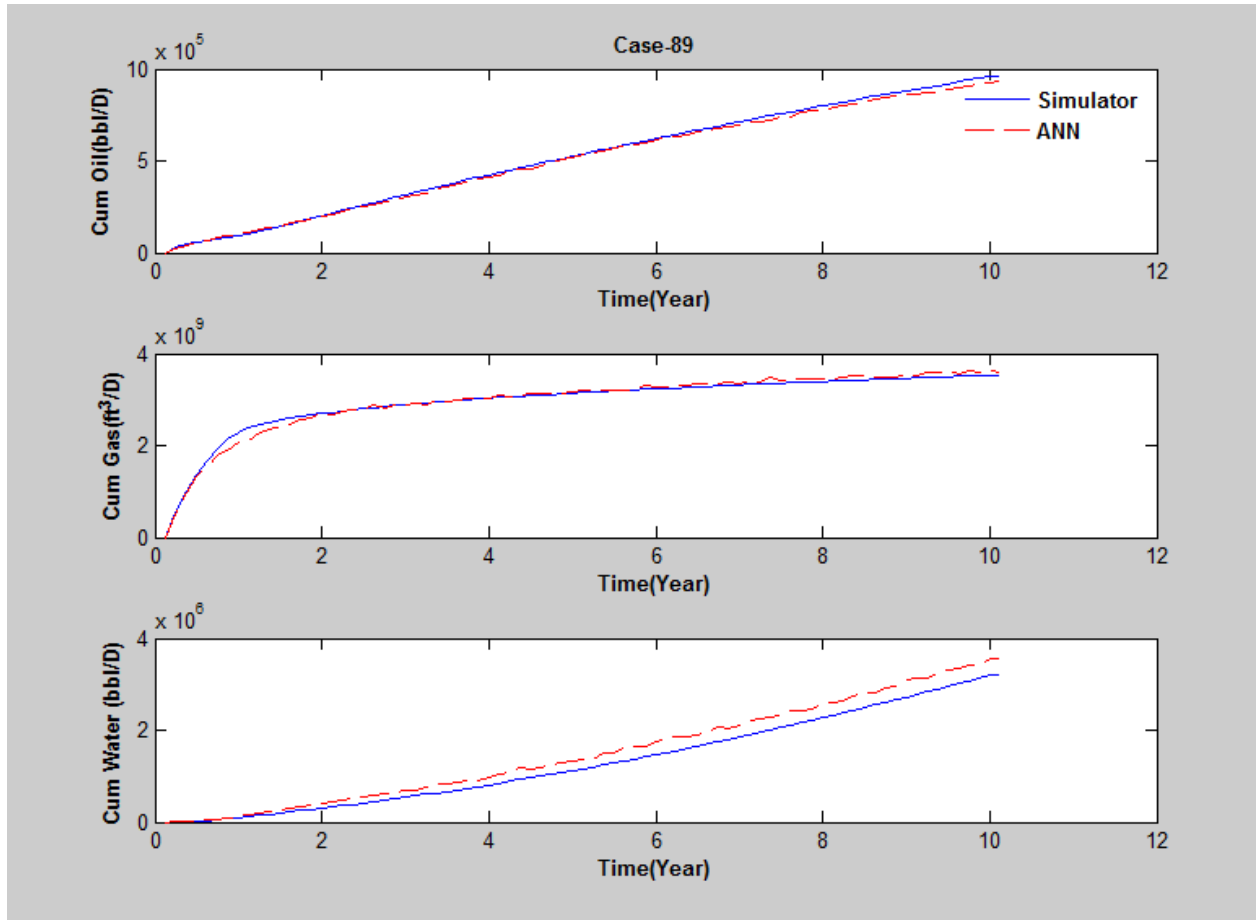


Figure 60: Comparison of cumulative production profiles generated by ANN and numerical simulator (Case-89)

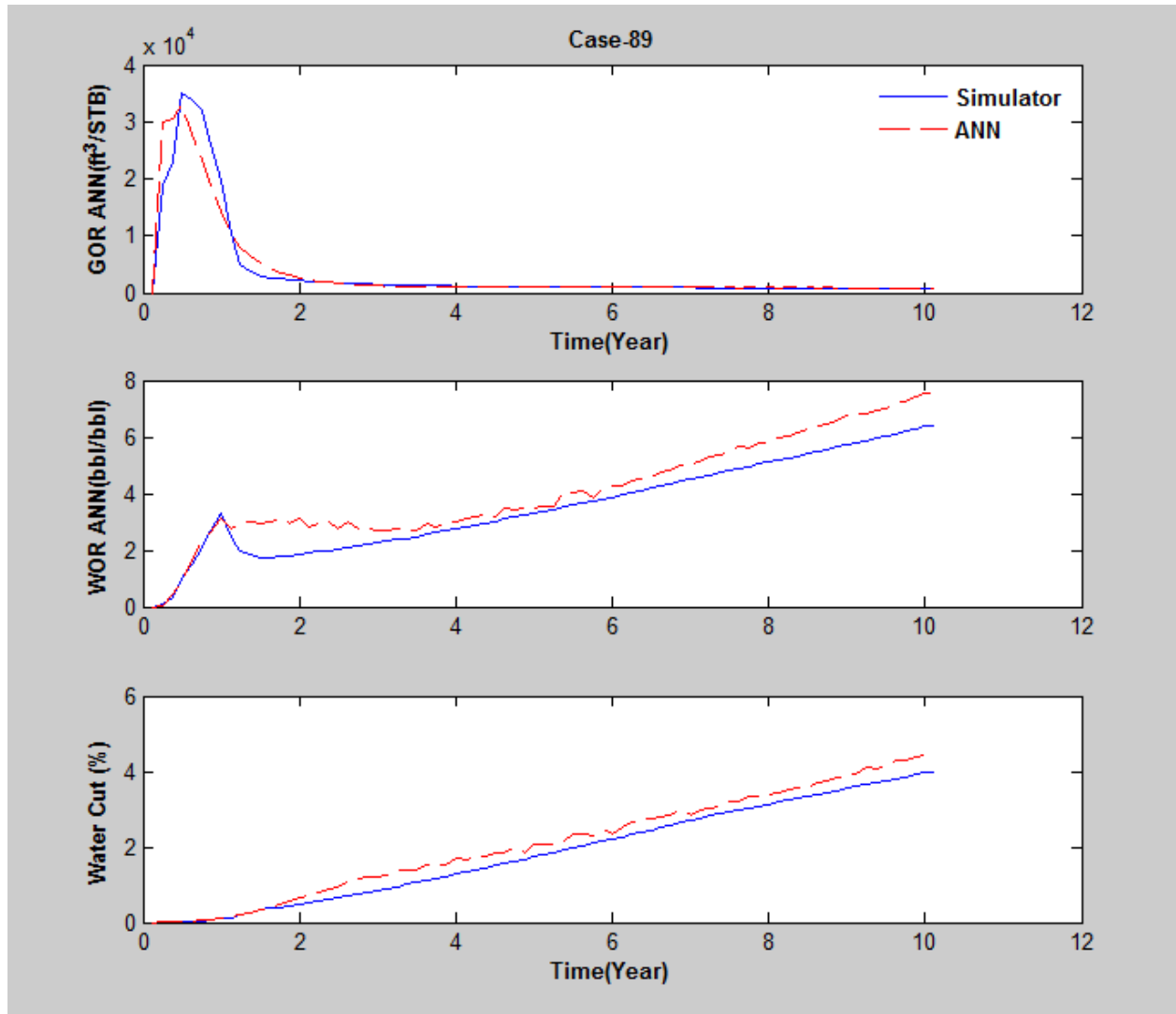


Figure 61: Comparison of Gas Oil Ratio, Water Oil Ratio and water cut production profiles generated by ANN and numerical simulator (Case-89)

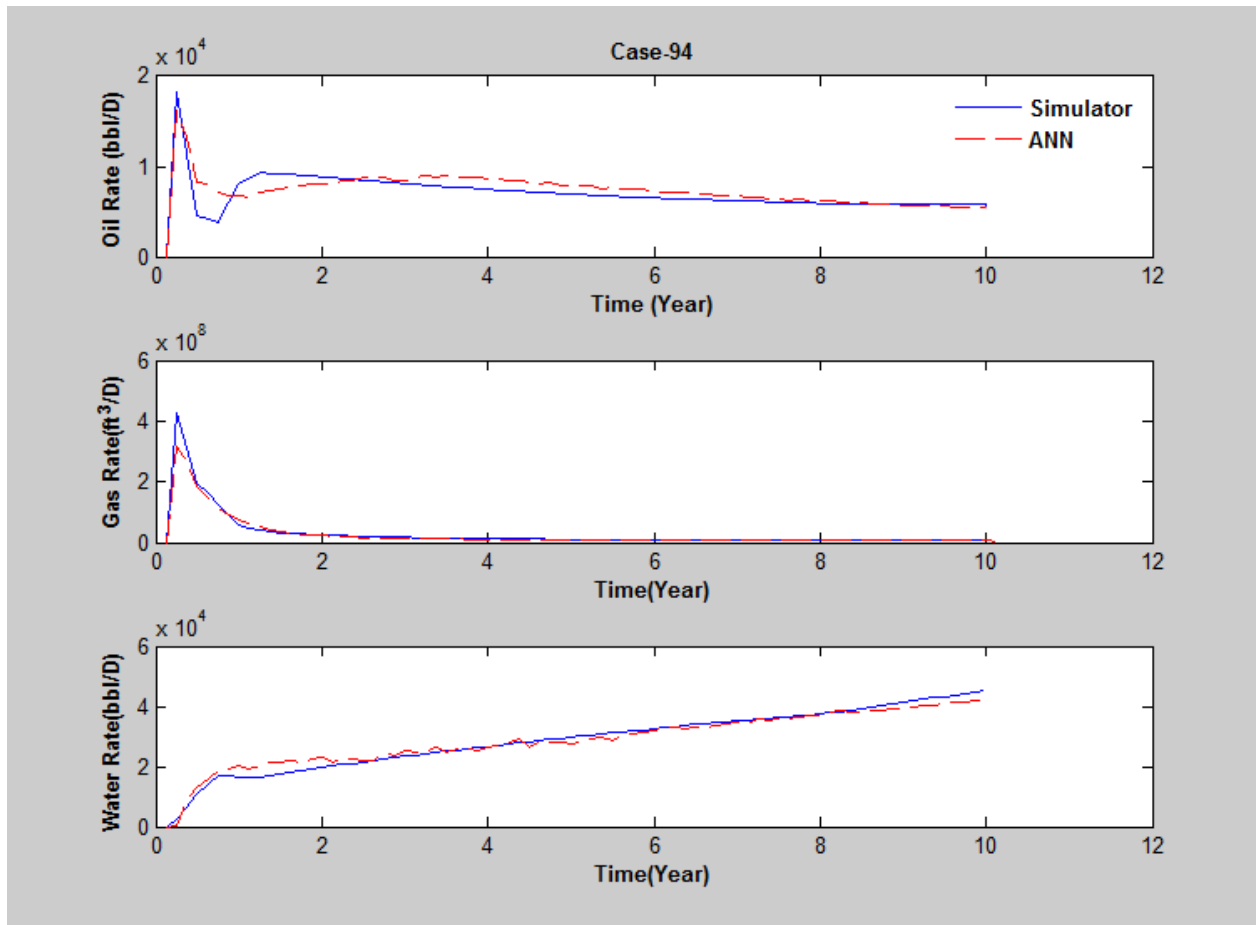


Figure 62: Comparison of production profiles generated by ANN and numerical simulator (Case-94)

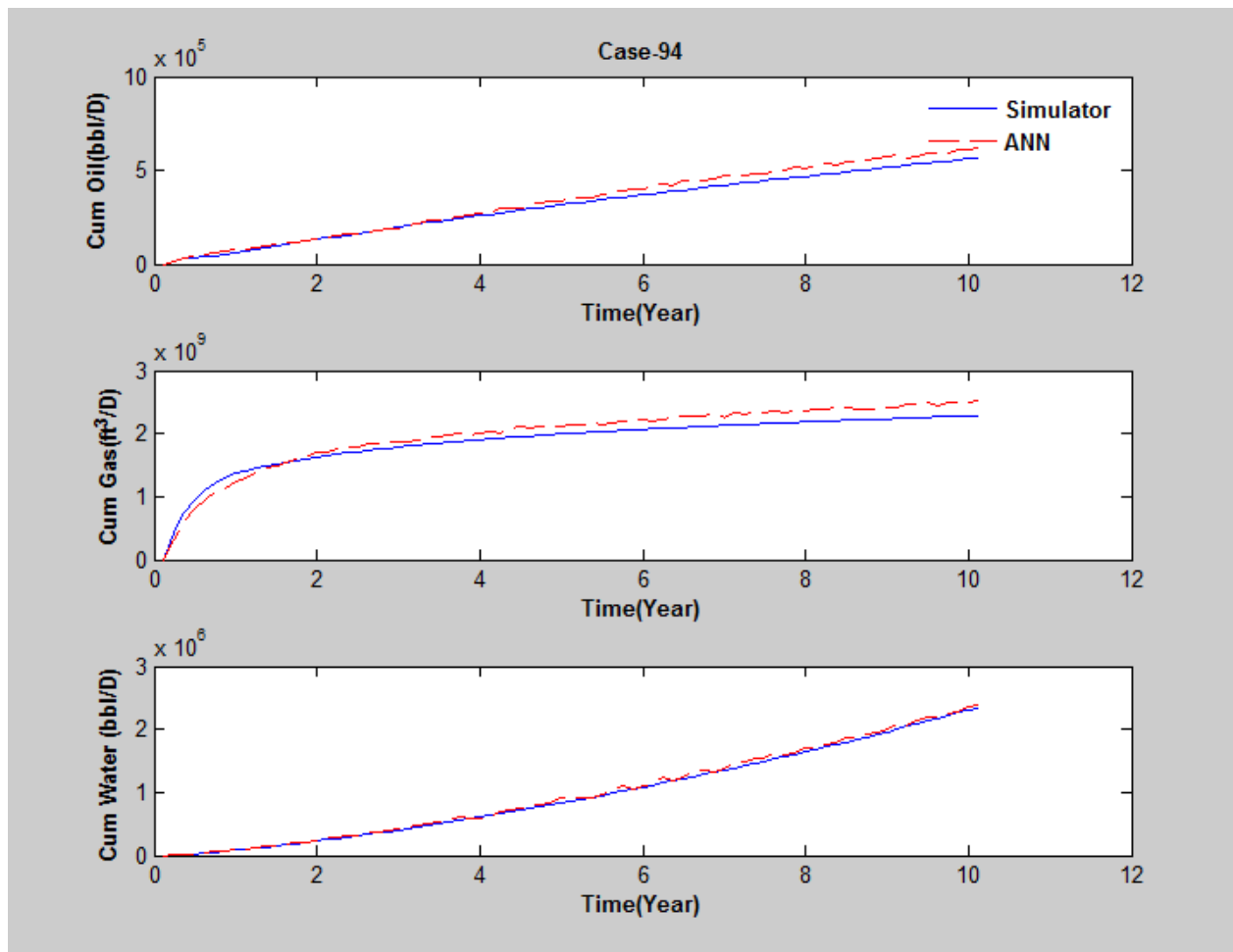


Figure 63: Comparison of cumulative production profiles generated by ANN and numerical simulator (Case-94)

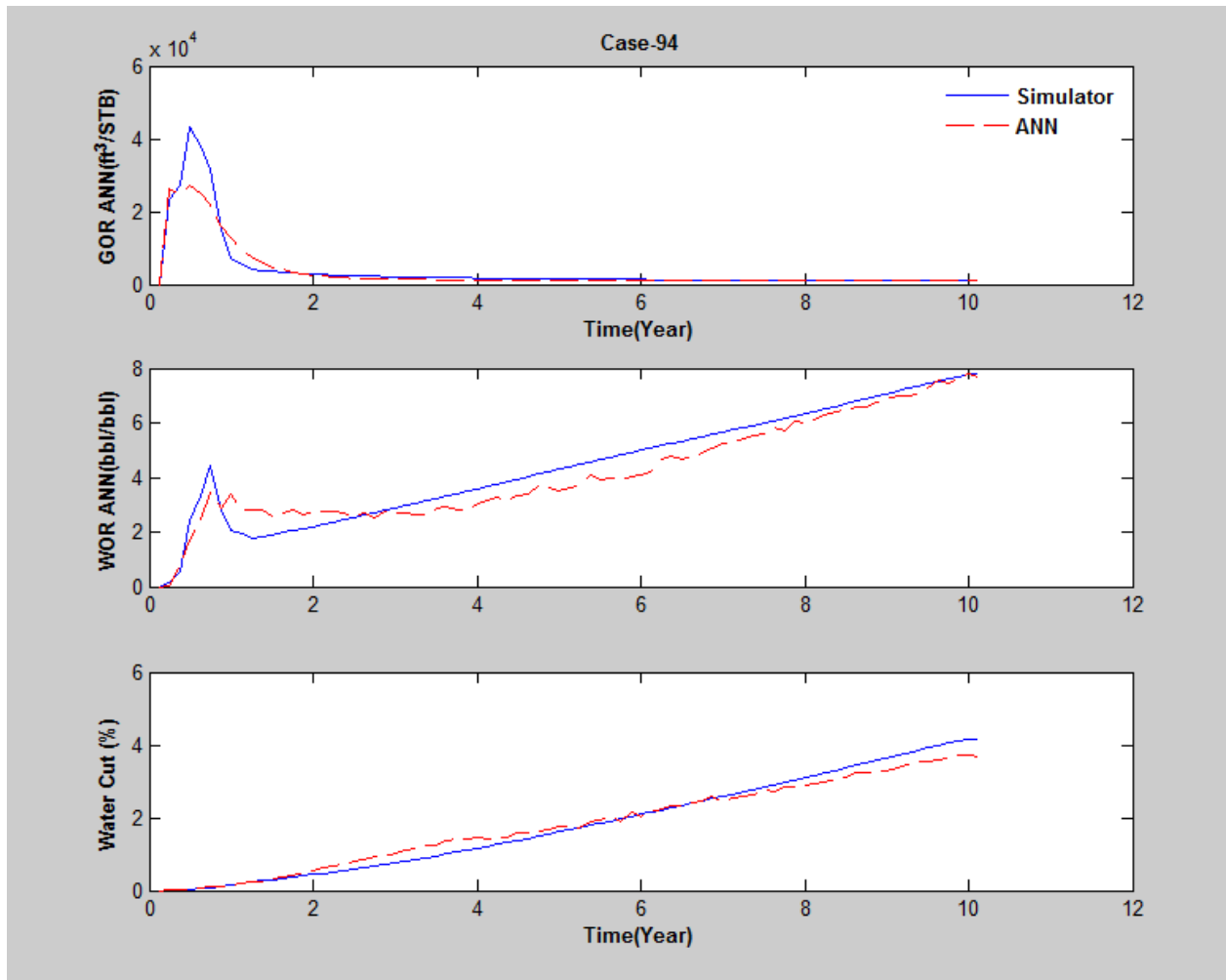


Figure 64: Comparison of Gas Oil Ratio, Water Oil Ratio and water cut production profiles generated by ANN and numerical simulator (Case-94)



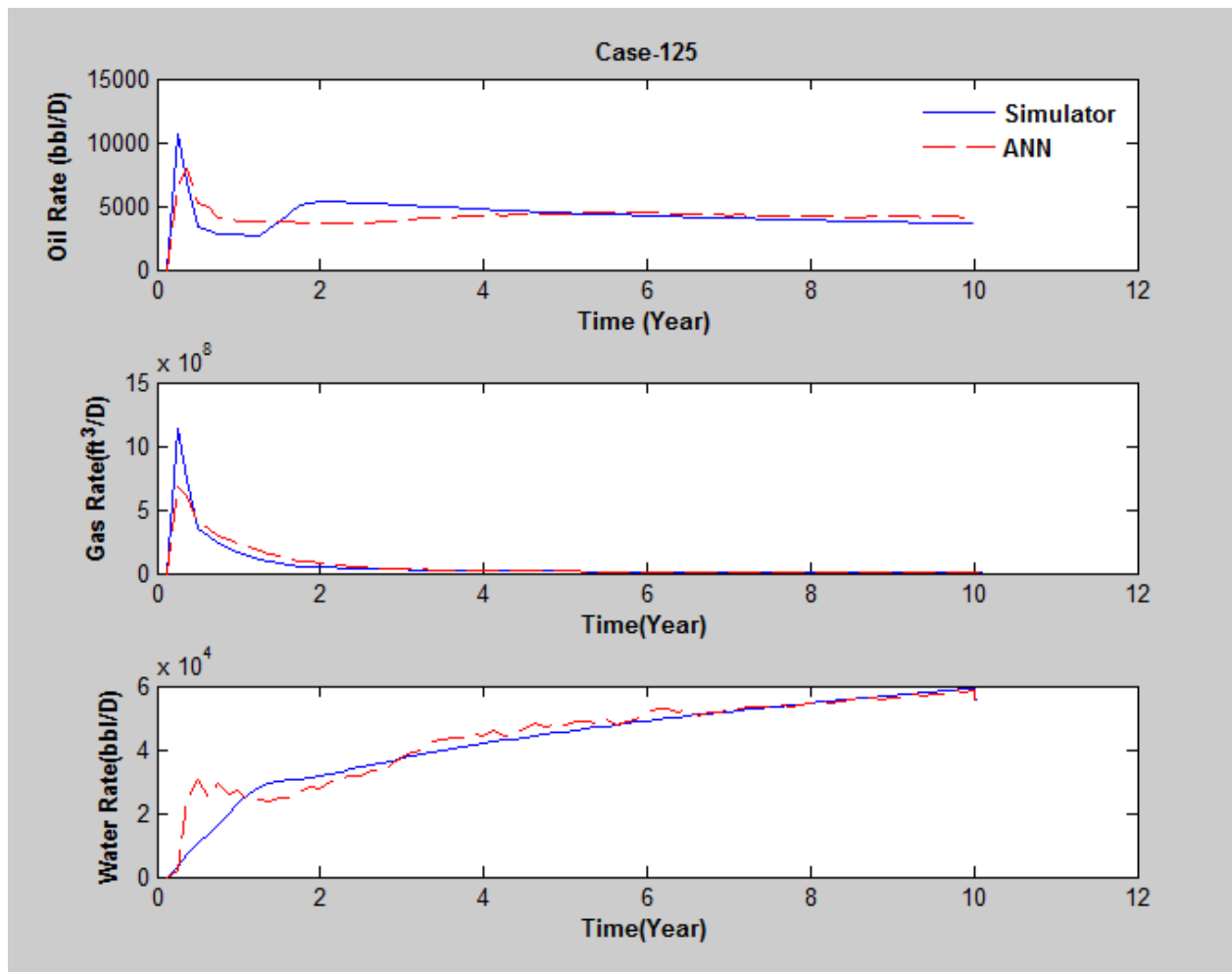


Figure 65: Comparison of production profiles generated by ANN and numerical simulator (Case-125)

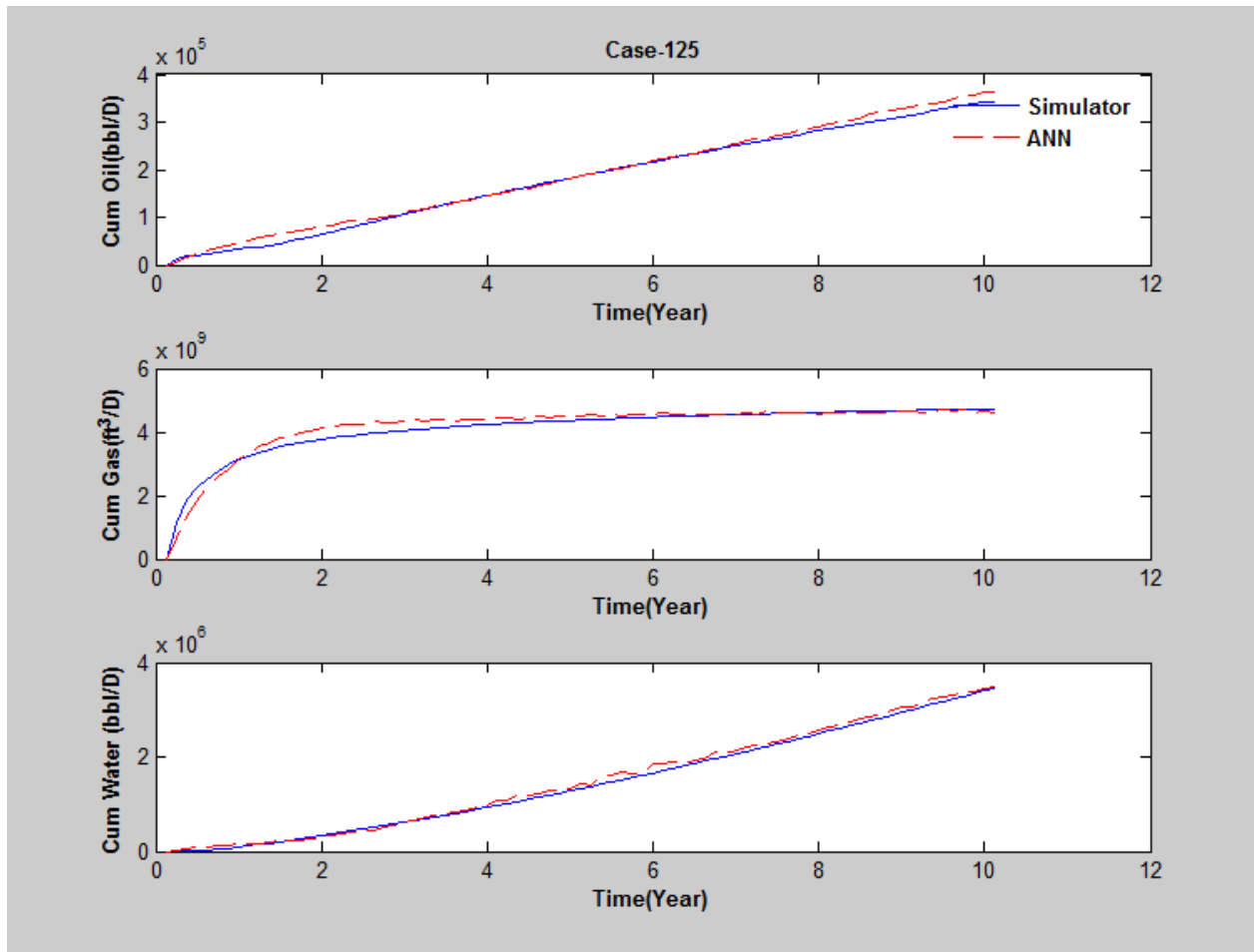


Figure 66: Comparison of cumulative production profiles generated by ANN and numerical simulator (Case-125)

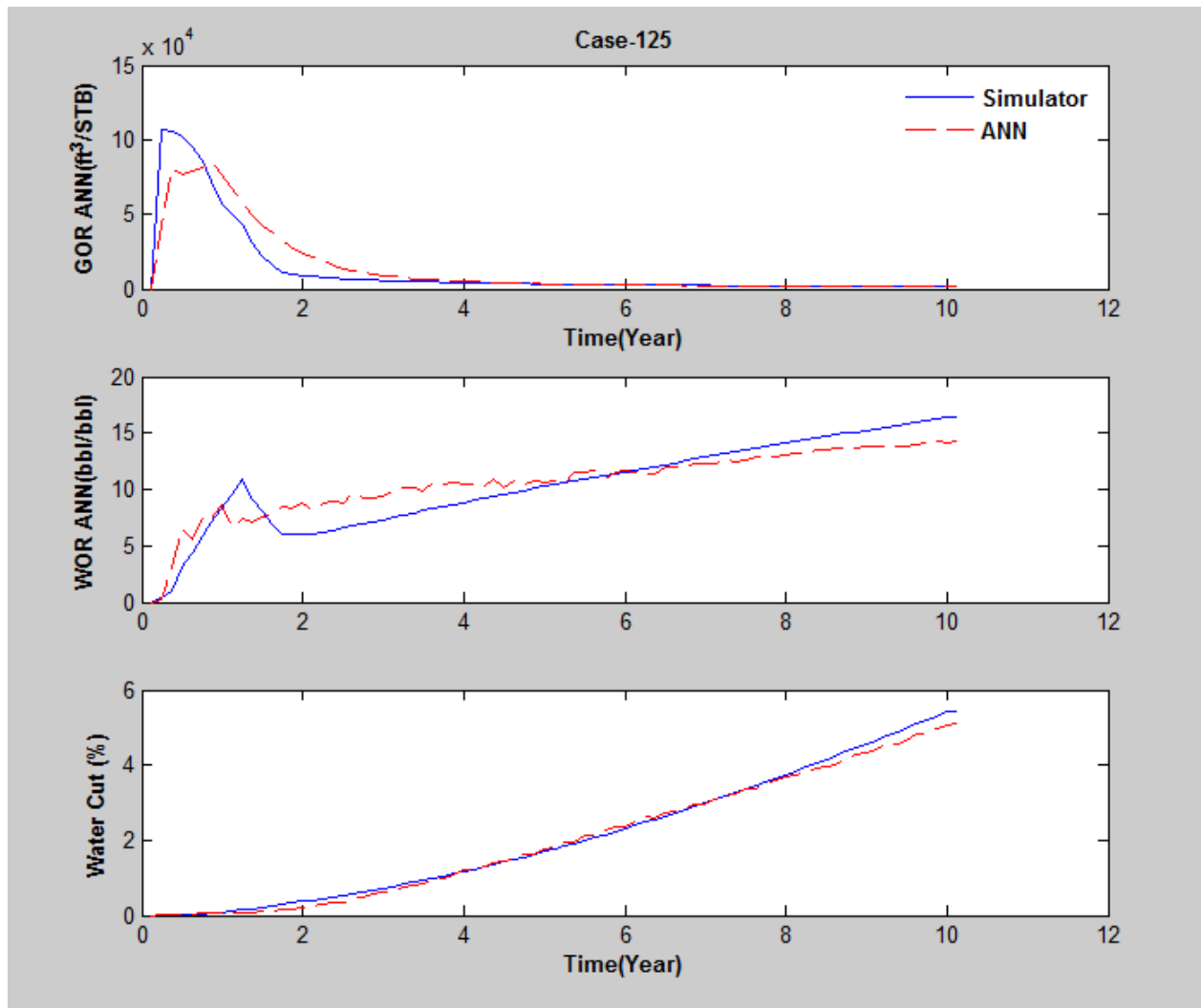


Figure 67: Comparison of Gas Oil Ratio, Water Oil Ratio and water cut production profiles generated by ANN and numerical simulator (Case-125)

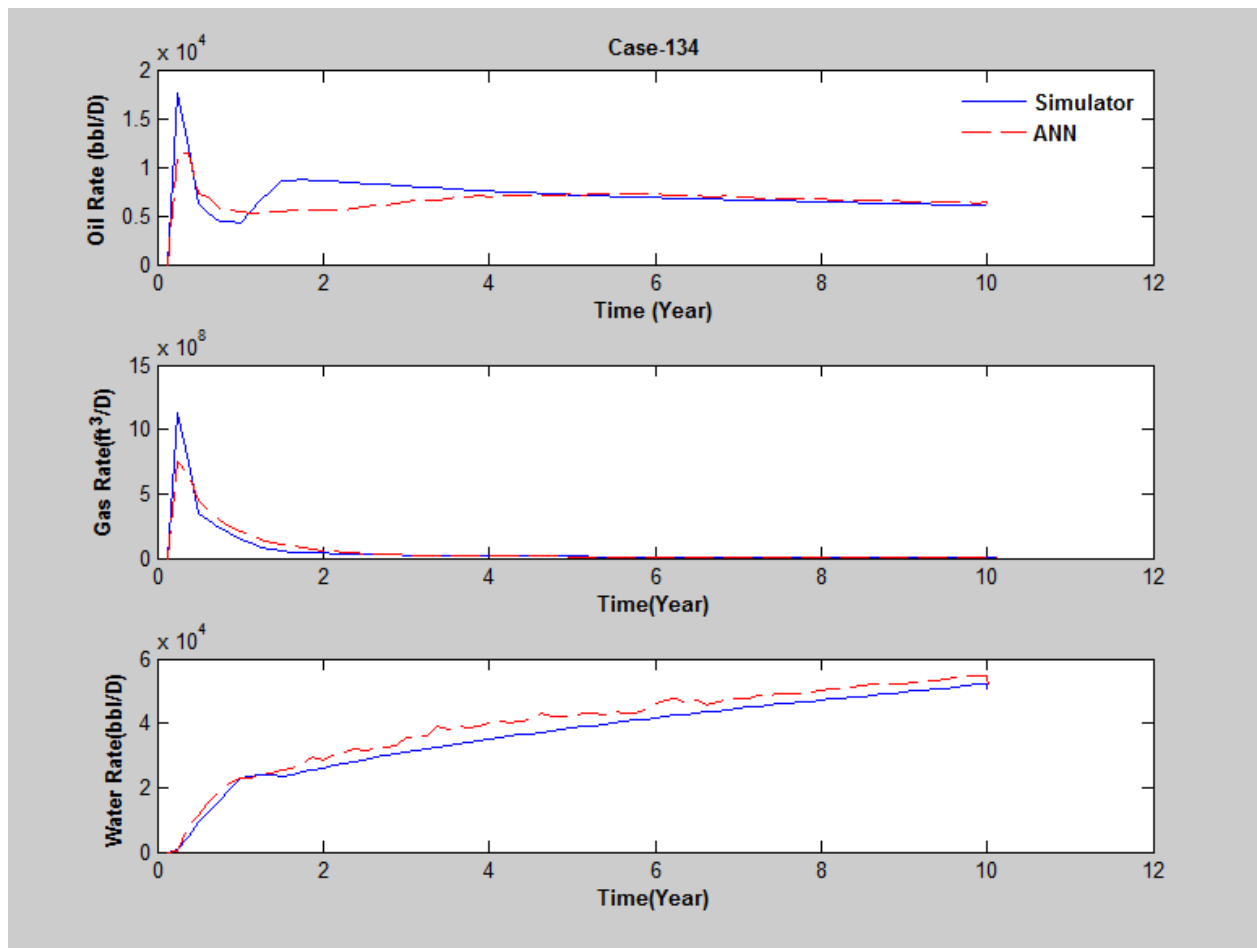


Figure 68: Comparison of production profiles generated by ANN and numerical simulator (Case-134)

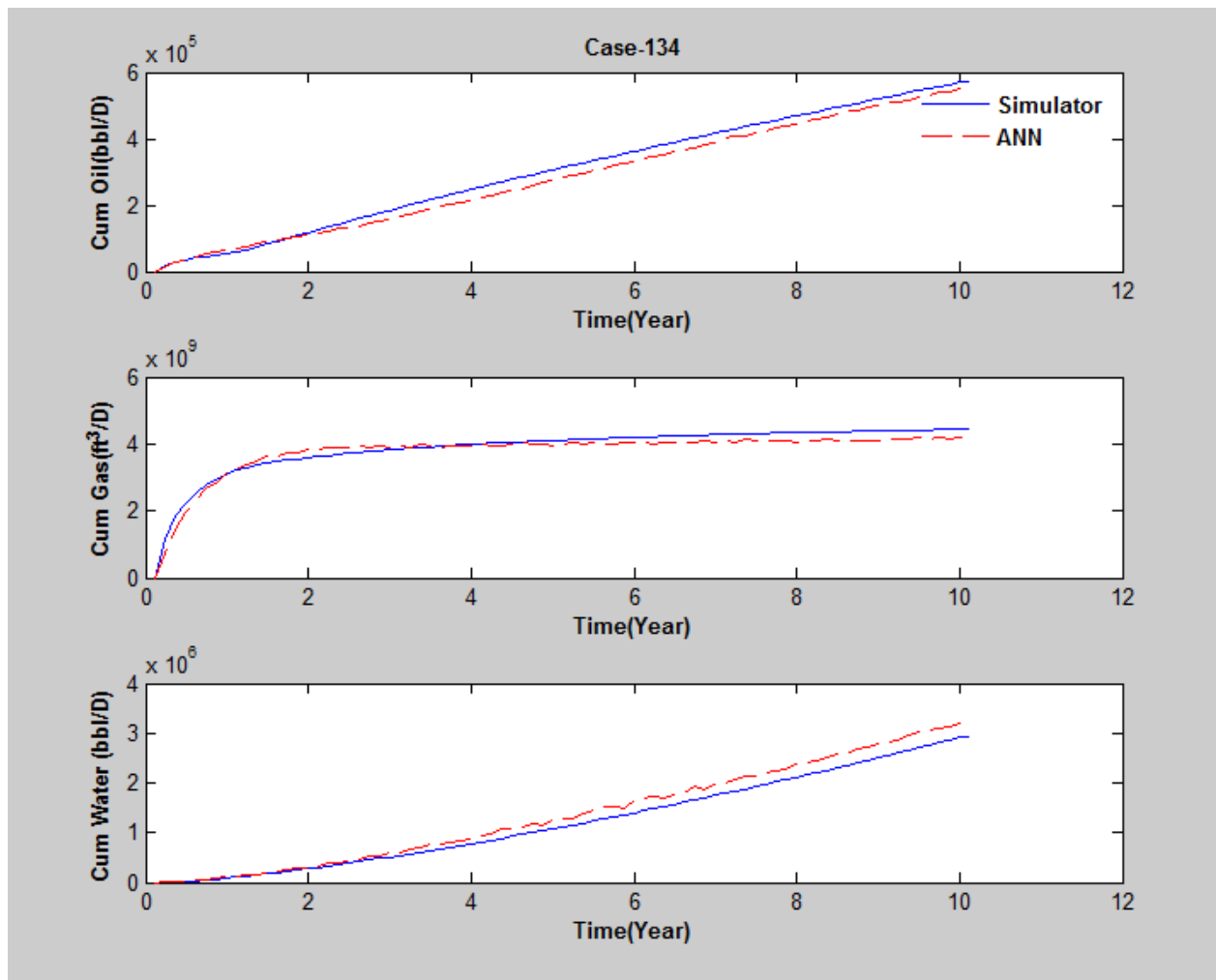


Figure 69: Comparison of cumulative production profiles generated by ANN and numerical simulator (Case-134)

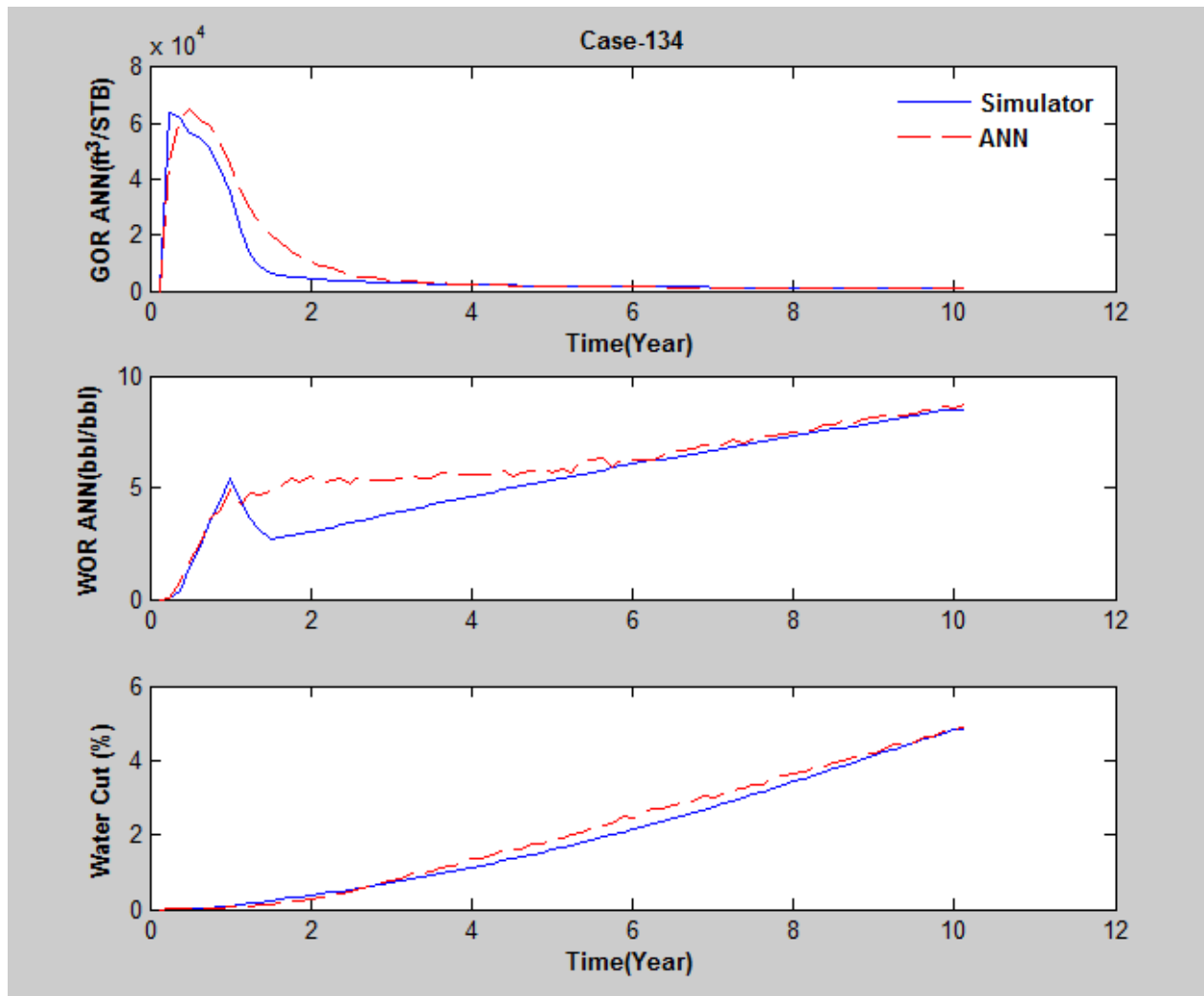


Figure 70: Comparison of Gas Oil Ratio, Water Oil Ratio and water cut production profiles generated by ANN and numerical simulator (Case134)

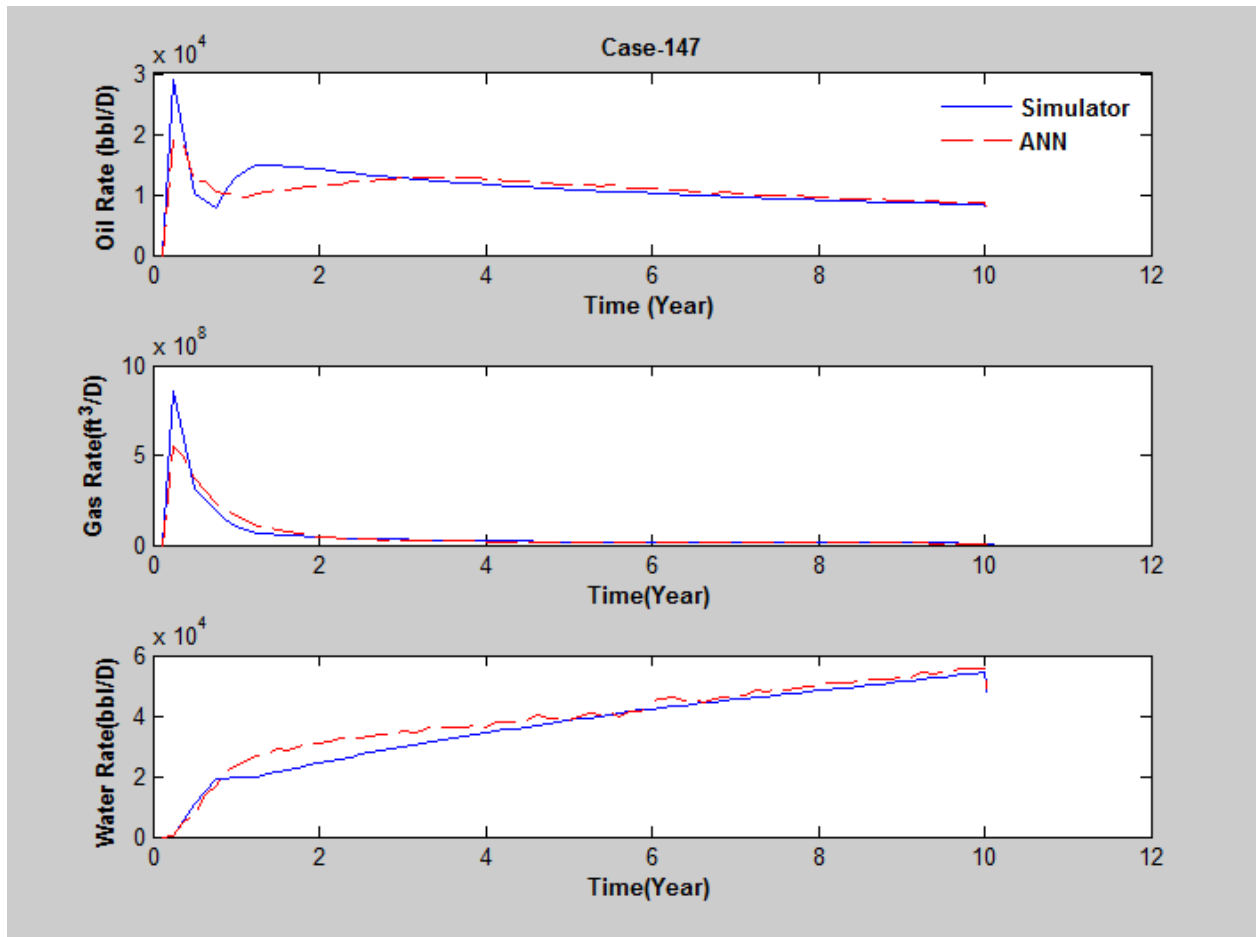


Figure 71: Comparison of production profiles generated by ANN and numerical simulator (Case-147)

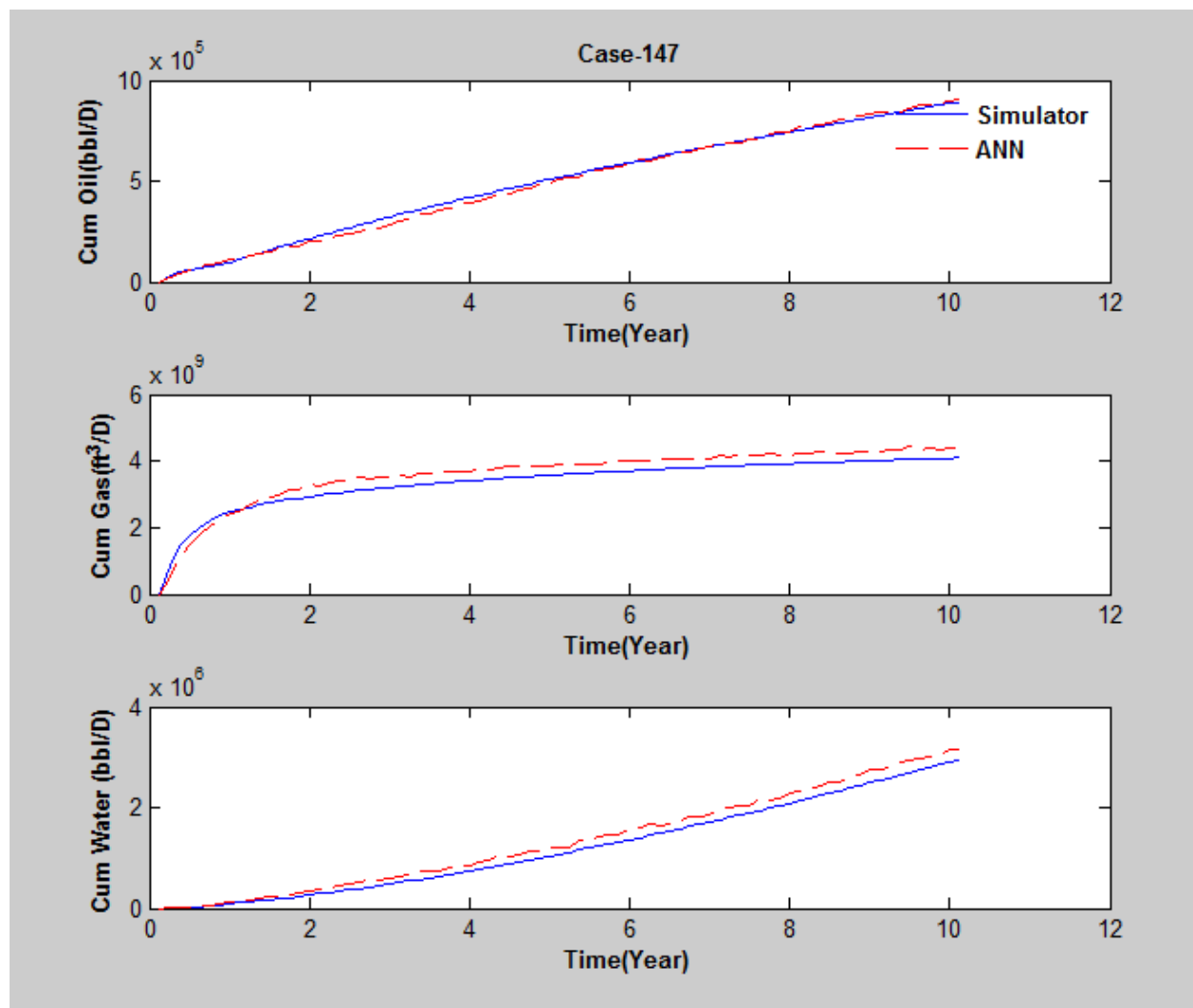


Figure 72: Comparison of cumulative production profiles generated by ANN and numerical simulator (Case-147)



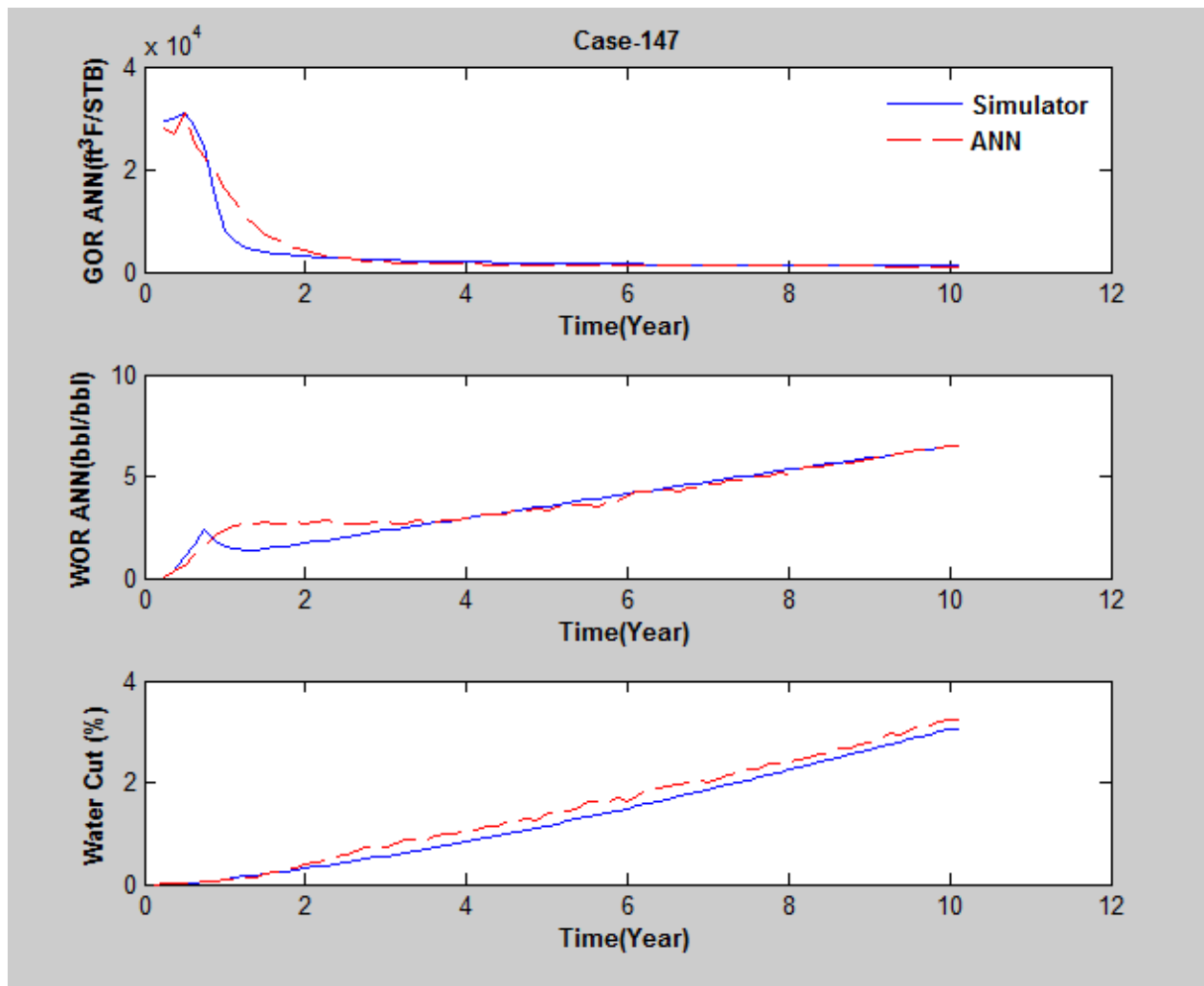


Figure 73: Comparison of Gas Oil Ratio, Water Oil Ratio and water cut production profiles generated by ANN and numerical simulator (Case-147)

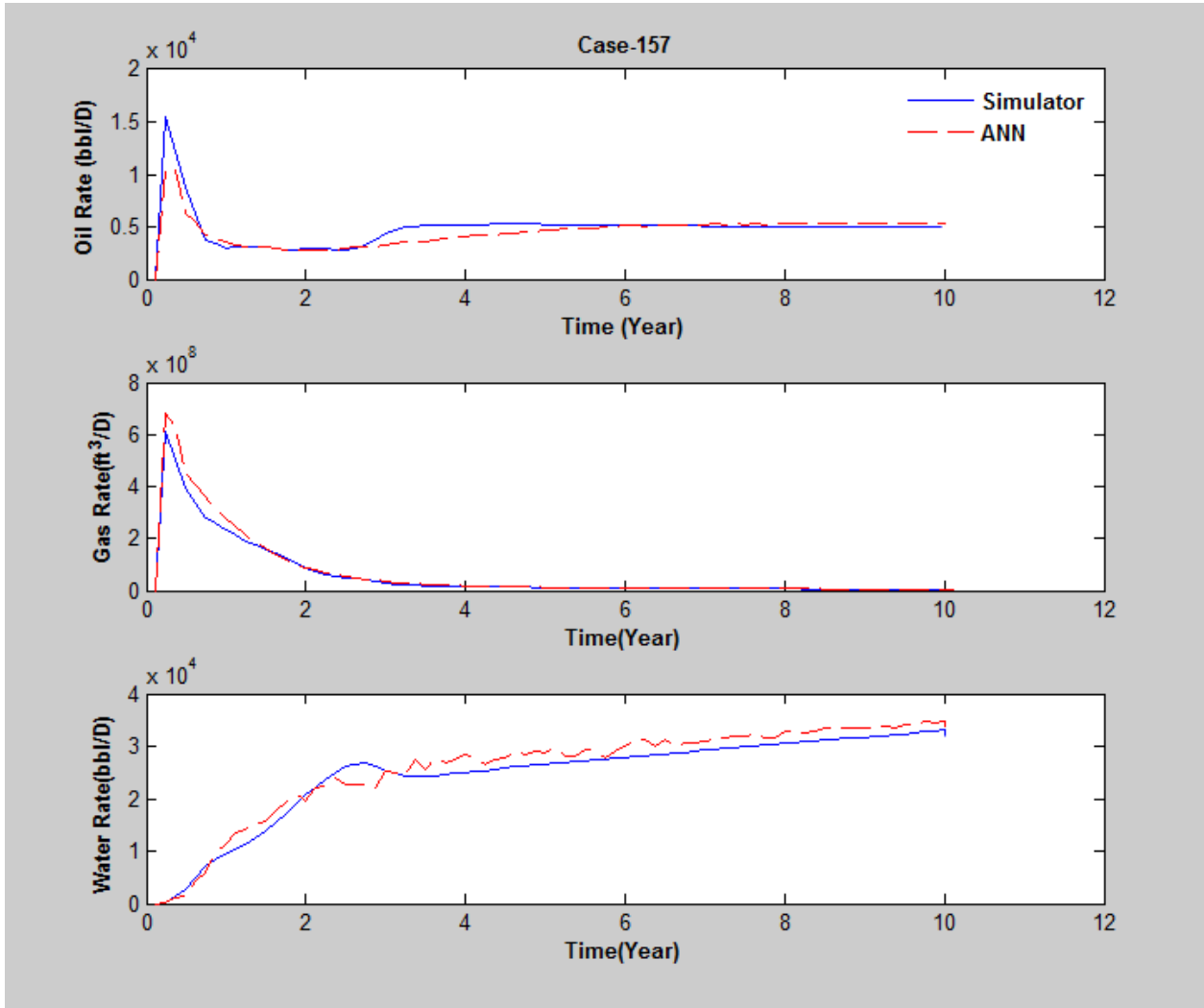


Figure 74: Comparison of production profiles generated by ANN and numerical simulator (Case-157)

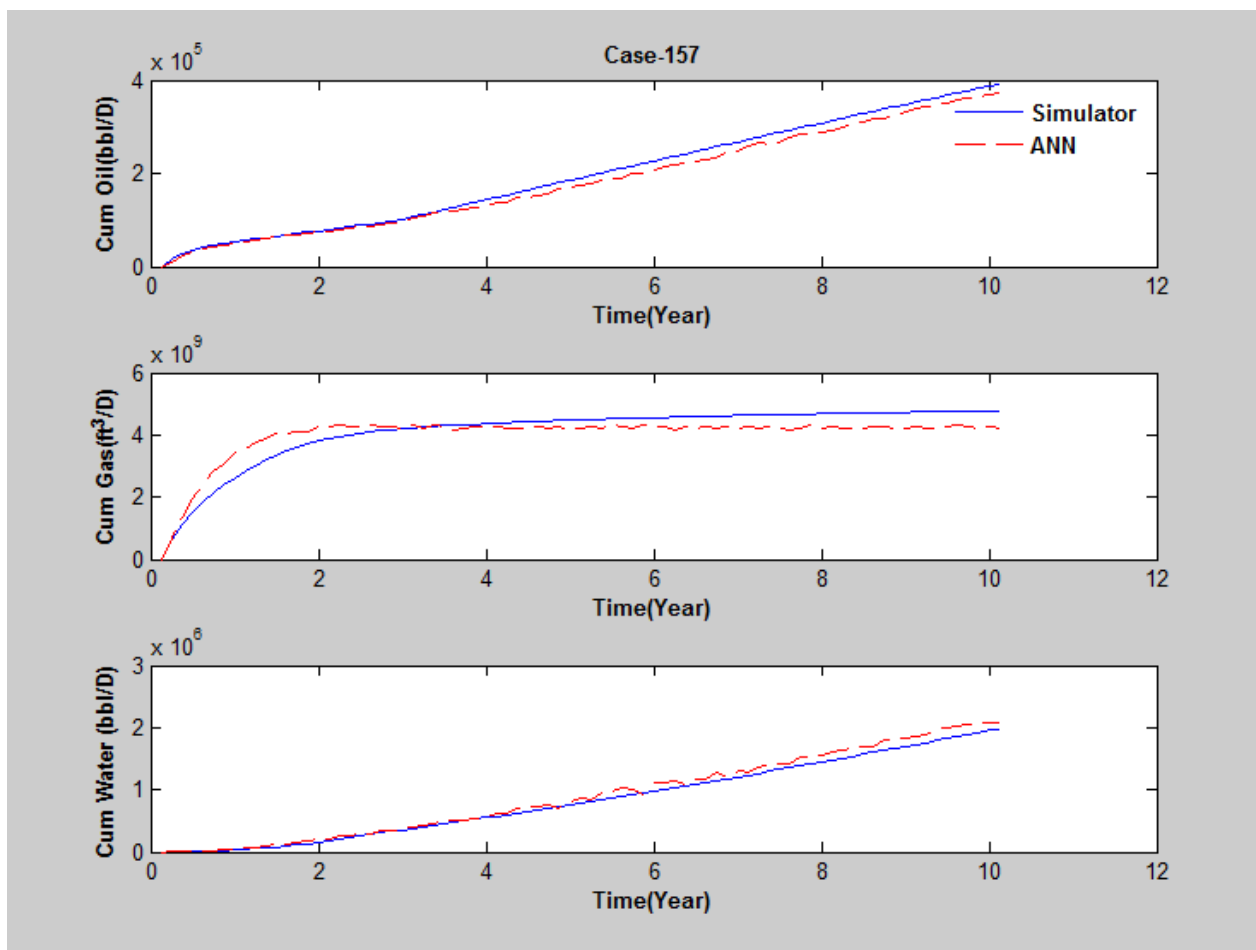


Figure 75: Comparison of cumulative production profiles generated by ANN and numerical simulator (Case-157)

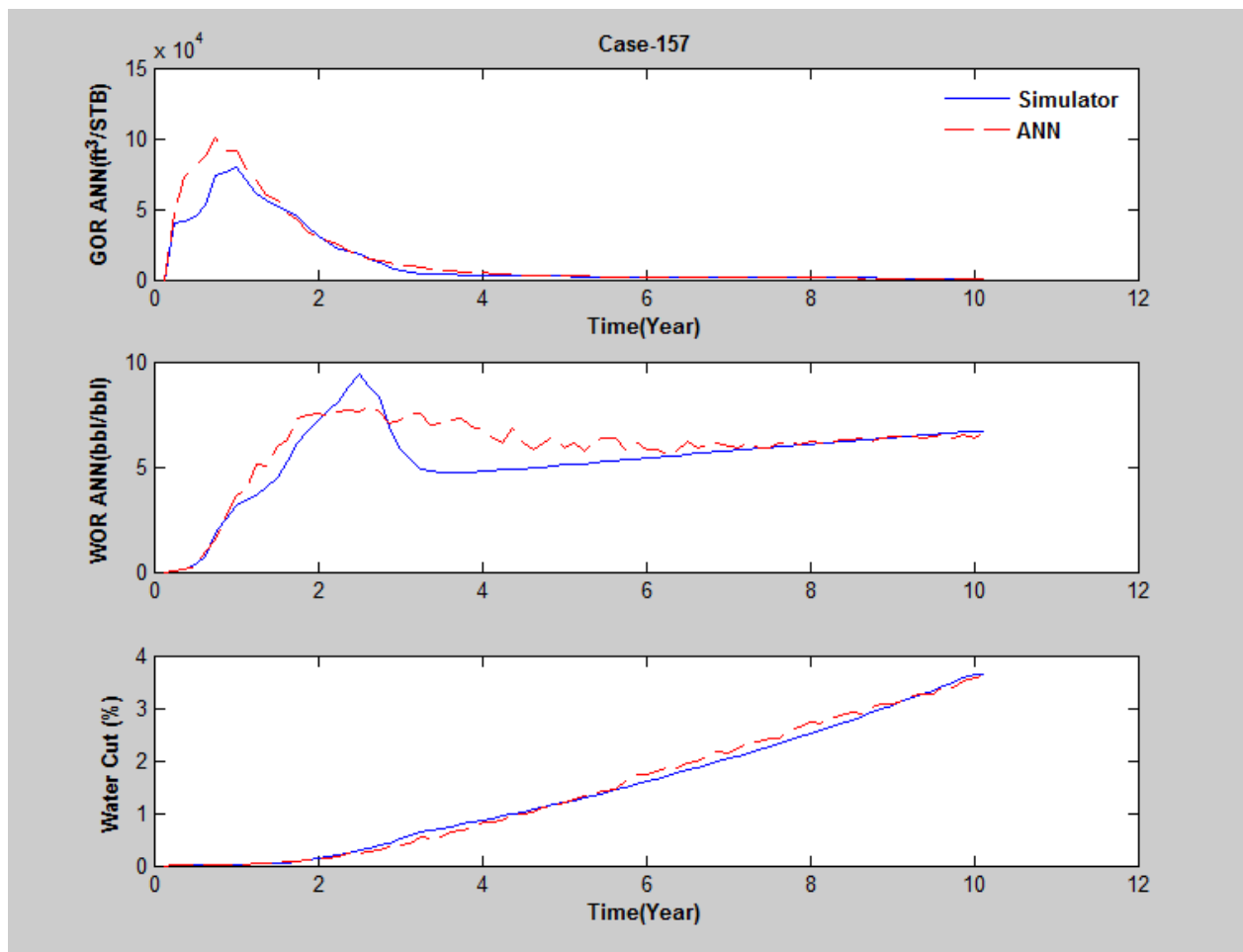


Figure 76: Comparison of Gas Oil Ratio, Water Oil Ratio and water cut production profiles generated by ANN and numerical simulator (Case-157)

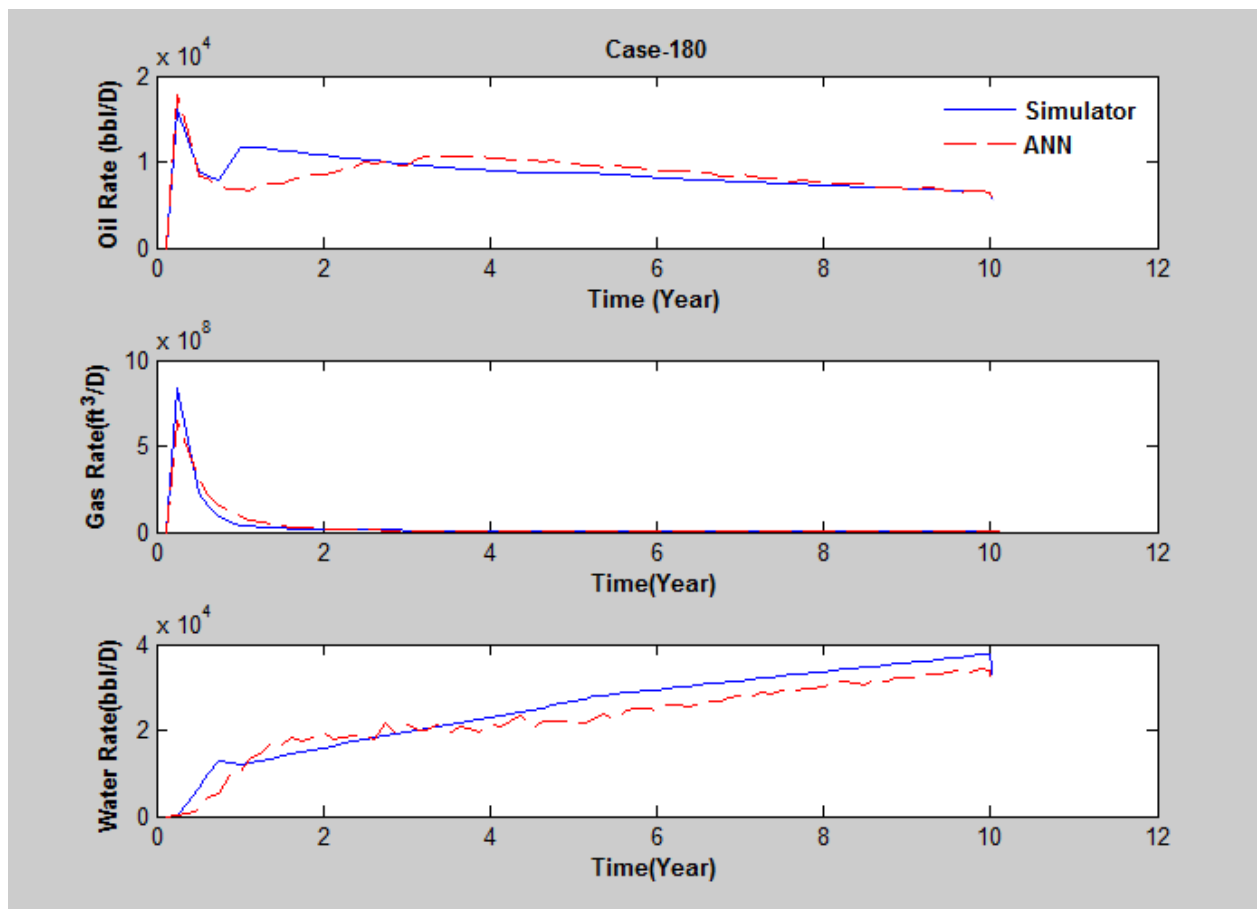


Figure 77: Comparison of production profiles generated by ANN and numerical simulator (Case-180)

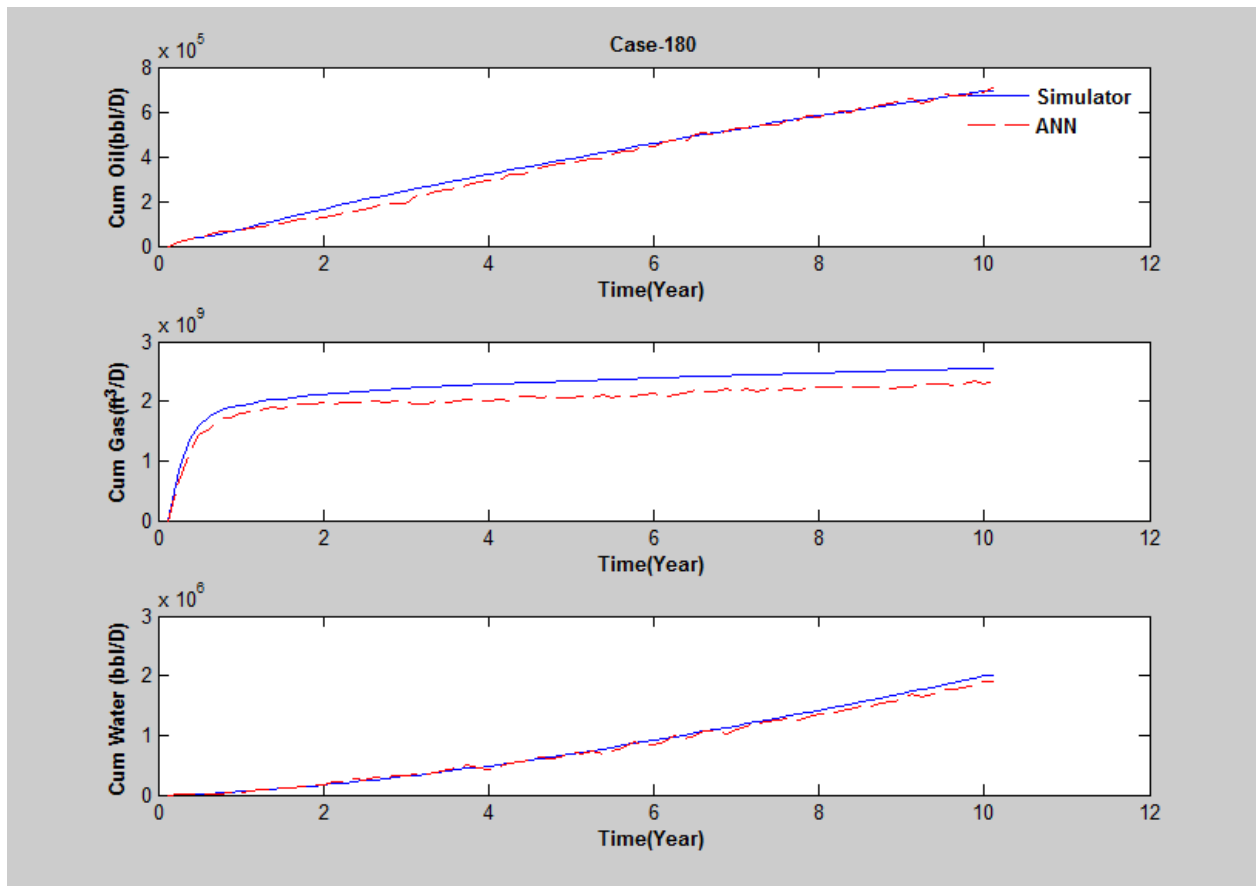


Figure 78: Comparison of cumulative production profiles generated by ANN and numerical simulator (Case-180)

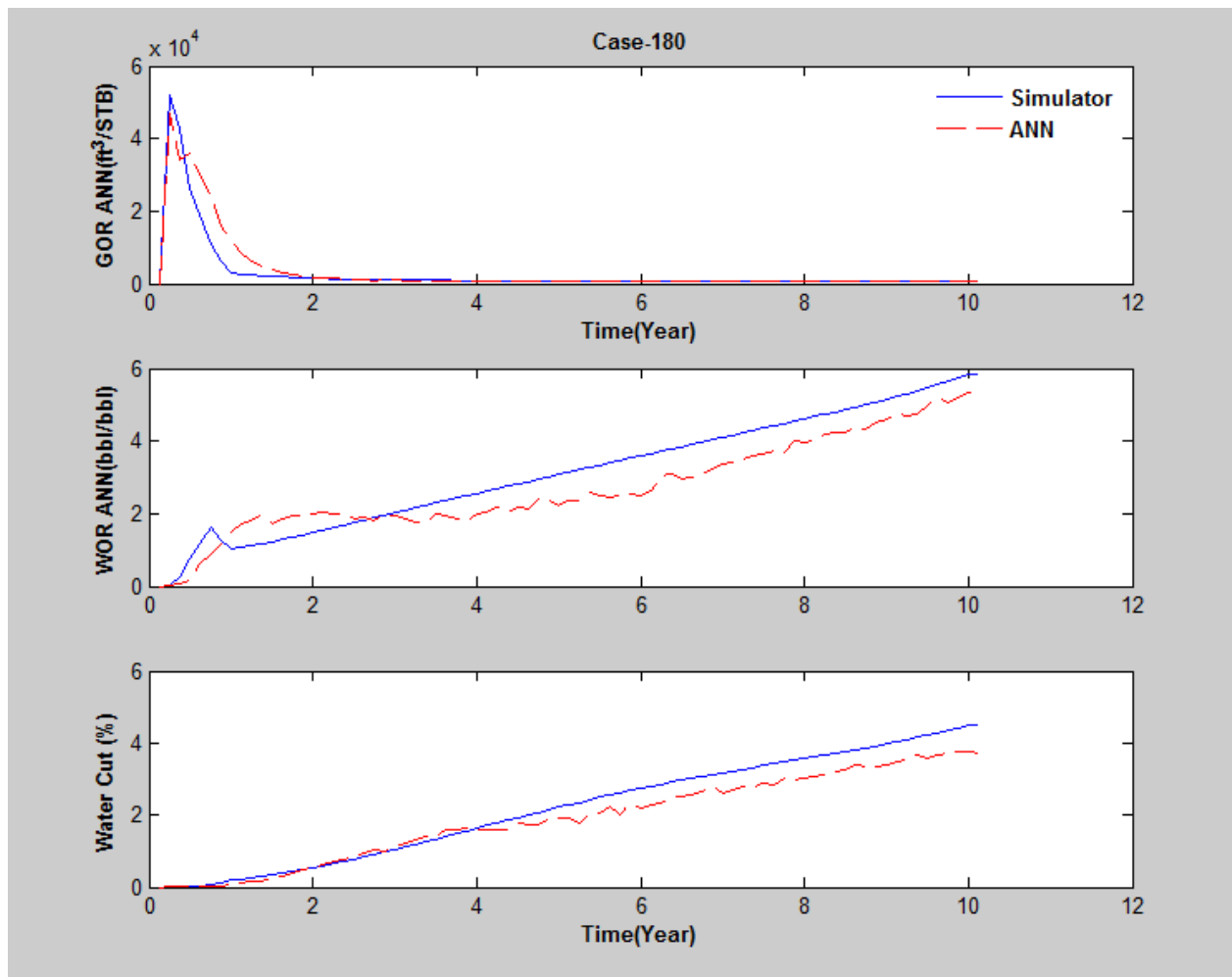


Figure 79: Comparison of Gas Oil Ratio, Water Oil Ratio and water cut production profiles generated by ANN and numerical simulator (Case-180)

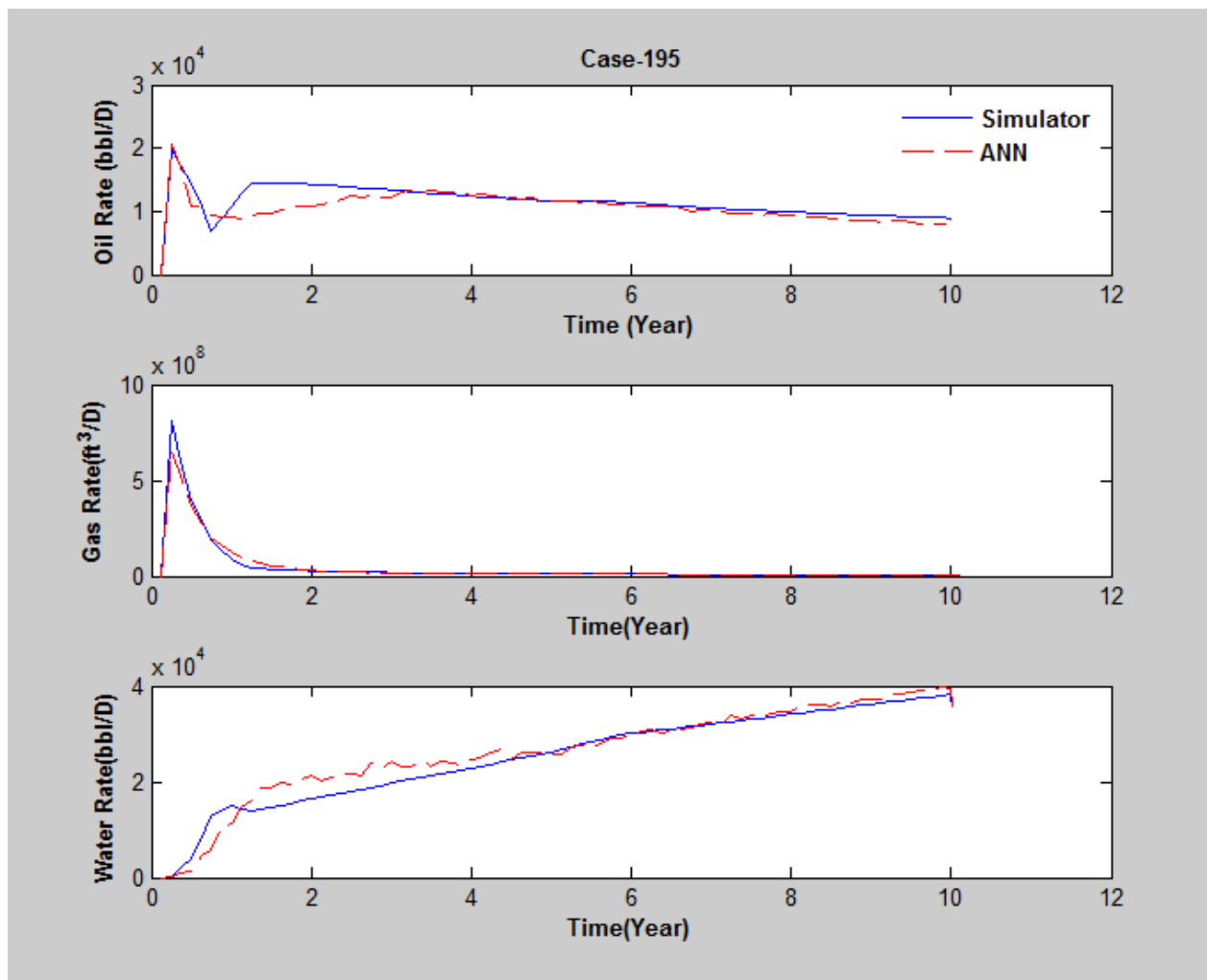


Figure 80: Comparison of production profiles generated by ANN and numerical simulator (Case-195)



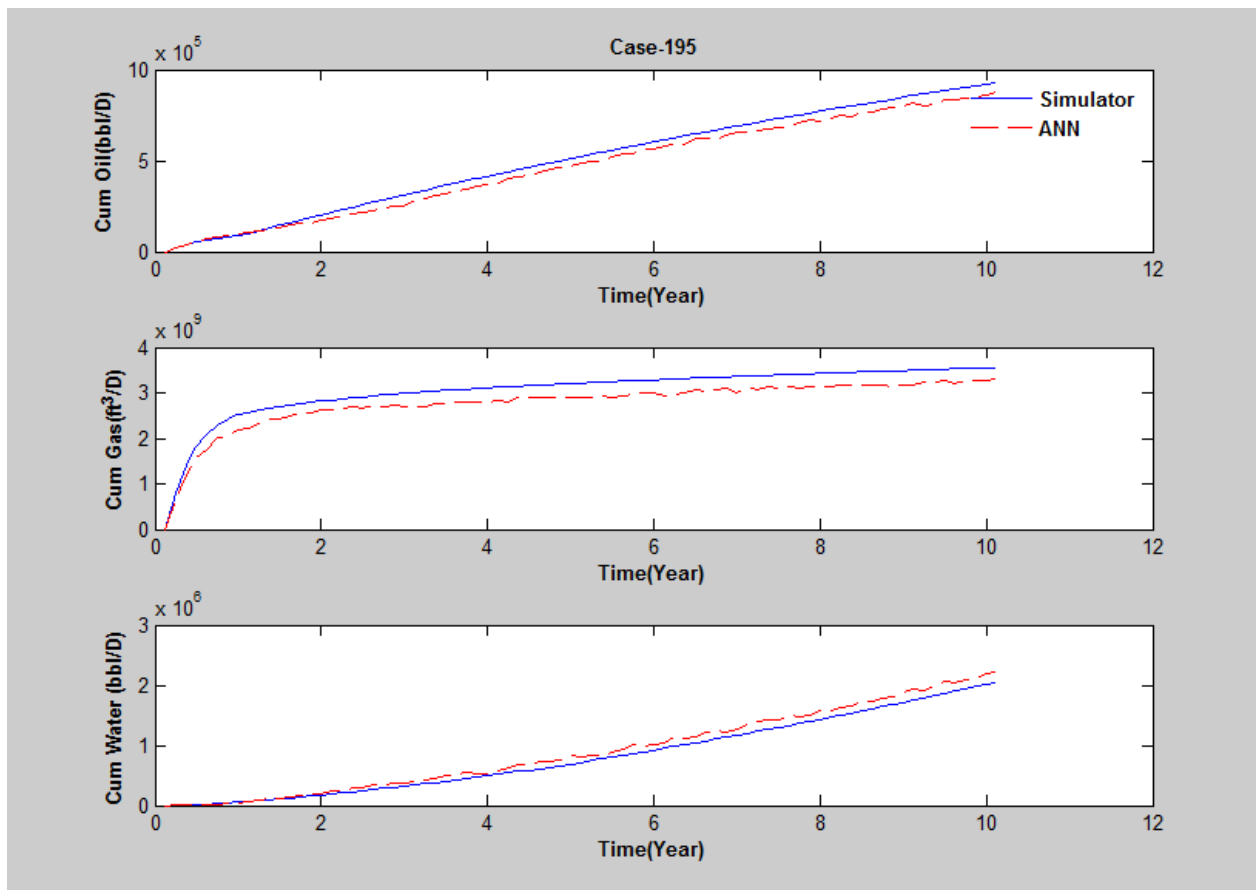


Figure 81: Comparison of cumulative production profiles generated by ANN and numerical simulator (Case-195)

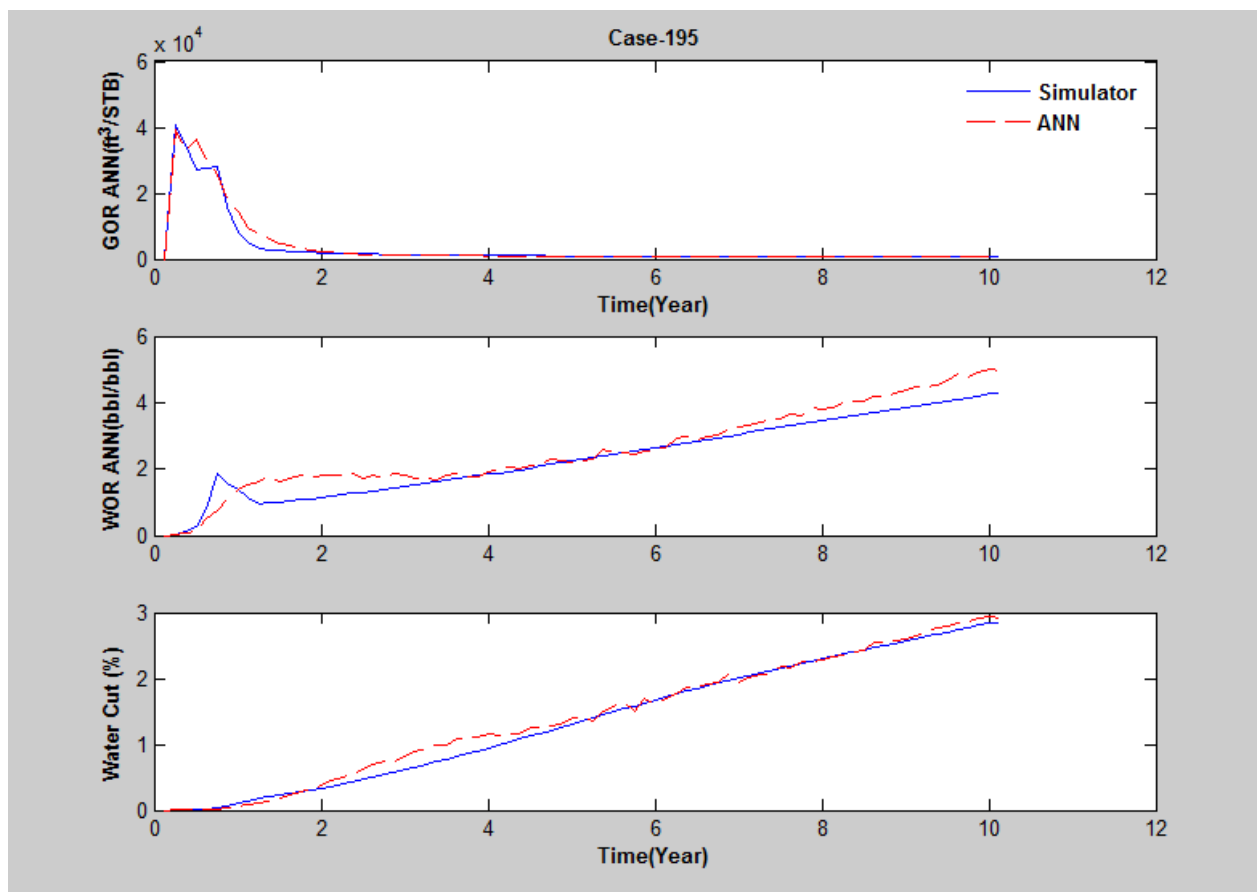


Figure 82: Comparison of Gas Oil Ratio, Water Oil Ratio and water cut production profiles generated by ANN and numerical simulator (Case-195)

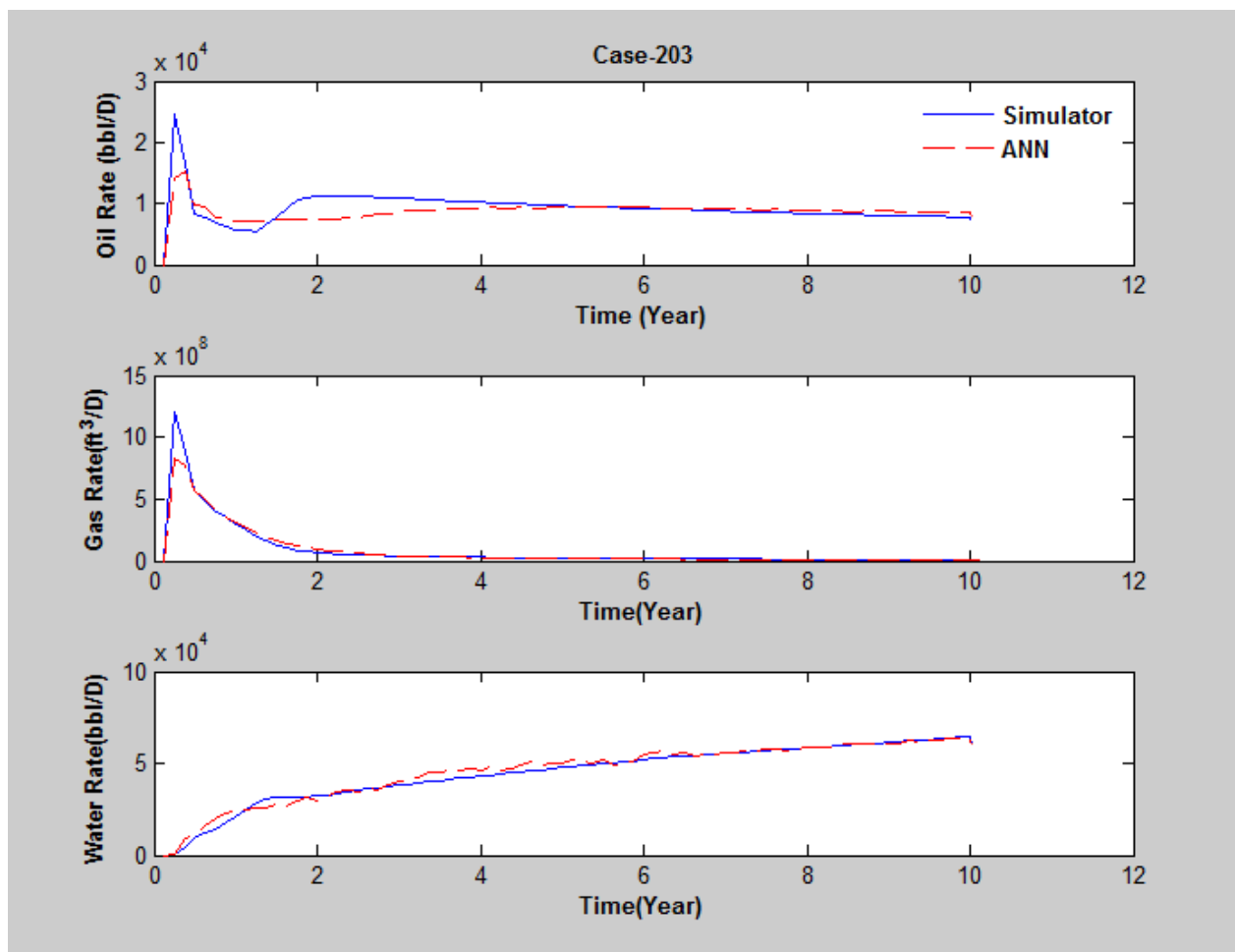


Figure 83: Comparison of production profiles generated by ANN and numerical simulator (Case-203)

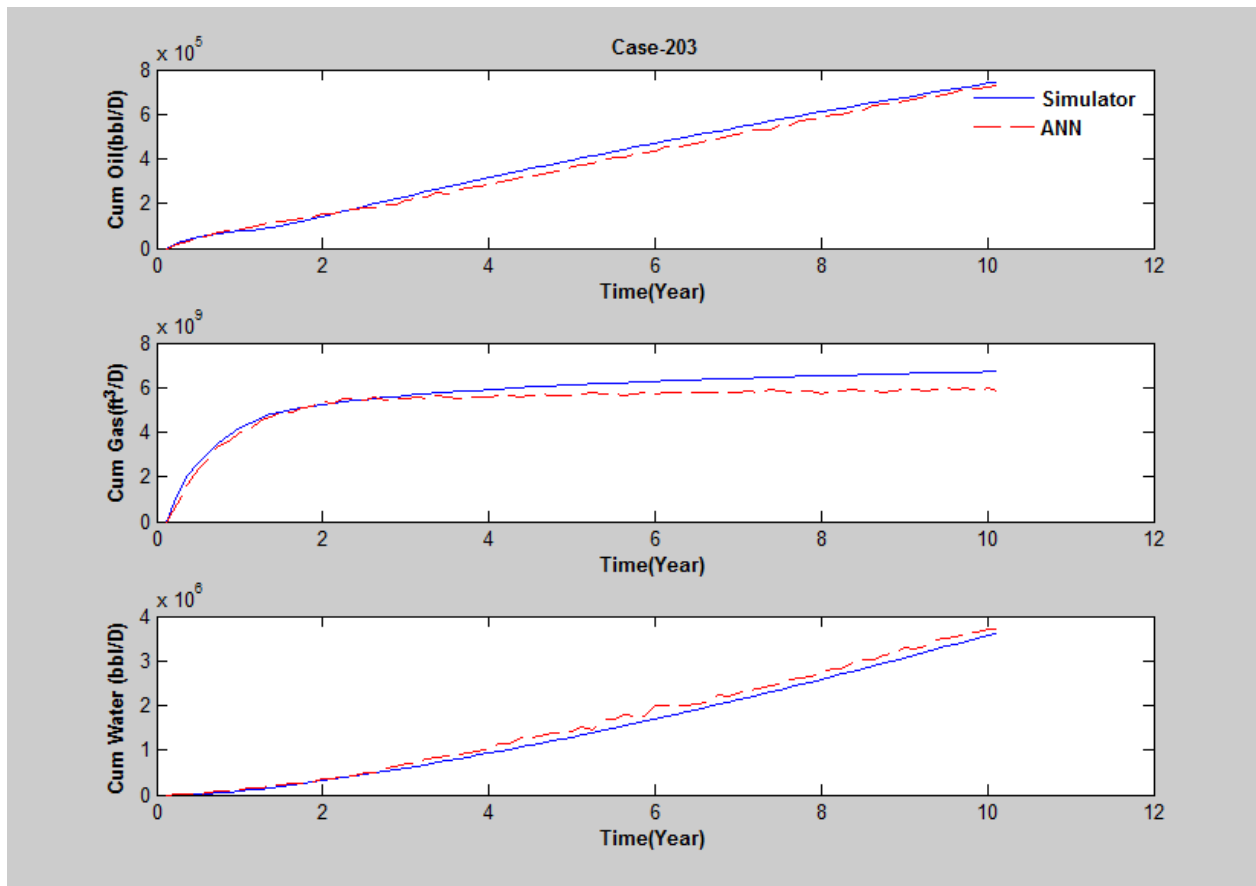


Figure 84: Comparison of cumulative production profiles generated by ANN and numerical simulator (Case-203)

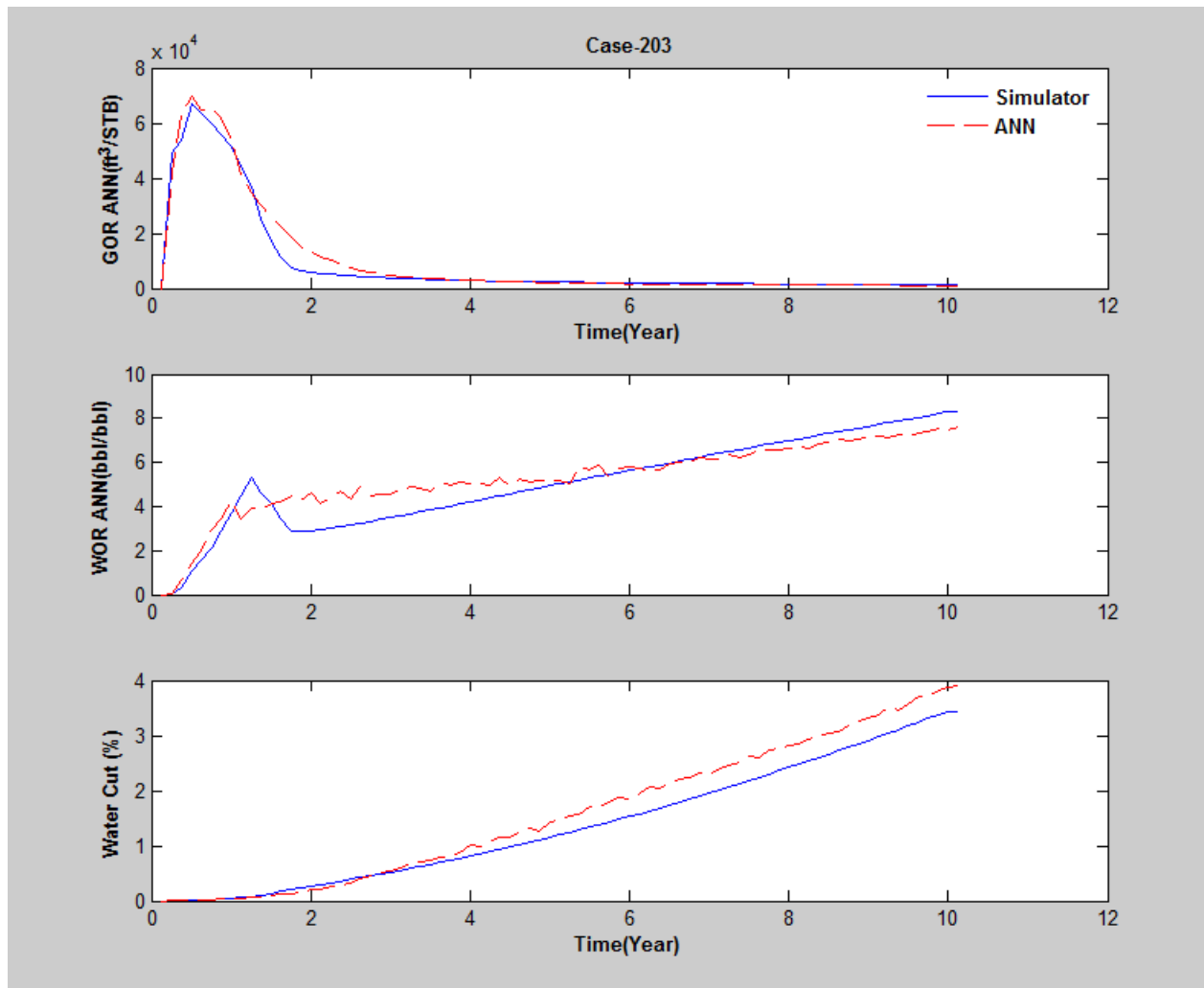


Figure 85: Comparison of Gas Oil Ratio, Water Oil Ratio and water cut production profiles generated by ANN and numerical simulator (Case-203)

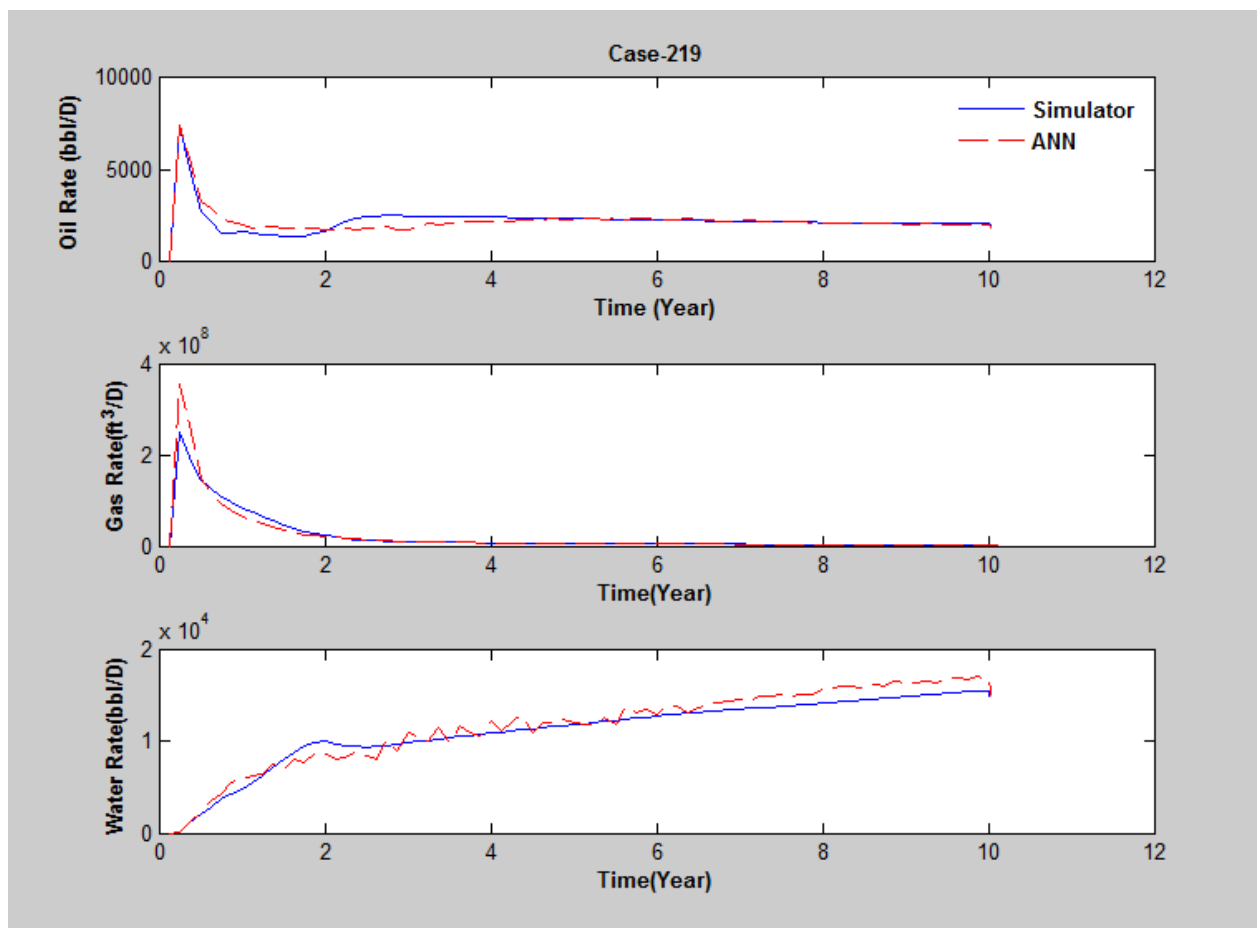


Figure 86: Comparison of production profiles generated by ANN and numerical simulator (Case-219)

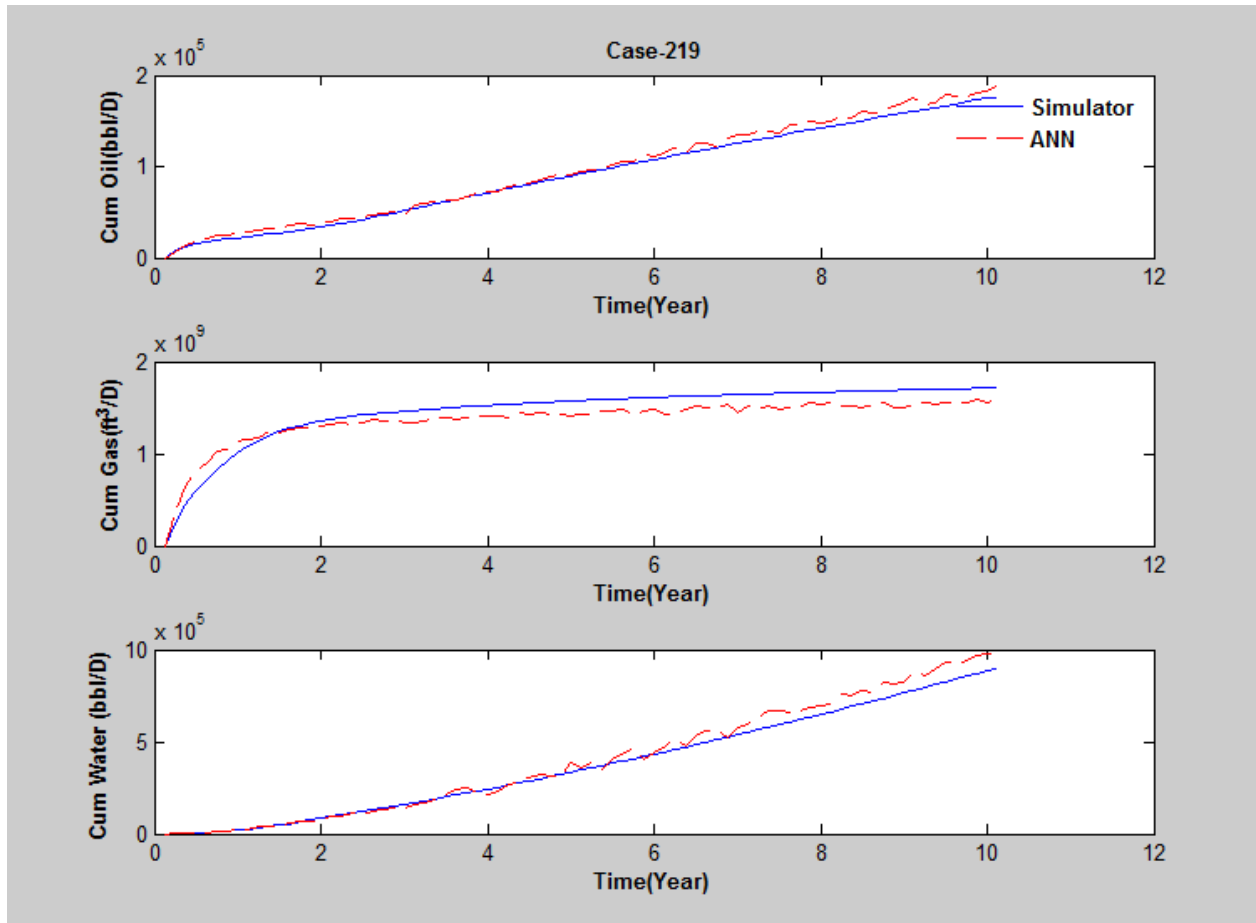


Figure 87: Comparison of cumulative production profiles generated by ANN and numerical simulator (Case-219)

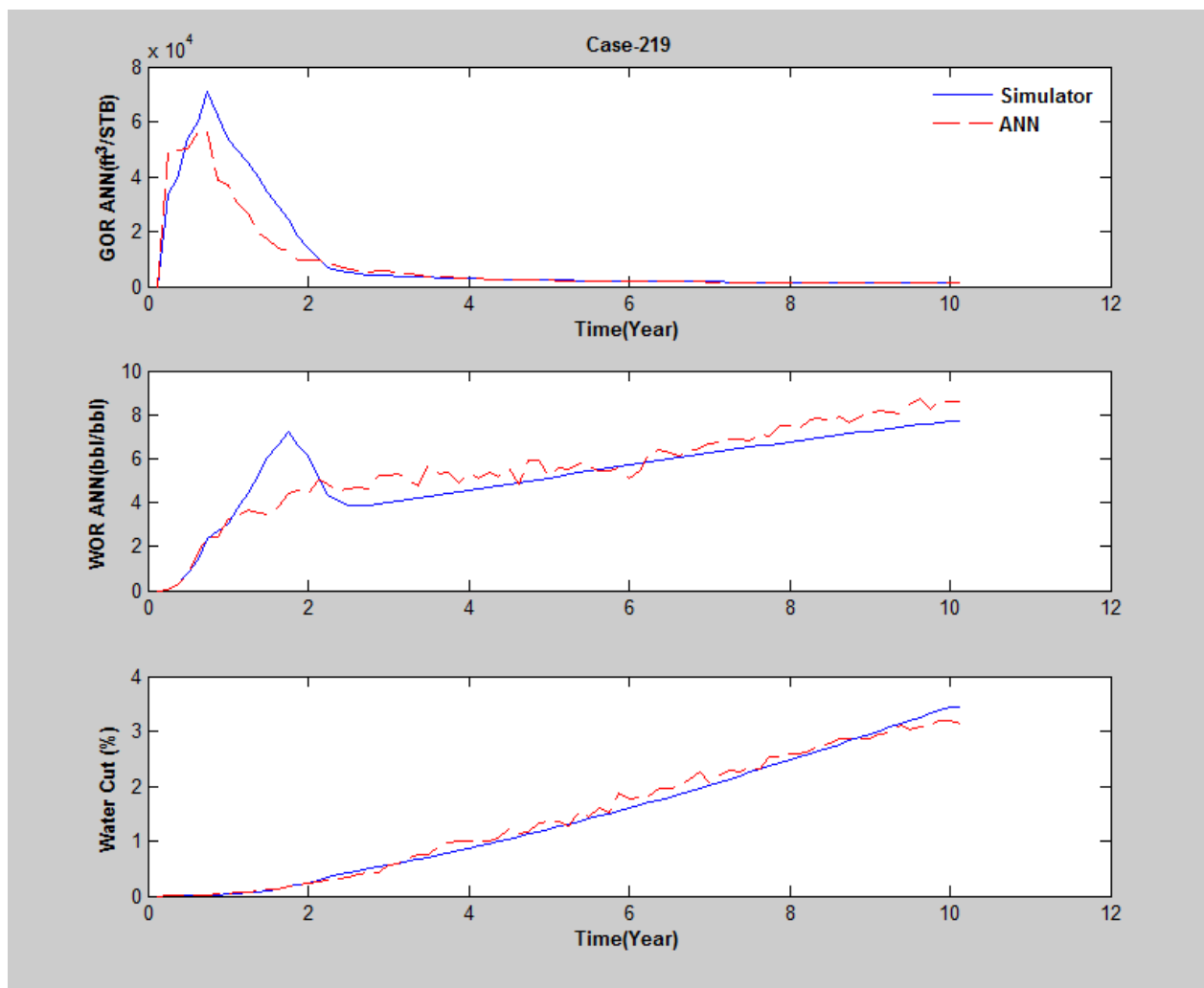


Figure 88: Comparison of Gas Oil Ratio, Water Oil Ratio and water cut production profiles generated by ANN and numerical simulator (Case-219)



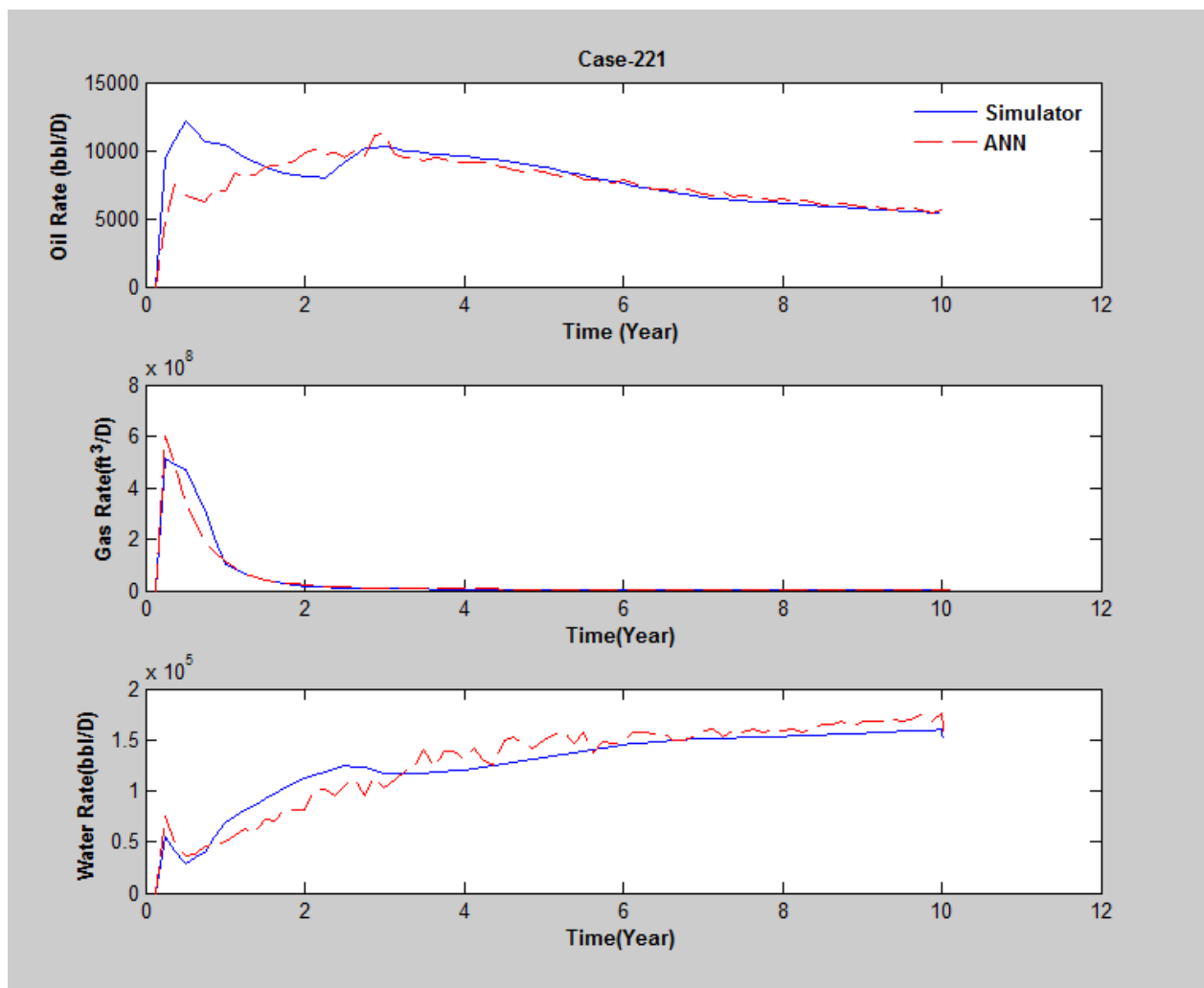


Figure 89: Comparison of production profiles generated by ANN and numerical simulator (Case-221)

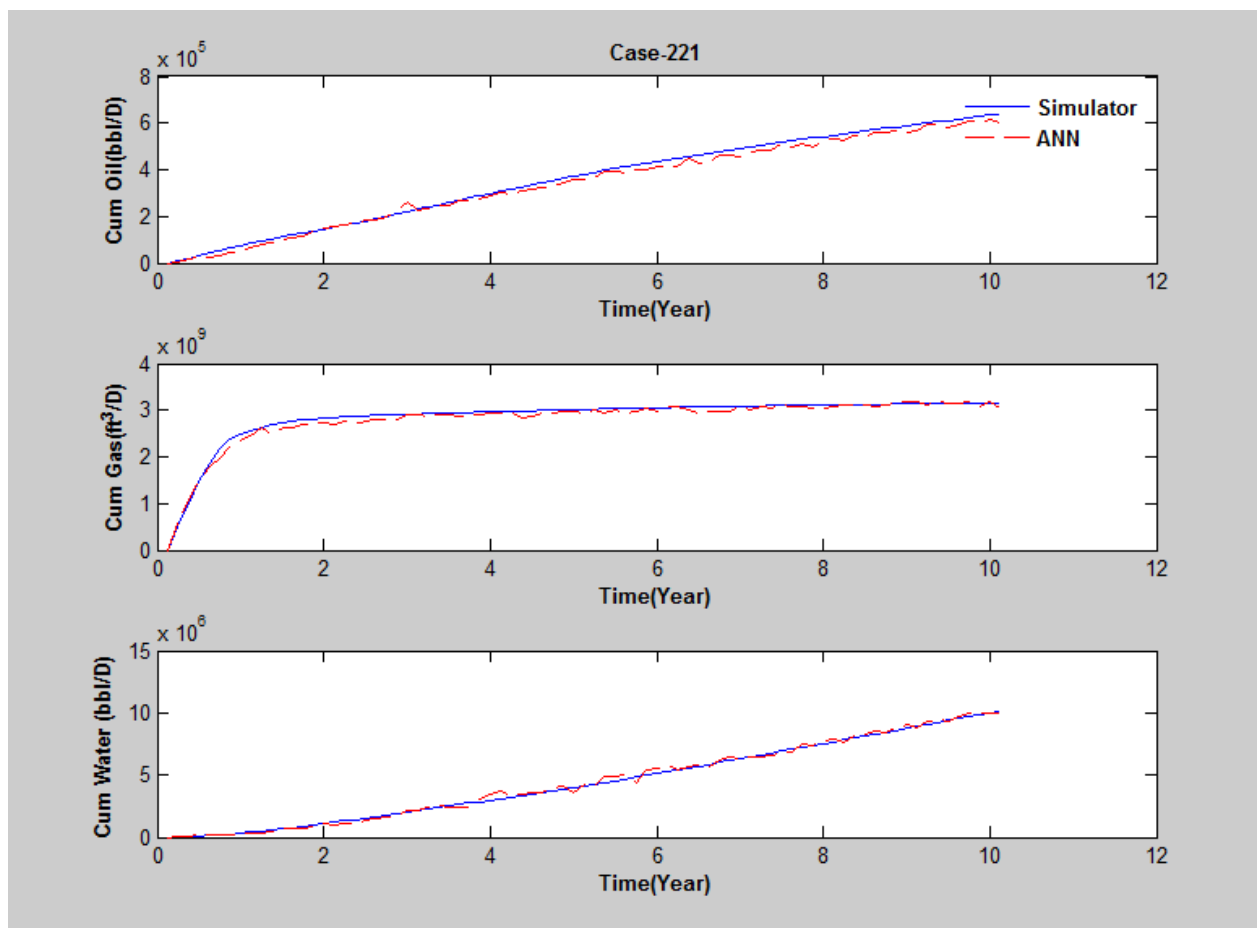


Figure 90: Comparison of cumulative production profiles generated by ANN and numerical simulator (Case-221)

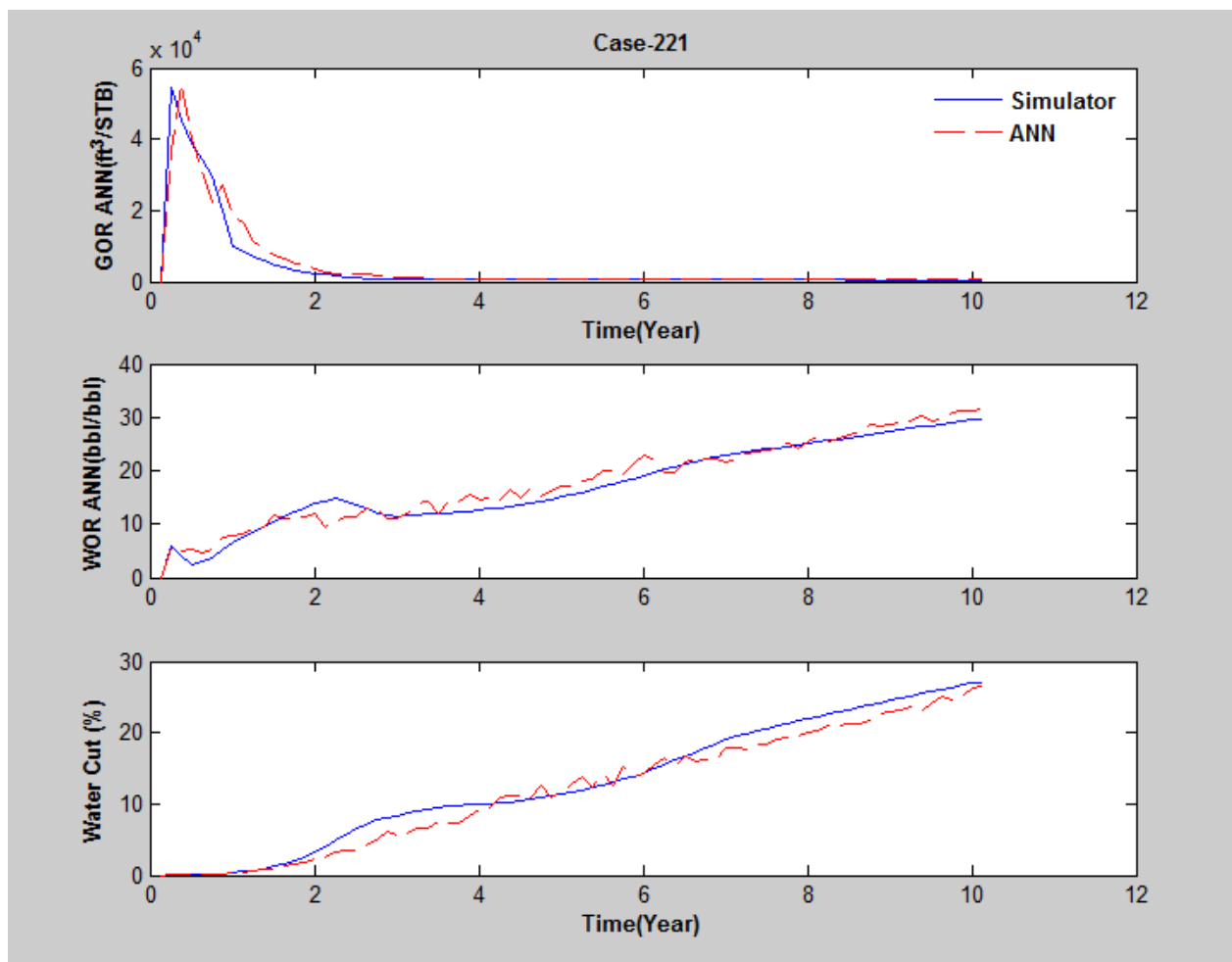


Figure 91: Comparison of Gas Oil Ratio, Water Oil Ratio and water cut production profiles generated by ANN and numerical simulator (Case-221)

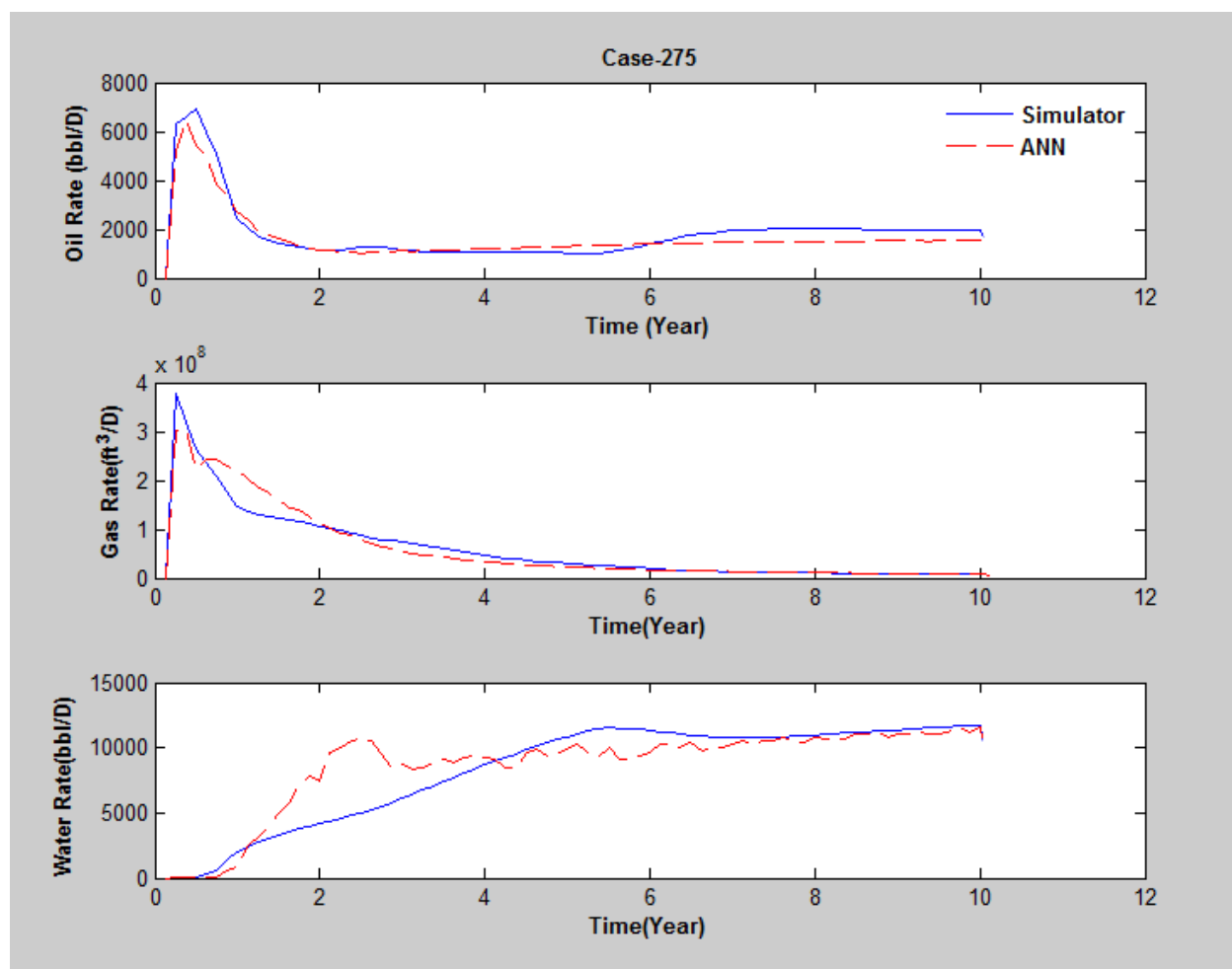


Figure 92: Comparison of production profiles generated by ANN and numerical simulator (Case-275)

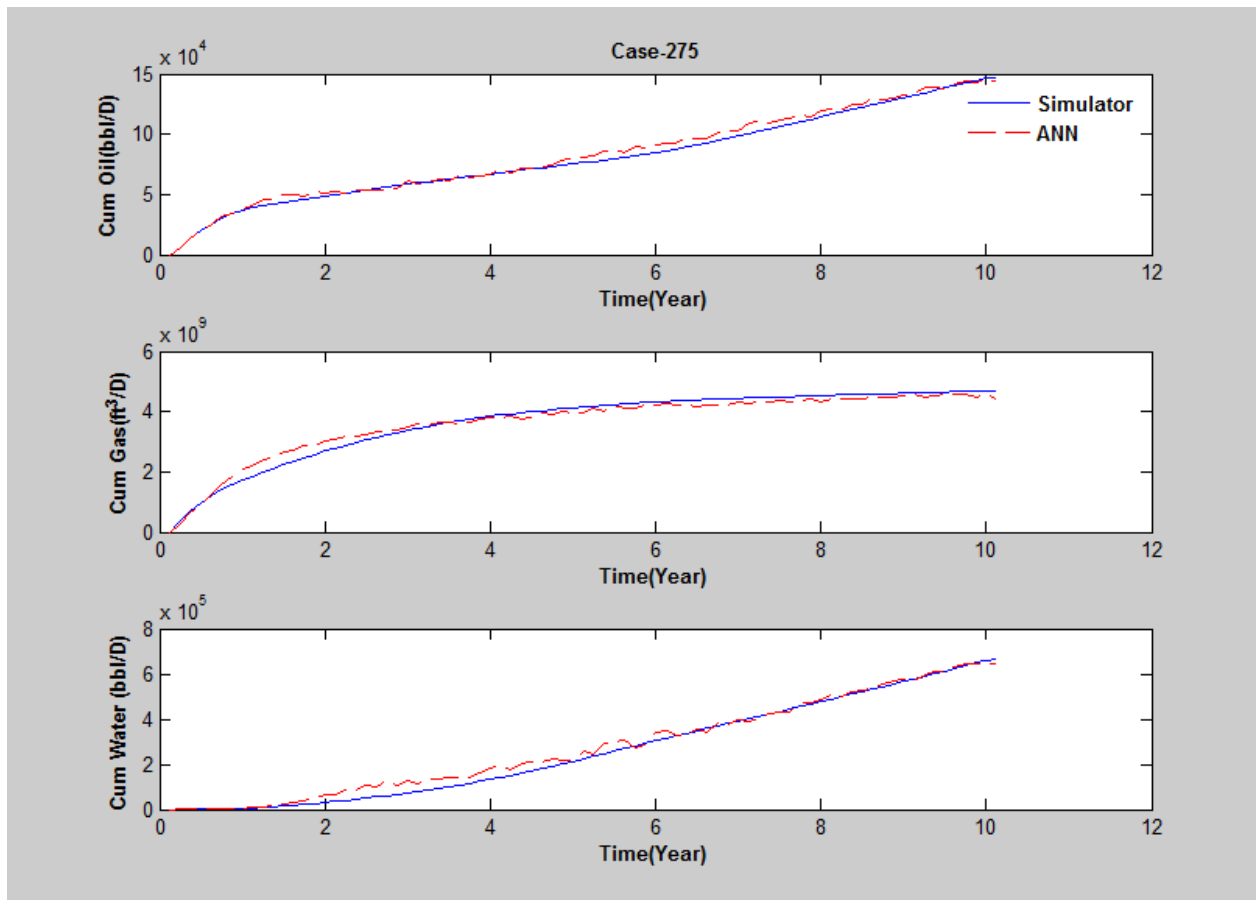


Figure 93: Comparison of cumulative production profiles generated by ANN and numerical simulator (Case-275)

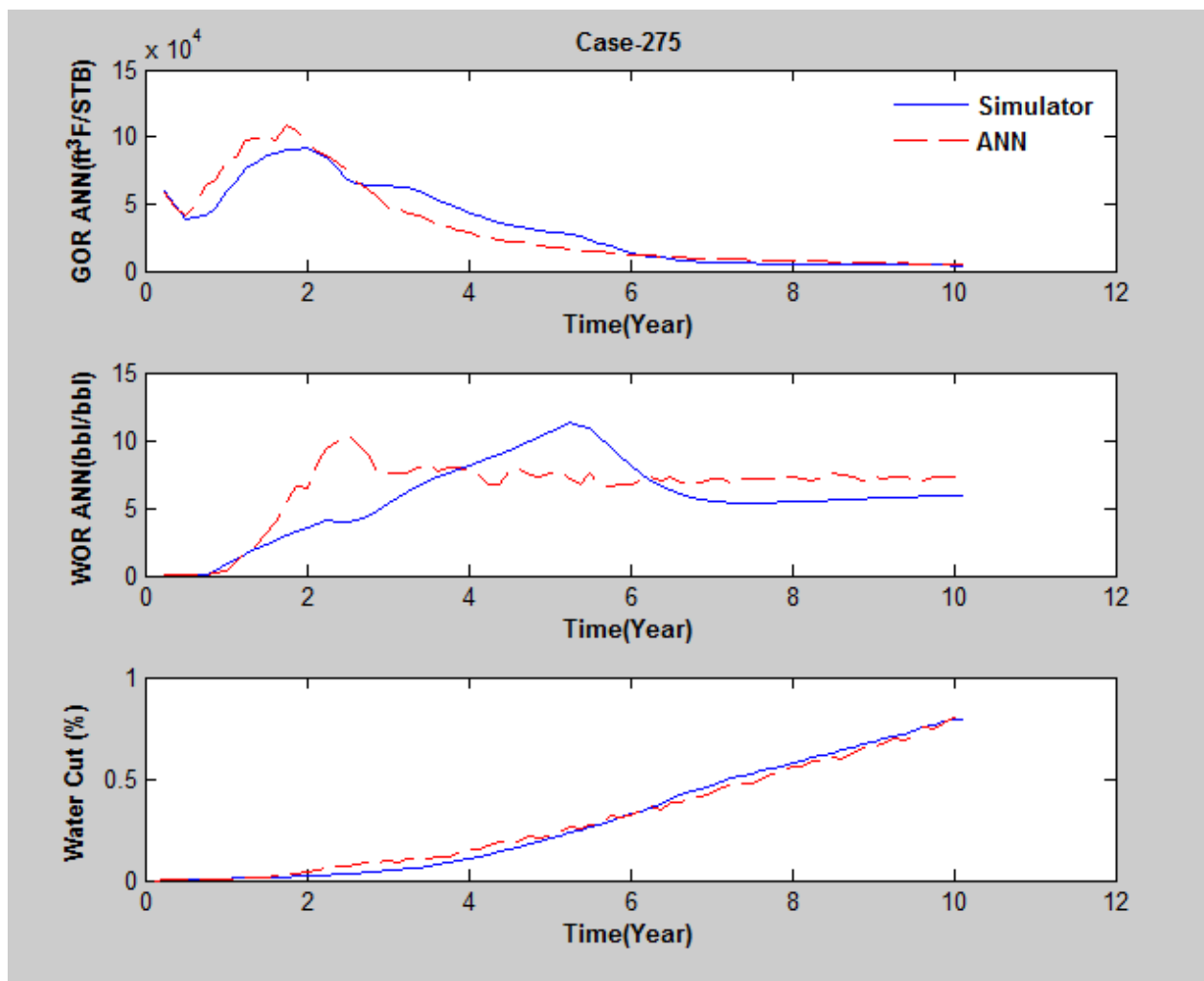


Figure 94: Comparison of Gas Oil Ratio, Water Oil Ratio and water cut production profiles generated by ANN and numerical simulator (Case-275)

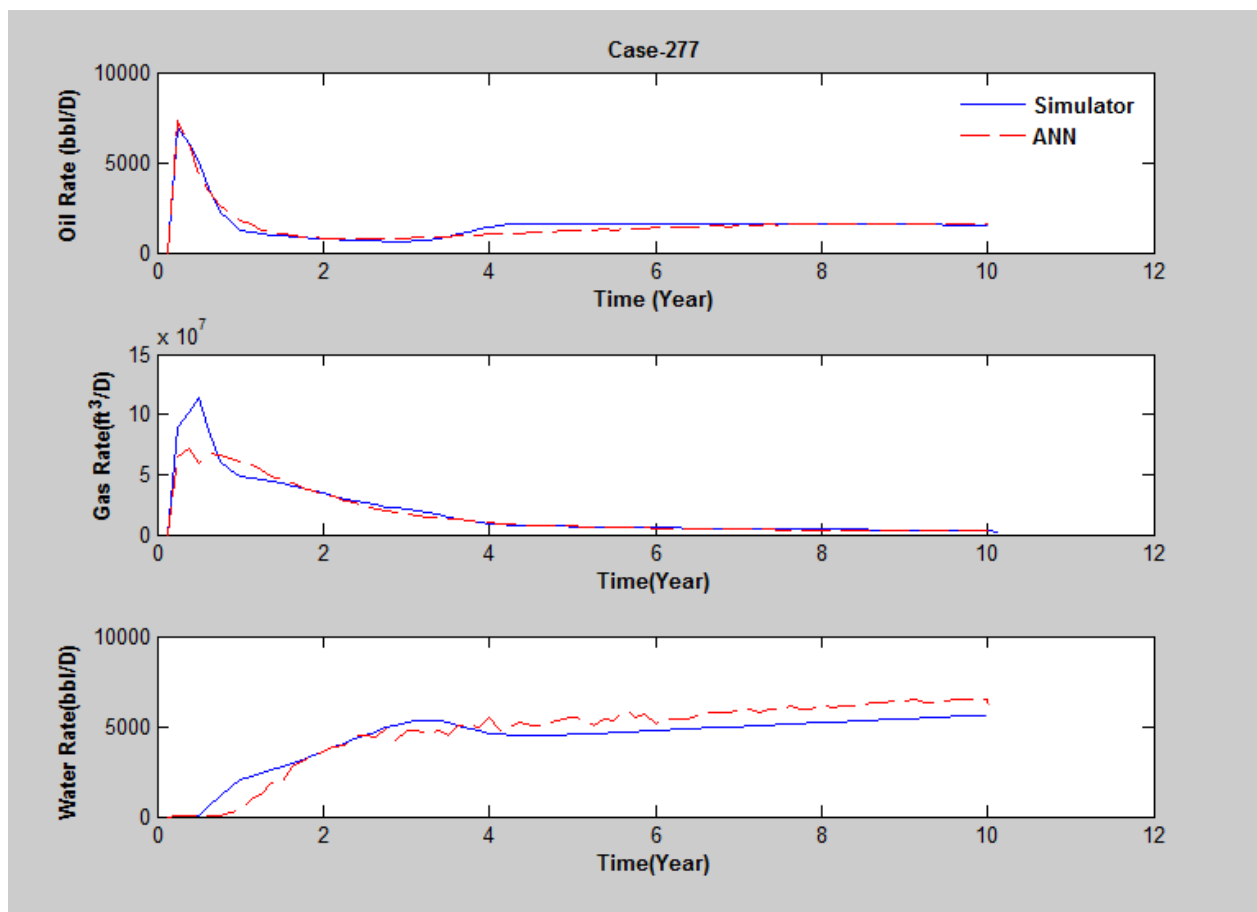


Figure 95: Comparison of production profiles generated by ANN and numerical simulator (Case-277)

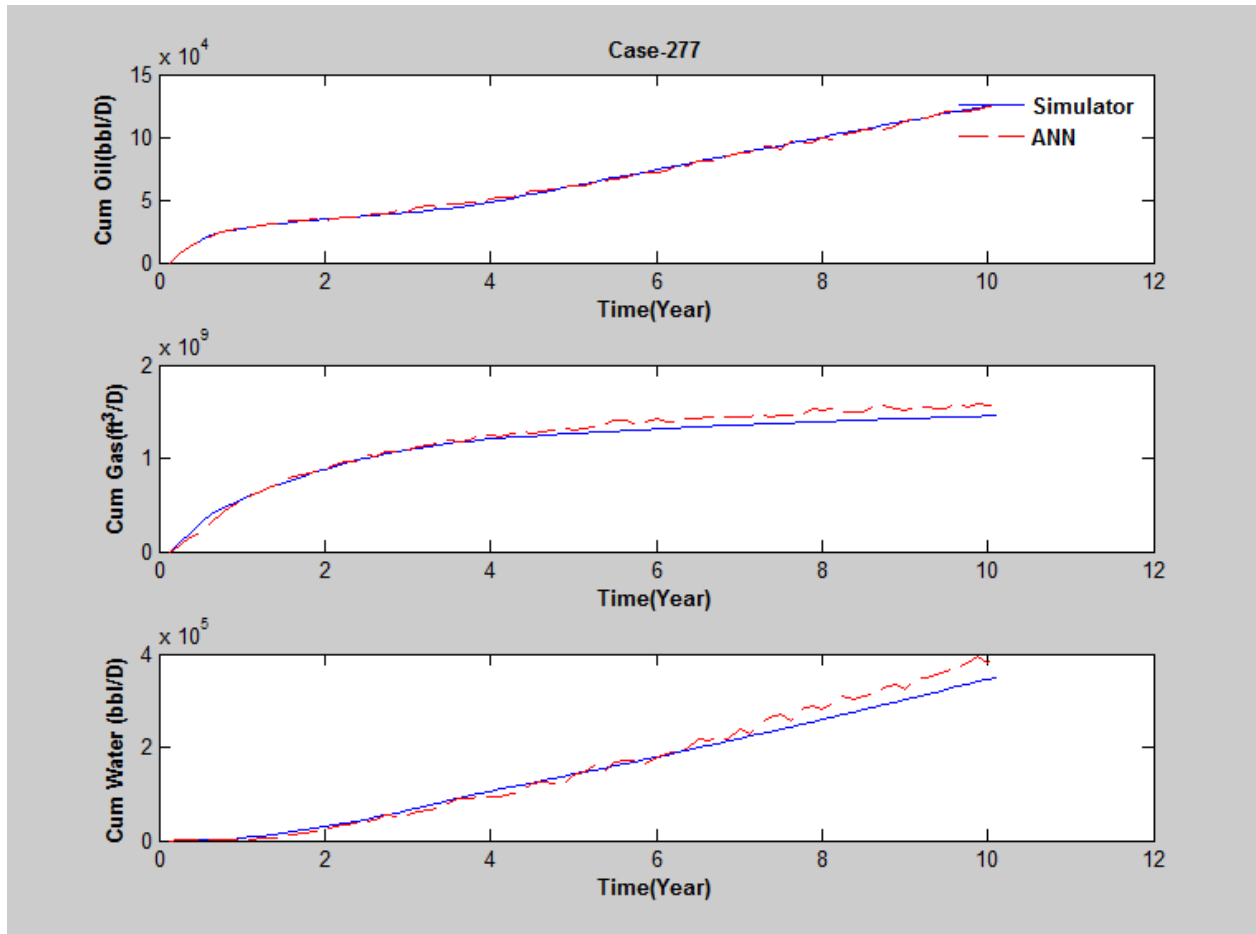


Figure 96: Comparison of cumulative production profiles generated by ANN and numerical simulator (Case-277)



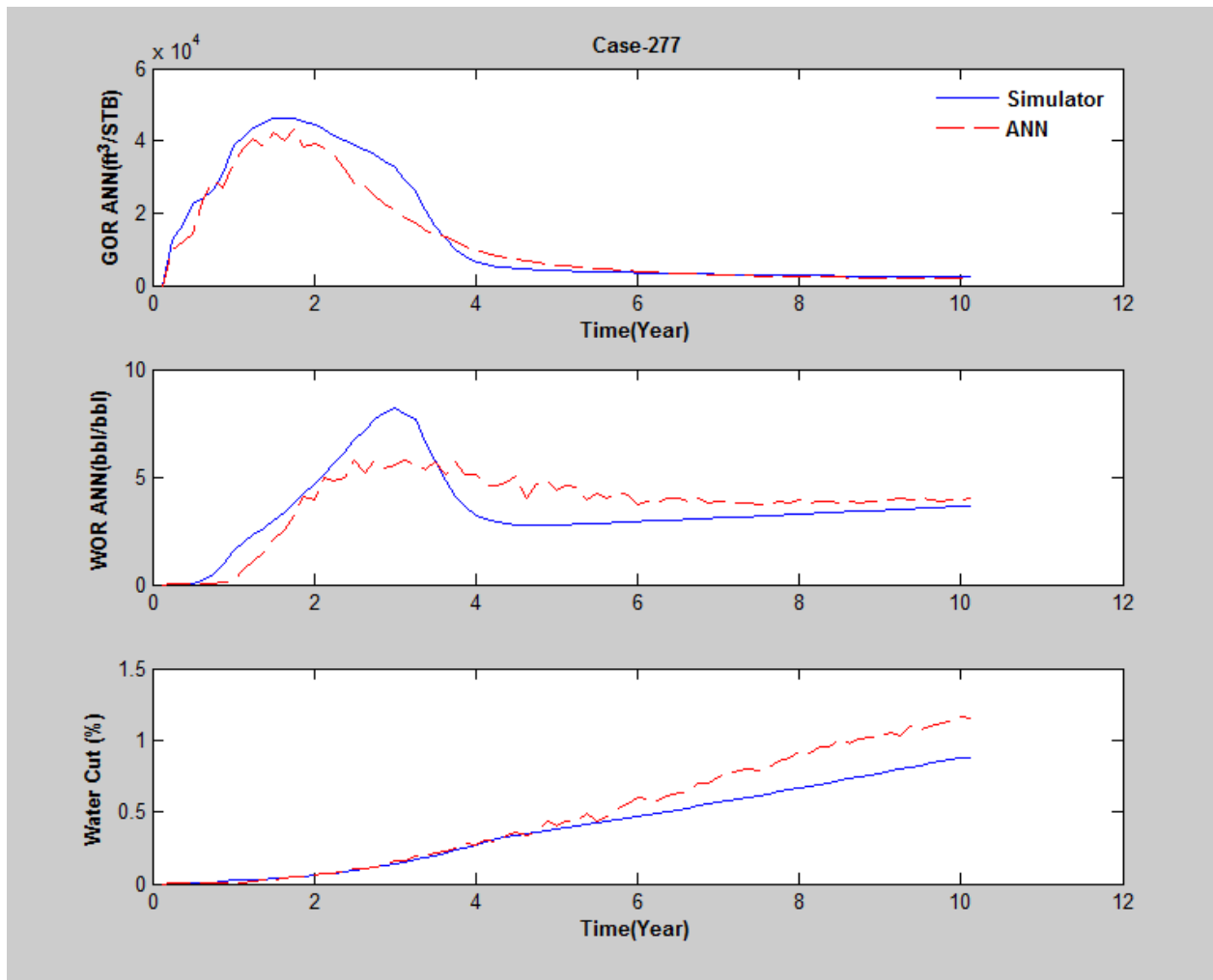


Figure 97: Comparison of Gas Oil Ratio, Water Oil Ratio and water cut production profiles generated by ANN and numerical simulator (Case-277)

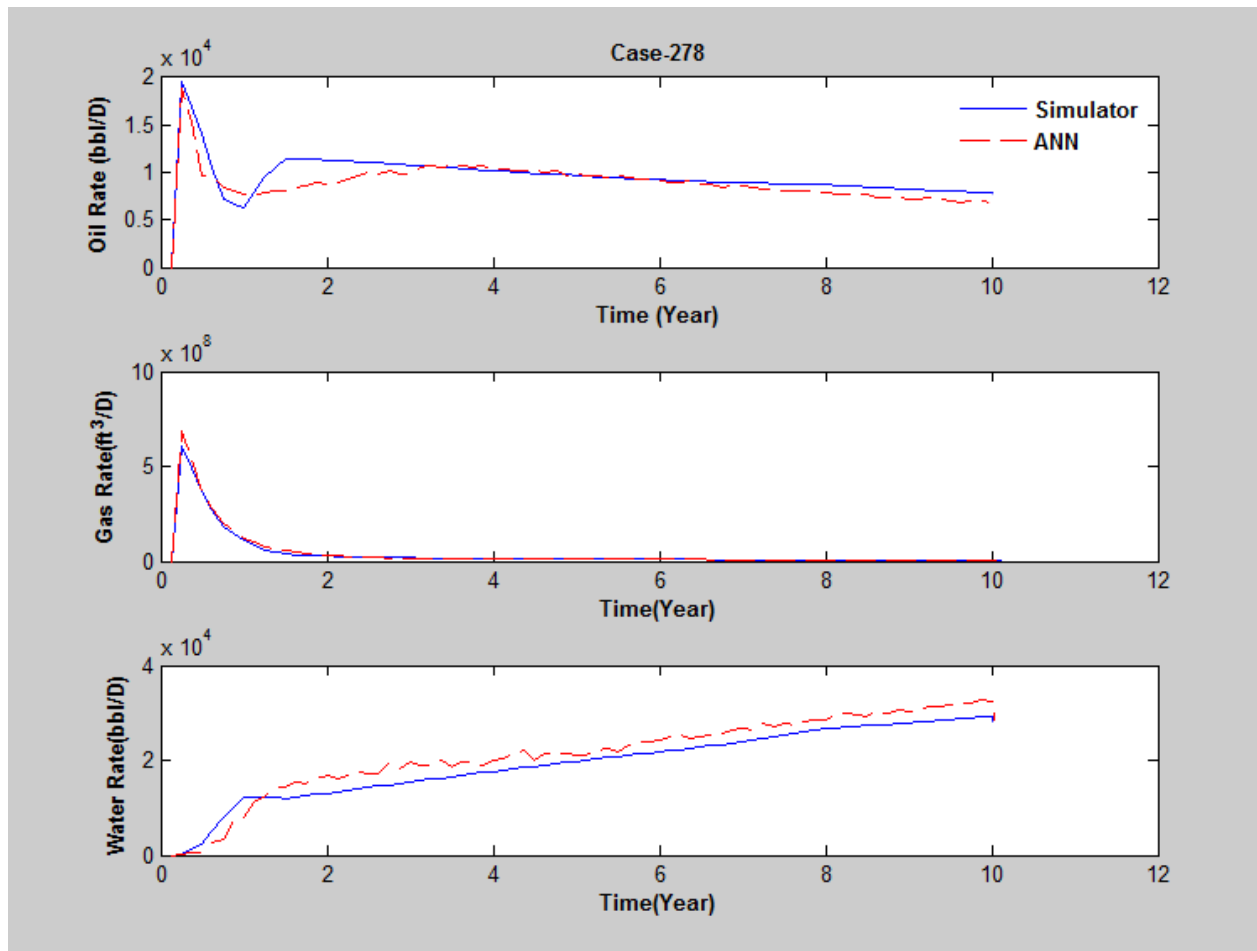


Figure 98: Comparison of production profiles generated by ANN and numerical simulator (Case-278)

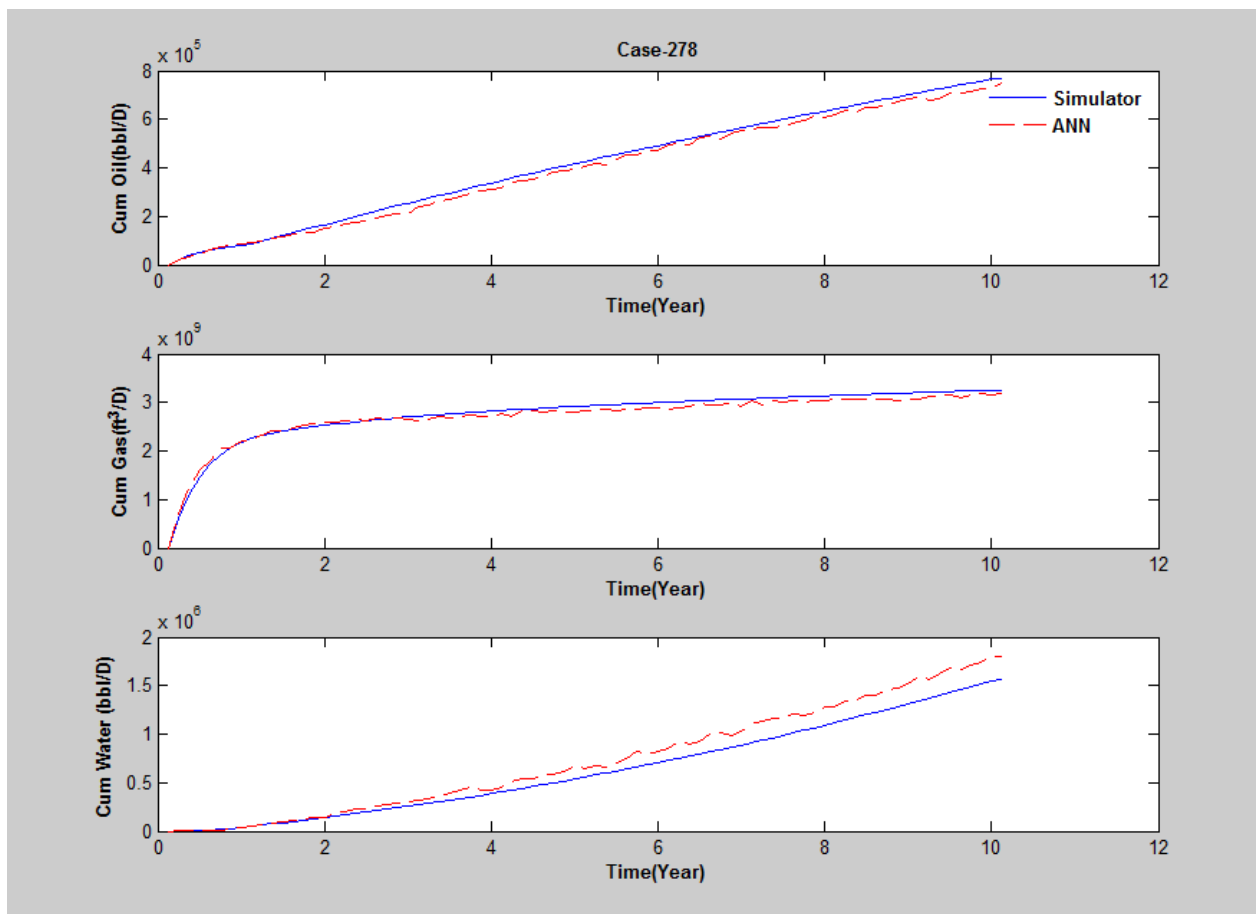


Figure 99: Comparison of cumulative production profiles generated by ANN and numerical simulator (Case-278)

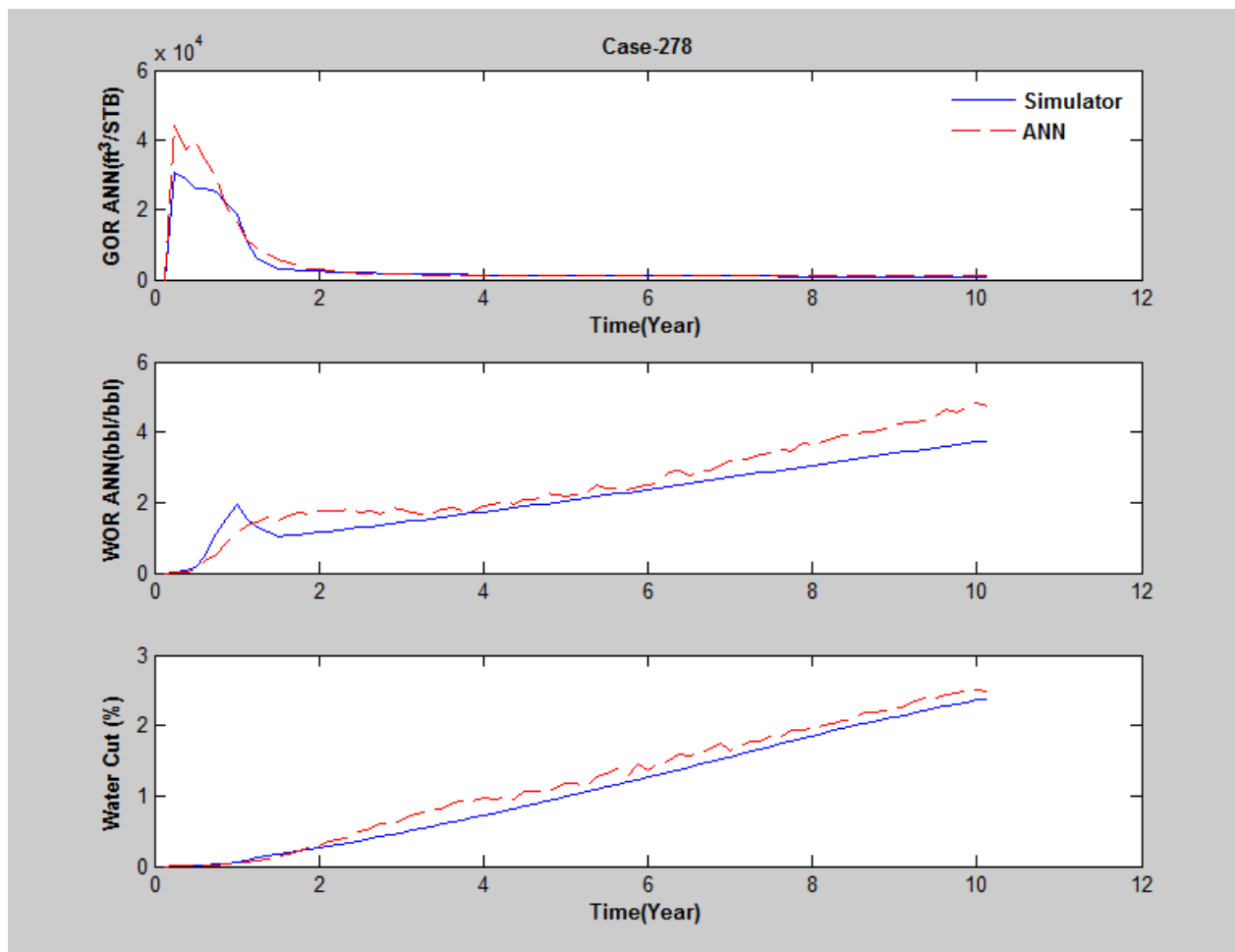


Figure 100: Comparison of Gas Oil Ratio, Water Oil Ratio and water cut production profiles generated by ANN and numerical simulator (Case-278)

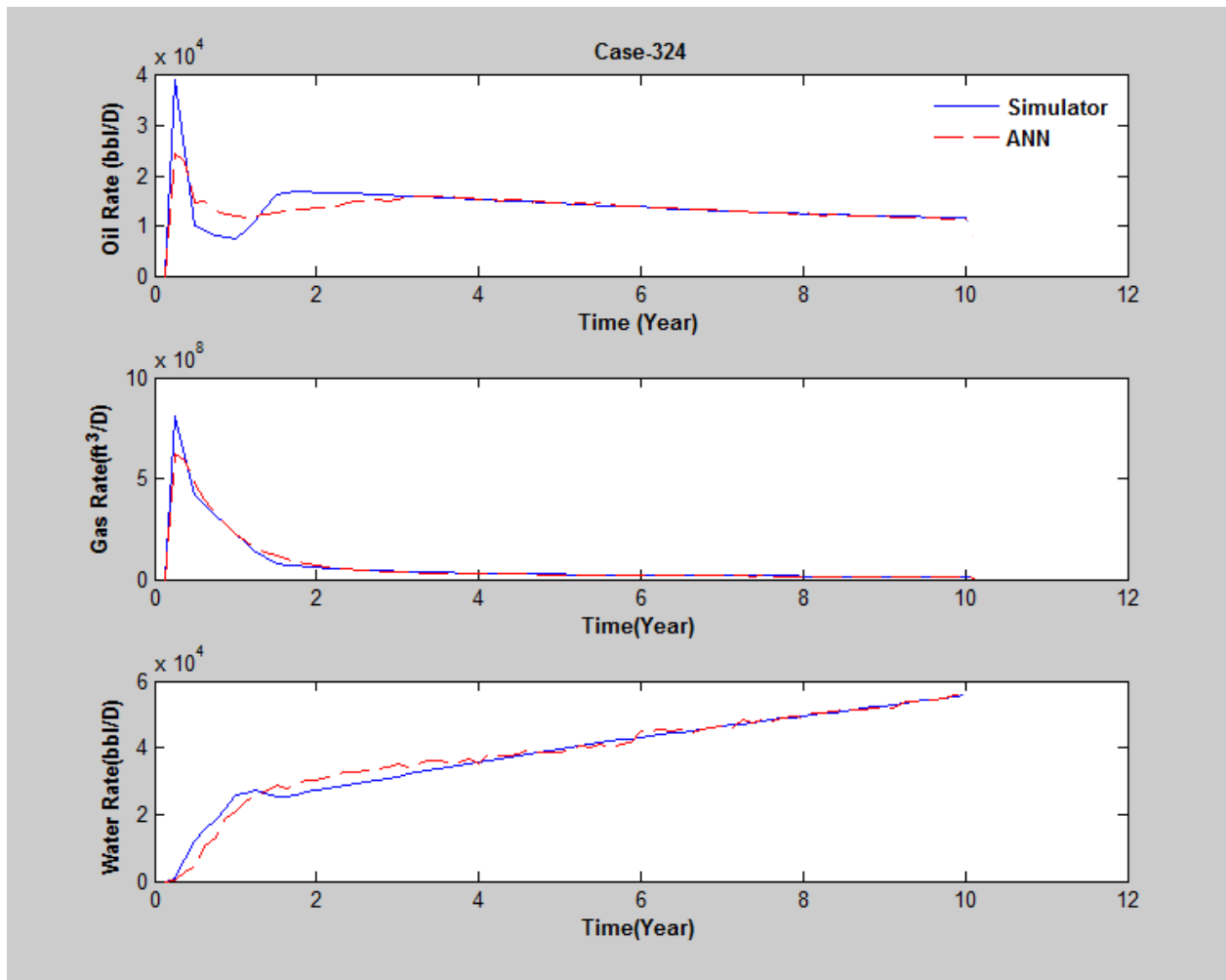


Figure 101: Comparison of production profiles generated by ANN and numerical simulator (Case-324)

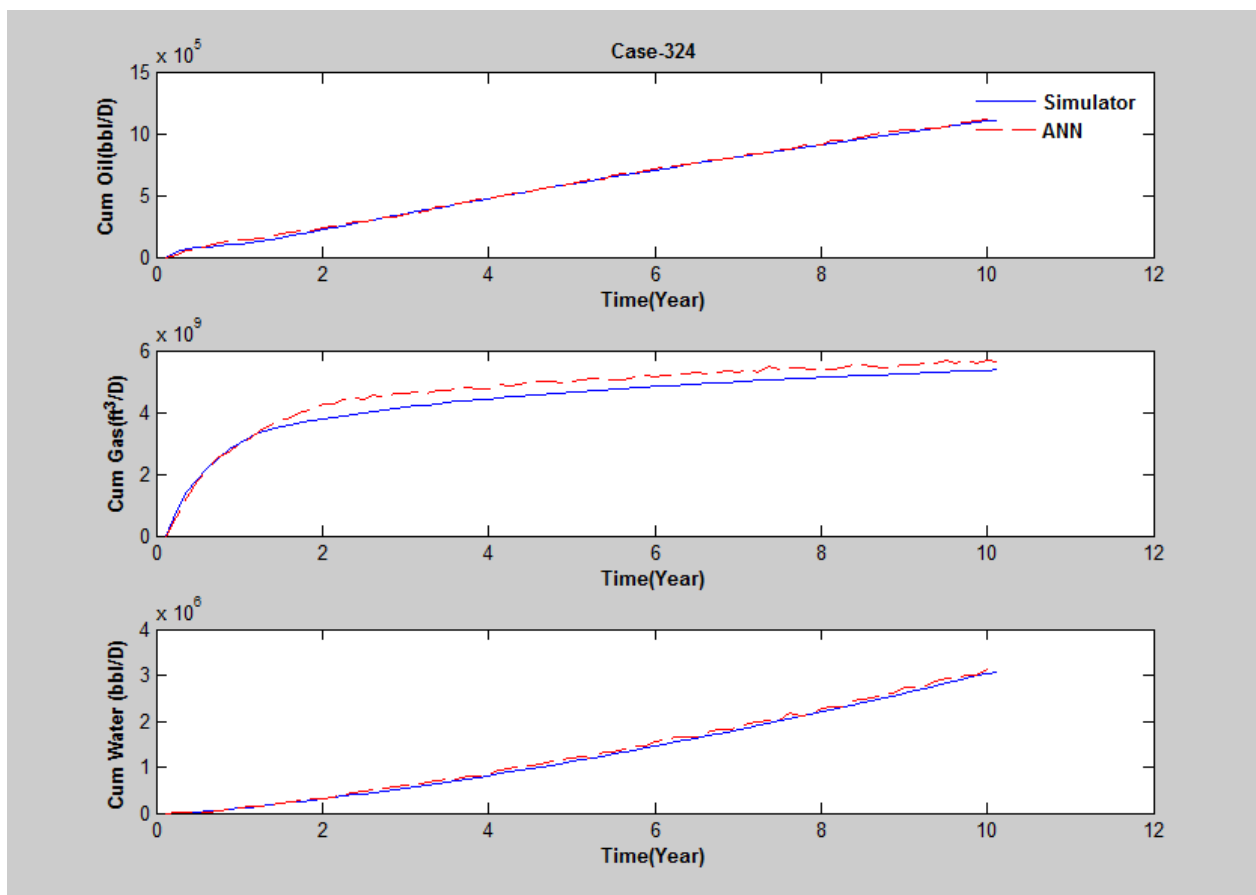


Figure 102: Comparison of cumulative production profiles generated by ANN and numerical simulator (Case-324)

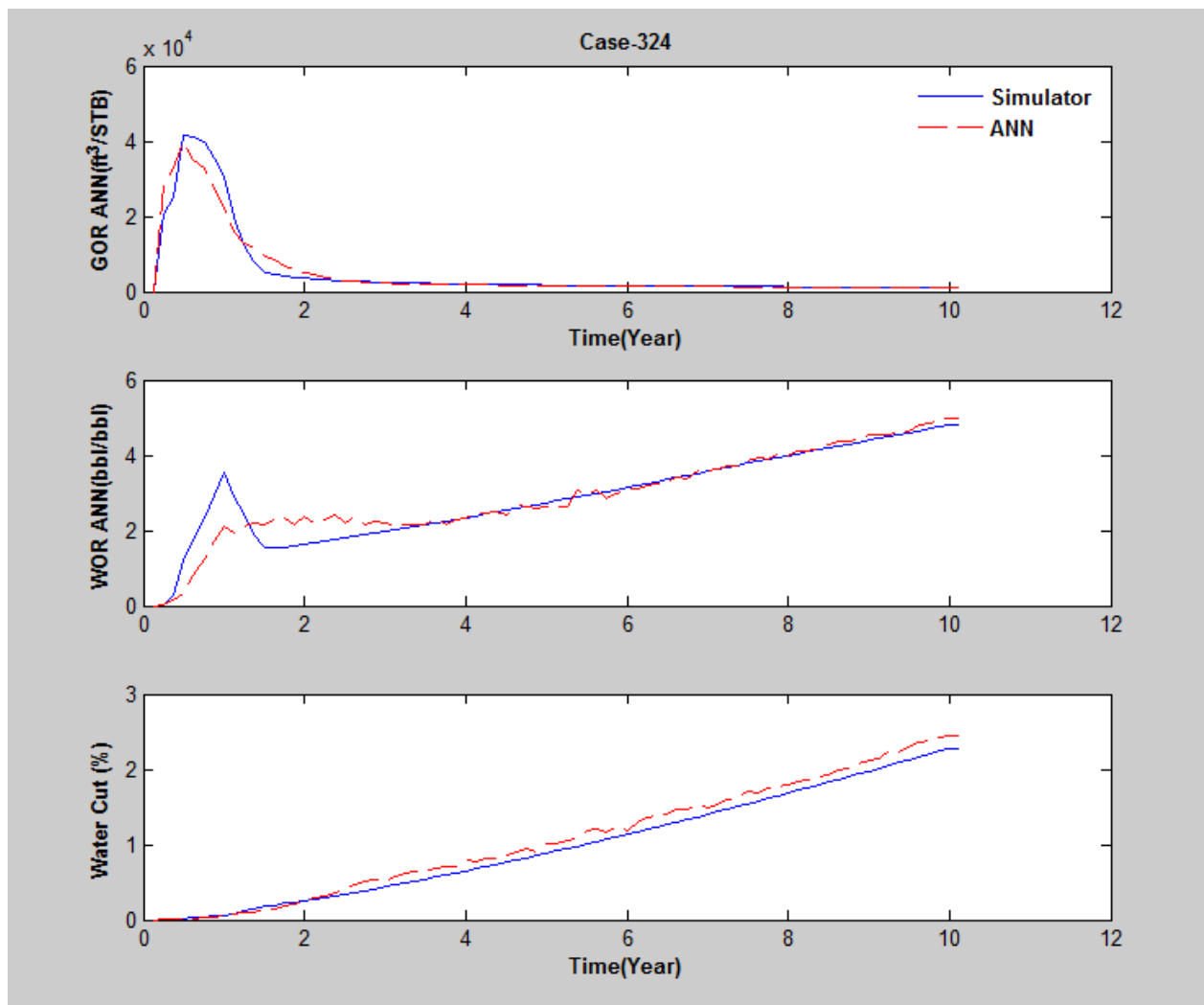


Figure 103: Comparison of Gas Oil Ratio, Water Oil Ratio and water cut production profiles generated by ANN and numerical simulator (Case-324)

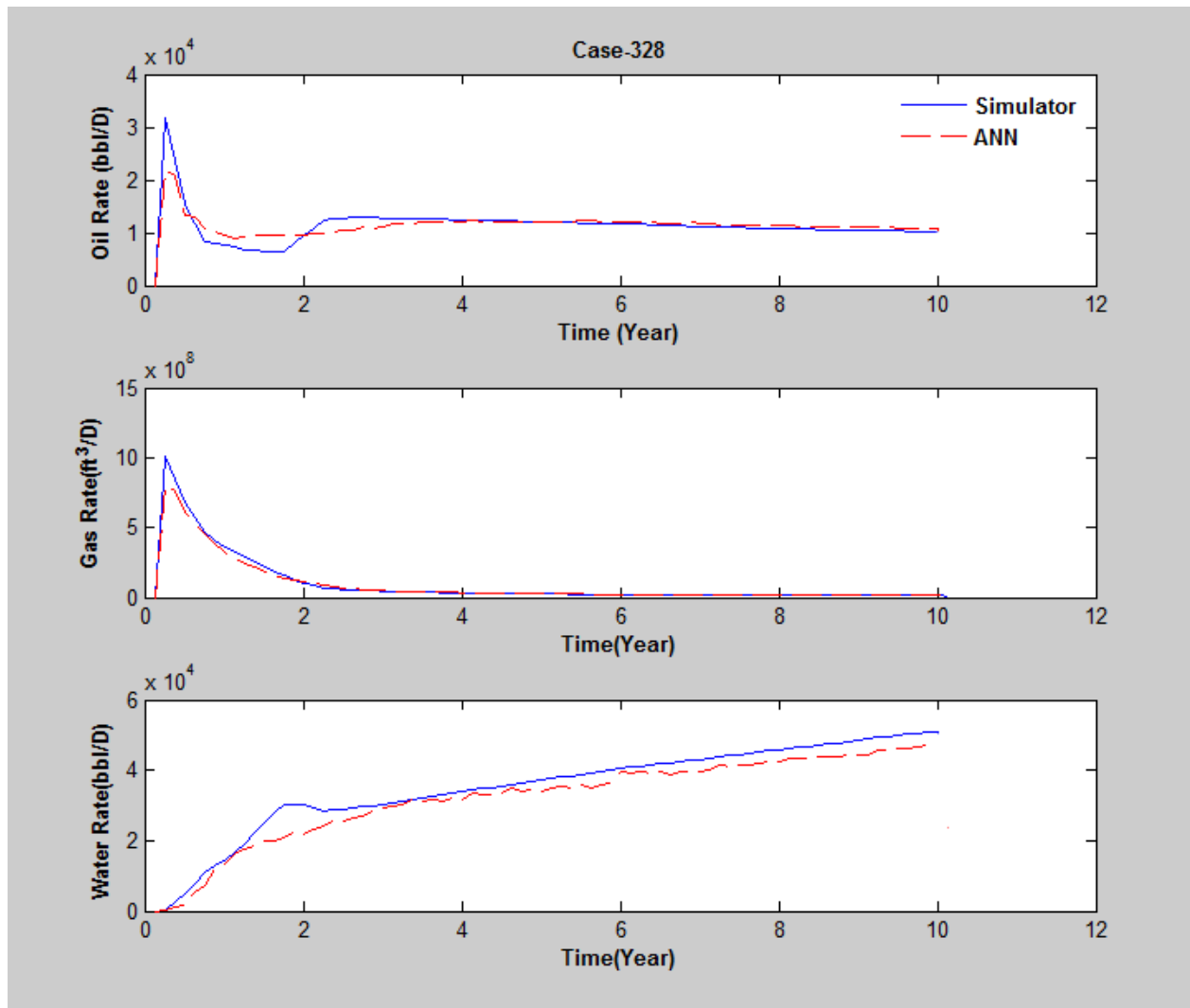


Figure 104: Comparison of production profiles generated by ANN and numerical simulator (Case-328)



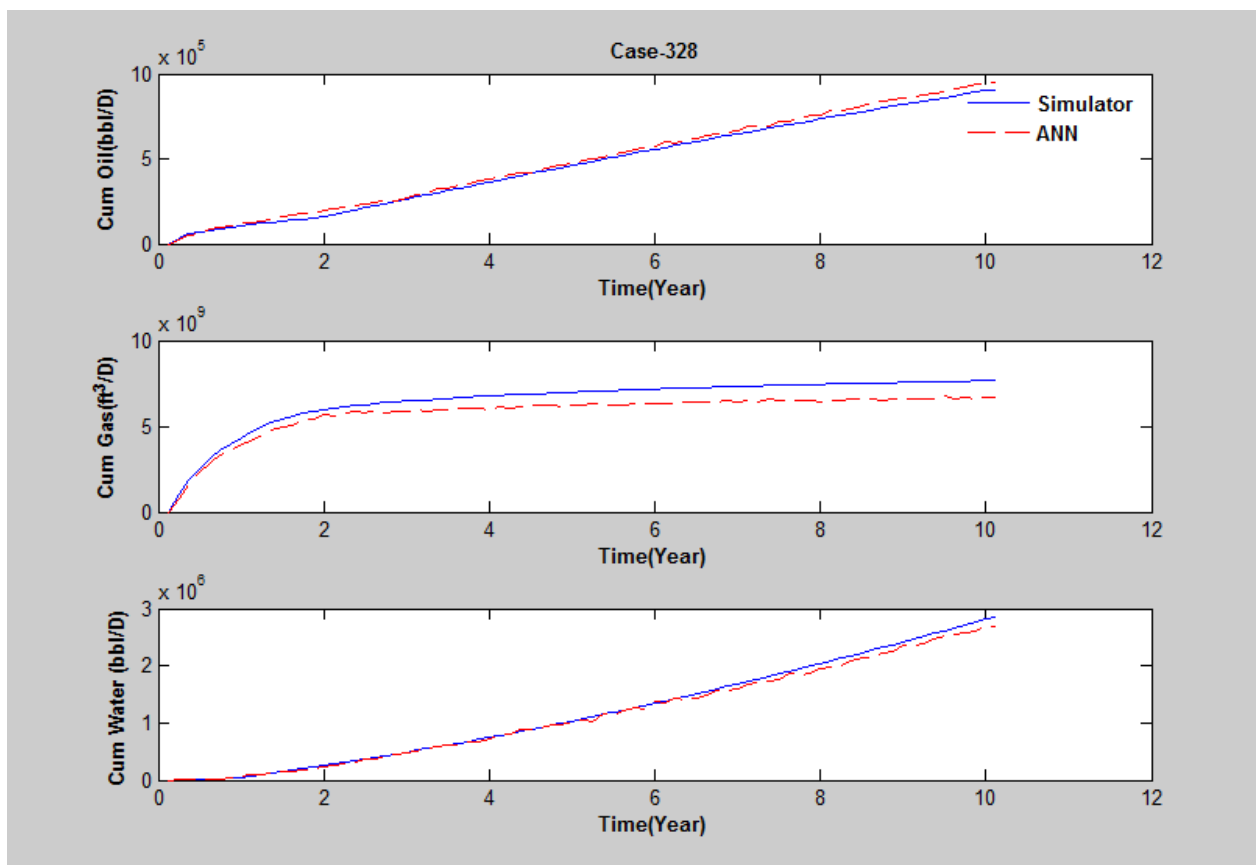


Figure 105: Comparison of cumulative production profiles generated by ANN and numerical simulator (Case-328)

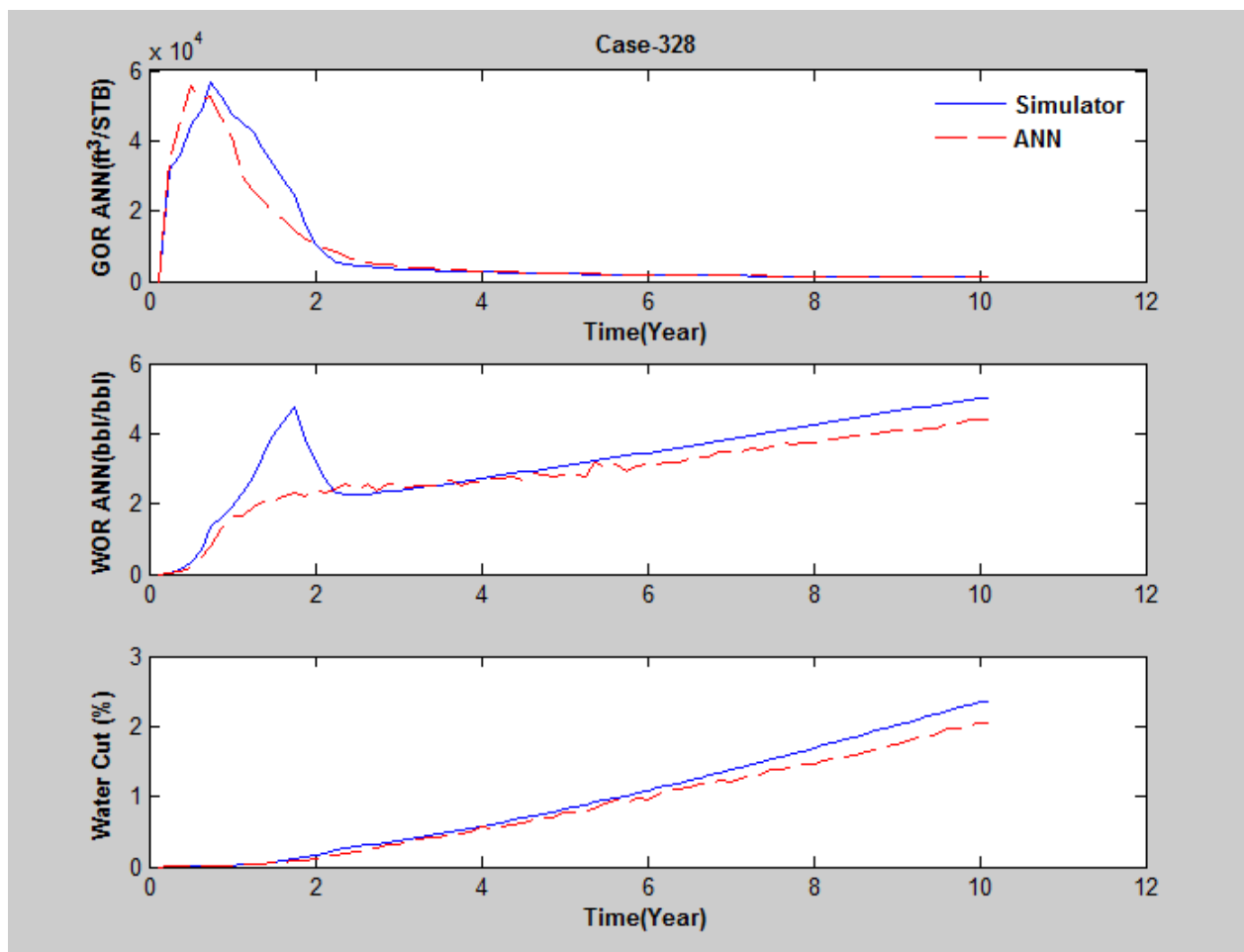


Figure 106: Comparison of Gas Oil Ratio, Water Oil Ratio and water cut production profiles generated by ANN and numerical simulator (Case-328)

## Appendix (B) Properties Distribution

---

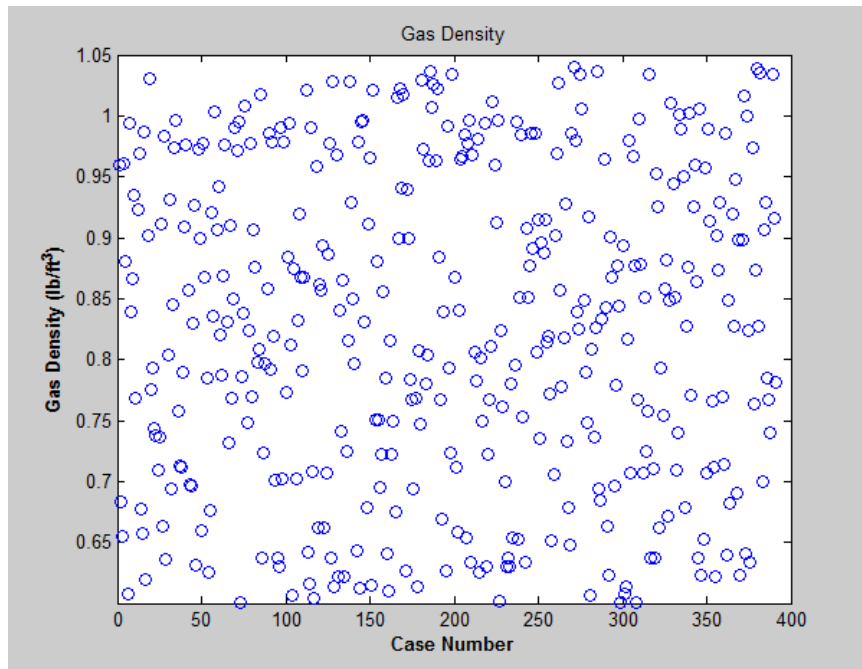


Figure 107: Gas Density distribution

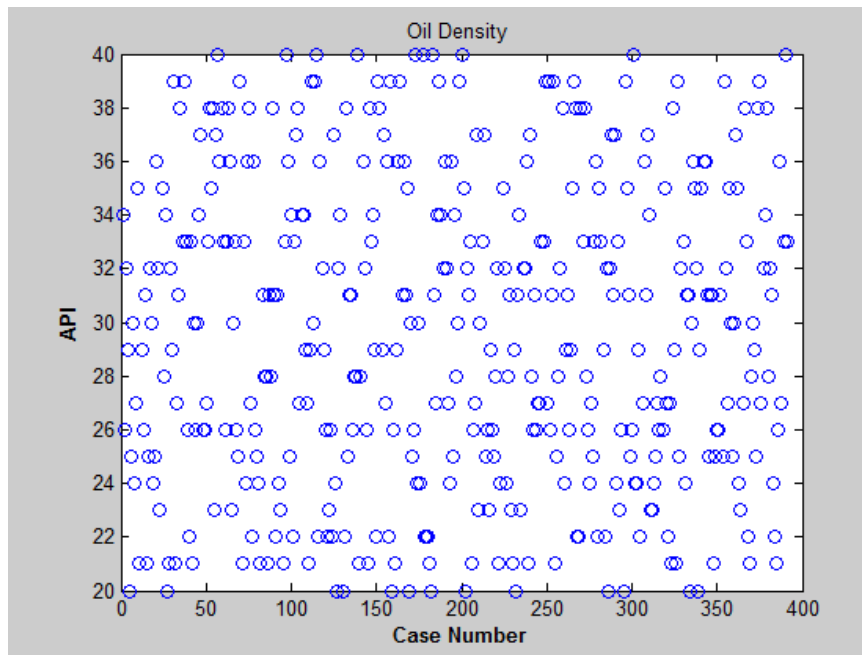


Figure 108: Oil Density distribution

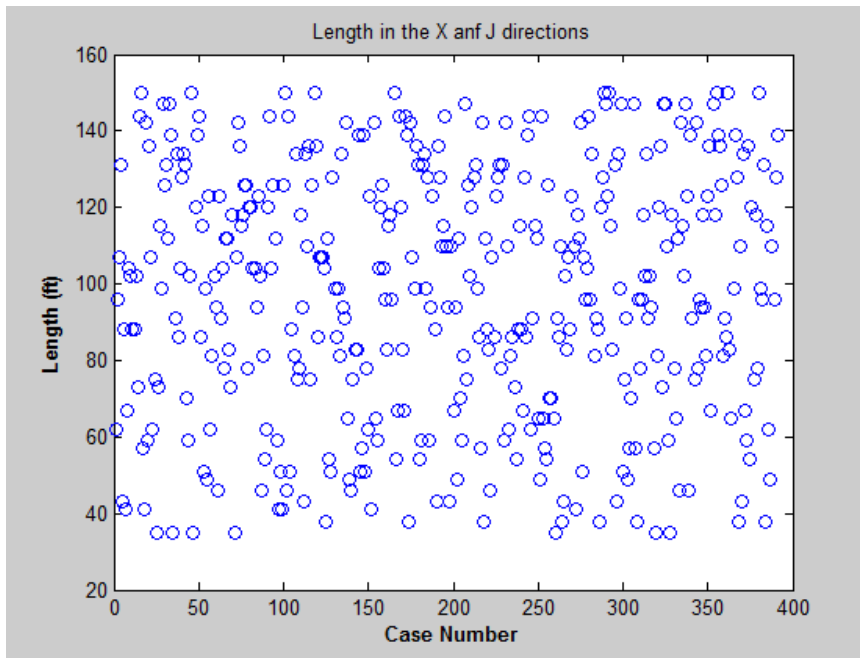


Figure 109: Grid block length in the x and y directions distribution

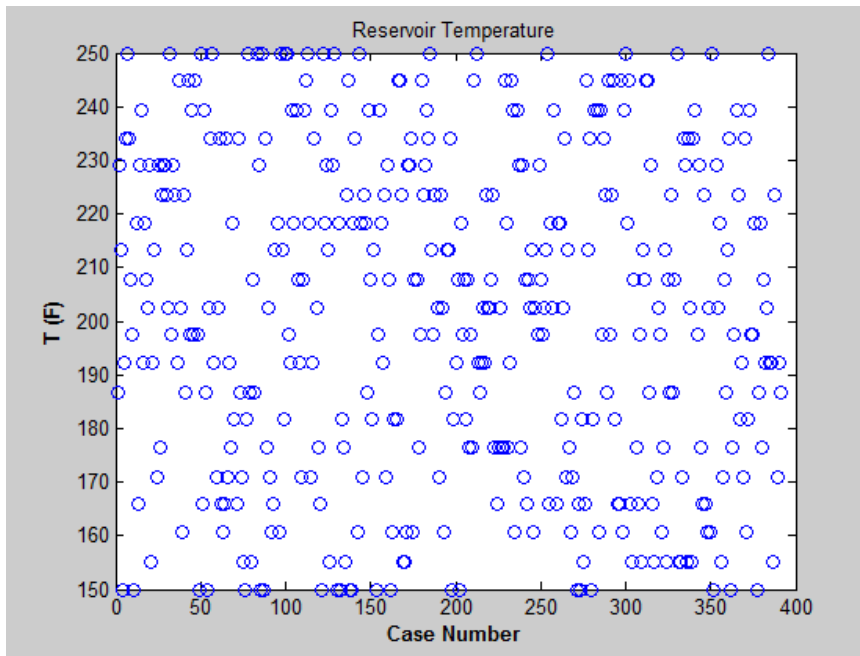


Figure 110: Reservoir temperature distribution

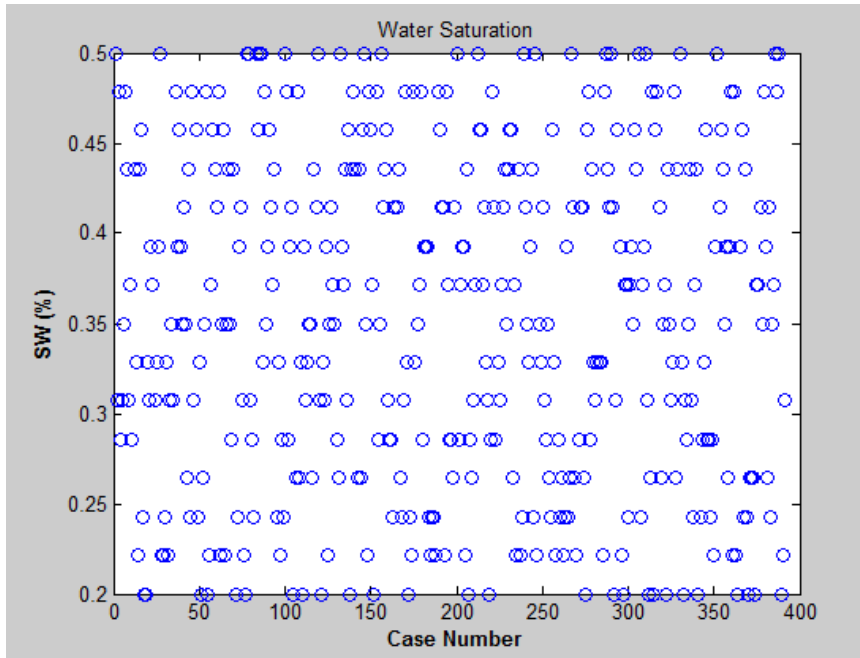


Figure 111: Water Saturation distribution

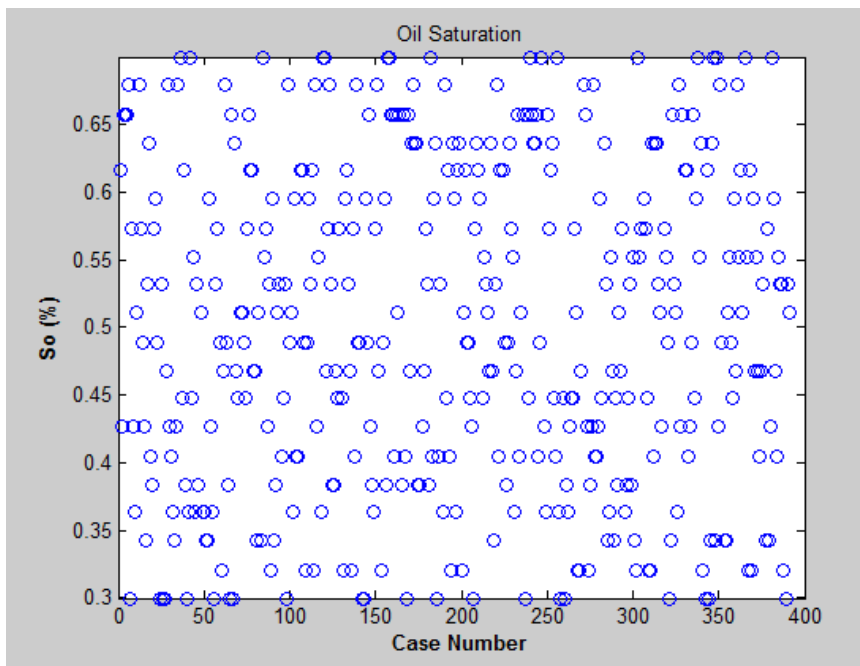


Figure 112: Oil saturation distribution

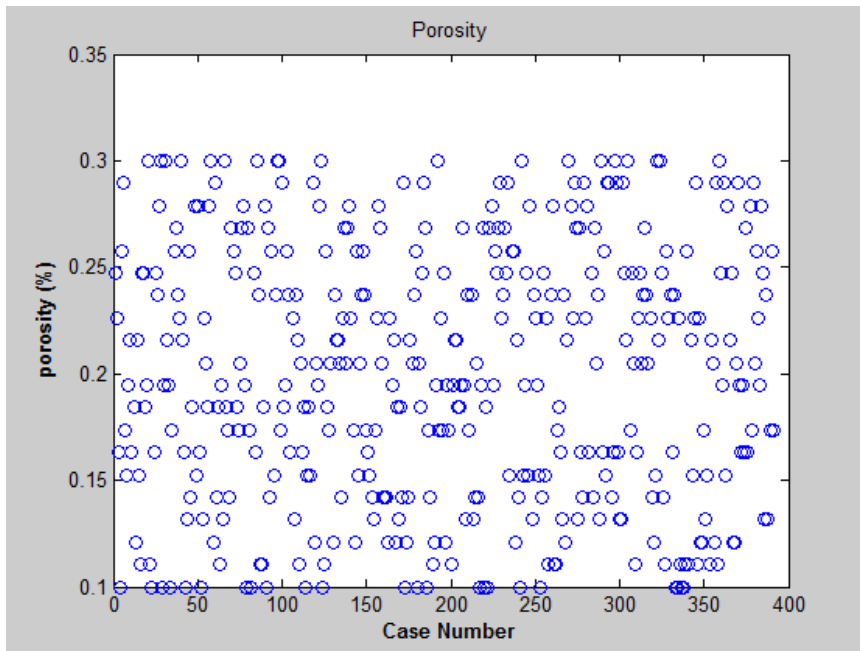


Figure 113: Porosity distribution

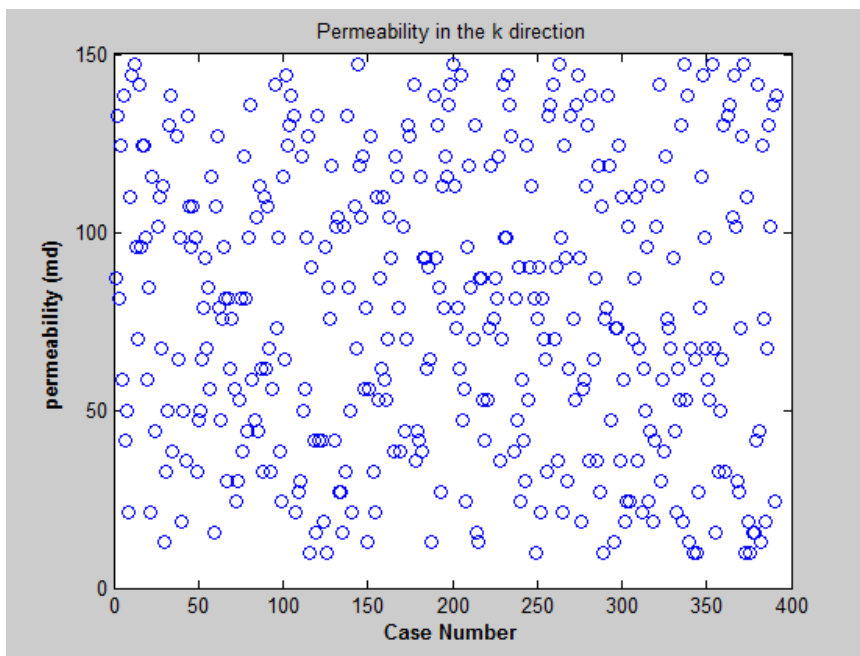


Figure 114: Permeability in the k direction distribution

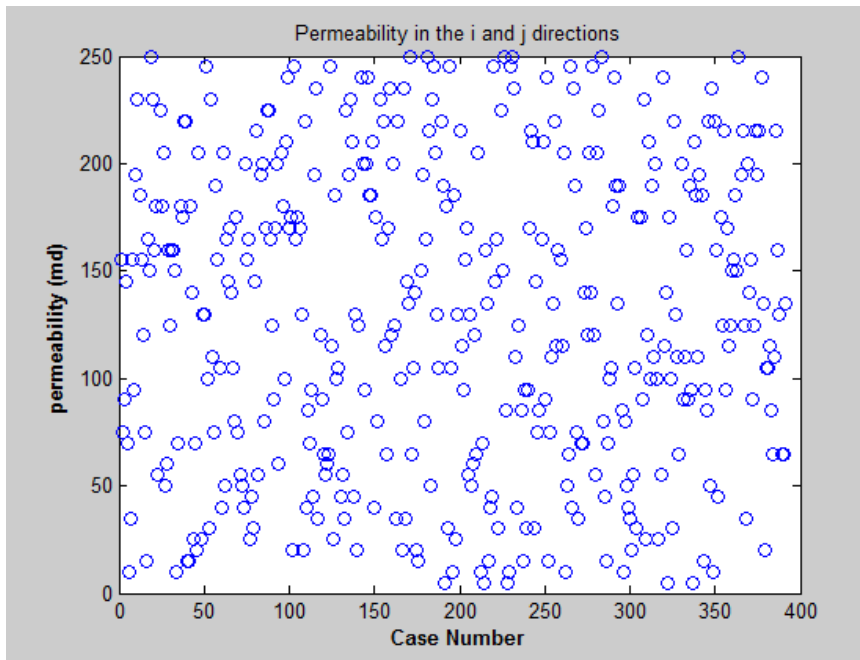


Figure 115: Permeability in the i and j directions distribution

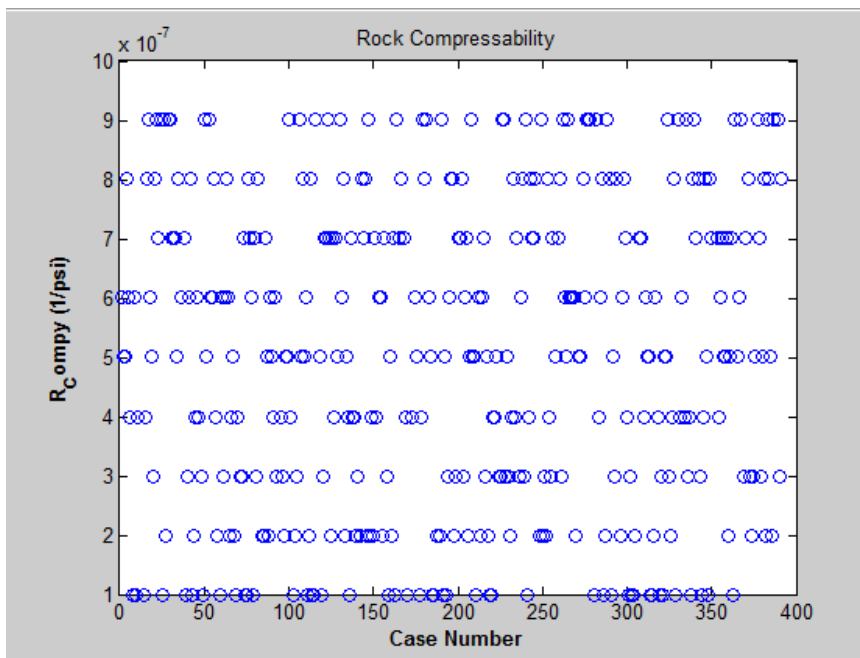


Figure 116: Rock Compressibility distribution

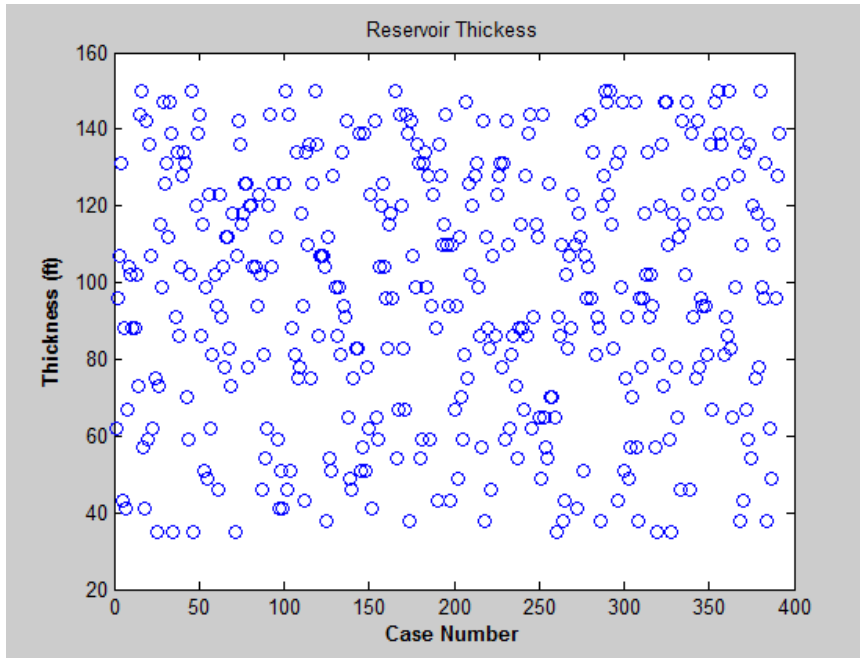


Figure 117: Reservoir thickness distribution

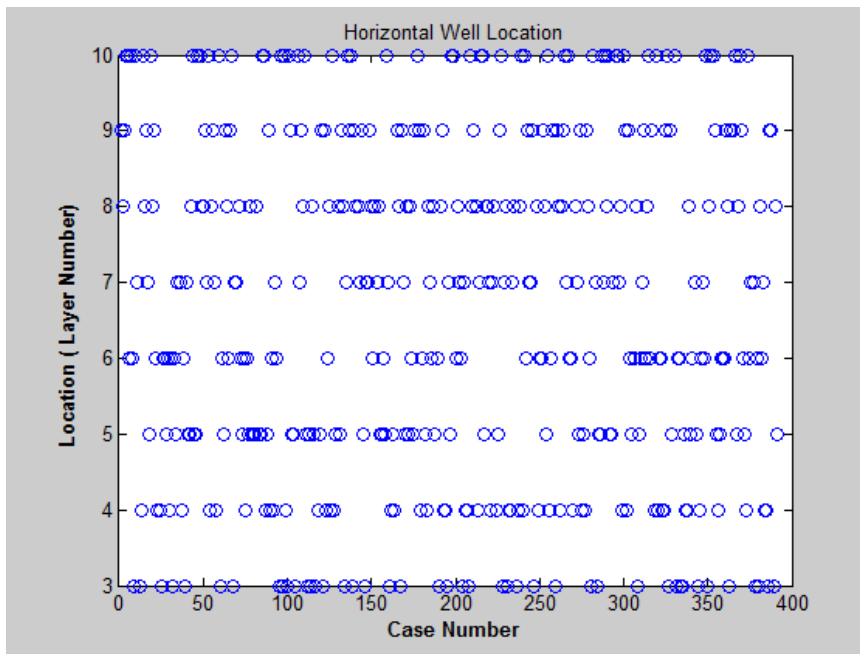


Figure 118: Location of the horizontal well in term of layer number distribution



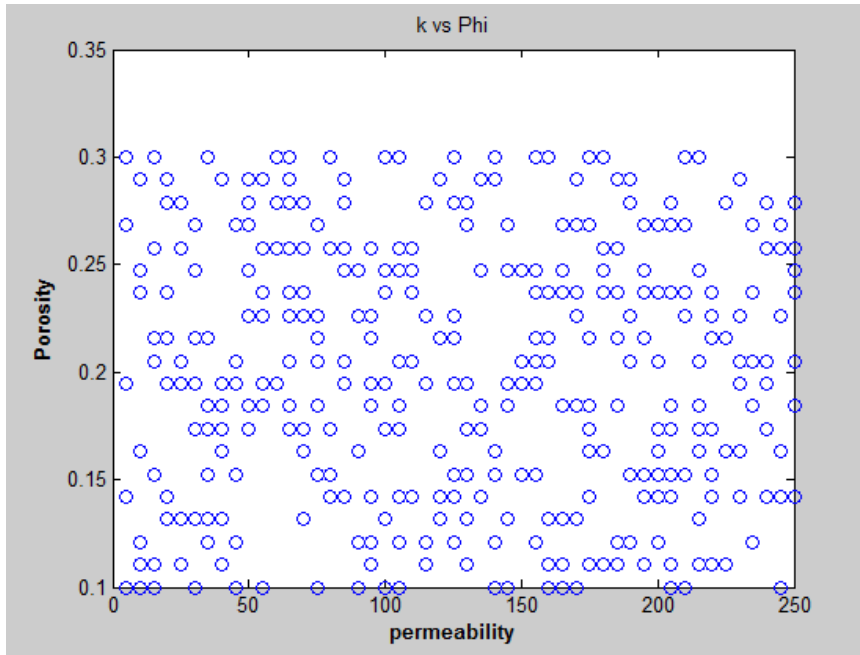


Figure 119: Permeability versus Porosity distribution

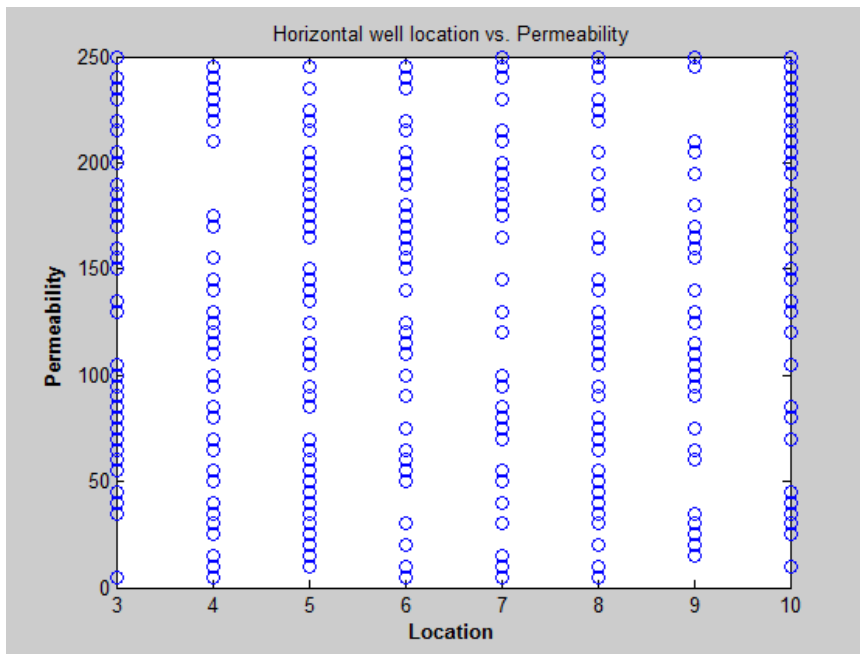


Figure 120: Horizontal well location versus Permeability distribution

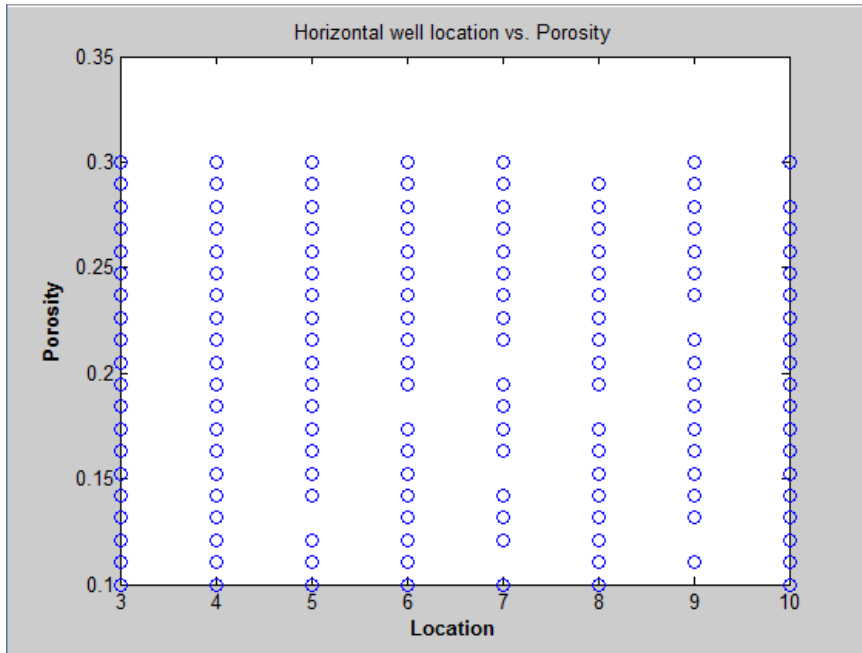


Figure 121: Porosity versus well location distribution

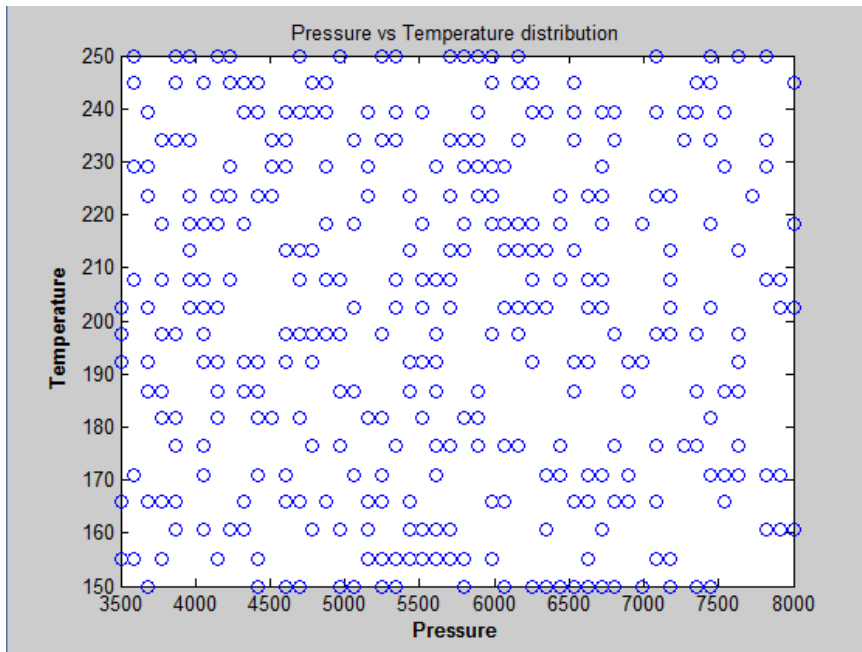


Figure 122: Temperature versus pressure distribution

## Appendix (C) ANN MATLAB Code

---

```
clc
clear all
format long

% load all input & output
Input=xlsread('output3.xlsx',4);
Oil_Rate=xlsread('output3.xlsx',1);
Gas_Rate=xlsread('output3.xlsx',2);
Water_Rate=xlsread('output3.xlsx',3);
Cum_Oil=xlsread('output3.xlsx',5);
Cum_Gas=xlsread('output3.xlsx',6);
Cum_Water=xlsread('output3.xlsx',7);
GOR=xlsread('output3.xlsx',8);
WOR=xlsread('output3.xlsx',9);
WC=xlsread('output3.xlsx',10);

In1_Location=Input(1,:);
In2_Length=(29*(Input(2,:))).^2/43560;
In3_PermI=Input(3,:);
In4_PermK=Input(4,:);
In5_Phi=Input(5,:);
In6_Press=Input(6,:);
In7_RComp=Input(7,:);
In8_So=Input(8,:);
In9_Sw=Input(9,:);
In10_Temp=Input(10,:);
In11_H=Input(11,:);
In13_API=Input(12,:);
In14_GD=Input(13,:);

%functional link

FL1=In3_PermI./In4_PermK;
FL2=In4_PermK./In3_PermI;
FL3=(In3_PermI+In4_PermK)./10;
FL4=In8_So./In9_Sw;
FL5=In8_So+In9_Sw;
FL6=In9_Sw./In8_So;
FL7=In7_RComp.*In6_Press.*1000;
FL8=In11_H./In2_Length;

for j=1:length(:,T_test);
    for i= 1:length(time);
        if Oil_Rate(i,j)==0;
            Oil_Rate(i,j)=1;
        else
            Oil_Rate(i,j)=Oil_Rate(i,j);
        end
    end
end
```

```

end
if Gas_Rate(i,j)==0;
    Gas_Rate(i,j)=1;
else
    Gas_Rate(i,j)=Gas_Rate(i,j);
end
if Water_Rate(i,j)==0;
    Water_Rate(i,j)=1;
else
    Water_Rate(i,j)=Water_Rate(i,j);
end

if Cum_Oil(i,j)==0;
    Cum_Oil(i,j)=1;
else
    Cum_Oil(i,j)=Cum_Oil(i,j);
end
if Cum_Gas(i,j)==0;
    Cum_Gas(i,j)=1;
else
    Cum_Gas(i,j)=Cum_Gas(i,j);
end
if Cum_Water(i,j)==0;
    Cum_Water(i,j)=1;
else
    Cum_Water(i,j)=Cum_Water(i,j);
end
if GOR(i,j)==0;
    GOR(i,j)=1;
else
    GOR(i,j)=GOR(i,j);
end
if WOR(i,j)==0;
    WOR(i,j)=1;
else
    WOR(i,j)=WOR(i,j);
end
if WC(i,j)==0;
    WC(i,j)=1;
else
    WC(i,j)=WC(i,j);
end
end
end
end

```

```

Reservoir=[In2_Length./1000;In3_PermI./100;In4_PermK./100;In5_Phi;In6_Press./1
000;In7_RComp.*1e5;In8_So;In9_Sw;In10_Temp./100;In11_H./100;In13_API./10;In14_
GD];
Design=In1_Location./10;

```

```

Feed=[(In1_Location);log(In2_Length);log(In3_PermI);log(In4_PermK);In5_Phi;log
(In6_Press).\10;In7_RComp.*1e5;In8_So;In9_Sw;log(In10_Temp).\10;log(In11_H).\1
0;log(In13_API).\10;In14_GD;In8_So\In9_Sw;1.\(In8_So.*In13_API*0.1);(In2_Lengt
h.*In11_H)];

```

```

OUTPUT=[Oil_Rate;Gas_Rate;Water_Rate;Cum_Oil;Cum_Gas;Cum_Water;GOR;WOR;WC];
Target=log(OUTPUT);

% normalize data to be from -1 to 1
[Pn,ps] = mapminmax(Feed,-1,1);
[Tn,ts] = mapminmax(Target,-1,1);

[mi,ni] = size(Pn);
[mo,no] = size(Tn);

% Defining some random variables required in the network
N_in = mi; % Number of inputs in the network
N_out = mo; % Number of outputs in the network
Tot_in = ni; % Total number of simulations

% [Pn_train,Pn_val,Pn_test,trainInd,valInd,testInd] =
divideind(Pn,1:350,351:370,371:391);
[Pn_train,Pn_val,Pn_test,trainInd,valInd,testInd] =
dividerand(Pn,0.9,0.05,0.05);

[Tn_train,Tn_val,Tn_test] = divideind(Tn,trainInd,valInd,testInd);

val.T = Tn_val;
val.P = Pn_val;
test.T = Tn_test;
test.P = Pn_test;

A= 13;
B= 19;
C=33;
D=39;
E=42;
F=43;
G=49;
Layer1=A;
Layer2=B;
Layer3=C;
Layer4=D;
Layer5=E;
Layer6=F;
Layer7=G;

% net = newff(Pn,Tn,[ Layer1,
Layer2],{'logsig','logsig'},'trainscg','learngdm','msereg'); %transfer
functions try logsig, tansig, purlin,..
% net = newff(Pn,Tn,[ Layer1,
Layer2],{'tansig','tansig'},'trainscg','learngdm','msereg');
% Training function: trainscg, trainrp, trainbr,..

```

```

%     net = newff(Pn,Tn,[ Layer1, Layer2,
Layer3],{'tansig','tansig','tansig'},'trainscg','learngdm','msereg');
%     net = newff(Pn,Tn,[ Layer1, Layer2,
Layer3],{'logsig','logsig','logsig'},'trainscg','learngdm','msereg');
%     net = newff(Pn,Tn,[ Layer1, Layer2, Layer3,
Layer4],{'logsig','logsig','logsig','logsig'},'trainscg','learngdm','msereg')
;
%     net = newff(Pn,Tn,[ Layer1, Layer2, Layer3,
Layer4],{'tansig','tansig','tansig','tansig'},'trainscg','learngdm','msereg')
;
%     net = newff(Pn,Tn,[ Layer1, Layer2, Layer3, Layer4,
Layer5],{'logsig','logsig','logsig','logsig','logsig'},'trainscg','learngdm',
'msereg');
%     net = newff(Pn,Tn,[ Layer1, Layer2, Layer3, Layer4,
Layer5],{'tansig','tansig','tansig','tansig','tansig'},'trainscg','learngdm',
'msereg');

%     net = newff(Pn,Tn,[ Layer1, Layer2, Layer3, Layer4, Layer5,
Layer6],{'logsig','logsig','logsig','logsig','logsig','logsig'},'trainscg','l
earngdm','msereg');
%     net = newff(Pn,Tn,[ ,[ Layer1, Layer2, Layer3, Layer4, Layer5,
Layer6],{'tansig','tansig','tansig','tansig','tansig','tansig'},'trainscg','l
earngdm','msereg');
%     NNeu7=0;
%     else
%     net = newff(Pn,Tn,[ ,[ Layer1, Layer2, Layer3, Layer4, Layer5,
Layer6,Layyer7],{'logsig','logsig','logsig','logsig','logsig','logsig','logsi
g'},'trainscg','learngdm','msereg');
%     net = newff(Pn,Tn,[ Layer1, Layer2, Layer3, Layer4, Layer5,
Layer6,Layyer7],{'tansig','tansig','tansig','tansig','tansig','tansig','tansi
g'},'trainscg','learngdm','msereg');

%

%

net.trainParam.goal = 1e-4; % Accuracy within this range
net.trainParam.epochs = 5000; % Number of iterations while training the
network
net.trainParam.show = 1;
net.trainParam.max_fail = 1000; % Number of validation check fails before
stopping a network. This is done to prevent over-learning
net.trainParam.mem_reduc = 60; % Done to reduce memory requirements
net.trainParam.showWindow = true; % To show the training window

% Training of network
[net,tr] = train(net,Pn_train,Tn_train,[],[],test,val);

% Getting data from the trained network
Tn_train_ann = sim(net,Pn_train);
Tn_test_ann = sim(net,Pn_test);

% Now, we need to denormalize the data sets using mapminmax
T_train = mapminmax('reverse',Tn_train,ts);
T_test = mapminmax('reverse',Tn_test,ts);

```

```

T_train_ann = mapminmax('reverse',Tn_train_ann,ts);
T_test_ann = mapminmax('reverse',Tn_test_ann,ts);

Pn_train = mapminmax('reverse',Pn_train,ps);
Pn_val = mapminmax('reverse',Pn_val,ps);
Pn_test = mapminmax('reverse',Pn_test,ps);

% conversion to original data
T_train=exp(T_train); T_train_ann=exp(T_train_ann);
T_test=exp(T_test);T_test_ann=exp(T_test_ann);
% net=feedforwardnet(100,'trainscg');
% net=feedforwardnet(100,'trainrp');
% net=feedforwardnet(100,'trainrb');

for j=1:length(:,T_test);
    for i= 1:length(time);
        if Oil_Rate(i,j)==1;
            Oil_Rate(i,j)=0;
        else
            Oil_Rate(i,j)=Oil_Rate(i,j);
        end
        if Gas_Rate(i,j)==1;
            Gas_Rate(i,j)=0;
        else
            Gas_Rate(i,j)=Gas_Rate(i,j);
        end
        if Water_Rate(i,j)==1;
            Water_Rate(i,j)=0;
        else
            Water_Rate(i,j)=Water_Rate(i,j);
        end

        if Cum_Oil(i,j)==1;
            Cum_Oil(i,j)=0;
        else
            Cum_Oil(i,j)=Cum_Oil(i,j);
        end
        if Cum_Gas(i,j)==1;
            Cum_Gas(i,j)=0;
        else
            Cum_Gas(i,j)=Cum_Gas(i,j);
        end
        if Cum_Water(i,j)==1;
            Cum_Water(i,j)=0;
        else
            Cum_Water(i,j)=Cum_Water(i,j);
        end
        if GOR(i,j)==1;
            GOR(i,j)=0;
        else
            GOR(i,j)=GOR(i,j);
        end
        if WOR(i,j)==1;
            WOR(i,j)=0;
        else
            WOR(i,j)=WOR(i,j);
        end
    end
end

```

```
end
  if WC(i,j)==1;
    WC(i,j)=0;
  else
    WC(i,j)=WC(i,j);
  end
end
end
```